12-2023

Using Noninvasive Calibrated Cuff Plethysmography to Observe the Effects of Cold-Water Immersion on Arterial Compliance

Rita M. Grigorian
California Polytechnic State University, San Luis Obispo, ritagrigorian21@gmail.com

USING NONINVASIVE CALIBRATED CUFF PLETHYSMOGRAPHY TO OBSERVE THE EFFECTS OF COLD-WATER IMMERSION ON ARTERIAL COMPLIANCE

A Thesis

presented to

the faculty of California Polytechnic State University

San Luis Obispo

In Partial Fulfillment

of the Requirements for the Degree

Master of Science

in Biomedical Engineering

by

Rita Grigorian

August 2023

COMMITTEE MEMBERSHIP

TITLE:	Using Noninvasive Calibrated Cuff Plethysmography to Observe the Effects of Cold-Water Immersion on Arterial Compliance
AUTHOR:	Rita Grigorian
DATE SUBMITTED:	August 2023
COMMITTEE CHAIR:	Michael Whitt, Ph.D. MBA Professor of Biomedical Engineering
COMMITTEE MEMBER:	David Clague, Ph.D. Professor of Biomedical Engineering
COMMITTEE MEMBER:	Justin Shaw, M.S. Design Engineer

ABSTRACT

Using Noninvasive Calibrated Cuff Plethysmography to Observe the Effects of Cold-Water Immersion on Arterial Compliance

Rita Grigorian

As the prevalence of cardiovascular diseases continues to exponentially grow in populations across the globe, the necessity of determining underlying factors, effective methods of diagnoses, and universally available preventive measures also grows. Early detection of endothelial dysfunction, a proven precursor of cardiovascular diseases, can be extremely impactful in encouraging preventative measures and early intervention before medical conditions become chronic. In recent years, ice plunging, a form of cryotherapy involving full body immersion in cold water, has gained popularity within circles of fitness and health practitioners, gaining the interest of people of all backgrounds. Certain parallels observed between the human physiological response to cold exposure and endothelial function encourage further study of the effects of ice plunging on cardiovascular health. Calibrated cuff plethysmography is a promising method of reflecting on endothelial function by measuring arterial compliance of select blood vessels. In this study, a calibrated cuff plethysmography device was built and tested for efficiency as it was used to measure compliance and cross-sectional area of the brachial artery of 14 participants 30 minutes before, immediately after, and 30 minutes after a 5-minute cold plunge in a temperature of 10°C - 15°C. Results found some significant differences between baseline measurements recorded immediately after the ice plunge and measurements recorded during reactive hyperemia conditions at normal body temperature but did not conclude that 5-minute cold-water immersion intervention had a significant impact on arterial compliance or area overall since this was a short term experiment with only acute intervention methods. The device used was concluded to effectively measure arterial compliance and area.

Keywords: Calibrated cuff plethysmography, oscillometry, cold-water immersion, reactive hyperemia, endothelial dysfunction, vasodilation, vasoconstriction, artereogenesis, angiogenesis, thermoregulation, cryotherapy

ACKNOWLEDGMENTS

I would like to acknowledge Dr. Michael Whitt for his unwavering support and expert help during the entire process of my thesis research. It wouldn't have been possible without his guidance and knowledge of the subject. I'm grateful to have been given the opportunity to continue building upon his work and having the honor of working with him in person. I truly could not imagine a better advisor. I also offer thanks to Nick Hughes who played a critical role in building the device which was used and helping me with data collection every step of the way.

I would also like to thank the 14 participants who volunteered to take part in my study with such excitement, despite the discomfort of sitting in a tub of 10°C ice water. I would like to thank Anahita Emami for helping with the whole data collection process.

I would like to give special thanks to my parents and my two brothers who have supported me throughout my whole life in all decisions and endeavors regardless of their perceived feasibility. I'd also like to thank my grandfather, Mark, for being such a great figure of inspiration and always pushing me to do more.

Finally, I would like to acknowledge the friends I have made at Cal Poly for being with me every step of the way and becoming my lifelong friends.

TABLE OF CONTENTS

Page

CHAPTER

LIST OF TABLES

Table Page

LIST OF FIGURES

Chapter 1

1. INTRODUCTION

The human vascular system is often credited for facilitating the flow and diffusion of blood, lymph, nutrients, and more throughout the body with the purpose of maintaining homeostatic conditions in response to the presence of gradients in temperature, shear stress, blood pressure, blood oxygen levels, among other regularly observed cycling physiologic changes. Arterial compliance is critical to the ability of the vascular system to properly perform its homeostatic responsibilities and continue to successfully supply blood to the body. In this way, arterial compliance can be referenced as the capability of an artery to comply to changes in blood flow among other stimulating factors via vasodilation and several additional regulatory mechanisms. Arterial compliance is heavily dependent on the healthy functionality of the endothelium within the vessel as endothelial cells play critical roles in many regulatory pathways. Vasodilation, arteriogenesis, and angiogenesis are among a plethora of regulatory pathways with several stimulants which aid in the restoration of appropriate blood flow to tissue in the presence of vessel occlusion, atherosclerosis development, and other vascular complications. This paper reviews human physiological responses to cold temperature exposure and its effects on endothelial function as they relate to the pathways and stimulants of these three regulatory mechanisms. The following study discusses the construction and implementation of a noninvasive calibrated cuff plethysmography device used to evaluate arterial compliance by aiding in the measurement/calculation of differences in the cross-sectional area of the brachial artery of subjects in normal and hyperemic conditions before and after full body exposure to cold water.

The noninvasive measurement of arterial luminal area via the combination of concepts involving both oscillometry and plethysmography has proven to be advantageous over the more common method of ultrasound imaging, which has been shown to yield greater error with several limitations including the need for very skilled technicians [1]. Particularly, a device which is very similar to the one used in this study was found to have a volume accuracy within 1.5% error as compared to ultrasound methods which yielded a 17% relative error [1]. The model used in this study was modeled after the aforementioned prototype device built by Dr. Michael Whitt which served as the precursor for the Cordex SmartCuff by Cordex Systems Inc. Our model of the calibrated cuff plethysmography device was built and used to generate arterial pressure-area curves and relations of arterial compliance versus transmural pressure as related to the brachial arteries of participants during baseline and hyperemic conditions before and after a short period of full body cold water exposure. The accurate measurement of arterial lumen area is critical in the assessment of endothelial function and evaluation of vasodilatory drugs, reaping many preventative benefits for hypertensive patients, patients undergoing anesthesia, and patients with coronary and peripheral artery disease [1]. Figures 1 and 2 below show examples of transmural arterial pressure - area curves and transmural pressure – arterial compliance curves which are generated by the device.

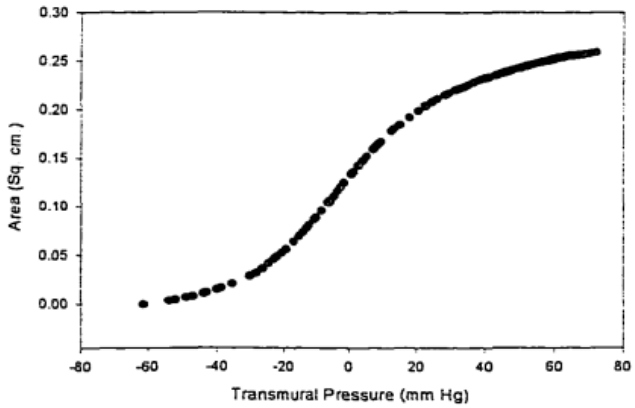

Figure 1. Arterial Pressure - Area (P-A) Curve [1]. This plot displays the cross-sectional arterial area of the brachial artery over the specified transmural arterial pressure range.

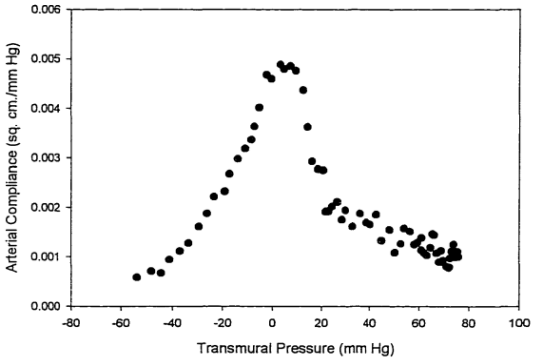

Figure 2. Arterial Compliance vs Transmural Pressure [1]. This plot represents the derivative of the plot shown in figure 1. It displays the compliance of a brachial artery over the noted transmural arterial pressure range.

Ultimately, the goal of this study is to use the calibrated cuff plethysmography device to observe cardiovascular responses to full body cold-water immersion intervention which has been claimed to reap many benefits in the realms of cardiovascular health, mental health, muscle recovery, and vascular health on multiple occasions. Results include the

effects of cold-water immersion on blood pressure and arterial compliance among other factors.

1.1 OSCILLOMETRY AND PLETHYSMOGRAPHY

1.1.1 Oscillometry

Oscillometry involves the measurement of pulsation changes in the arteries and results in the acquisition of data that provides systolic, diastolic, and mean arterial pressure which is observed at maximal pressure oscillations. Systolic pressure is observed at 55% of the maximum pulse wave amplitude while diastolic pressure is observed at 85% [2]. This data is acquired through gradual release of cuff pressure from levels greater than that of the patient's systolic pressure. The pressure of the cuff as well as oscillations in cuff pressure resulting from increased blood flow and pulse against the cuff itself is collected by a pressure sensor, recorded, and filtered using a high pass filter greater than 0.5 Hz [1]. Oscillometric volume pulses are collected through segmental plethysmography techniques which involve the use of an instrument to measure variability size and blood flow through organs and limbs. Example data displaying cuff pressure and oscillations in cuff pressure can be observed in figure 3 below.

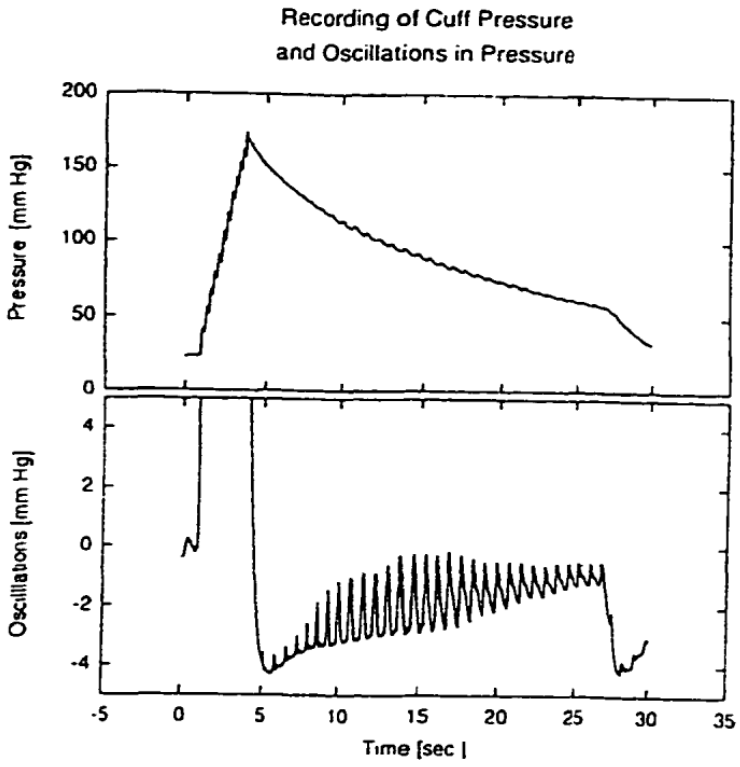

Figure 3. Cuff Pressure and Oscillations in Cuff Pressure Over Time as Seen During Gradual Pressure Release [2]. As cuff pressure is decreased over time, oscillations in pressure can be seen spiking as a result of increased blood flow and pulse against the cuff. Greater spikes are representative of greater arterial compliance.

1.1.2 Segmented Plethysmography

Segmented plethysmography essentially relates changes in the volume of the limb under observation to the pressure of the cuff. Diaphragm displacement is related to limb volumetric displacement through the equation, $A \times d = k\Delta V$, in which A represents the cross-sectional area of the diaphragm, d is diaphragm displacement, and k is a variable constant, $k = \frac{V_0}{V_0+V_1}$, that differs at each pressure level. Here V_0 represents the initial volume of the inactive section of the system and V_1 represents the initial volume of the active section. ΔV represents the limb volumetric displacement. Volumetric changes in

vasculature have been observed to be directly proportional to volume changes in active sections of pneumatic systems in segmental plethysmography. Here, changes in pressure caused by changes in vascular volume directly affect cuff compliance, which is defined as $[\Delta\ Cuff\ Volume\ (ml)]/[\Delta\ Cuff\ Pressure\ (mmHg)]$ [1]. It should be noted that diaphragm displacement differs with each system pressure and volume and can also be affected by cuff tightness around the limb of interest, causing variation in cuff compliance at each cuff pressure. For this reason, the pressure-volume relationship in the cuff is nonlinear and in turn results in a nonlinear cuff compliance relationship which can be observed in figure 4 below.

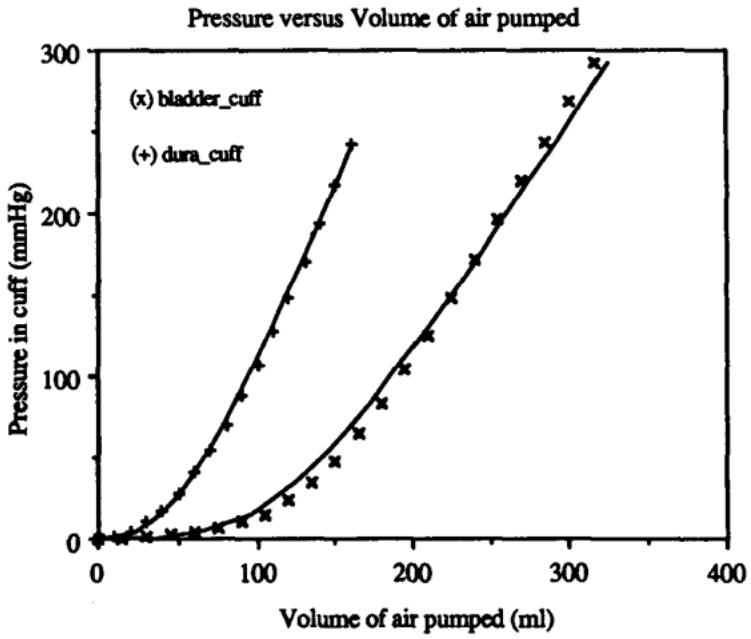

Figure 4. Pressure-Volume Curve from Occlusive Cuffs [2].

Furthermore, it has been found that maximal arterial compliance occurs when the transmural pressure of an artery is at or close to zero, also the oscillometric maximum. This occurs when the arterial pressure is equal to the pressure of the cuff [2]. Segmental

plethysmography essentially collects limb volumetric displacement at a range of different cuff pressures with the calculation of constant k at each pressure. Knowledge of the cuff pulse pressure (dP_{cuff}) and the cuff compliance $(\frac{dV}{dP})_{cuff}$ can be used to find the cuff volumetric displacement (dV_{cuff}) using the equation: $dV_{cuff} = (\frac{dV}{dP})_{cuff} \times dP_{cuff}$, where differences in cuff volume are directly correlated to differences in limb volume (dV_{artery}). As follows, the limb volumetric displacement can be discovered at any chosen cuff pressure with the acquisition of $(\frac{dV}{dP})_{cuff}$ and dP_{cuff} using the equation $dV_{artery} = dV_{cuff} = (\frac{dV}{dP})_{cuff} \times dP_{cuff}$. In order for $dV_{artery} = dV_{cuff}$ to be true, the pressure applied by the cuff onto the artery must be consistent throughout the entirety of the cuff length [1]. For the purposes of this thesis, the general concept of segmental plethysmography and oscillometry are used in what is referred to as calibrated cuff plethysmography where limb volume pulse is assumed to be equal to arterial volume pulse as one is essentially the result of the other.

1.2 BACKGROUND

1.2.1 Cardiovascular disease

Cardiovascular diseases (CVD) currently take the title of the leading cause of death for both men and women across the entire globe, claiming approximately 17.9 million lives every year [3]. In the United States alone, according to the American Heart Association, around 82.6 million people live with at least one type of cardiovascular disease. Some common types of CVD include coronary and peripheral artery disease, stroke, hypertension, congestive heart failure, atrial and ventricular arrhythmias, congenital cardiovascular disorders, rheumatic heart disease, and other conditions related to the circulatory system [4].

Coronary and peripheral artery disease, with approximate global prevalence of 154 and 120 million people respectively in 2016, is often caused by the development of atherosclerosis in the coronary or peripheral arteries [5]. These conditions often result from dysfunction of endothelial cells, the accumulation of lipids in these vessels, and the formation of plaque in the luminal area and can eventually lead to other cardiovascular complications like myocardial infarctions, stroke, limb ischemia, and death if not treated properly [5].

Current treatments for patients with coronary artery disease include beta blockers, ARB/ACE inhibitor and statins as well as surgical interventions like coronary artery bypassing, angioplasty, or the insertion of a stent to hold the occluded artery open [5]. Peripheral artery disease involves blockages in the peripheral arteries that supply the upper and lower extremities as well as vital organs with the blood needed to survive. It can be harder to diagnose because it can remain asymptomatic for years before causing serious issues like critical ischemia. Treatments for peripheral artery disease are similar to those of coronary artery disease, including pharmacologic agents, surgical intervention like balloon angioplasty, atherectomy, endarterectomy, bypass surgery, and stent insertion [6]. Stent insertion can be more difficult in the peripheral arteries as compared to coronary arteries since these arteries are relatively smaller and more prone to adverse events involving stents.

While surgical intervention does offer sufficient results in treatment of both coronary and peripheral artery disease at times, it can also result in complications like movement of stents, stent material deterioration, damage from graft retrieval for bypass surgery, among other issues. Typically, if a patient is already suffering from

blockages in major arteries, invasive and complex procedures can negatively affect their overall health and result in a longer recovery time than that which would be seen in a healthy patient. In response to these concerns, a newer approach which could potentially help patients with arterial disease without invasive intervention is cell therapy, where cells which are known to release angiogenic properties like VEGF, bFGF, HGF, and TB4 are injected into patient [7], [8]. No such products have yet been released into the market as production of the ideal angiogenesis stimulating cell therapy has not yet been successful in a clinical setting.

1.2.2 Endothelial Dysfunction

The endothelium is composed of a layer of endothelial cells which make up the inner lining of the entire vascular system, allowing blood to flow through the body while keeping it separate from surrounding tissues. Endothelium is very important as it plays a major role in maintaining homeostasis between vasculature and tissue by producing both agonistic and antagonistic secretions, overseeing both vasodilation and vasoconstriction of vessels. Homeostasis is also maintained by the controlled production of prothrombic and antithrombic elements as well as antifibrinolytics and fibrinolytics [9]. Endothelial cells also play major roles in cell proliferation and migration during angiogenesis.

Endothelial cells respond to both chemical and mechanical stimuli and are able to change their morphology relative to shear stimulus from blood flow. Increased shear stress in blood vessels cause smooth muscle cells to relax and endothelial cells to flatten out, dilating the vessel, increasing the area of the vessel cross section, causing slower blood flow, and in turn decreasing and regulating shear stress in a healthy negative feedback loop [10]. Conversely, a low shear stress in an arterial vessel

stimulates contraction of smooth muscle cells and causes endothelial cells to increase their volume and reduce their surface area along the vessel, constricting the vessel, decreasing the cross-sectional area of the vessel, causing faster blood flow, and increasing and regulating shear stress in another negative feedback loop [10]. In both of these mechanisms, shear stress is actually stimulating the release of nitric oxide by endothelium, which travels to the smooth muscle of arterial wall where it plays a role in the degradation of GTP to cGMP which regulates Ca^{2+} levels in the cytosol, causing muscle relaxation and ultimately vasodilation of the vessel [7]. Low shear, in turn, results in low nitric oxide release and constriction instead of dilation.

Significant problems can arise when endothelial cells are damaged. Endothelial dysfunction is caused by insufficient nitic oxide in the blood vessel walls, resulting in the inability of the endothelium to perform the homeostatic tasks that it is responsible for. This can lead to inflammatory responses and vascular disease as vessels are unable to properly dilate and contract. Hypertension, diabetes mellitus, and smoking, among other risk factors, can all act as contributors to endothelial dysfunction and decreased nitric oxide activity. Nitric oxide plays roles in anti-arteriosclerotic mechanisms like suppression of endothelin, a vasoconstrictive factor, and also impedes platelet aggregation and slows down adhesive molecule expression, making it harder for plaque to form. Nitric oxide also inhibits LDL oxidation and smooth muscle proliferation and migration, slowing down atherosclerosis development [11] The optimal levels of shear stress that allow the endothelium to function properly are typically above 15 $dynes/cm^3$ [12]. Shear stress too low results in insufficient nitric oxide and increase in adhesion molecules and growth factors, creating a very pro-

inflammatory environment and allowing for plaque accumulation. On the flip side, a shear stress too high can cause endothelial cells to erode and cause plaque to rupture.

1.2.3 Methods of Detection

Endothelial dysfunction can be assessed by observing nitric oxide production of endothelial cells as well as vasodilation capacity. To evaluate endothelial dysfunction, endothelium independent vasodilation caused by a nitric oxide donor drug can be compared to natural endothelium dependent flow-mediated vasodilation after an induced acute ischemic state. This is usually observed in the brachial, radial, or femoral arteries where vasodilation is quantified by arterial diameter measurements typically using Laser-Doppler methods or high-resolution ultrasounds [7]. Vascular echography and peripheral arterial tonometry can also be used to measure flow mediated dilation noninvasively. Endothelial function has also been evaluated by looking at bone marrow derived endothelial progenitor cell (EPC) count as they are presumed to play a role in endothelium repair as well as angiogenesis. Many studies have found correlations between a high amount of cardiovascular risk factors and lower EPC counts in patients and found lower numbers of EPCs in patients with more endothelial dysfunction, implying the potential of EPC count as a marker for endothelial function assessment [9].

Early detection of endothelial dysfunction can be lifechanging to patients as the dysfunction of these vital cells can create the perfect environment for the onset of arteriosclerosis development and eventual cardiovascular disease. Decreased flow mediated dilation and circulating EPC counts, both related to endothelial dysfunction, have been found to be correlated with greater incidences of cardiovascular events,

highlighting endothelial dysfunction as a marker for cardiovascular disease and its detection as a very promising preventative measure [9].

1.2.4 Reactive Hyperemia and Arterial Compliance

Since endothelium has many roles, there are various methods of assessing its many different functions separately. Common functional assessments include evaluation of vascular tone mediation, endothelial cell permeability, anticoagulation and fibrinolysis, as well as endothelial function biomarkers [13]. Endothelial function in accordance with vascular tone relates to the dilative and constrictive functions of endothelial cells. Measurement of endothelium dependent dilation is a common form of evaluation of vascular tone. One way of utilizing endothelial dependent dilation in order to assess endothelial function is called post occlusive reactive hyperemia in which acute avascularization or ischemia is temporarily induced on the measurement site for approximately five minutes and then blood flow is restored. The immediate rush of blood after the ischemic intervention results in endothelium dependent dilation as a result of increased shear, pressure, and flow. Many characteristics of blood flow can be measured using the aforementioned method, including peak blood flow[13]. This type of endothelial cell evaluation is usually done on the brachial artery since nitric oxide is the only driver of flow mediated dilation in that specific artery. After reactive hyperemia has occurred, ultrasound technology has been commonly used to measure arterial dilation and consequently, arterial compliance. This study will utilize the ability of a pressure cuff to stop blood flow to the arm before being released. The device that was built during this study uses the collection of pulse waves that are utilized in the calculation of arterial area at baseline and hyperemic conditions.

1.2.5 Properties of Thermogenesis and Thermoregulation

The use of cold temperature exposure as a therapeutic method has been engrained in human civilization for centuries, ranging from as far back as the times of Hippocrates in ancient Greece to current day sport medicine. Cryotherapy is the therapeutic use of various modalities of cold exposure, commonly thought to treat muscle tissue soreness, reduce sensory nerve conduction speed to reduce pain, and alter blood flow. Some common cryotherapy methods include cold-water immersion, ice application, cold air application typically through whole-body cryotherapy chambers, and cryopneumatic devices, among others [14].

Before going into cold exposure as therapy, it is important to understand the human physiologic responses to cold and thermogenesis, as understanding these pathways can help find areas that can be capitalized off of. On a cold day out, a person might put on a jacket or sweater to regulate their body temperature, it is when these outer interventions are not enough or available in a situation, when the body's natural temperature regulating pathways kick in to maintain homeostasis.

Thermoregulation occurs in a sort of balance between cardiac output and heat transfer between the body and environment [15]. When the environment outside of the body is colder than the body's core temperature, heat flows from the core to the outside environment through conductive and convective mechanisms. Vasomotor responses to cold stimulus aid in thermoregulation by causing peripheral vasoconstriction, decreasing blood flow to the peripheral limbs, and conserving heat in the body's core. Peripheral vasoconstriction consequently results in a decrease in skin temperature as heat is not being replaced as fast as it is being lost due to a decrease in warm blood perfusion do these areas. Excessive continuous cold exposure and vasoconstriction

can be dangerous as the reduction of blood flow can result in a reduction of nutrients reaching tissue, eventually leading to tissue damage and necrosis [16]. In extreme cases, cold injuries like frostbite can occur due to excessive cold exposure at temperatures as low as -0.55°C, during which cell temperature can drop below freezing and lead to crystallization [17]. This is an extreme occurrence that is typically seen when frostbite victims are unprepared for certain environmental factors. The topic of this paper does not include the examination of such low temperatures but rather higher temperatures which have been cited as typical temperatures for muscle recovery in athletic procedures by multiple sources.

Metabolic responses to the cold are also important in thermoregulation. Heat production via muscle contraction plays a great role in thermoregulation as 70% of the total energy expended by muscle contraction is released as heat [15]. Though voluntary muscle contraction is one way of producing heat, so are involuntary contraction pathways like shivering. Shivering is the activation of rhythmic muscle contractions that results in an increase of whole-body oxygen uptake and great increases in metabolic rate. One study observed increases in metabolism related to up to 588% increases in carbohydrate oxidation and 63% in fat oxidation, citing blood glucose as a likely source of carbohydrates, energy, for shivering thermogenesis [18]. The importance of maintaining an appropriate blood glucose level is highlighted by this relationship as a decreased metabolic rate can lead to a decreased core temperature and decrease of shivering when there are inadequate concentrations of blood glucose. In contrast, voluntary muscle contraction in the form of exercise

typically increases metabolic production in greater magnitudes. Though metabolic heat production is increasing here, total body heat is ultimately decreasing as blood flow to the skin and outer body is increasing in convective heat transfer from the central body to the periphery [15].

Thermoregulation also varies among different people depending on multiple factors. Body mass and adipose tissue thickness are factors that contribute to a person's thermal response to cold as a greater surface area to body mass ratio usually correlates with greater heat loss. Body fat is also responsible for providing a significant amount of insulation as it is known to hold greater thermal resistivity than that of skin and muscle tissue, causing people with thicker layers of adipose tissue to shiver less. Other factors that affect thermoregulatory pathways include age and biological sex. Older people, for example, can have impaired thermoregulatory abilities because of impaired vasoconstriction and vasodilation ability that ultimately results from endothelial dysfunction. Loss of muscle mass due to aging can also dampen ones shivering thermogenesis response [15]. Differences in thermoregulation between males and females have also been noted in various studies, citing general differences in average body fat percentage between sexes as well as significant changes in leptin, adiponectin, and plasma glucose levels as a response to acute cold exposure, but no differences in resting energy expenditure [19]. Figure 5 below displays the physiological effects of cold exposure on the human body.

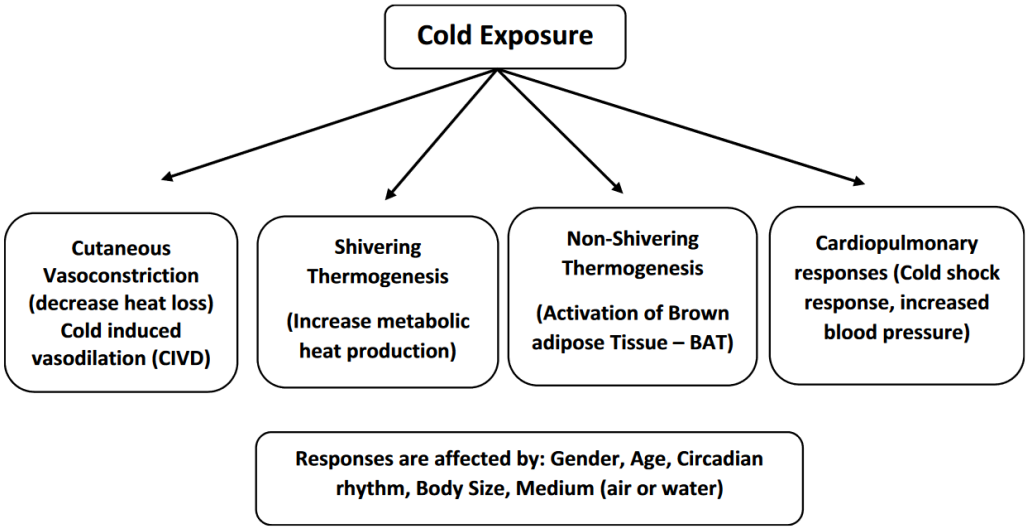

Figure 5. Physiologic Effects of Acute Cold Exposure.

Brown adipose tissue (BAT), specifically, plays multiple significant roles in non-shivering thermogenesis. The mechanisms behind non-shivering thermogenesis include the cold induced stimulation of the uncoupling protein 1 (UCP1) in the mitochondria membrane. UCP1 plays a critical role in differentiating respiratory chain activity and adenosine triphosphate synthesis. This is done through creating a proton leak by redirecting protons through the mitochondrial membrane, resulting in heat release[19]. BAT differ from white adipose tissue in that it typically has a greater number of mitochondria, making it more capable of going through with non-shivering thermogenic pathways [18]. It has been found in a comparison between average body weight males and females, that females were more sensitive to cold exposure and elicited a shivering response as well as changes in resting energy expenditure at higher temperatures than males. Metabolic responses to cold exposure as well as hormonal changes were found to be generally more distinct in females than males[19]. The same study also observed greater decreases in plasma leptin concentration and significant increases in plasma

adiponectin concentrations in females as compared to males. Decreases in leptin, which is involved with energy expenditure and appetite regulation, can be the result of energy usage during thermogenesis as lower leptin levels encourage energy intake via food consumption[19].

CHAPTER 2

2. LITERATURE REVIEW

2.1 Atherogenesis

While the study at hand examined the arterial compliance of healthy participants with no known signs of atherosclerosis, it is important to know the implication of atherogenesis and how it relates to endothelial dysfunction. Atherosclerosis is the thickening of arteries caused by plaque accumulation inside the arterial lining. It plays a key role in peripheral and coronary artery disease as well as other cardiovascular events by inhibiting proper blood flow through the body. Atherosclerosis is common in bifurcated lesions of vessels because areas of branching facilitate a continuous turbulent shear stress on the vessel walls, causing constant irritation and activation of the endothelial cells [20]. It should be noted that it is typical for blood vessels to experience constant wall shear stress as blood should always be flowing through a healthy body. It is in regions of low wall shear stress or regions of oscillatory flow where atherosclerotic plaque typically begins to form in an unhealthy patient [20]. After plaque has already formed, high wall shear stress in that area is associated with the formation of a type of plaque with a thin fibrous cap which is vulnerable to rupture. Endothelial cells which line the arterial walls are quite sensitive to changes in blood flow patterns. The changes in wall shear stress that follow open the door for atherogenesis[21]. Low shear stress along the arterial walls from constant blood flow results in the recruitment of adhesive proteins by endothelial cells which trigger the release of cytokines [22]. This abundance of cytokines then results in an influx of phagocytic leukocytes, such as macrophages. Atherosclerosis begins with an increase in low density lipoproteins (LDL) in the intima of an artery. When an LDL is oxidized by

the macrophages that were recruited by the activated endothelial cells, this oxidized LDL (OxLDL) acts as a cytokine in encouraging more endothelial activation, feeding into a positive feedback loop. OxLDL can also then be phagocytosed by a macrophage via scavenger receptor, and will then either become a yellow foam cell, or begin to present OxLDL surface antigens. In the case that the macrophage presents OxLDL antigens, T-helper cells are able to bind and release interferon-gamma (IFN-γ), a cytokine which also triggers endothelial activation and again feeds into the positive feedback loop. Alternatively, after phagocytosing large amounts of OxLDL, macrophages can also become yellow foam cells which secrete coagulation factors which encourage smooth muscle cell proliferation, adding to plaque mass, as well as chemokine tumor necrosis factor alpha (TNF-α) and metalloproteinases (MMPs). TNF-α contributes to atherogenesis by stimulating more endothelial cell activation and again feeding the positive feedback loop while MMPs contribute by breaking down the matrix of accumulated plaque and causing plaque rupture which can then trigger immune response and additional clotting as the rupture is exposed to blood in the arterial lumen. Figure 6 depicts the steps of atherosclerotic plaque formation.

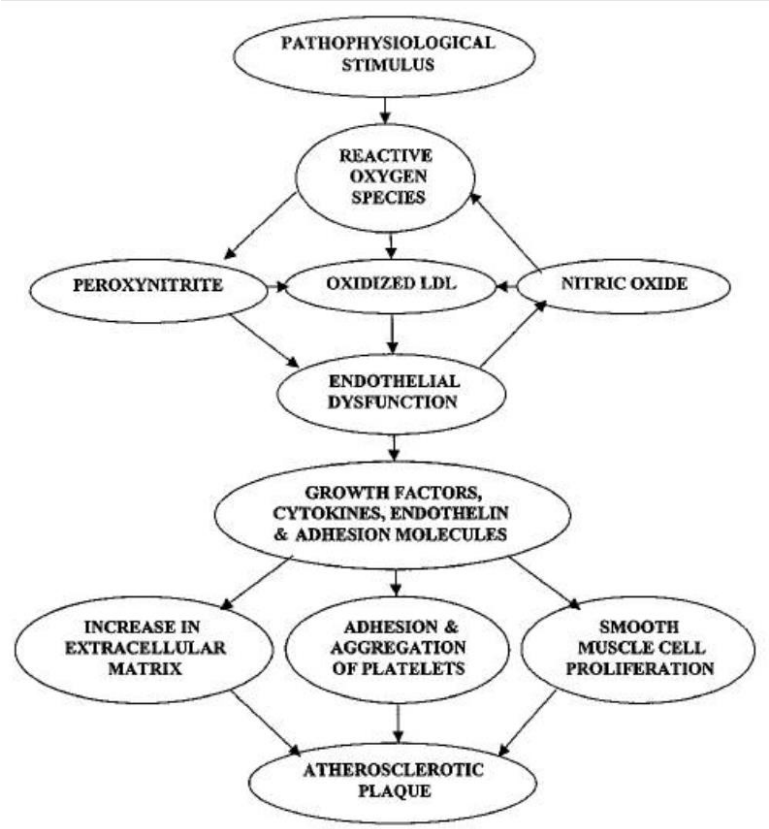

Figure 6. Diagram of Key Events in Atherosclerotic Plaque Formation [19].

2.2 Anti-Atherogenic Pathways

While atherosclerotic pathways are always stimulated via continuous shear in bifurcated arteries, the human body also has natural anti-atherosclerotic pathways which regulate atherosclerosis in healthy physiologic conditions. Anti-atherogenic pathways include high density lipoprotein (HDL) intervention, B cell activation, and T regulatory cell activation [23].

Reverse cholesterol transport involves the transport of LDL by HDL to the liver, regulating the amount of LDL in the arterial intima and therefore regulating the amount of LDL that is able to be oxidized and trigger endothelial cell activation. This can also be facilitated by macrophage activity [20].

B cell activation contributes to anti-atherogenic pathways as B cells produce anti-OxLDL antibodies which bind to OxLDL and inhibit their ability to be phagocytosed by macrophages, therefore inhibiting the macrophage's transition into a yellow foam cell and halting its potential to release MMPs and TNF-α which would induce more endothelial activation and plaque buildup. By stopping the phagocytosis of OxLDL, this mechanism also inhibits the OxLDL antigen presentation of the macrophage and in turn inhibits T helper cell binding and additional IFN-γ secretion from said T helper cell [24].

T regulatory cell activation serves as another anti-atherogenic pathway as these cells regulate T helper cell activity within atherogenic pathways. T regulatory cells play a role in atherosclerosis regulation by secreting TGF-β, which, in contrast to TNF-α which was seen in pro-atherogenic pathways, suppresses endothelial cell activation by stopping the secretion of IFN-γ by T helper cells. In doing so, TGF- β decreases the overall endothelial activation and counteracts the effects of increased shear stress, which continues to irritate endothelial carry on the positive feedback loop. TGF- β can be seen as a regulator of this loop.

2.3 Arteriogenesis

Arteriogenesis is the remodeling, widening, and growth of mature arteries and collateral vessels. Arteriogenic pathways often serve as loopholes which aid in revascularization when a vessel has a blockage. Typically, in a healthy bifurcated arterial structure, uniform blood pressure is observed on all sides of the structure [25]. Arteriogenesis can be triggered when an occlusion forms on one side of the bifurcation, resulting in a pressure gradient across the structure. Blockage on one side of the artery causes an increase of blood flow through the collateral vessel connecting both sides as a means of restoring

blood flow. Increased blood flow through the collateral means an increase in pressure as well as an increase in shear stress on the endothelial cells lining the inside of the vessel. As noted earlier, increased shear stress causes endothelial cell activation signified by initial adhesion protein recruitment, cytokine secretion, and macrophage recruitment. Macrophages recruited to the site of the collateral artery then release mitogens vascular endothelial growth factor (VEGF) and platelet-derived growth factor (PDGF) as well as MMP [22]. VEGF is responsible for the proliferation of endothelial cells while PDGF encourages smooth muscle cell proliferation. With the additional vessel matrix degradation due to MMP secretion, the collateral vessel is able to degrade and reassemble its new endothelial and smooth muscle cells into a wider vessel which can facilitate blood flow at a regulated pressure and velocity as arteriogenesis acts to protect against atherosclerosis.

2.4 Angiogenesis

Angiogenesis is the process by which new blood vessels grow from previously existing vessels via cell proliferation, sprouting, and migration. Two main types of angiogenesis are known as sprouting angiogenesis and splitting angiogenesis, also known as intussusception [26]. Angiogenesis is a major driving factor behind capillary growth and nutrient diffusion throughout the body. Angiogenic responses are directly related to oxygen levels found in the body.

Sprouting angiogenesis is heavily regulated by oxygen availability in the tissue as it is greatly triggered by hypoxic conditions. For some background, hypoxia inducible factor alpha (HIF-α) is a major driving force of sprouting angiogenesis. Under normal conditions it, along with the available partial pressure of oxygen, can be credited for

regulation of the expression of erythropoietin (EPO), which is responsible for stimulating red blood cell production, linking the importance of oxygen levels to red blood cell counts and vascularization [27]. The HIF family includes three oxygen regulated subdivisions, HIF-1α, HIF-2α, and HIF-3α, all of which have similar and intertwining responsibilities within multiple various pathways. These structurally homologous α subunits contain a common domain that facilitates DNA binding as well as specific domains that facilitate the heterodimerization of these units with their transcriptional partners, Arly hydrocarbon receptor nuclear translocator (Arnt). Arnt is a transcriptional factor of the β subdivision of the HIF family also known as HIF-β, including subunits Arnt, Arnt2, and Arnt3. Similar to HIF- α subunits, Arnt, Arnt2, and Arnt3 are structurally homologous to each other, however they do not all have adaptive responses to hypoxic conditions. While Arnt3, also known as BMAL, is involved with regulating circadian rhythms, Arnt2 is involved with neural development and some transcriptional response to hypoxia, it is Arnt that is mainly involved with hypoxic responses [11]. Under normoxic conditions, HIF activity is regulated by PHDI-3 via hydroxylation of HIF-α within the HIF-α oxygen dependent degradation domain where HIF-α degradation is fueled by oxygen and 2-oxoglutarate. The mechanism behind this involves binding to the E3 ubiquitin ligase complex which alters HIF-α such that it is targeted for proteasomal degradation [11]. The examination of the HIF family is important in this subject because of its shared presence in angiogenic and thermoregulatory pathways, which will be discussed in further sections.

It is in hypoxic conditions where low oxygen and 2-oxoglutarate levels result in the inability of HIF-α to be degraded. HIF-α accumulation resulting from a decrease in its

hydroxylation stimulates the translocation of HIF-α to the nucleus where it binds to Arnt, creating a HIF-α/HIF-β heterodimer which consequently binds to the hypoxia response element (HRE) in target gene promoters in DNA, inducing transcription. Co-activator proteins p300 and CBP supplement the HIF heterodimer in kickstarting the transcription of genes involved with hypoxia response [11]. In this way, angiogenesis can be a long-term adaptive response to local hypoxia as pro-angiogenic genes including VEGF, angiopoietin-2, Tie2, platelet derived growth factor (PDGF), basic fibroblast growth factor (bFGF), and monocyte chemoattractant protein-1 (MCP-1) are all activated, resulting in increased vascular permeability, endothelial cell proliferation, sprouting, migration, adhesion, and vessel formation [11]. These mechanisms are observed at the earliest stages of human vascularization where the low oxygen environment of the uterus drive hypoxia and HIF induced epithelial progenitor cell (EPC) differentiation and angiogenesis [11]. The expression of the VEGF gene specifically is a significant contributing factor in angiogenesis as VEGF stimulates the detachment and migration of endothelial cells from their parent vessel. Meanwhile, increases in MMPs facilitate the degradation of the vessel's extracellular matrix. MMP-2 specifically, a transcriptional target of HIF-1α, fuels the migration of endothelial cells in a hypoxic environment. Newly formed endothelial cells then adhere to each other to form a sprout, led by the tip followed by trailing stalk cells. Transmembrane receptors like VEGF-R2 on the tip cell are activated by VEGF and stimulate cell migration toward more hypoxic areas of tissue. To ensure that sprouts are not forming infinitely from all cells, delta-notch signaling aids in the specification of tip cell migration. Once VEGF binds to a tip cell via receptor tyrosine kinases (RTKs), ligand Delta-like-4 production is activated in the tip cell,

resulting in activation of notch receptors in neighboring stalk cells [10]. Notch receptor activation, in turn, inhibits VEGF-R2 production on stalk cells, making them less capable in binding to VEGF, migrating and creating more sprouts. This way, only tip cells are able to lead sprouting mechanisms [10]. Once endothelial tubing is formed by the previously mentioned sprouts, supporting cells of the vasculature like pericytes and smooth muscle cells are recruited to aid in the formation of the vessel's basement membrane. Macrophages are also recruited to the scene and aid in the connection of two tip cells and anastomosis of two separate vacuoles in two separate sprouts, creating one complete capillary tube to restore oxygen diffusion to the hypoxic tissue [11].

HIF also plays a role in short term hypoxia adaptation response by increasing oxygen levels via stimulation of vasodilatory enzymes like nitric oxide synthase (iNOS) which produces NO, causing short term vasodilation and increased blood flow [11]. This can be related to the human thermoregulatory responses in which blood vessels on the outer surface of the body constrict at low temperatures, to preserve core heat. Decreased blood flow to the peripheries means decreased oxygen which can be related to elevated HIF levels as have been observed as a response to cold exposure. This subject is discussed more thoroughly in further sections.

Splitting angiogenesis, or intussusceptive angiogenesis, is different from sprouting angiogenesis as it takes place inside the lumen of a vessel rather than towards the outer walls of the vessel [28]. Since splitting angiogenesis is a quite recent discovery in comparison to sprouting angiogenesis, its mechanisms are not as well understood, though it is said to be a faster and more efficient form of angiogenesis since it solely depends on rearrangement of pre-existing endothelial cells rather than their proliferation.

Intussusceptive angiogenesis is known to play a significant role in the development of vessel bifurcation and relies on VEGF for stimulation. This type of angiogenesis occurs when endothelial cells on opposing walls of a vessel come into contact with each other or if intralumenal sprouting occurs along the length of the vessel, creating a cylindrical pillar, splitting the lumen lengthwise into two lumens, and ultimately two initially parallel vessels [28].

2.5 The Hunting Response: Cold-Induced Vasodilation

The hunting response, also known as cold-induced vasodilation, refers to a phenomenon that has been observed in the toes, fingers, face, and even forearms in which cyclic vasodilation occurs after a short period of constriction in a cold environment. A general schematic of the hunting response in action can be seen in figure 7 below. Though little research has been done on the mechanism of the hunting response, it is thought be a protective mechanism to restore warmth to cold extremities in the form of increased blood flow [29].

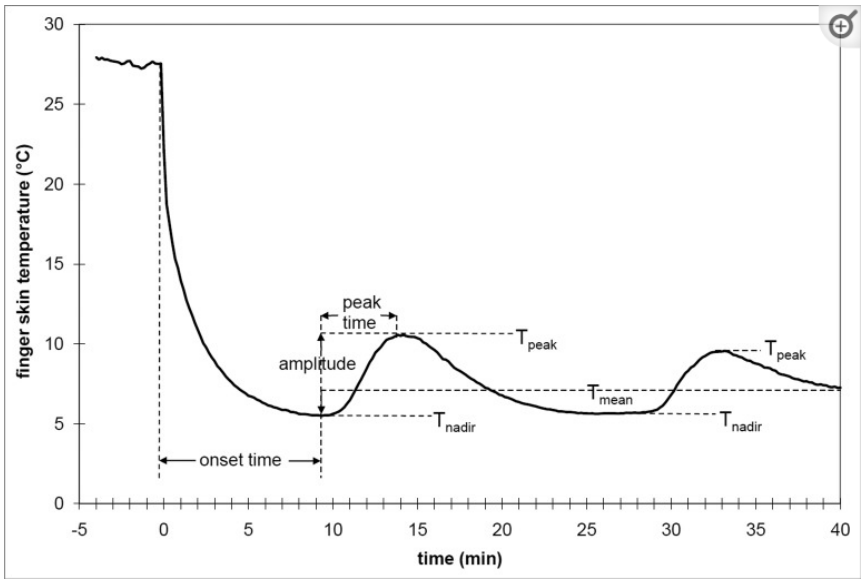

Figure 7. The hunting response, cycles of increased finger temperature with cyclic vasodilation [26].

This phenomenon is believed to be heavily correlated with arteriovenous anastomoses, which are shunts that allow blood to flow straight from the arterioles to venules while bypassing capillary beds. They typically jump into action in their thermoregulatory role in the unclothed human body an environmental temperature level of 26°C to 36°C [30]. Arteriovenous anastomoses are typically found in mucous and skin membranes with short complexions and thick, muscular, and densely innervated walls. Since they transport blood straight from the arterioles to venules, completely bypassing any capillary action, their sole transport function is that of heat transport, rather than the transport of substances [30]. Cold induced vasodilation has been theorized to involve cyclic and sudden dilation of arteriovenous anastomoses, as has been seen through ultrasound and laser-Doppler techniques [31]. This is supported by the notion that the most arteriovenous anastomose dense regions are also the regions where the hunting response typically occurs, with the exception of its observation in the forearms. Furthermore, the role of arteriovenous anastomoses in the hunting response is supported by noting that capillary

flow alone is too miniscule to create such a difference in fingertip temperature as is seen during the response. Figure 8 below models the general path of arteriovenous anastomoses in dilated and constricted states.

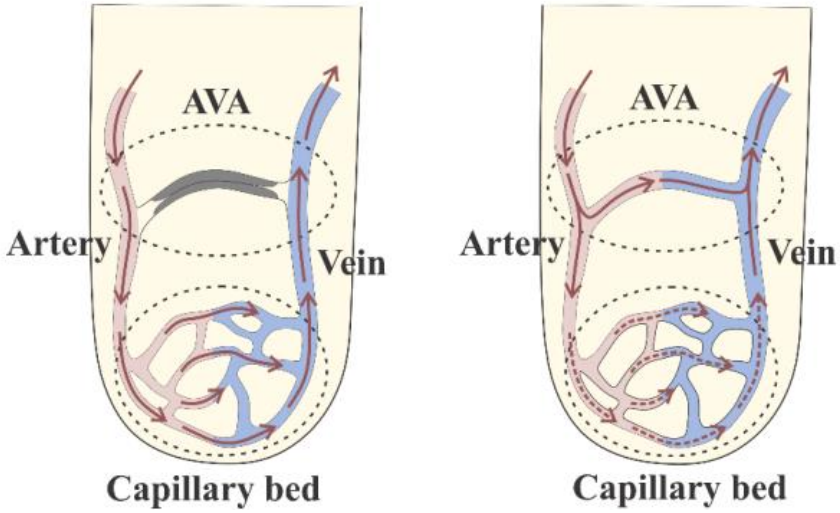

Figure 8. Arteriovenous Anastomoses (AVA) in the fingertips (constricted and dilated) [29].

Several studies have observed the effects of repeated local cold exposure on cold induced vasodilation to explain the exhibition of stronger hunting responses in populations who live in colder regions of the world. It is yet unclear whether these differences in cold exposure responses stem from acclimatization to the environment or genetic pre-disposition. Other studies observe differences in cold exposure responses in populations whose occupations involve exposure to cold temperatures. One study reviewing the trainability of cold induced vasodilation found that repeated cold exposure did not change the dynamic flow of blood within the peripheries over time [16].

2.6 Adiponectin

Adiponectin, produced by adipose tissue, is an adipokine that circulates in the blood associated with antidiabetic and anti-atherosclerotic pathways [32]. Several studies have observed the effects of cold exposure on plasma adiponectin levels, generally finding increasing trends and even significant increases in both male and female populations [32] [13]. Not only does adiponectin act as a regulator in areas including insulin resistance, inflammation, and atherosclerosis, it also contributes to the vascular homeostasis regulation with its involvement in endothelial signaling pathways. It is also important to note the loss of adiponectin in the state of insulin resistance as observed in patients with obesity, type 2 diabetes, and coronary artery disease, all of which can be associated with endothelial dysfunction through one pathway or another [33]. In terms of vascular homeostasis, adiponectin contributes by decreasing endothelial cell and macrophage expression of adhesive molecules that are typically recruited in response to shear stress and fuel atherosclerotic pathways via continuous endothelial cell activation. Endothelial dysfunction, as previously noted to be in association with hypertension, cardiovascular disease, insulin resistance, and more, can be heavily correlated with hypoadiponectinemia, or low plasma adiponectin levels [33]. Furthermore, adiponectin slows down atherosclerotic pathways by inhibiting the extracellular regulated kinase (ERK), which then inhibits proliferation and migration of smooth muscle cells which are critical in plaque formation. Adiponectin also binds directly to PDGF, stopping it from fueling even more smooth muscle cell proliferation and migration [34]. This protein can also be credited for the inhibition of the transcription factor known as nuclear factor kappa-light chain-enhancer of activated B cells (NF-kB), dramatically decreasing the activity of TNF-α (in turn decreasing endothelial activity) and adhesion molecule

expression [33]. As for relation to vasodilatory pathways, adiponectin is responsible for AMP kinase activation and nitric oxide production within endothelial cells, implying the correlation between low adiponectin levels and hypertension, as hypoadiponectinemia results in decreased nitric oxide production and availability, leading to impaired vasodilation capability and ultimately hypertension [18]. The formation of an oxLDL rich macrophage to a foam cell can also be inhibited by adiponectin driven inhibition of scavenger receptors on macrophage cell surfaces [34]. It should also be noted that healthy forearm blood flow peaks during reactive hyperemia have been correlated to adiponectin levels, implying the promising potential of adiponectin levels as a biomarker for endothelial dysfunction and risk of cardiovascular disease [34].

2.7 Cold Exposure and Resistance Training

With the increase of muscle fiber size which results from resistance training, the body compensates by inducing angiogenesis in order to maintain blood flow in a larger volume of muscle. This is done by maintaining capillary density within skeletal muscle. Many studies have looked into the effects of cold-water immersion on muscle recovery, but few have reviewed the angiogenic biomarkers which parallel it. One study found that men who recovered from resistance training using cold water immersion intervention showed a significantly larger number of capillaries per fiber as compared to men who participated in active recovery after the same schedule of resistance training [35]. They also saw a significant increase in VEGF in the cold-water immersion group while an increase in EVH1 domain containing protein 1, related to angiogenic sprouting, was observed in both groups. The study concluded that cold water immersion, as a form of recovery after resistance training changed angiogenic and fiber type altering responses to resistance therapy via altered microRNA, gene, and protein expression. Cold-water immersion is

also known to alter muscle fiber development after resistance training as different myosin heavy chain genes (MYHs) are observed among groups that recover with cold water immersion and groups that go forth with active recovery. Typically, resistance training has been known to encourage a shift from less fatigue resistant fiber phenotypes like type IIx to more resistant phenotypes like type IIa. Type II muscle fibers, found in higher ratios in power athletes are known as fast twitch fibers whereas type I fibers are slow twitch fibers which are more evident in endurance athletes [36]. Type IIx fibers have the highest twitch speeds but are also much more sensitive to fatigue as compared to type IIa fibers. The study mentioned above found that cold water immersion decreased the transition of type IIx fibers to type IIa fibers as compared to the active recovery test group [35]. A separate study examining rat soleus muscle found that cold-water exposure induced transition from type I to II muscle fibers [37].

2.8 VEGF and HIF Related to Cold Exposure

2.8.1 VEGF

It is quite clear that VEGF plays critical roles in the formation, development, growth, and functionality of blood vessels throughout the body in several pathways including arteriogenesis and angiogenesis from stages as early as embryonic development to stages much later in the human lifetime. As mentioned in earlier sections VEGF is an inducer of angiogenesis and the proliferation of endothelial cells in arteriogenic pathways. As a major driving factor with significant involvement in these pathways, its relationship with cold exposure makes it a good target of research in the field of cryotherapy. Several studies have observed increases in VEGF levels of populations after cold exposure interventions. One study in particular looked at the effects of cold exposure in on gene and protein expression of VEGF in male adult Wistar rats, specifically in the heart and

skeletal muscles [38]. In this study, rats were submerged in 18°C water up to shoulder height for one hour a day, five days a week, for twenty weeks and then tested for VEGF mRNA and protein in the heart, gastrocnemius, and soleus muscles. Researchers found significant increases in VEGF mRNA and protein expressions in groups undergoing chronic exposure, specifically in cardiac muscles. Conclusions suggested that the VEGF gene plays a major regulatory role in cardiovascular and skeletal muscle adaptation efforts to the cold by acting as a stimulator of angiogenesis and in turn thermogenesis [36]. Another study which observed the effects of cold exposure on both wild-type mice and UCP knockout mice which are more sensitive to cold temperatures, found that both displayed activation of angiogenesis in white and brown adipose tissue. VEGF, among other proangiogenic factors increased while angiogenesis inhibitors, like thrombospondin, downregulated [39]. It was also found that while hypoxia occurred in the wild-type mouse, it didn't occur in the UCP knockout mouse, rendering the angiogenic response as independent of hypoxia. Blocking VEGFR2 resulted in the halting of the angiogenic response and a decrease in non-shivering thermogenesis capabilities, while blockage of VEGFR1 did the opposite [37].

2.8.2 HIF

HIF also plays significant roles in blood vessel growth and regulation. More specifically, it is responsible for regulating cellular responses to hypoxia. Cold exposure can result in the upregulation of HIF-2α as it plays a role in cold-induced thermogenesis. It has even been said that a lack of adipocyte HIF-2α in the Western-diet contributes to the growing prevalence of atherosclerosis in the area as it allows for increased adipose ceramide levels, hindering the elimination of hepatocyte cholesterol and thermogenesis capabilities

[40]. Other studies found significant increases in HIF-1α signaling after cold exposure [41].

2.9 Effects of Cold Exposure on Endothelial Function

Endothelial function is highly dependent on the physiological balance of endothelin (ET) and nitric oxide produced in endothelial cells. ET, initially thought to be a vasoconstrictive peptide, has been found to have three isoforms, one of which, ET-1, is very involved in many cardiovascular diseases as the most potent mammalian vasoconstrictor discovered [42]. It has been found that extreme levels of cold exposure can result in increased ET-1 and could be associated with cold-induced hypertrophy. Another study investigating the effects of cold-water immersion after high-intensity interval training increased a marker for endothelial damage and suggested that this type of post-exercise recovery method may not be the best for endothelial health [43]. A different study also observing the effects of cold exposure on endothelial function found that smooth muscle endothelial cells had increased migratory capacity after cold exposure during a rewarming period, suggesting that cold stress in itself might not be pro-angiogenic in that aspect, but when accompanied by a rewarming period, could encourage angiogenesis [44].

CHAPTER 3

3. METHODS

3.1 Experiment Overview

This study was designed to observe the effects of acute cryotherapy interventions, specifically full body cold water immersion, on the human cardiovascular response, by measuring arterial compliance and cross-sectional area of the brachial artery of participants before, immediately after, and 30 minutes after partaking in 5-minute ice bath with non-invasive calibrated cuff plethysmography techniques. IRB approval was received from the Cal Poly IRB on Tuesday, May 30th, 2023. All testing took place on June 12th, 2023. 14 participants, 9 females and 5 males between the ages of 18-24 were tested after signing a written consent form. All participants were self-identified as not having any history of cardiovascular issues and were assumed to have healthy endothelial function. Materials used included a conventional folding ice bath typically used for athletic purposes, a thermometer, and the noninvasive calibrated cuff device described in later sections, and lots of ice.

Figure 9. Portable Ice Bath Used in the Experiment [45].

The experimental protocol was as follows. Participants were asked to sit on a chair with their right arm placed at rest on a table. The data collection for each participant included a baseline and five-minute hyperemia state recording. For baseline measurements, after the entire plethysmography device was turned on, the blood pressure cuff was wrapped around the right upper arm, pumped up to a pressure of 160 mmHg, and slowly released over a span of one minute until cuff pressure read 0 mmHg. Next, the same data was recorded in a state of reactive hyperemia. Participants sat in the same position and the blood pressure cuff was pumped up to 160 mmHg. The pressure was held at 160 mmHg for 5 minutes, collapsing the brachial artery and stopping blood flow to the limb. After five minutes the pressure was again released over a span of one minute until the cuff pressure read 0 mmHg. This pair of recording (baseline and hyperemia) were recorded once before any cold-water immersion intervention, once immediately after, and once 30

minutes after the cold plunge. The cold-water intervention protocol required that participants sat in an ice-water bath with their full body immersed up to the neck for 5 minutes. The water was kept at 10 - 15°C throughout all experimentation as this was found to be a common temperature range for ice bath therapy used by many professional athletes as a treatment for muscle injury and soreness. A protocol summary is provided below.

1. Cuff Plethysmography Recording Round 1 (6 minutes)
    a. Baseline 1
    b. Hyperemia 1
2. Participant Rest Time (20 minutes)
3. Cold-Water Immersion (5 minutes)
4. Cuff Plethysmography Recording Round 2 (6 minutes)
    a. Baseline 2
    b. Hyperemia 2
5. Participant Rest Time (25 minutes)
6. Cuff Plethysmography Recording Round 3 (6 minutes)
    a. Baseline 3
    b. Hyperemia 3

3.2 A Brief History of Calibrated Cuff Plethysmography

The device used in this study is based on the calibrated cuff plethysmography device designed and built by Dr. Michael Whitt in 1999. The measurement of arterial luminal area via calibrated cuff plethysmography requires the collection of the subjects arterial

pressure pulse around 1 Hz and a pump pressure pulse with a set stroke volume greater than 20 Hz [1]. The pressure area curve of an artery measuring from full arterial collapse to the point where the cuff pressure is 0 mmHg can provide the following information:

- Pump stroke volume (mL)
- Magnitude of pump pulse pressure at cuff (mmHg)
- Magnitude of arterial pulse pressure at cuff (mmHg)
- Magnitude of arterial pressure (mmHg)
- Mean cuff pressure at a time interval (mmHg)

The following arrangement of equipment, diagramed and developed in 1995 by Pilla, was used as inspiration by Dr. Whitt in his own upgraded device [1][46]. Equipment included a blood pressure cuff, pressure transducer, electronic circuit, pump, and two valves as shown below in figure 10.

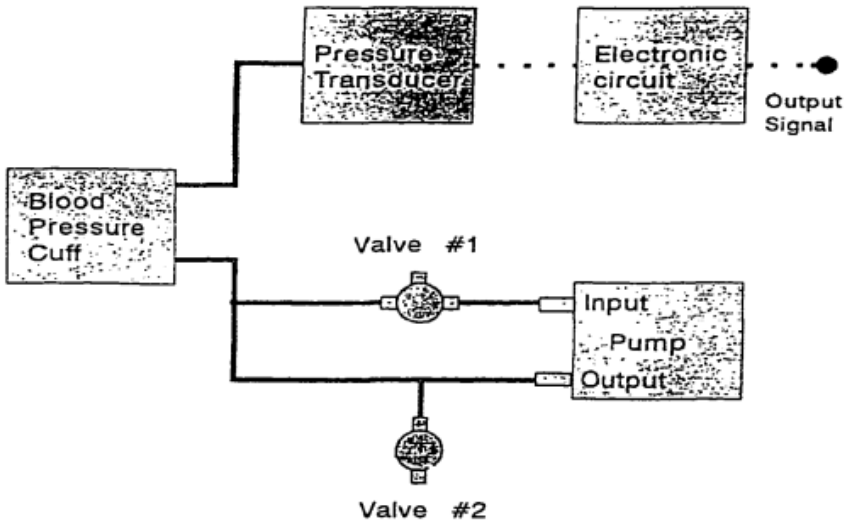

Figure 10. Schematic of Equipment (1995) [43].

This arrangement relied on the manual release of pressure from the inflated cuff in incremental drops of 3-5 mm Hg as well as the pumping of water through the pump for the measurement of volumetric flow and acquisition of pump stroke volume. Pump stroke volume was calculated using the following equation: $Pump\ Stroke\ Volume(mL) = \frac{Volume\ Water\ Pumped\ Over\ Time(\frac{mL}{sec})}{Pump\ Oscillation\ Frequency\ (Hz)}$ [1]. This model was deemed questionable because there was difficulty confirming the consistency of a constant pump output flow rate throughout the range total range of transmural pressures because of variance that was found to be related to the effect of the medium being used (water) on head pressure and output flow, limiting the accuracy of the pump stroke volume being calculated. Secondly, the incremental method of cuff pressure release that can be observed in figure 11 below left out critical data points in areas of steep pressure drops where data could not be collected.

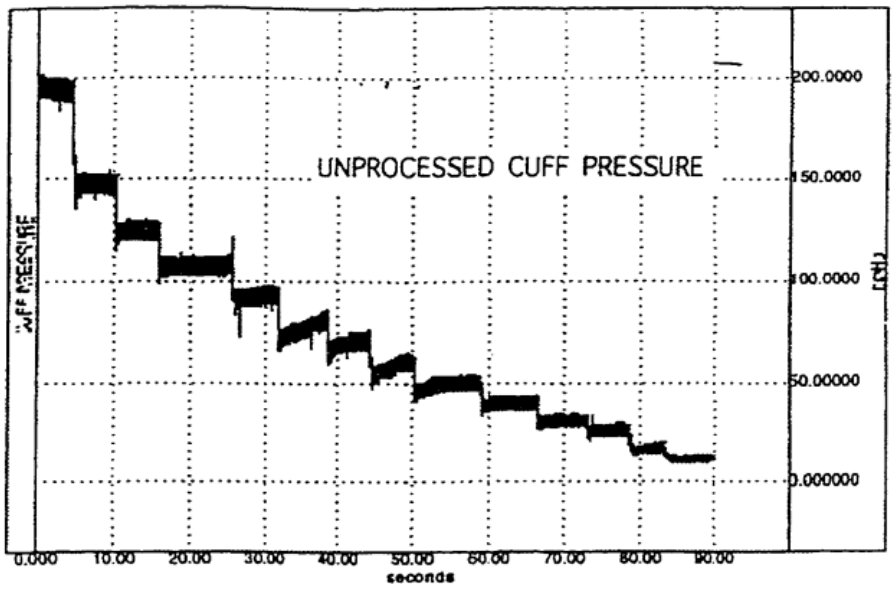

Figure 11. Data Acquisition Protocol by Pilla in 1995 [43].

The following iteration of the calibrated cuff plethysmography device designed by Dr. Whitt himself was finalized in 1999 and reaped many improvements that contributed to its greater effectiveness and accuracy. These improvements included the incorporation of a diaphragm pump with a lower pump curve, an inline flowmeter for recording of real time flow, and a new method of collecting data from the continuous pressure decline curve instead of collection from step like pressure drops as seen in the previous method, allowing for data collection at more pressure points [1].

3.3 New Calibrated Cuff Plethysmography Assembly

The model used in this study was assembled in a manner very similar to that of Dr. Whitt's. The new arrangement includes an adult sized blood pressure cuff, a pressure transducer, an amplifier, a very similar inline flowmeter, diaphragm pump, and power supply. These components were connected using mainly clear and solid black tubing, electrical tape, male and female luer locks, and multiple zip ties. It should be noted that the flowmeter used in the new schematic came from the manufacturer, Omega, and not Kobold, which manufactured the model used in Dr. Whitt's model. Regardless of this difference, the two models are physically exactly the same and have the same device housing. This notion justified the use of an equation supplied by Kobold to calculate the actual flow in the following sections. Figure 12 depicts the schematic of equipment used as well as the specific equipment models.

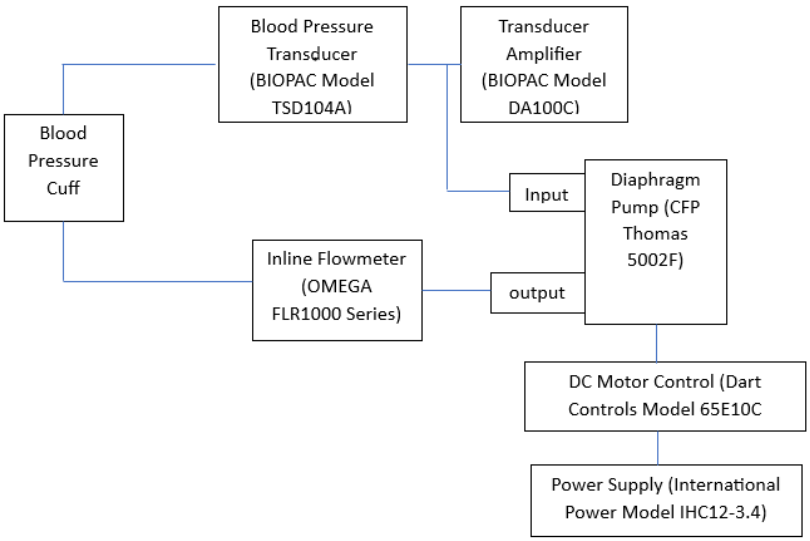

Figure 12. New Calibrated Cuff Plethysmography Schematic (2023).

In this model, the pump frequency of the diaphragm pump was able to be manually adjusted, per the incorporation of the DC motor control unit. The power supply diagramed in the bottom right of figure 11 serves the purpose of supplying the pump and motor control unit and also converting AC to DC for compatibility of the wall outlet to motor control. The outlet of the pump then pumps air through the inline flowmeter which is able to measure real time air flow rates in liters per minute. This air flows through the blood pressure cuff and makes its way to the blood pressure transducer. Setting the pump pulse to a frequency higher than that of a patient's arterial pulse frequency allows for the accurate measurement of and cyclic changes in cuff pressure and volumetric air flow resulting from the combination of both pulse frequencies.

3.4 Data Collection

Figure 13 below depicts the raw data measurements which were collected through use of the device. Cuff pressure was recorded as it slowly declined and volumetric flow through the system as a whole was recorded by the inline flowmeter throughout the entire data recording.

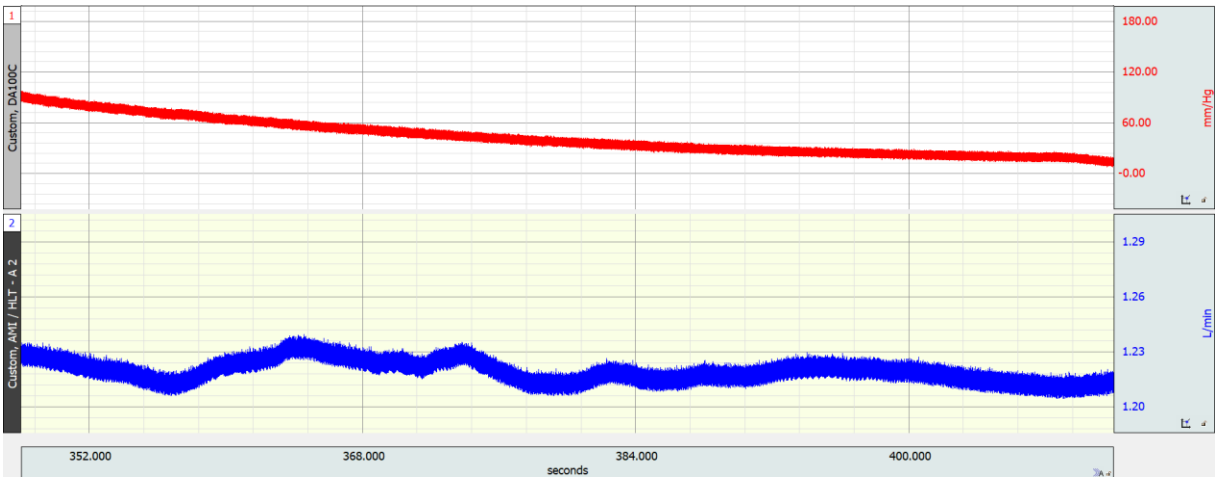

Figure 13. Recorded Pressure Drop and Volumetric Flow. The red plot represents the cuff pressure over time while the blue data represents the volumetric flow rate of the pump.

The pump pressure pulse and arterial pressure pulse can be distinguished from each other because they have different constant frequencies. While arterial blood pressure pulse energy typically stays under 10 Hz, pump pulse energy is set between 25 and 30 Hz [1]. In this study it was set at a sweet spot of approximately 27 Hz, as seen in the Fast Fourier Transform (FFT) pictured in Figure 14.

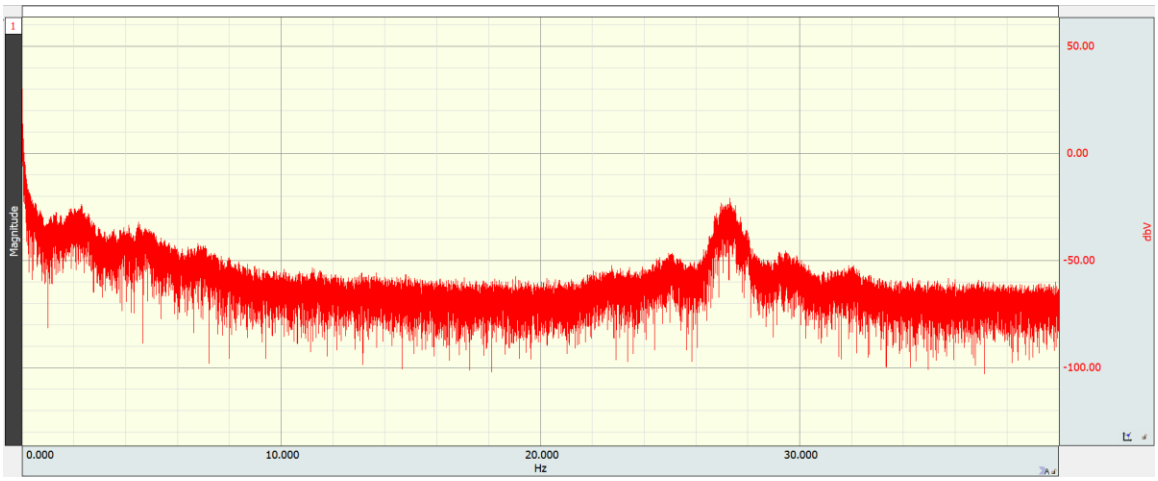

Figure 14. Fast Fourier Transform of Cuff Pressure Data Collection.

The pump pulse energy determined by the FFT was used to decide the limits of the band pass filter that would separate the pump calibration pulse. A band pass filter with upper and lower limits of the observed pump pulse energy ± 5 was applied to the original recorded cuff pressure curve. In the common case where the pump pulse energy was 27, for example, a band pass filter of 22-32 Hz was used to isolate the pump pulse. Figure 15 depicts a sample of pump pulses which were isolated during this study using a band pass filter of 22 - 32 Hz.

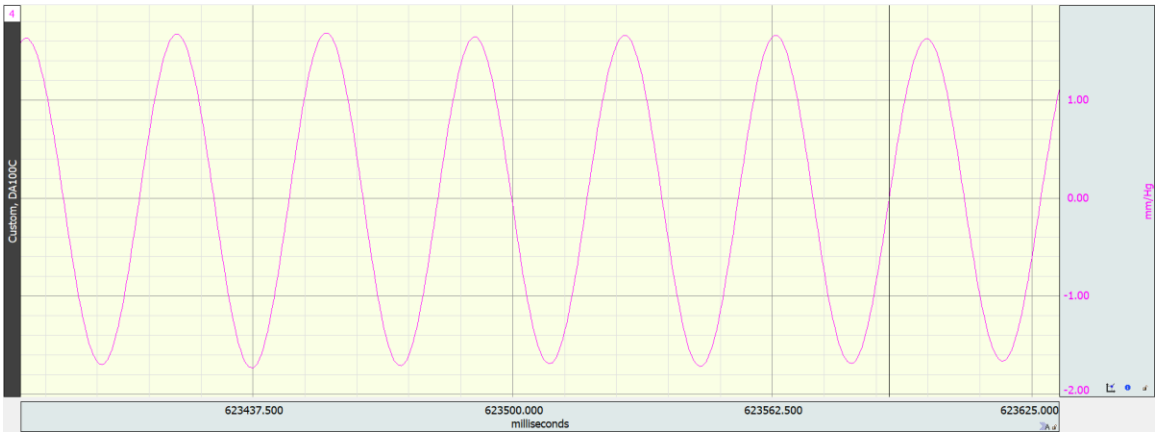

Figure 15. Pump Pulse – Band Pass Filter of 22-32 Hz.

Arterial pressure pulse was isolated by incorporation of a band pass filter with upper and lower limits of 0.5 and 5.0 Hz. The limits of the band pass were decided based on Dr. Whitt's past protocol and experiment comparing band pass filters 0.5-5.0 Hz and 0.5-10.0 Hz, which found that the 0.5-5.0 range was sufficient in the acquisition of arterial pulse magnitudes while also omitting unnecessary information about the constant pressure decline. Figure 16 depicts a sample of arterial pulses which were isolated during this study using a band pass filter of 0.5-5.0 Hz.

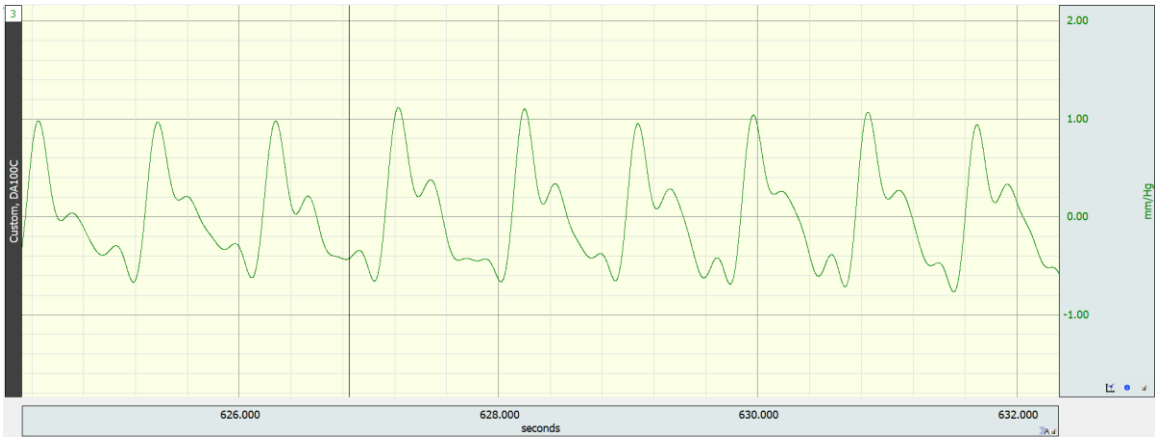

Figure 16. Arterial Pressure Pulse – Band Pass filter of 0.5 - 5.0 Hz.

An example of raw data and its associated band pass waveforms can be seen in figure 17 below.

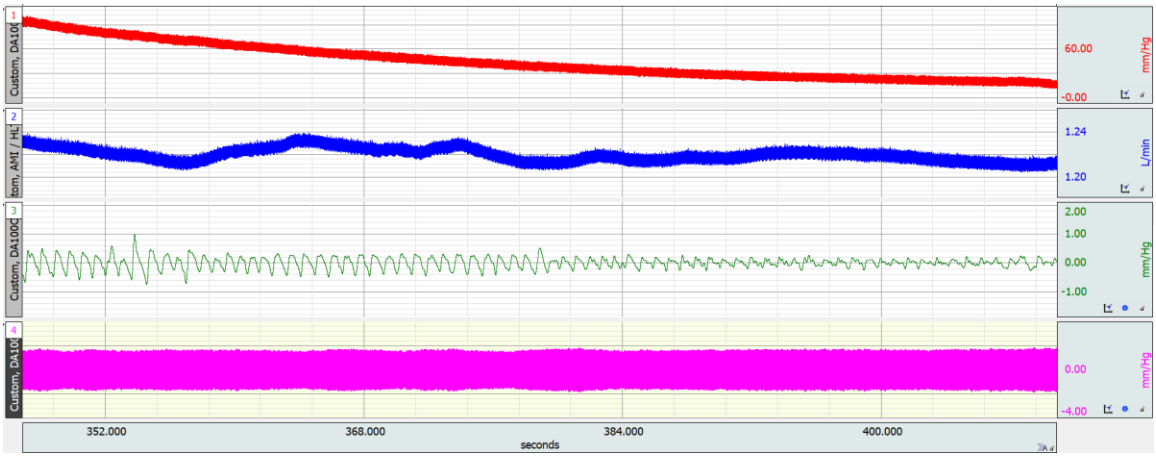

Figure 17. Example of Raw Data and Band Pass Waveforms (0.5–5.0 Hz and 22–32 Hz). The top channel represents raw cuff pressure data. The second channel from the top represents raw flowmeter data. The third channel represents arterial pressure pulses. The fourth channel represents pump pulse data.

Acqknowledge 5 software and a Biopac data collection system were used to analyze digital signals acquired through use of the pressure transducer. All data was analyzed on a Lenovo YOGA 730 laptop. The actual device used in this study is pictured below in Figure 18.

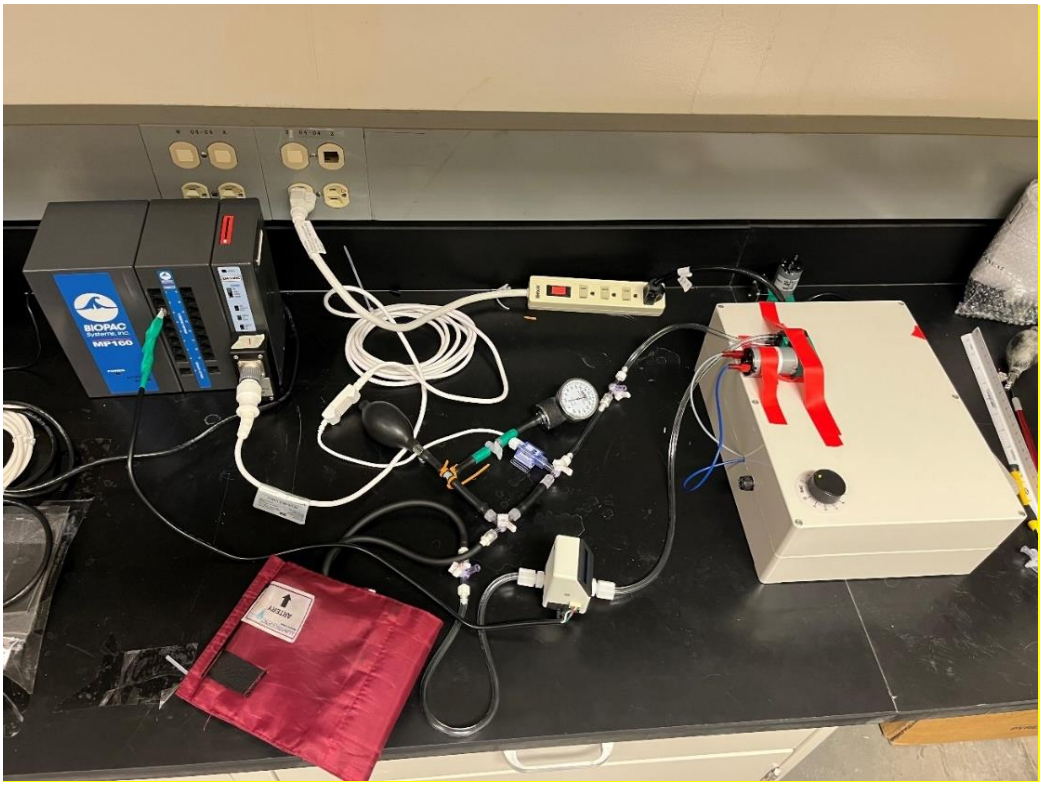

Figure 18. Calibrated Cuff Plethysmography Device Built and Used in Study.

3.5 Data Analysis

According to manufacturers, Kobold, output voltage of the flowmeter in use required correction because pressure changes with its housing could cause error [47]. For this reason, the following equation was supplied and used to calculate the "actual flow".

$$Indicated\ Flow\ (VDC) = Actual\ Flow\ \times \left(\sqrt[0.84]{\frac{P_{STP}(atm)}{P_{Hsg}(atm)}}\right)$$

Here, P_{Hsg} represents the pressure of the system while P_{STP} represents standard pressure, or 0 mm Hg cuff pressure. The resulting value was then used to compute the pump stroke volume using the following relationship [1].

$$Pump\ Stroke\ Volume\ (at\ 0\ mmHg\ cuff\ pressure) = \frac{\text{Actual Flow } at\ STP\ Value}{Observed\ Pump\ Frequency}$$

Boyle's Law, $P_1V_1 = P_2V_2$, was used to adjust the calculated pump stroke volume to consider the total system pressure, giving the following relationship [1]. It should be recalled that the diaphragm pump in use pumps air.

$$Pump\ Stroke\ Volume\ at\ System\ Pressure = \frac{760\ mmHg \times Pump\ Stroke\ Volume\ at\ 0\ mmHg\ Cuff\ Pressure}{System\ Pressure}$$

These values were calculated for each arterial pulse collected at each cuff pressure. Transmural pressure was taken to be the arterial blood pressure, set to be approximately 85mmHg minus the recorded cuff pressure. This assumed that each participant had a mean arterial pressure of 85 mmHg, as a healthy mean arterial pressure is said to be anywhere between 70 mmHg – 100 mmHg [48]. Key elements which were acquired through the oscillometric process included the following:

- Arterial pressure pulse measured at the cuff (dP_{artery}) in mmHg
- Pump pressure pulse measured at the cuff (dP_{pump}) in mmHg
- Pump stroke volume at total system pressure (dV_{pump}) in ml
- Systolic and diastolic blood pressures in mmHg
- Transmural arterial pressure in mmHg

After collection of these values, the following equation was used to calculate arterial volume compliance, $(\frac{dV}{dP})_{artery,}$ at each cuff pressure [1].

$$(\frac{dV}{dP})_{artery} = (dP_{artery\ at\ cuff})[\frac{\left(\frac{dV}{dP}\right)_{pump\ at\ cuff}}{Systolic\ Pressure - Diastolic\ Pressure}]$$

The term $\left(\frac{dV}{dP}\right)_{pump\ at\ cuff}$ is cuff compliance. The numerator of the term, (dV), is found by taking the pump flowmeter rate per second (ml/s) and dividing it by the frequency of the pump (Hz). The denominator of the term (dP) is found by determining the magnitude of pump pulses associated with the time of the arterial pulse. Typically, it is expected that cuff compliance would increase as cuff pressure decreases. In this study, however, it was seen that cuff compliance was slowly decreasing as the cuff pressure was dropped. More information on why this result may have been seen can be found in the discussion of limitations section of this paper. The plot in Figure 19 below depicts how cuff compliance changed as cuff pressure changed.

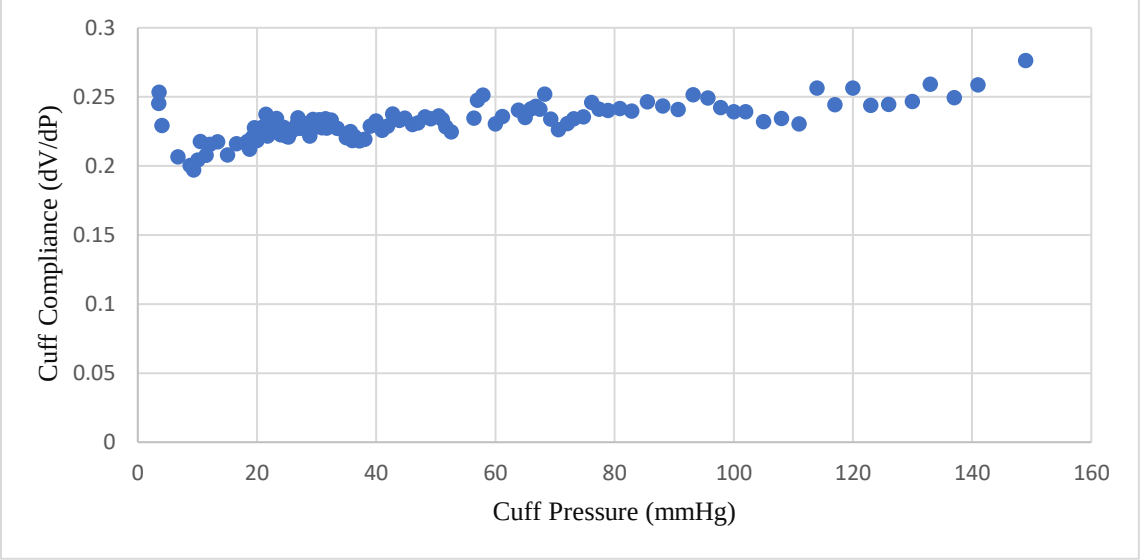

Figure 19. Cuff Compliance vs. Cuff Pressure. This figure plots the cuff compliance as cuff pressure changed, showing the variability in cuff compliance in a range of different cuff pressures.

To find arterial area compliance, $(\frac{dA}{dP})_{artery}$, the arterial volume compliance was normalized by considering the length of the artery being observed, which in this case was taken to be equal to the cuff length at 13.5 cm. This was done through the use of the equation below. Arterial area compliance was calculated at each cuff pressure.

$$\left(\frac{dA}{dP}\right)_{artery} = \frac{\left(\frac{dV}{dP}\right)_{artery}}{Cuff\ Length}$$

Arterial area compliance was calculated at each cuff pressure recorded and was plotted against the transmural arterial pressure. This process was done for all 14 participants 30 minutes before, immediately after, and 30 minutes after 5-minute full body, cold water immersion. Figures 19, 20, and 21 shown below depict this relationship as plotted for a female participant (Participant: F3) as collected 30 minutes before cold water immersion intervention, immediately after, and 25 minutes after.

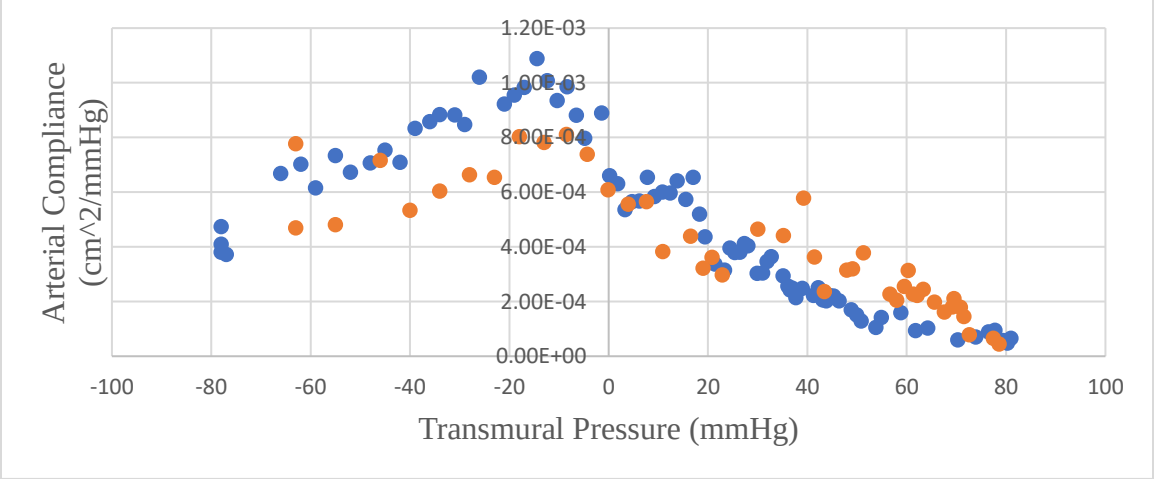

Figure 20. Arterial Area Compliance vs. Transmural Arterial Pressure of Female Participant (F3) 30 Minutes Before Cold-Water Immersion. Blue data points represent baseline measurements while orange data points represent measurements collected during 5-minute reactive hyperemia.

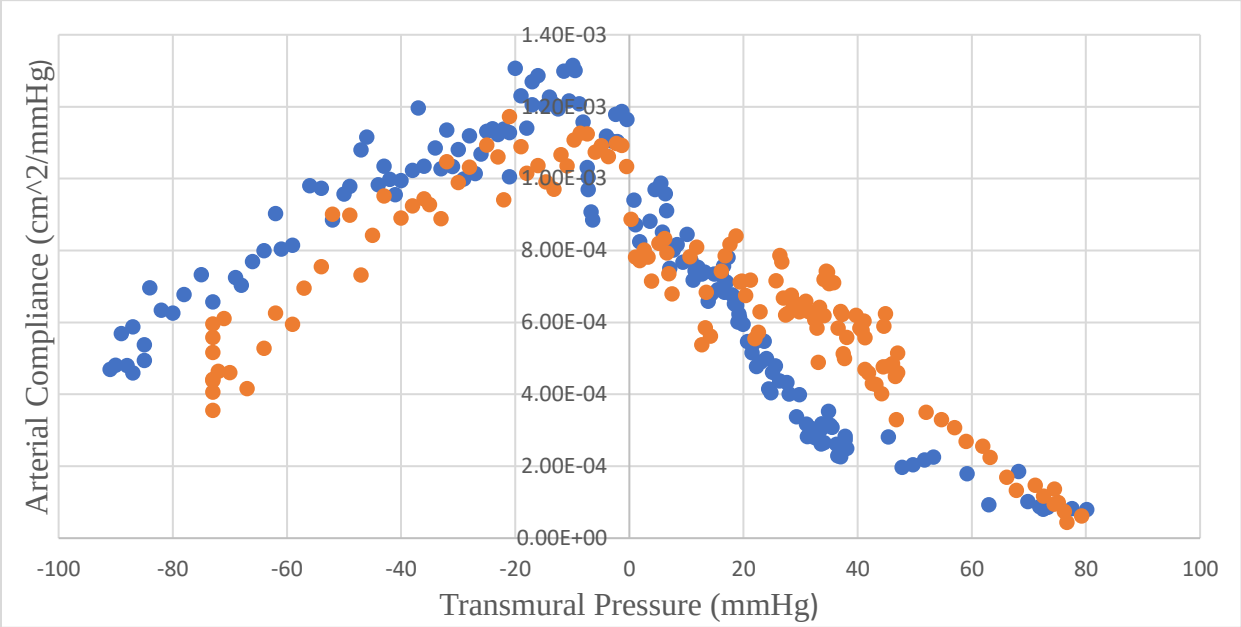

Figure 21. Arterial Area Compliance vs. Transmural Arterial Pressure of Female Participant (F3) Immediately After Cold-Water Immersion. Blue data points represent baseline measurements while orange data points represent measurements collected during 5-minute reactive hyperemia.

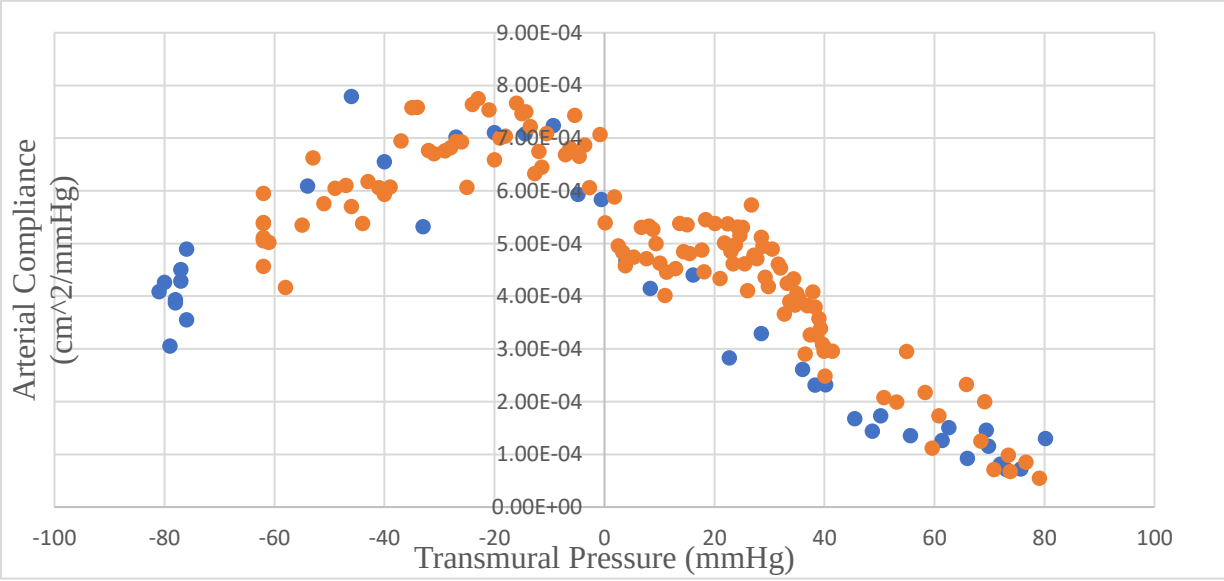

Figure 22. Arterial Area Compliance vs. Transmural Arterial Pressure of Female Participant (F3) 30 Minutes After Cold-Water Immersion. Blue data points represent baseline measurements while orange data points represent measurements collected during 5-minute reactive hyperemia.

Next, the arterial area compliance curve was integrated for each plot with respect to transmural pressure, giving the arterial luminal area at each cuff pressure. This relationship was also plotted, as seen in Figures 22, 23, and 24 (collected from Participant F2) to show differences in lumen area between baseline and hyperemic circumstances under different conditions (before/after cold water immersion).

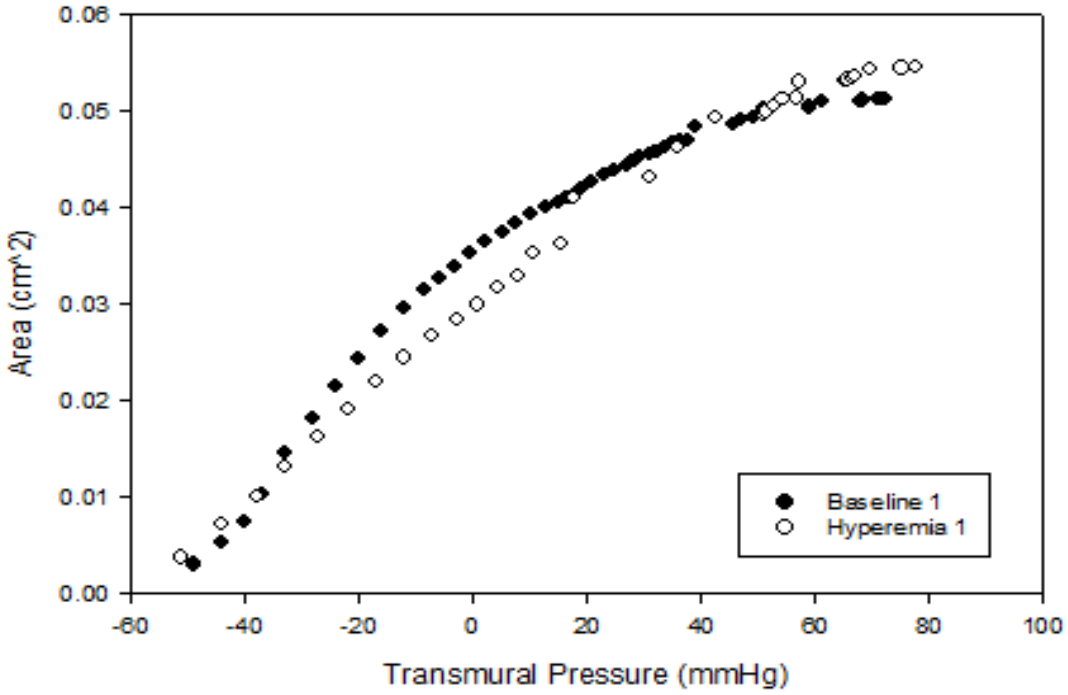

Figure 23. Arterial Lumen Area vs. Arterial Transmural Pressure of Female Participant (F2) 30 Minutes Before Cold-Water Immersion. Black data points represent baseline measurements while white data points represent measurements collected during 5-minute reactive hyperemia.

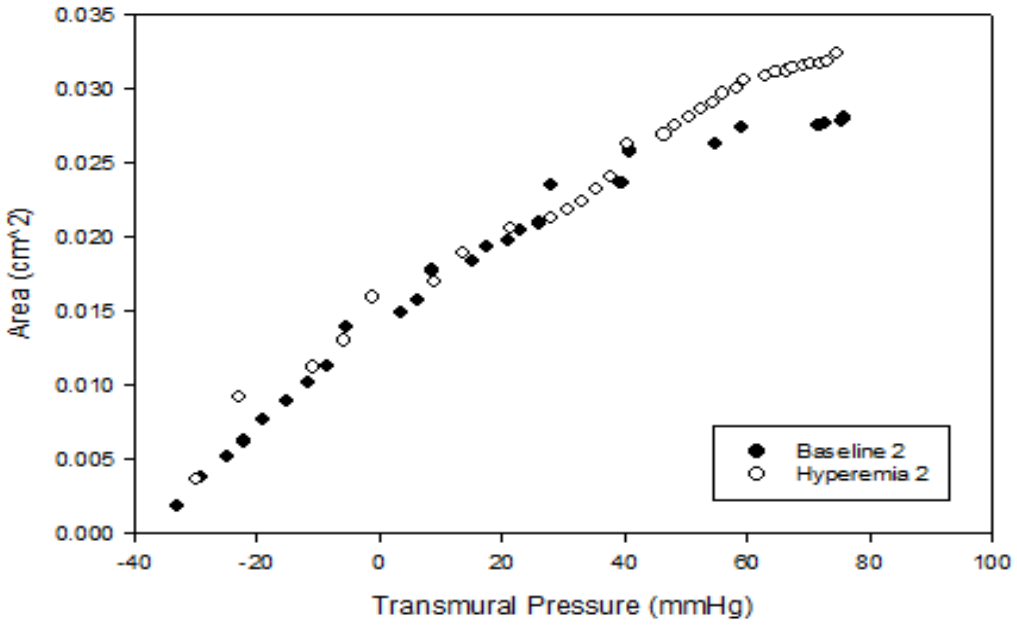

Figure 24. Arterial Lumen Area vs. Arterial Transmural Pressure of Female Participant (F2) Immediately after Cold-Water Immersion. Black data points represent baseline measurements while white data points represent measurements collected during 5-minute reactive hyperemia.

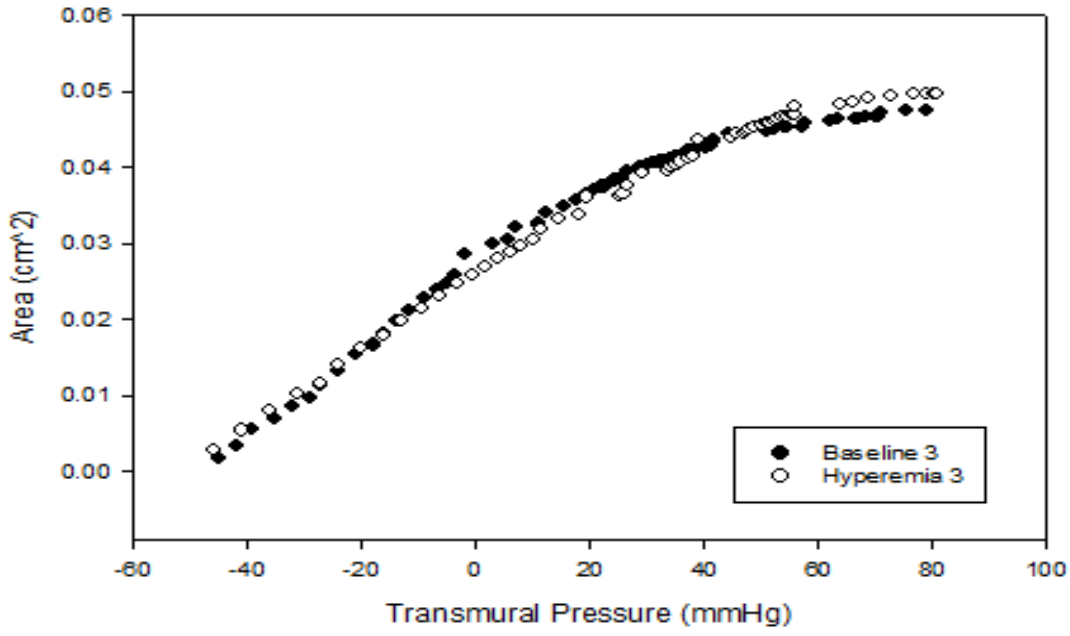

Figure 25. Arterial Lumen Area vs. Arterial Transmural Pressure of Female Participant (F2) 30 Minutes After Cold-Water Immersion. Black data points represent baseline measurements while white data points represent measurements collected during 5-minute reactive hyperemia.

Since these plots were integrated from the completes range of transmural pressures collected, they were then integrated from 0 mmHg to 80 mmHg, as it is known that the positive transmural pressure region is where differences in compliance can typically be seen during reactive hyperemia. A modified Maxwell model used in a different study approximated the different contribution of collagen, elastin, and smooth muscle in the mechanical responses of the arterial wall at different pressure ranges [49].

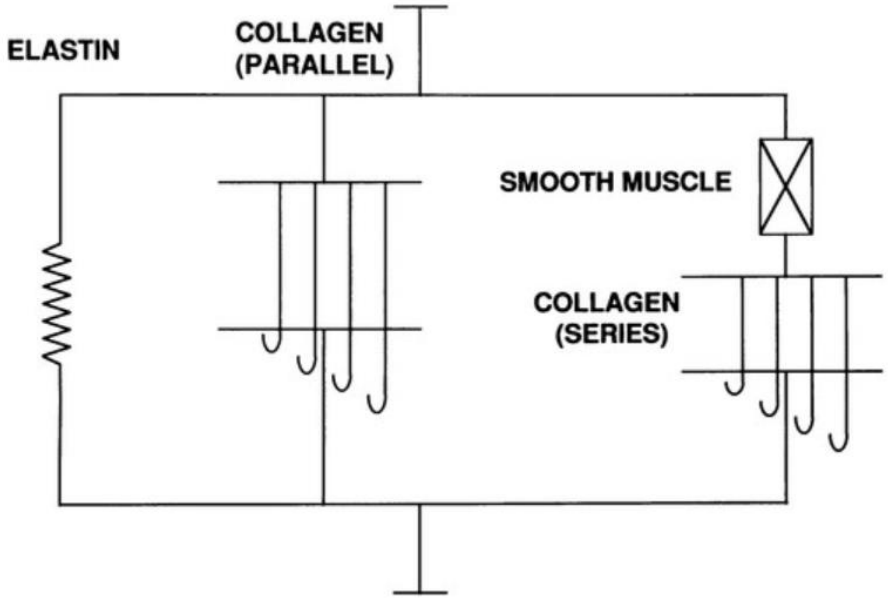

Figure 26. Modified Maxwell Model of Brachial Artery Wall [48].

Within the positive transmural pressure range, smooth muscle activity drives arterial compliance, which is why the 0 mmHg – 80 mmHg range was selected as the range of interest in this study. Since that is where it is expected that differences between hyperemia and baseline curves will be observed. This eliminated the compounding of noise from the negative transmural pressure range and shows, more clearly and accurately, the differences in arterial lumen area as the arterial transmural pressure

increases from 0 mmHg to approximately 80 mmHg. This integration was also plotted, as seen in Figures 26, 27, and 28 (collected from Participant F2) to show differences in lumen area between baseline and hyperemic circumstances under different conditions (before/after cold water immersion). All curves associated with each participant can be found in Appendix A.

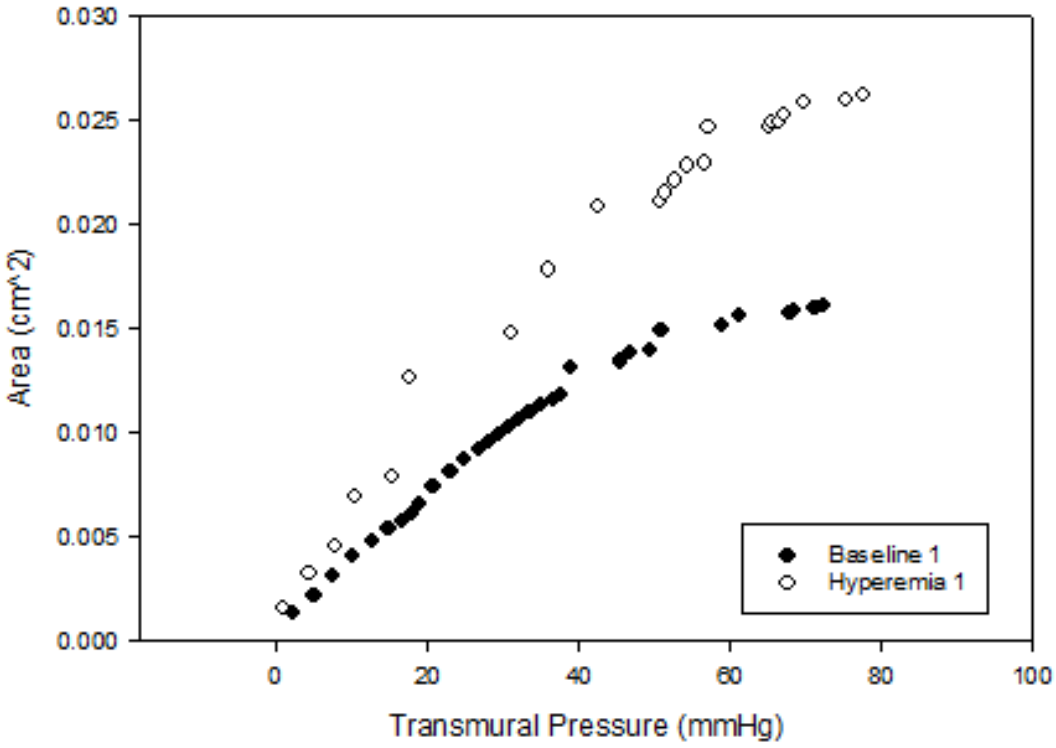

Figure 27. Arterial Lumen Area vs. Arterial Transmural Pressure of Female Participant (F2) 30 Minutes Before Cold-Water Immersion. Black data points represent baseline measurements while white data points represent measurements collected during 5-minute reactive hyperemia. Integrated from 0 mmHg to 80 mmHg transmural pressure.

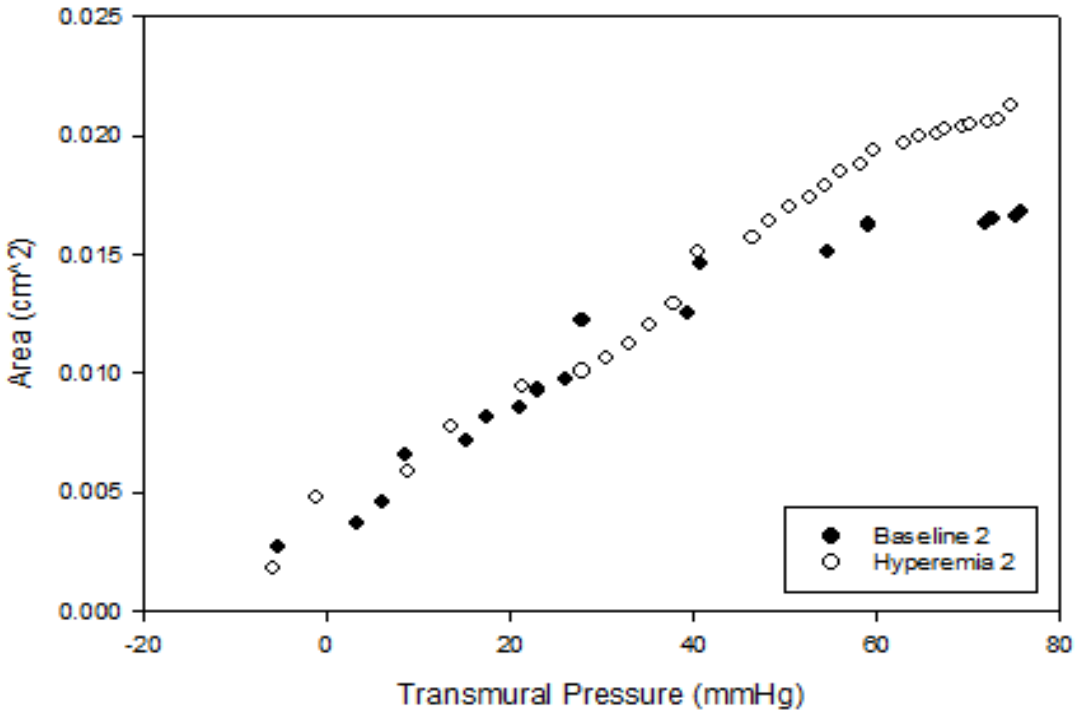

Figure 28. Arterial Lumen Area vs. Arterial Transmural Pressure of Female Participant (F2) Immediately After Cold-Water Immersion. Black data points represent baseline measurements while white data points represent measurements collected during 5-minute reactive hyperemia. Integrated from 0 mmHg to 80 mmHg transmural pressure.

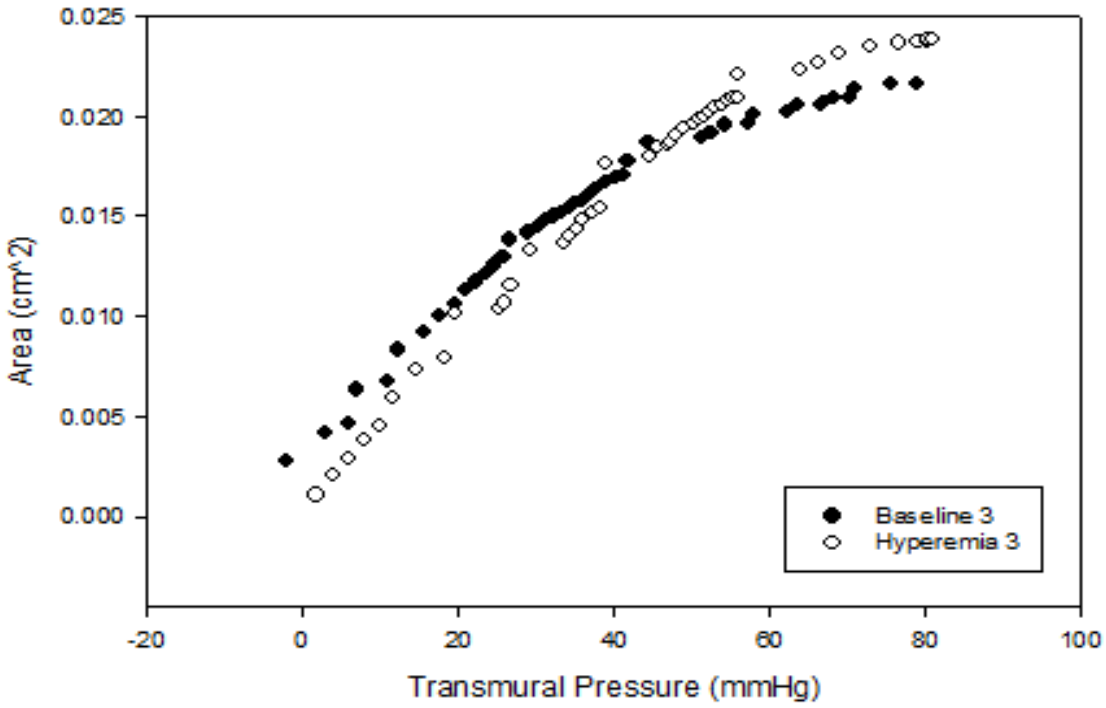

Figure 29. Arterial Lumen Area vs. Arterial Transmural Pressure of Female Participant (F2) 30 Minutes After Cold-Water Immersion. Black data points represent baseline measurements while white data points represent measurements collected during 5-minute reactive hyperemia. Integrated from 0 mmHg to 80 mmHg transmural pressure.

The total area under each arterial area compliance curve for each data collection (six per participant), was calculated by taking the integral of the curve from ranges 0-75 mmHg, 20-75 mmHg, and 50-75 mmHg. This includes the areas under arterial area compliance curves at baseline and 5-minute reactive hyperemia conditions 30 minutes before cold water immersion intervention, immediately after, and 30 minutes after. From here on, these recordings will be referred to as Baseline 1, Hyperemia 1, Baseline 2, Hyperemia 2, Baseline 3, and Hyperemia 3 where Baseline 1 and Hyperemia 1 represent measurements recorded 30 minutes prior to the 5 minutes cold water immersion intervention, Baseline 2 and Hyperemia 2 represent measurements recorded immediately after the intervention, and Baseline 3 and Hyperemia 3 represent measurements recorded 30 minutes after the

intervention. Total area under each curve from integration ranges on 0-75 mmHg, 20-75 mmHg, and 50-75 mmHg were recorded. Next each participant's data recordings (3 per participant, each including a baseline and hyperemia recording) was scored. The score represents the percent difference in the area under the arterial area compliance curve measured at baseline and hyperemia for each of the three measuring rounds (30 minutes before intervention, immediately after, and 30 minutes after). The following equation, where $A_{Hyperemia}$ represents the area under the baseline arterial area compliance curve and $A_{Baseline}$ represents the area under the reactive hyperemia arterial compliance curve, was used in the scoring of each measurement round.

$$Score = \frac{A_{Hyperemia} - A_{Baseline}}{A_{Baseline}} \times 100$$

3.6 Statistical Analysis

One way ANOVA tests were performed to compare the area under each curve between males and females and across all test rounds. Tukey-Kramer tests were also performed for comparisons of all pairs. The same was done again for the comparison of scores between male and female participants in each data recording round. All categories were tested to find any statistically significant differences among groups and trials within groups.

3.7 Device Validation Testing

The calibrated cuff plethysmography setup used in this study was validated by use of a noncompliant steel cylinder and a clear medical IV bag and syringe. All equipment was set up as it would have been during data collection except the cuff was wrapped around a steel cylinder with a diameter of approximately 5 inches. A clear medical IV bag filled with water and no air bubbles was placed in between the fastened cuff and the cylinder.

Figures 29 and 30 below depict a general schematic of the arrangement of equipment for validation as well as a picture of the actual setup which was used.

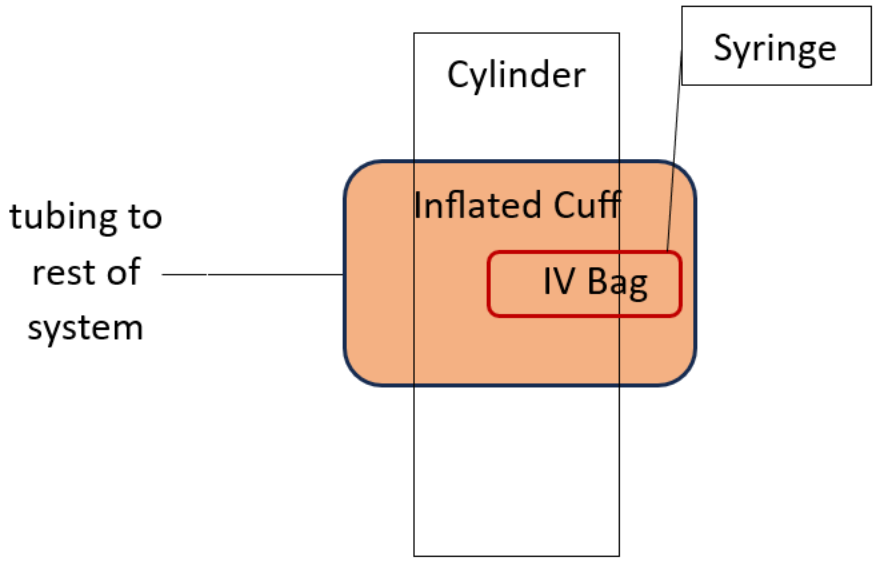

Figure 30. Schematic of Equipment Used During Validation Testing.

Figure 31. Steel Cylinder and Medical IV Bag Used for Device Validation.

Next, the cuff was pumped up and kept at a constant pressure such that it firmly surrounded the cylinder and IV bag, the device was turned on, and data was collected as approximately 2 milliliters of additional water was injected into the IV bag using a syringe that was attached via a stopcock, creating a slight pressure change in the cuff which can be observed in figure 31 below.

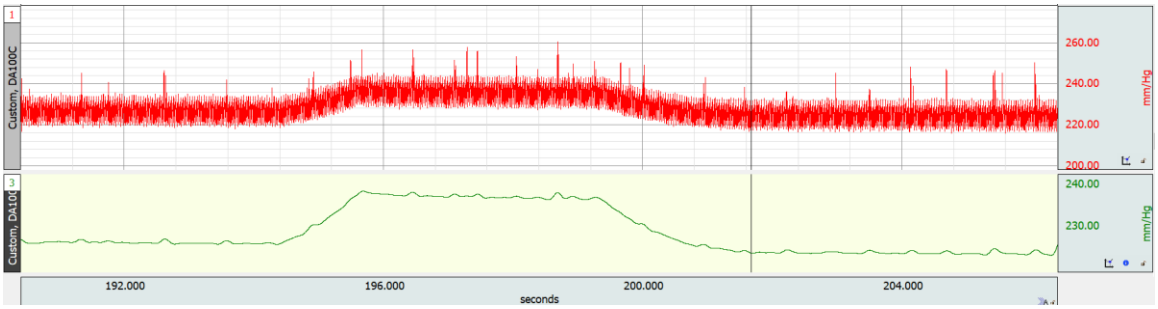

Figure 32. Cuff Pressure Change Observed as 2 mL of Water is Injected and Removed from the IV Bag. The red plot above represents the cuff pressure as it increases and decreases with **additions of water. The green plot below represents changes in pump pressure pulse.**

Changes in cuff pressure as well as pump pulse, frequency, and flowmeter measurements were all recorded and used to calculate the volumetric difference in accordance with changes in the aforementioned recorded measurements. Percent error between the calculated change in volume and the actual volume of water injected into the system was then recorded. This process was repeated at multiple constant cuff pressure ranges at pump pulse frequencies of 24 Hz and 28 Hz to determine the setting of the device which reap the most accurate results. Tables 1 and 2 below show the results of the validation testing at pump frequencies of approximately 24 Hz and 28 Hz respectively. It was observed that a pump pulse frequency of approximately 28 Hz showed the most accurate readings.

Table 1. Device Validation and Measurement Error Recorded at 28Hz Pump Frequency.

Cuff Pressure Range (mmHg)	Actual Volume Increase (mL)	Calculated Volume Increase (mL)	Error (%)
40-50	2	1.858	-7.065
40-50	2	1.847	-7.6455
40-50	2	1.807	-9.62
90-100	2	1.955	-2.247
90-100	2	1.947	-2.639
90-100	2	2.101	5.092
130-140	2	2.131	6.5747
130-140	2	2.100	5.033
130-140	2	2.005	0.254
190-200	2	1.940	-2.995
190-200	2	2.018	0.908
190-200	2	2.190	9.534
230-240	2	2.0111	0.556
230-240	2	1.9965	-0.172
230-240	2	2.100	5.041

Table 2. Device Validation and Measurement Error Recorded at 23-24 Hz Pump Frequency.

Cuff Pressure Range (mmHg)	Actual Volume Increase (mL)	Calculated Volume Increase (mL)	Error (%)
40-50	2	2.119	5.987
40-50	2	2.073	3.671
40-50	2	2.020	1.009
90-100	2	1.902	-4.85
90-100	2	1.972	-1.369
90-100	2	2.0747	3.738
130-140	2	2.0003	0.015
130-140	2	2.1801	9.003
130-140	2	2.422	21.1222
190-200	2	3.325	61.76
190-200	2	3.177	58.856
190-200	2	2.066	3.309
240-250	2	2.053	2.681
240-250	2	2.861	43.079
240-250	2	2.662	33.096

CHAPTER 4

4. RESULTS

4.1 Data Result Summary

The following tables display the areas under each arterial area compliance curve for all recordings for all participants. Participants are grouped based on biological sex and are referred to by their assigned code. M1-M5 are representative of the male participants while F1-F9 are representative of the female participants. Scores representing differences in area below the curve between reactive hyperemia and baseline recordings are also recorded in tables 3-8 below. Rounds 1, 2, and 3 are representative of the recordings taken 30 minutes before cold water immersion, immediately after cold water immersion, and 30 minutes after cold water immersion.

Table 3. Areas Under Baseline and Reactive Hyperemia Arterial Area Compliance Curves and Scoring Per Male Participant From 0 mmHg – 75 mmHg Transmural Pressure.

	Round 1			Round 2			Round 3		
	30 min Before Cold Water Immersion			Right After Cold Water Immersion			30 min After Cold Water Immersion		
Participant	Baseline 1	Hyperemia 1	Score	Baseline 2	Hyperemia 2	Score	Baseline 3	Hyperemia 3	Score
M1	0.03847782	0.037173679	-3.389333708	0.029161912	0.03446559	18.18700479	0.057215687	0.068911028	20.440794
M2	0.04389506	0.0589053	34.19575042	0.036488777	0.04003401	9.715953654	0.05006687	0.059445131	18.731472
M3	0.01905695	0.029163347	53.03262499	0.014840689	0.025355442	70.85083399	0.03053569	0.035119401	15.010994
M4	0.02195721	0.030557653	39.16909137	0.018842677	0.02495047	32.41467804	0.037724773	0.040416391	7.1348816
M5	0.03987983	0.04484301	12.44534811	0.047092716	0.043979575	-6.610664988	4.01E-02	4.90E-02	22.234043
Average	0.03265337	0.040128598	27.09069624	0.029285354	0.033757017	24.9115611	0.043127035	0.050579642	16.710437

Table 4. Areas Under Baseline and Reactive Hyperemia Arterial Area Compliance Curves and Scoring Per Male Participant From 20 mmHg – 75 mmHg Transmural Pressure.

	Round 1			Round 2			Round 3		
	30 min Before Cold Water Immersion			Right After Cold Water Immersion			30 min After Cold Water Immersion		
Participant	Baseline 1	Hyperemia 1	Score	Baseline 2	Hyperemia 2	Score	Baseline 3	Hyperemia 3	Score
M1	0.02225288	0.021148186	-4.964272426	0.015316512	0.021313537	39.15398354	0.03270507	0.044093513	34.821642
M2	0.02421287	0.041986049	73.40384189	0.020702239	0.022758974	9.934842091	0.033196036	0.040875567	23.133882
M3	0.01073364	0.018626263	73.53173621	9.12E-03	0.016122247	76.68719884	0.017168197	0.020893435	21.698483
M4	0.01199933	0.022501935	87.52662158	0.011680688	0.016117613	37.98512898	0.01898326	0.022375459	17.869424
M5	0.01941547	0.026475499	36.36293086	0.022328596	0.030932615	38.53362915	2.08E-02	3.33E-02	60.28552
Average	0.01772284	0.026147587	53.17217162	0.015830555	0.021448997	40.45895652	0.024562947	0.032303346	31.56179

Table 5. Areas Under Baseline and Reactive Hyperemia Arterial Area Compliance Curves and Scoring Per Male Participant From 50 mmHg – 75 mmHg Transmural Pressure.

	Round 1			Round 2			Round 3		
	30 min Before Cold Water Immersion			Right After Cold Water Immersion			30 min After Cold Water Immersion		
Participant	Baseline 1	Hyperemia 1	Score	Baseline 2	Hyperemia 2	Score	Baseline 3	Hyperemia 3	Score
M1	5.09E-03	7.09E-03	39.20415198	4.54E-03	6.36E-03	40.03653147	9.42E-03	0.012724828	35.040822
M2	7.09E-03	0.012115728	70.77122807	5.11E-03	7.34E-03	43.57649157	6.91E-03	0.011234846	62.701681
M3	2.13E-03	5.38E-03	153.1316718	3.26E-03	4.45E-03	36.59802968	4.72E-03	6.38E-03	35.089337
M4	3.98E-03	7.14E-03	79.47551083	4.02E-03	4.55E-03	13.14329128	4.80E-03	6.97E-03	45.283389
M5	4.30E-03	7.93E-03	84.49671816	0.010854409	0.010758655	-0.882163583	5.46E-03	8.61E-03	57.626477
Average	4.52E-03	7.93E-03	85.42	5.56E-03	6.69E-03	26.49	6.26E-03	9.18E-03	47.15

Table 6. Areas Under Baseline and Reactive Hyperemia Arterial Area Compliance Curves and Scoring Per Female Participant From 0 mmHg – 75 mmHg Transmural Pressure.

	Round 1			Round 2			Round 3		
	30 min Before Cold Water Immersion			Right After Cold Water Immersion			30 min After Cold Water Immersion		
Participant	Baseline 1	Hyperemia 1	Score	Baseline 2	Hyperemia 2	Score	Baseline 3	Hyperemia 3	Score
F1	0.03309027	0.036297	9.69232329	2.35E-02	0.0418375	77.74429207	0.028424024	0.0327480670	15.21263584
F2	0.01602244	0.025847003	61.3175453	0.013788499	0.015930739	15.53642967	0.018595151	0.023450081	26.10857743
F3	0.02294026	0.024564379	7.0797875	0.028622014	0.037726705	31.8100991	0.017575882	0.025944537	47.61442045
F4	0.0204262	0.022075323	8.0735616	0.015187081	0.01617745	6.521133392	0.025996353	0.031533063	21.29802322
F5	0.04466029	0.044843961	0.41126557	0.031540538	0.037519923	18.95777722	0.044025544	0.041245138	-6.315437062
F6	0.02924749	0.036156227	23.6216427	0.024785713	0.027126235	9.443029231	0.024606463	0.034132286	38.71268557
F7	0.01510947	0.019961906	32.1152178	0.014890245	0.021255407	42.74719311	0.018310526	0.022084242	20.60954663
F8	0.01660312	0.023949208	44.2452365	0.012145114	0.016149574	32.9717784	0.01455635	0.017188121	18.07987859
F9	0.02546393	0.027257228	7.04251343	0.025972145	0.03047824	17.34972207	0.029886004	0.033056241	10.60776807
Average	0.02484038	0.028994747	21.5110104	0.021163265	0.027133533	28.12016158	0.024664033	0.02904242	21.32534431

Table 7. Areas Under Baseline and Reactive Hyperemia Arterial Area Compliance Curves and Scoring Per Female Participant From 20 mmHg – 75 mmHg Transmural Pressure.

	Round 1			Round 2			Round 3		
	30 min Before Cold Water Immersion			Right After Cold Water Immersion			30 min After Cold Water Immersion		
Participant	Baseline 1	Hyperemia 1	Score	Baseline 2	Hyperemia 2	Score	Baseline 3	Hyperemia 3	Score
F1	0.01580036	0.021045	33.1904666	0.013455916	0.0247097	83.63478725	0.016137676	0.0179084421	10.97286775
F2	9.44E-03	0.018023515	90.9126374	8.43E-03	0.012919427	53.23351589	0.011349712	0.015572481	37.20595669
F3	0.01078037	0.01671123	55.0154364	0.013653116	0.02278901	66.91435352	9.91E-03	0.015987459	61.29535151
F4	0.01073511	0.012507313	16.5084956	9.48E-03	0.012161746	28.29946174	0.013235539	0.016899538	27.68303421
F5	0.02562499	0.026168571	2.12129586	0.01949727	0.022065433	13.17190778	0.02332004	0.021268467	-8.797468973
F6	0.01289171	0.0180716	40.1800093	0.013428057	0.019067355	41.99637729	0.014995214	0.020671654	37.85500779
F7	9.45E-03	0.014179361	50.0719441	9.04E-03	0.013716594	51.79907699	0.011278587	0.014120301	25.19565572
F8	9.51E-03	0.014920564	56.8779013	7.70E-03	0.010891053	41.41185596	8.69E-03	0.010623282	22.24118387
F9	0.01386482	0.018730567	35.0941935	0.014895027	0.020019356	34.40294593	0.01507869	0.019032552	26.2215172
Average	0.01312193	0.017817477	42.2191533	0.012175272	0.017593302	46.09603137	0.013777534	0.016898242	26.65256731

Table 8. Areas Under Baseline and Reactive Hyperemia Arterial Area Compliance Curves and Scoring Per Female Participant From 50 mmHg – 75 mmHg Transmural Pressure.

	Round 1			Round 2			Round 3		
	30 min Before Cold Water Immersion			Right After Cold Water Immersion			30 min After Cold Water Immersion		
Participant	Baseline 1	Hyperemia 1	Score	Baseline 2	Hyperemia 2	Score	Baseline 3	Hyperemia 3	Score
F1	3.77E-03	0.004625	22.7795131	4.11E-03	0.0071058	72.99816115	5.05E-03	0.0057121860	13.00659829
F2	2.21E-03	5.03E-03	127.278322	2.22E-03	4.31E-03	94.33356841	2.61E-03	4.04E-03	55.13689192
F3	2.63E-03	5.67E-03	115.734114	3.75E-03	5.18E-03	38.20131005	3.12E-03	4.46E-03	43.10176942
F4	2.62E-03	3.68E-03	40.8522648	2.93E-03	3.82E-03	30.28830396	3.10E-03	4.73E-03	52.8383769
F5	5.22E-03	6.27E-03	20.0573286	5.12E-03	5.93E-03	15.94648323	5.59E-03	7.39E-03	32.11695527
F6	3.55E-03	6.17E-03	73.8775162	6.56E-03	7.40E-03	12.79083149	5.29E-03	5.15E-03	-2.707825471
F7	2.68E-03	4.00E-03	49.2650675	2.89E-03	4.09E-03	41.72801451	3.26E-03	3.30E-03	1.27369124
F8	3.24E-03	5.59E-03	72.6889104	3.13E-03	3.71E-03	18.45812811	3.03E-03	3.60E-03	18.78612249
F9	3.73E-03	6.61E-03	77.1471009	4.37E-03	5.96E-03	36.45355729	4.92E-03	5.97E-03	21.35893783
Average	3.29E-03	5.29E-03	66.63	3.90E-03	5.28E-03	40.13	4.00E-03	4.93E-03	26.10

4.2 Baseline vs Hyperemia and Scores Within and Between Male and Female Groups

It should be recalled that the area under each arterial area compliance curve is representative of the actual cross-sectional area of the brachial artery as transmural pressure changes upon cuff pressure release. Calculating the total area essentially compounds each area at each transmural pressure point, meaning that a greater value represents a greater summed cross-sectional area and more blood flow over time.

When observing pressure-area curves within the range 0mmHg – 75 mmHg transmural pressure, one-way ANOVA comparison and comparison for all pairs using a Tukey Kramer test within the male participants found no significant differences in any baseline or hyperemia measurements except for Hyperemia 3, which was found to be significantly greater than Baseline 2, citing a p-value of 0.0431. No significant differences were found when comparing baseline and hyperemia measurements within the female group across all trial rounds. When comparing male and female results it was found that the female Baseline 2 trial was significantly different than males' Baseline 3 as well as males' Hyperemia 1 and 3 trials, with p-values of 0.0007, 0.0391, and 0.0001. No other statistical significance was observed between the hyperemia and baseline pressure-area curves of male and female participants. No statistical significance was detected in a comparison of and Scores either, between and within male and female groups. There are, however, some interesting trends worth noting. It was observed in the female group that while the scores were not significantly different between trials 1, 2, and 3, the average scores of trials 1 and 3 were relatively close at 21.511% and 21.325%, while trial 2 had a higher average score of 28.120%. These differences were associated with a greater difference in baseline and hyperemia curves in trial 2. It can also be seen within the female group that hyperemia measurements seem to stay relatively close throughout each trial, at 0.0289, 0.0271, 0.0290, while baseline measurements do not follow the same trend. Baseline measurements in the female group had averages of 0.0248, 0.0211, 0.02466, where the Baseline 2 measurement is seemingly the outlier in comparison the other two averages.

When looking at the male group, the same trends are not seen. Instead, it is observed that Score 1 is largest at 27.091%, followed by Score 2 at 24.911%, and Score 3 at 16.710%. Hyperemia and baseline measurements were slightly lower in trial 2, and highest in trial 3, relative to the tree trials done within the male group. Hyperemia measurements were 0.04012, 0.0337, and 0.0505 whereas baseline measurements were 0.0326, 0.0292, and 0.0431. As expected, the hyperemia measurement in each trial was always greater than its associated baseline measurement. One exception was seen in one male participant's data, where his Baseline 2 measurement was greater than his Hyperemia 2 measurement. This was most likely the result of motion artifacts as that specific participant exhibited the greatest amount of uncontrollable shivering immediately after the cold-water immersion intervention, making room for greater error during the second round of data collection for the participant.

In an integration of the same curves over a smaller range of 20 mmHg – 75 mmHg similar statistical results were observed. Withing the male group a one-way ANOVA comparison and comparison for all pairs using a Tukey Kramer test found that Hyperemia 3 was significantly greater than Baseline 1 and Baseline 2 with p-values of 0.0075 and 0.0013. No significant differences were found when comparing baseline and hyperemia measurements within the female group across all trial rounds withing the 20 mmHg – 75 mmHg. When comparing the hyperemia and baseline curves between male and female groups, the male Hyperemia 3 measurement is significantly greater female Baseline 1, 2, and 3 with p-values <0.0001 as well as female Hyperemia 1, 2, 3 with p-values 0.0013, 0.0010, and 0.0005 respectively. Male Baseline 3 measurements were found to be significantly greater than female Baseline 1 and 2 measurements with p-values 0.0289

and 0.0119, respectively. Male Hyperemia 1 was found to be significantly greater than female Baseline 1, 2, 3 with p-values 0.0063, 0.0023, 0.0122 respectively. No statistical significance was detected when comparing Scores 1, 2, and 3. The 20 mmHg – 75 mmHg pressure range had trends similar to those seen when observing the 0 mmHg – 75 mmHg range.

When observing the same curves from the pressure range 50 mmHg – 75 mmHg, similar statistical results were seen, however it was decided that the 0 mmHg – 75 mmHg is most reflective of the results of the experiment since the shortening of the range of observation of data amplifies the impacts of noise and possible incorrect outlying data points.

CHAPTER 5

5. DISCUSSION

5.1 Discussion of Results

This paper begins with an overview of cardiovascular disease, endothelial dysfunction, natural bypass pathways like vasodilation, arteriogenesis, and angiogenesis, as well as the parallels they may have with the human body's physiologic response to cold therapies. Similar research can be done using the cold pressor test, in which participants submerge one hand into cold water and changes in heart rate and blood pressure are monitored. This method also relies on the stimulation of the body's physiological response to cold exposure in order to determine certain cardiovascular properties. This study did a similar thing but involved full body immersion into cold water instead of a single hand. The objective of this experiment was to test the efficiency of a calibrated cuff plethysmography device by using it to distinguish any differences in brachial artery cross-sectional area observed before and after full body cold-water immersion. While not all results showed significant differences, the trends that were seen were quite expected and follow trends that are seen during acute cold exposure.

As mentioned in the results, the 0 mmHg – 75 mmHg transmural pressure range was paid the most attention when observing the areas under pressure – compliance curves of baseline and hyperemia measurements as well as the scores used to compare them. This was because it captured the full range of arterial compliance where baseline and hyperemia curves began to diverge while minimizing the impact of noisy data as much as possible in comparison to the 20 mmHg – 75 mmHg and 50 mmHg -75 mmHg ranges which were also observed and analyzed.

Observation of the 0 mmHg – 75 mmHg range within the male group found that only the Hyperemia 3 and Baseline 2 measurements were significantly different. In reflecting on this trend it is important to recall that all hyperemia measurement for each participant stayed relatively close to each, since reactive hyperemia is thought to be a situation in which arterial compliance and arterial area should be the greatest, considering blood is rushing through the artery at such speed after being released from a hyperemic condition for 5 minutes, causing an abnormally large momentary increase in shear stress and greater vasodilation. Therefore, it is expected that hyperemia measurements are the largest in all participants measurements and are not greatly affected by differences in environmental conditions since they should theoretically display the maximal arterial compliance and cross-sectional area. Baseline measurements, however, were subject to change depending on environmental changes within the experiment. It aligns with common knowledge of human physiology that the Baseline 2 measurement was significantly lower than the Hyperemia 3 measurement because it is known that vessels closer to the bodies surface contract in response to the cold as a mechanism to keep the core warm. This is especially apparent when observing the female test sample, where hyperemia measurements of each of the three trials stayed at relatively similar values of 0.0289, 0.0271, and 0.0291, respectively, while Baselines 1 and 3 were similar (0.0248 and 0.0246) with Baseline 2 trailing behind at 0.0211. Here the total cross-sectional area of the brachial artery is smaller in the Baseline 2 measurement because it was measured immediately after participants came out of a five-minute cold-water immersion intervention period, resulting in vessel constriction. Baseline 1 and 3 measurements were taken before the cold exposure and thirty minutes after, times at which participants were

at normal body temperatures. A much higher score is also seen in trial 2, within the female group, denoting the larger difference between baseline and hyperemia measurements immediately after cold exposure as compared to the other two trials, which again can be explained by the vasoconstriction that results from exposure to lower temperatures. Variance in scores can largely be attributed to conditional changes baseline measurements.

When comparing male and female groups to each other, significant differences between groups can be explained by anatomical differences between males and females, like larger body frames and larger blood vessels. This is exemplified by the observation that all average measurements from the male group, including baseline measurements, where larger than both average baseline and hyperemia measurements in the female group. This could be the result of anatomical differences as well as physiologic differences in the responses of males and females to reactive hyperemia or low temperature exposure.

Within the male group, though it was found that Hyperemia 3 was significantly larger than Baseline 2, other trends seen in the female group were not as apparent. The scores for each trial decreased as the number of trials increased, while there didn't seem to be any clear trend when observing the baseline and hyperemia curves, except for slightly lower areas seen in trial two, which again aligns with the human physiologic response to cold exposure.

Overall, it can be said that the calibrated cuff plethysmography device used in this study was quite successful in efficiently measuring arterial compliance. The setup used was based on Dr. Whitt's prior device with slightly different tubing and different equipment models. Since the basic setup has been arranged and determined to work efficiently, a

great foundation has been built for future students to continue working on this device as well as data collection and analysis methods.

5.2 Limitations and Future Studies

There is lots of room for improvement within the setup of this experiment in areas where limitations were met within device setup, data collection, and analysis. To begin with, the device construction itself included some limiting components. This includes the handheld inflation bulb used to inflate the blood pressure cuff placed around participants' upper arms. The release valve on the bulb which was used to slowly release pressure during data collection was manually loosened during each trial, opening the door for human error which resulted in an inconsistent release of pressure in cases where a more constant and slower release of pressure would have been more desirable to include all data points. Sudden drops of pressure which sometimes resulted from the initial unscrewing of the valve resulted in the unintentional exclusion of chunks of data. Future studies should look into a mechanism which can be programmed to fill the cuff to the desired pressure consistently and also release pressure at the desired constant rate.

It should also be recalled that there were very interesting findings seen when the calculated cuff compliance was plotted against the cuff pressure as it was released. Instead of seeing the expected trend, where cuff compliance increases as cuff pressure decreases, cuff compliance decreased with decreasing cuff pressures. Figure 33 below shows a plot of the expected trend. Figure 34 shows the trend that was actually seen during this study.

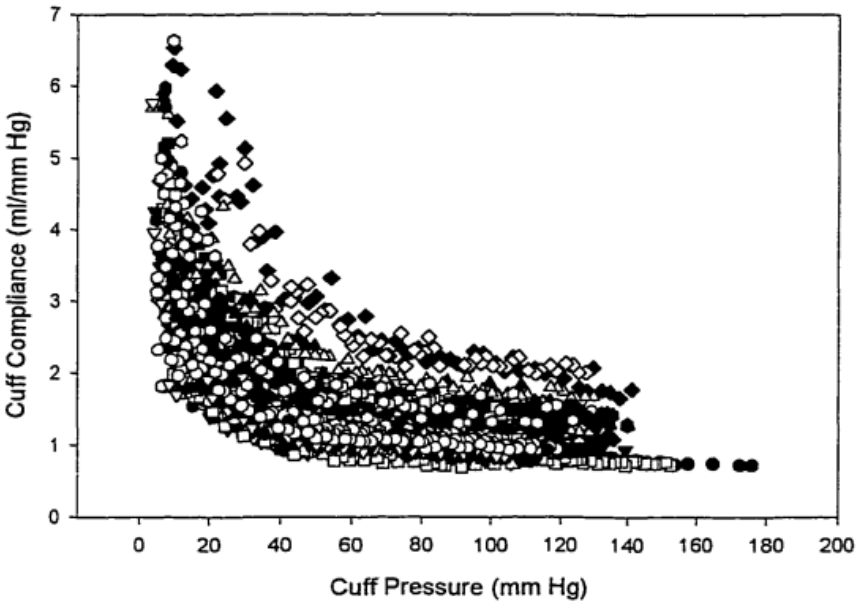

Figure 33. Calculated Cuff Compliance vs Cuff Pressure. This plot represents the trend that was expected based on previous research [1].

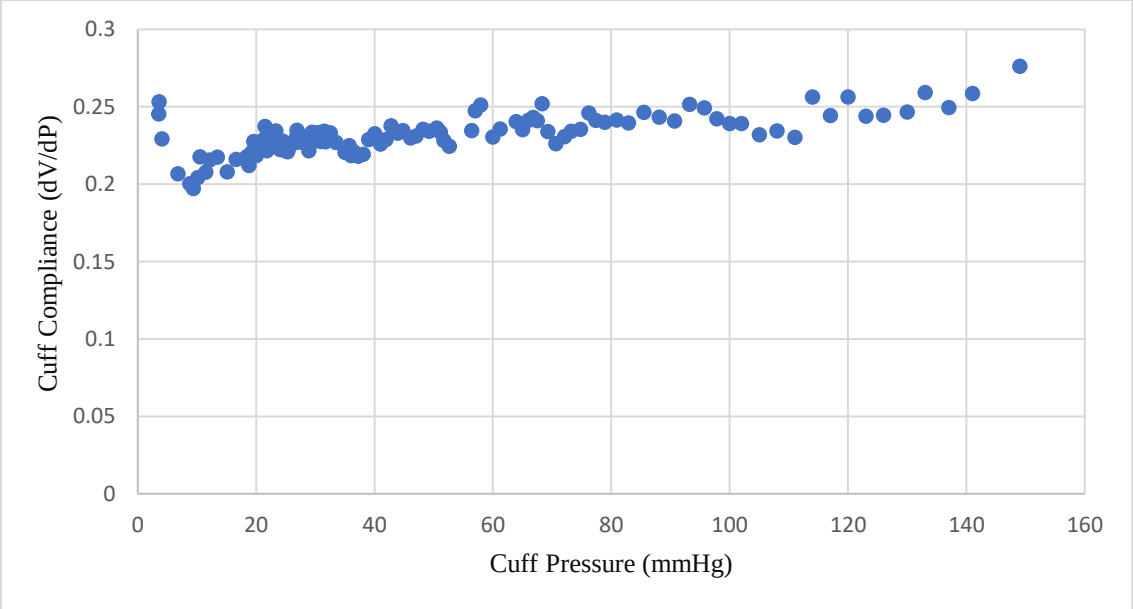

Figure 34. Cuff Compliance vs Cuff Pressure. This plot represents the trend which was seen during this study.

Differences in these trends can be explained by examining the equations used to calculate cuff compliance. Since cuff compliance is equal to the pump stroke volume (mL) divided by the pump pulse pressure (mmHg), and the pump stroke volume is equal to the pump flow rate (mL/sec) divided by the pump pulse frequency (Hz), it is important to look into the trends in which all these values vary with cuff pressure changes. Typically, it is expected that a release of cuff pressure would enable the diaphragm pump to pump harder, increasing overall pump flow rates as cuff pressure is decreased. This would, in turn, result in a higher pump stroke volume and an increasing cuff compliance as cuff pressure decreases. In this study, however, it was seen that the pump flow rate actually decreased as the cuff pressure was decreased, ultimately resulting in lower values obtained when calculating the cuff compliance. The following plot in Figure 34 shows the pump flow rate as it decreases with decreasing cuff pressure.

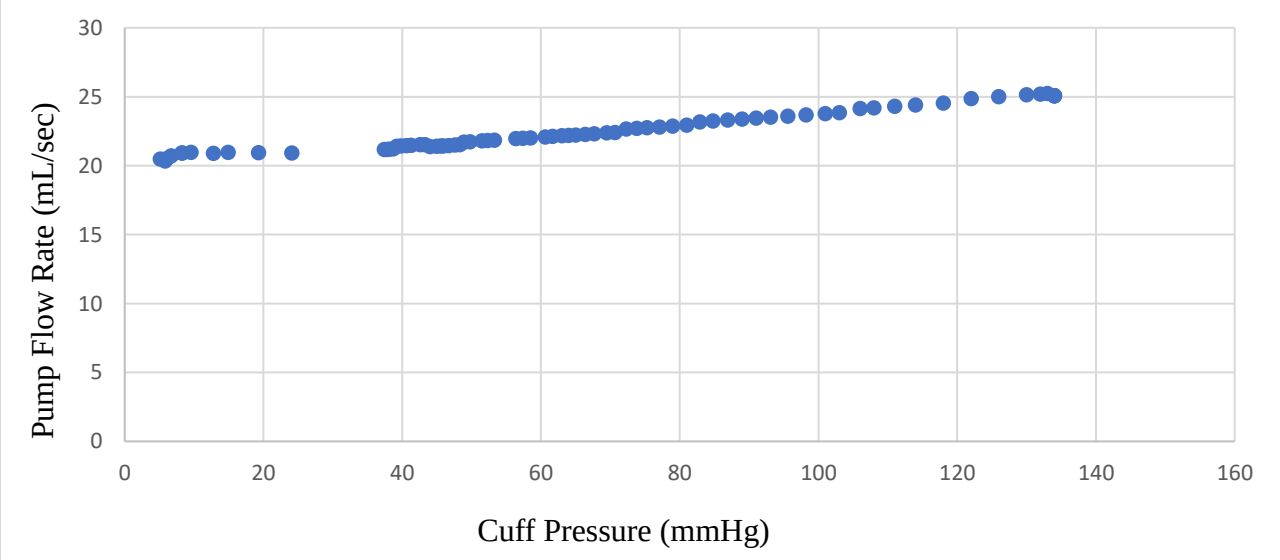

Figure 35. Pump Flow Rate vs Cuff Pressure.

It was seen that pump frequency (Hz) and pump pressure pulses (mmHg) both stayed relatively constant during data recordings, pointing at pump flow rate as the main issue in creating this trend. This was most likely related to issues with the pump itself. Future studies could be recommended to look into a newer pump model and test that it behaves consistently with past research.

Limitations that were also discovered during device validation methods included the inaccuracy of the syringe used to inject water into the medical bag which was placed in between the cuff and the steel column. This was also done manually and was subject to human error. The tubing of the medical bag and the medical bag itself were also quite compliant and may have been ununiformly affected by the pressure of the cuff as it was it was difficult to ensure that the cuff was uniformly applying pressure to the medical bag. Minimal volumes of water which got stuck at the end of the tubing could have also affected the results. In regard to the ununiform application of pressure on the bag, the "edge effect" of the cuff was also not accounted for. The edge effect refers to the notion that the cuff pressure seems to attenuate down to 0 mmHg toward the edges [50]. There was no way of ensuring that this had no effect on data collected during validation measures. Future studies should try to incorporate a device which accurately measures and injects fluid into a more efficient enclosure than the medical bag used at a constant rate which is difficult to do by hand. Mathematically accounting for the edge effect or obtaining a wider blood pressure cuff such that the medical bag is less affected in the center region of the cuff would also improve the overall validation model.

Limitations during data analysis included difficulty isolating good arterial pulse curves and omitting noise from that data collection process. Many arterial pulses were manually

selected during data collection, making the process very tedious and susceptible to human error. Additionally, the mean arterial pulse used to determine the transmural pressure range at each cuff pressure was assumed to be 85 mmHg for each participant. Future studies could determine the actual mean arterial pulse of each participant and use those values instead. It should be noted that this assumption did not affect intrasubject error as it did intersubject error.

Another limitation was a lack of male participants. Having 9 female participants seemed to reap much more consistent results than the male group which only had 5. Participants also varied in their responses to cold as some seemed more sensitive to the sensation. Measurements in trial 2 which came immediately after participants came out of the cold water were especially variable because some participants experienced uncontrollable shivering for parts of the data collection procedure which resulted in various chunks of inconclusive data.

Another key factor to consider is that the long-term effect of consistent cold-water immersion therapy were not tested in this experiment. This study only observed the effects of acute cold-water immersion after a single intervention period. Future studies should create a more long-term intervention schedule to see the long-term effects of cold exposure on physiologic pathways such as vasodilation, arteriogenesis, and angiogenesis as the full capabilities of the human body have not yet been uncovered and nor has the great potential of various modes of cryotherapy on preventative health.

BIBLIOGRAPHY

[1] D. Whitt, Michael, “NONINVASIVE DETERMINATION OF PERIPHERAL ARTERIAL LUMEN AREA,” Graduate School-New Brunswick Rutgers, The State University o f New Jersey and The Graduate School o f Biomedical Sciences Robert Wood Johnson Medical School, New Brunswick, New Jersey, 1999.

[2] G. Drzewiecki, R. Hood, and H. Apple, “Theory of the oscillometric maximum and the systolic and diastolic detection ratios,” *Ann. Biomed. Eng.*, vol. 22, no. 1, pp. 88–96, 1994, doi: 10.1007/BF02368225.

[3] “Cardiovascular diseases.” https://www.who.int/health-topics/cardiovascular-diseases (accessed Apr. 26, 2023).

[4] I. of M. (US) C. on a N. S. S. for C. and S. C. Diseases, “Cardiovascular Disease,” in *A Nationwide Framework for Surveillance of Cardiovascular and Chronic Lung Diseases*, National Academies Press (US), 2011. Accessed: Apr. 26, 2023. [Online]. Available: https://www.ncbi.nlm.nih.gov/books/NBK83160/

[5] R. Bauersachs, U. Zeymer, J.-B. Brière, C. Marre, K. Bowrin, and M. Huelsebeck, “Burden of Coronary Artery Disease and Peripheral Artery Disease: A Literature Review,” *Cardiovasc. Ther.*, vol. 2019, p. 8295054, Nov. 2019, doi: 10.1155/2019/8295054.

[6] “Stenting for Peripheral Artery Disease of the Lower Extremities,” *Ont. Health Technol. Assess. Ser.*, vol. 10, no. 18, pp. 1–88, Sep. 2010.

[7] N. G. Frangogiannis, “Cell therapy for peripheral artery disease,” *Curr. Opin. Pharmacol.*, vol. 39, pp. 27–34, Apr. 2018, doi: 10.1016/j.coph.2018.01.005.

[8] “Evidence supporting paracrine hypothesis for Akt-modified mesenchymal stem cell-mediated cardiac protection and functional improvement - Gnecchi - 2006 - The FASEB Journal - Wiley Online Library.” https://faseb.onlinelibrary.wiley.com/doi/10.1096/fj.05-5211com (accessed Apr. 26, 2023).

[9] R. J. Esper, R. A. Nordaby, J. O. Vilariño, A. Paragano, J. L. Cacharrón, and R. A. Machado, “Endothelial dysfunction: a comprehensive appraisal,” *Cardiovasc. Diabetol.*, vol. 5, no. 1, p. 4, Feb. 2006, doi: 10.1186/1475-2840-5-4.

[10] M. Ercan and C. Koksal, “The Relationship Between Shear Rate and Vessel Diameter,” *Anesth. Analg.*, vol. 96, no. 1, p. 307, Jan. 2003, doi: 10.1213/00000539-200301000-00073.

[11] Y. Hirata, D. Nagata, E. Suzuki, H. Nishimatsu, J. Suzuki, and R. Nagai, “Diagnosis and Treatment of Endothelial Dysfunction in Cardiovascular Disease: A Review,” *Int. Heart. J.*, vol. 51, no. 1, pp. 1–6, 2010, doi: 10.1536/ihj.51.1.

[12] S. S. Thosar, B. D. Johnson, J. D. Johnston, and J. P. Wallace, “Sitting and endothelial dysfunction: The role of shear stress,” *Med. Sci. Monit. Int. Med. J. Exp. Clin. Res.*, vol. 18, no. 12, pp. RA173–RA180, Dec. 2012, doi: 10.12659/MSM.883589.

[13] P. Y. Chia, A. Teo, and T. W. Yeo, “Overview of the Assessment of Endothelial Function in Humans,” *Front. Med.*, vol. 7, p. 542567, Oct. 2020, doi: 10.3389/fmed.2020.542567.

[14] “Cold for centuries: a brief history of cryotherapies to improve health, injury and post-exercise recovery - PMC.” https://www.ncbi.nlm.nih.gov/pmc/articles/PMC9012715/#CR57 (accessed Apr. 02, 2023).

[15] I. of M. (US) C. on M. N. Research, B. M. Marriott, and S. J. Carlson, “Physiology of Cold Exposure,” in *Nutritional Needs In Cold And In High-Altitude Environments: Applications for Military Personnel in Field Operations*, National Academies Press (US), 1996. Accessed: May 17, 2023. [Online]. Available: https://www.ncbi.nlm.nih.gov/books/NBK232852/

[16] S. S. Cheung and H. A. m. Daanen, “Dynamic Adaptation of the Peripheral Circulation to Cold Exposure,” *Microcirculation*, vol. 19, no. 1, pp. 65–77, 2012, doi: 10.1111/j.1549-8719.2011.00126.x.

[17] “Frostbite,” *nhs.uk*, Oct. 19, 2017. https://www.nhs.uk/conditions/frostbite/ (accessed Aug. 17, 2023).

[18] A. L. Vallerand and I. Jacobs, “Rates of energy substrates utilization during human cold exposure,” *Eur. J. Appl. Physiol.*, vol. 58, no. 8, pp. 873–878, 1989, doi: 10.1007/BF02332221.

[19] L. A. Mengel *et al.*, “Gender Differences in the Response to Short-term Cold Exposure in Young Adults,” *J. Clin. Endocrinol. Metab.*, vol. 105, no. 5, pp. e1938–e1948, May 2020, doi: 10.1210/clinem/dgaa110.

[20] C. M. Gibson *et al.*, “Relation of vessel wall shear stress to atherosclerosis progression in human coronary arteries,” *Arterioscler. Thromb. J. Vasc. Biol.*, vol. 13, no. 2, pp. 310–315, Feb. 1993, doi: 10.1161/01.atv.13.2.310.

[21] M. Zhou *et al.*, “Wall shear stress and its role in atherosclerosis,” *Front. Cardiovasc. Med.*, vol. 10, 2023, doi: 10.3389/fcvm.2023.1083547.

[22] R. B. Singh, S. A. Mengi, Y.-J. Xu, A. S. Arneja, and N. S. Dhalla, “Pathogenesis of atherosclerosis: A multifactorial process,” *Exp. Clin. Cardiol.*, vol. 7, no. 1, pp. 40–53, 2002.

[23] L. Lu, X. Sun, Y. Qin, and X. Guo, “The Signaling Pathways Involved in the Antiatherosclerotic Effects Produced by Chinese Herbal Medicines,” *BioMed Res. Int.*, vol. 2018, p. 5392375, Jun. 2018, doi: 10.1155/2018/5392375.

[24] T. Pattarabanjird, C. Li, and C. McNamara, “B Cells in Atherosclerosis: Mechanisms and Potential Clinical Applications,” *JACC Basic Transl. Sci.*, vol. 6, no. 6, pp. 546–563, Jun. 2021, doi: 10.1016/j.jacbts.2021.01.006.

[25] “Artery Formation (Physiology) - an overview | ScienceDirect Topics.” https://www.sciencedirect.com/topics/immunology-and-microbiology/artery-formation-physiology (accessed Aug. 07, 2023).

[26] T. H. Adair and J.-P. Montani, “Overview of Angiogenesis,” in *Angiogenesis*, Morgan & Claypool Life Sciences, 2010. Accessed: May 14, 2023. [Online]. Available: https://www.ncbi.nlm.nih.gov/books/NBK53238/

[27] B. L. Krock, N. Skuli, and M. C. Simon, “Hypoxia-Induced Angiogenesis,” *Genes Cancer*, vol. 2, no. 12, pp. 1117–1133, Dec. 2011, doi: 10.1177/1947601911423654.

[28] A. Uccelli *et al.*, “Vascular endothelial growth factor biology for regenerative angiogenesis,” *Schweiz. Med. Wochenschr.*, vol. 149, Jan. 2019, doi: 10.4414/smw.2019.20011.

[29] S. S. Cheung, “Responses of the hands and feet to cold exposure,” *Temp. Multidiscip. Biomed. J.*, vol. 2, no. 1, pp. 105–120, Feb. 2015, doi: 10.1080/23328940.2015.1008890.

[30] L. Walløe, “Arterio-venous anastomoses in the human skin and their role in temperature control,” *Temp. Multidiscip. Biomed. J.*, vol. 3, no. 1, pp. 92–103, Oct. 2015, doi: 10.1080/23328940.2015.1088502.

[31] T. K. Bergersen, J. Hisdal, and L. Walløe, “Perfusion of the human finger during cold-induced vasodilatation,” *Am. J. Physiol.-Regul. Integr. Comp. Physiol.*, vol. 276, no. 3, pp. R731–R737, Mar. 1999, doi: 10.1152/ajpregu.1999.276.3.R731.

[32] P. Imbeault, I. Dépault, and F. Haman, “Cold exposure increases adiponectin levels in men,” *Metabolism.*, vol. 58, no. 4, pp. 552–559, Apr. 2009, doi: 10.1016/j.metabol.2008.11.017.

[33] E. Rojas *et al.*, “The Role of Adiponectin in Endothelial Dysfunction and Hypertension,” *Curr. Hypertens. Rep.*, vol. 16, no. 8, p. 463, Jun. 2014, doi: 10.1007/s11906-014-0463-7.

[34] K. Shimada, T. Miyazaki, and H. Daida, “Adiponectin and atherosclerotic disease,” *Clin. Chim. Acta*, vol. 344, no. 1, pp. 1–12, Jun. 2004, doi: 10.1016/j.cccn.2004.02.020.

[35] R. F. D’Souza *et al.*, “Divergent effects of cold water immersion versus active recovery on skeletal muscle fiber type and angiogenesis in young men,” *Am. J. Physiol.-Regul. Integr. Comp. Physiol.*, vol. 314, no. 6, pp. R824–R833, Jun. 2018, doi: 10.1152/ajpregu.00421.2017.

[36] D. L. Plotkin, M. D. Roberts, C. T. Haun, and B. J. Schoenfeld, “Muscle Fiber Type Transitions with Exercise Training: Shifting Perspectives,” *Sports*, vol. 9, no. 9, p. 127, Sep. 2021, doi: 10.3390/sports9090127.

[37] “Intermittent cold exposure causes a muscle-specific shift in the fiber type composition in rats | Journal of Applied Physiology.” https://journals.physiology.org/doi/abs/10.1152/jappl.1993.75.1.264?casa_token=E_8yioRIJYMAAAAA:Lkfb44WBSxit2ZZg42X1O3U22rDHizwvae8ndMt-1ioIRaamexbSlf0iUnkdDfCikP9OBPxLI97r8w (accessed Aug. 07, 2023).

[38] J. C. Kim *et al.*, “Effects of cold-water immersion on VEGF mRNA and protein expression in heart and skeletal muscles of rats,” *Acta Physiol. Scand.*, vol. 183, no. 4, pp. 389–397, Apr. 2005, doi: 10.1111/j.1365-201X.2005.01415.x.

[39] Y. Xue *et al.*, “Hypoxia-Independent Angiogenesis in Adipose Tissues during Cold Acclimation,” *Cell Metab.*, vol. 9, no. 1, pp. 99–109, Jan. 2009, doi: 10.1016/j.cmet.2008.11.009.

[40] X. Zhang *et al.*, “Adipocyte Hypoxia-Inducible Factor 2α Suppresses Atherosclerosis by Promoting Adipose Ceramide Catabolism,” *Cell Metab.*, vol. 30, no. 5, pp. 937-951.e5, Nov. 2019, doi: 10.1016/j.cmet.2019.09.016.

[41] W. Chen *et al.*, “Cold exposure alters lipid metabolism of skeletal muscle through HIF-1α-induced mitophagy,” *BMC Biol.*, vol. 21, no. 1, p. 27, Feb. 2023, doi: 10.1186/s12915-023-01514-4.

[42] T. Masaki and T. Sawamura, “Endothelin and endothelial dysfunction,” *Proc. Jpn. Acad. Ser. B Phys. Biol. Sci.*, vol. 82, no. 1, pp. 17–24, Mar. 2006.

[43] Z. Sun, “Cardiovascular responses to cold exposure,” *Front. Biosci. Elite Ed.*, vol. 2, pp. 495–503, Jan. 2010.

[44] P. Lemieux, E. Roudier, and O. Birot, “Angiostatic freeze or angiogenic move? Acute cold stress prevents angiokine secretion from murine myotubes but primes primary endothelial cells for greater migratory capacity,” *Front. Physiol.*, vol. 13, 2022, Accessed: Aug. 07, 2023. [Online]. Available: https://www.frontiersin.org/articles/10.3389/fphys.2022.975652

[45] “nurecover® - Portable Ice Bath,” *nurecover*. https://us.nurecover.com/products/nurecover-portable-ice-bath (accessed Apr. 12, 2023).

[46] Pilla, JJ, “Calibrated cuff plethysmography: Development and application o f a device for use in evaluation of the effect o f arterial pressure-volume curve alterations on systemic blood pressure,” PhD Dissertation, Rutgers University, 1995.

[47] McMillan Company, “McMillan Company MODEL 100 FLO-Sensor Frequently Asked Questions,” May 1996.

[48] "Mean Arterial Pressure (MAP): Understanding Readings and Mmore," *Healthline*, Apr. 10, 2018. https://www.healthline.com/health/mean-arterial-pressure (accessed Aug. 17, 2023).

[49] A. J. Bank, H. Wang, J. E. Holte, K. Mullen, R. Shammas, and S. H. Kubo, "Contribution of Collagen, Elastin, and Smooth Muscle to In Vivo Human Brachial Artery Wall Stress and Elastic Modulus," *Circulation*, vol. 94, no. 12, pp. 3263–3270, Dec. 1996, doi: 10.1161/01.CIR.94.12.3263.

[50] G. Drzewiecki and J. J. Pilla, "Noninvasive Measurement of the Human Brachial Artery Pressure–Area Relation in Collapse and Hypertension," *Ann. Biomed. Eng.*, vol. 26, no. 6, pp. 965–974, Nov. 1998, doi: 10.1114/1.130.

APPENDIX

APPENDIX A: Pressure-Area and Pressure Compliance Curves for All Participants

Participant: F1

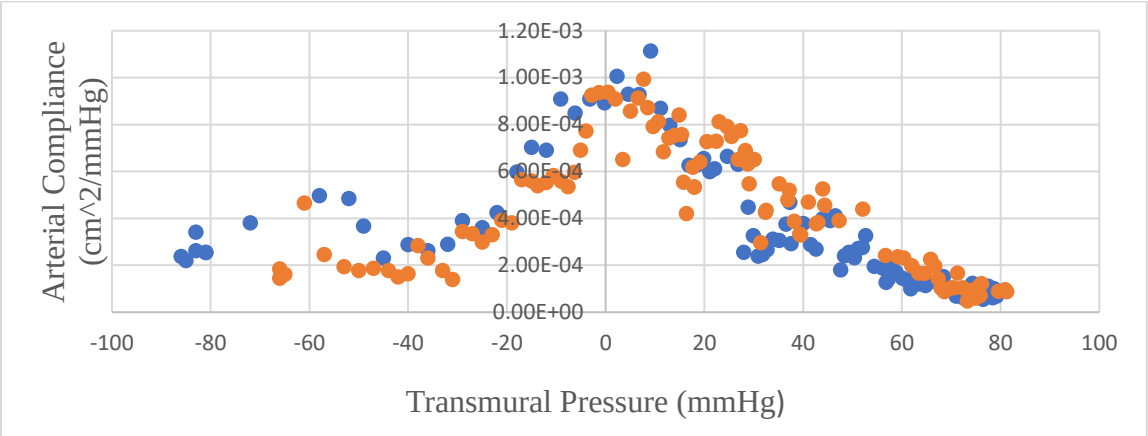

Figure 36. Arterial Area Compliance vs. Transmural Arterial Pressure of Female Participant (F1) 30 Minutes Before Cold-Water Immersion. Blue data points represent baseline measurements while orange data points represent measurements collected during 5-minute reactive hyperemia.

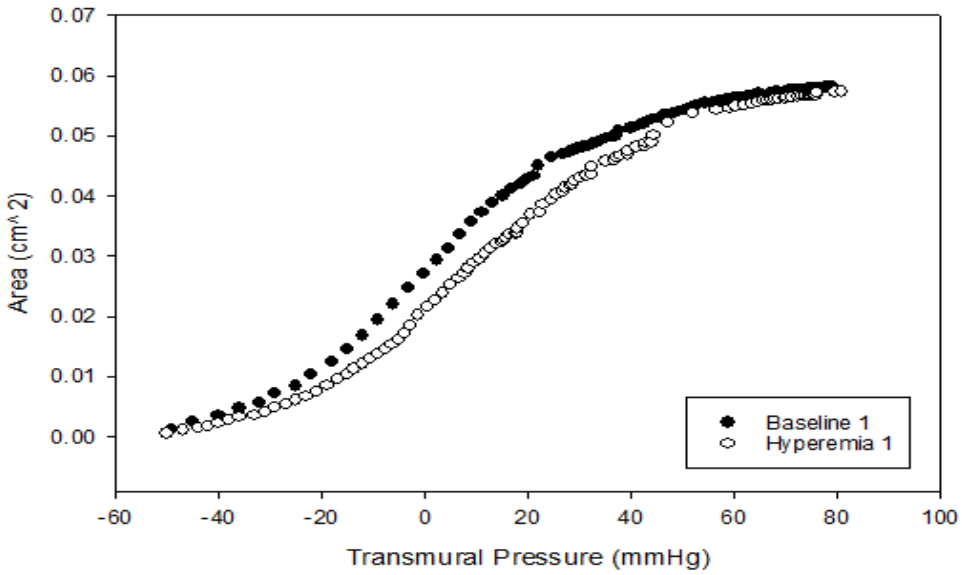

Figure 37. Arterial Lumen Area vs. Arterial Transmural Pressure of Female Participant (F1) 30 Minutes Before Cold-Water Immersion. Black data points represent baseline measurements while white data points represent measurements collected during 5-minute reactive hyperemia.

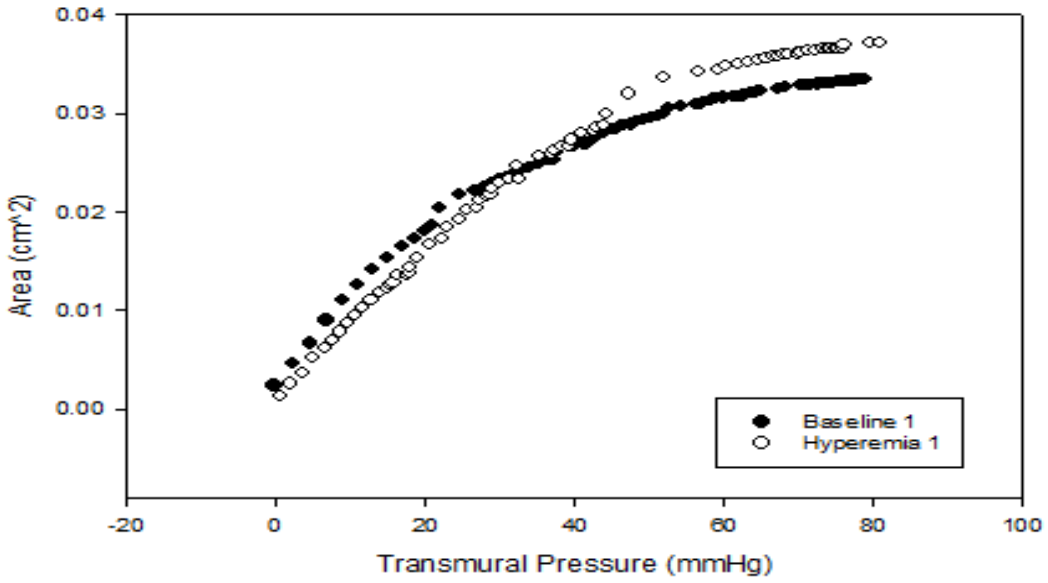

Figure 38. Arterial Lumen Area vs. Arterial Transmural Pressure of Female Participant (F1) 30 Minutes Before Cold-Water Immersion. Black data points represent baseline measurements while white data points represent measurements collected during 5-minute reactive hyperemia. Integrated from 0 mmHg to 80 mmHg transmural pressure.

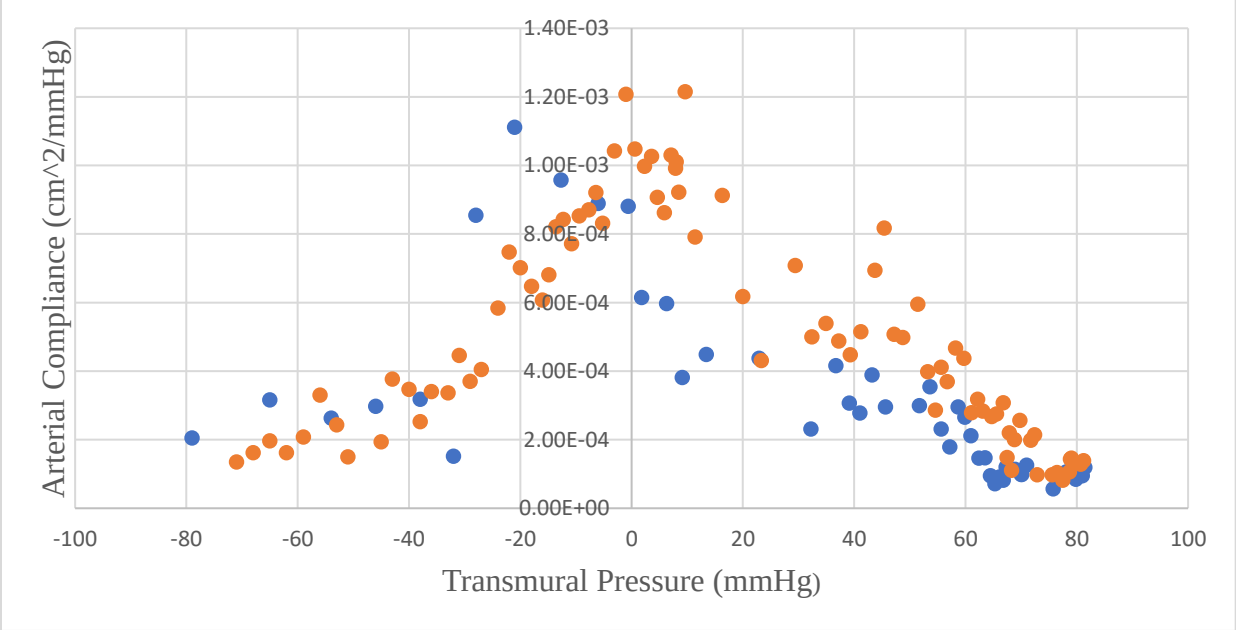

Figure 39. Arterial Area Compliance vs. Transmural Arterial Pressure of Female Participant (F1) Immediately After Cold-Water Immersion. Blue data points represent baseline measurements while orange data points represent measurements collected during 5-minute reactive hyperemia.

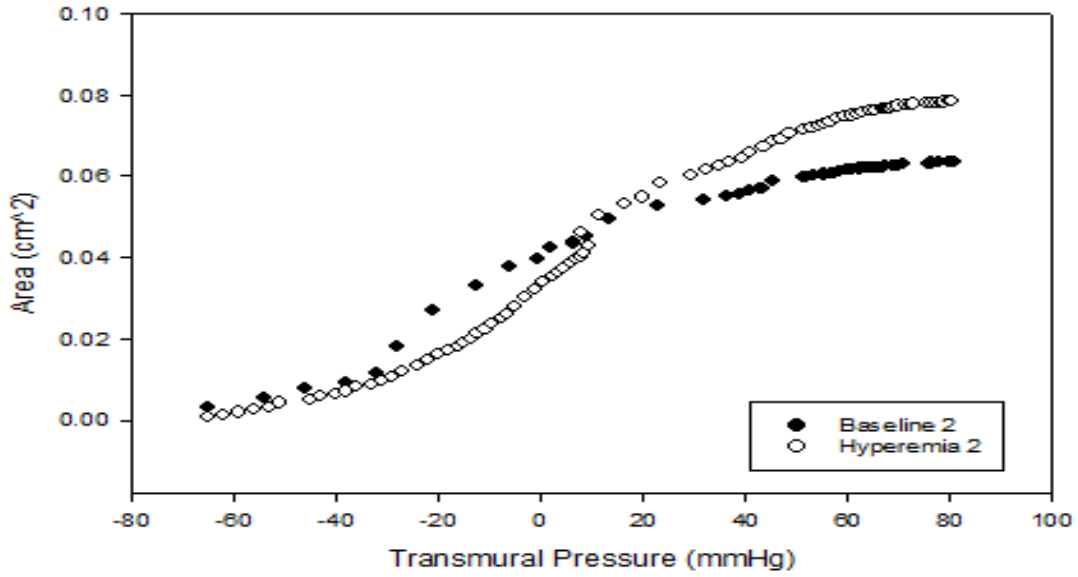

Figure 40. Arterial Lumen Area vs. Arterial Transmural Pressure of Female Participant (F1) Immediately After Cold-Water Immersion. Black data points represent baseline measurements while white data points represent measurements collected during 5-minute reactive hyperemia.

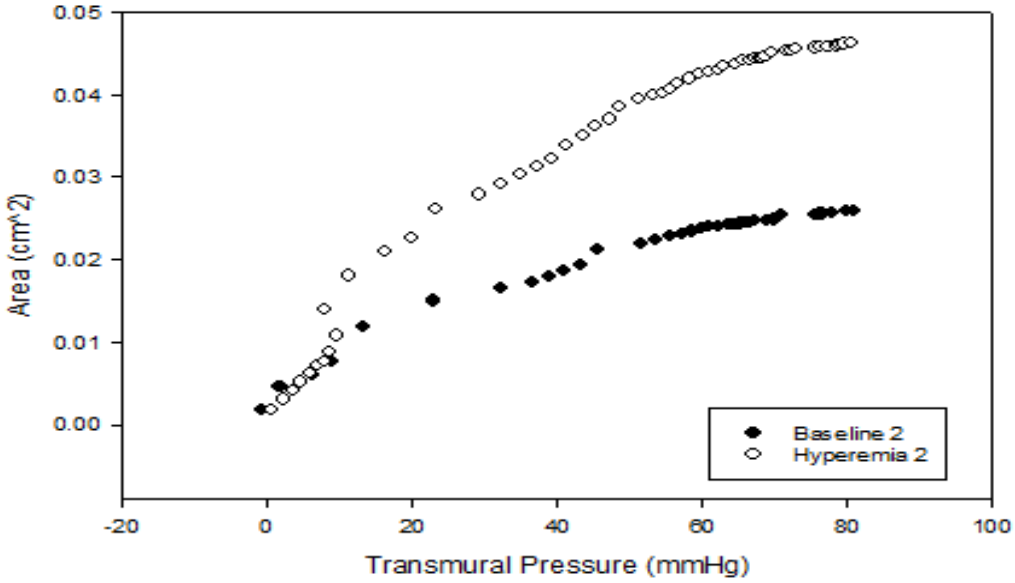

Figure 41. Arterial Lumen Area vs. Arterial Transmural Pressure of Female Participant (F1) Immediately After Cold-Water Immersion. Black data points represent baseline measurements while white data points represent measurements collected during 5-minute reactive hyperemia. Integrated from 0 mmHg to 80 mmHg transmural pressure.

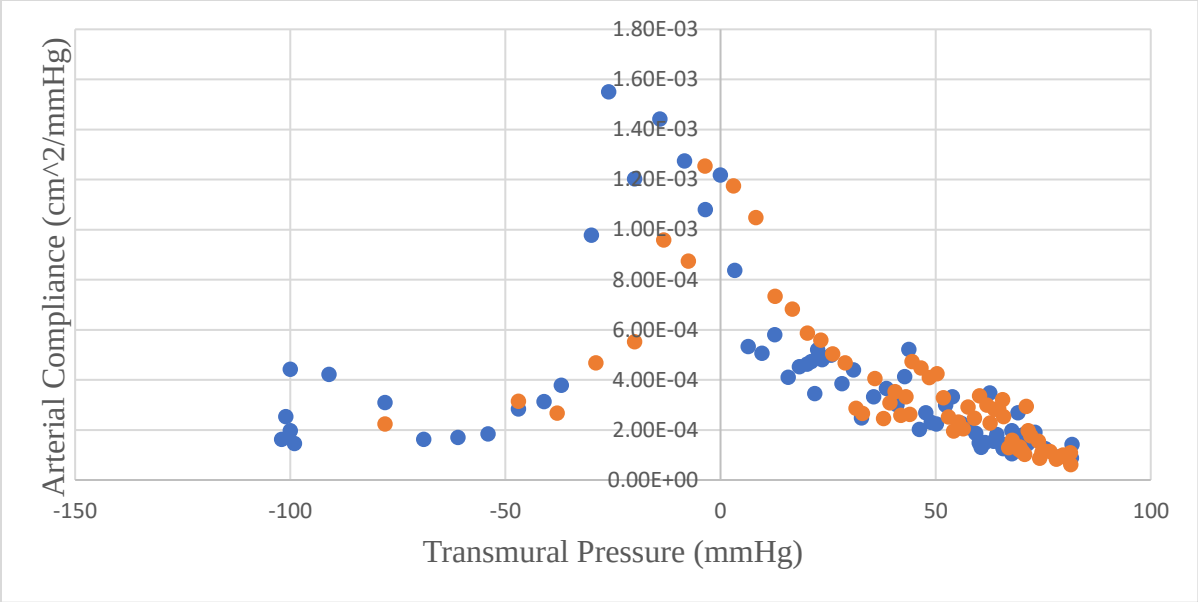

Figure 42. Arterial Area Compliance vs. Transmural Arterial Pressure of Female Participant (F1) 30 Minutes After Cold-Water Immersion. Blue data points represent baseline measurements while orange data points represent measurements collected during 5-minute reactive hyperemia.

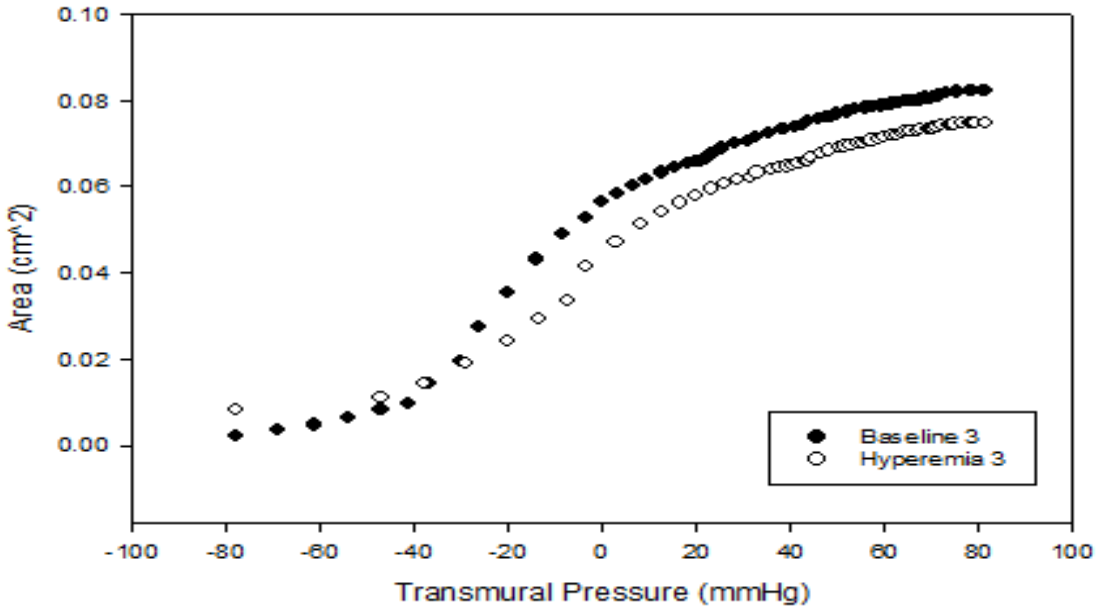

Figure 43. Arterial Lumen Area vs. Arterial Transmural Pressure of Female Participant (F1) 30 Minutes After Cold-Water Immersion. Black data points represent baseline measurements while white data points represent measurements collected during 5-minute reactive hyperemia.

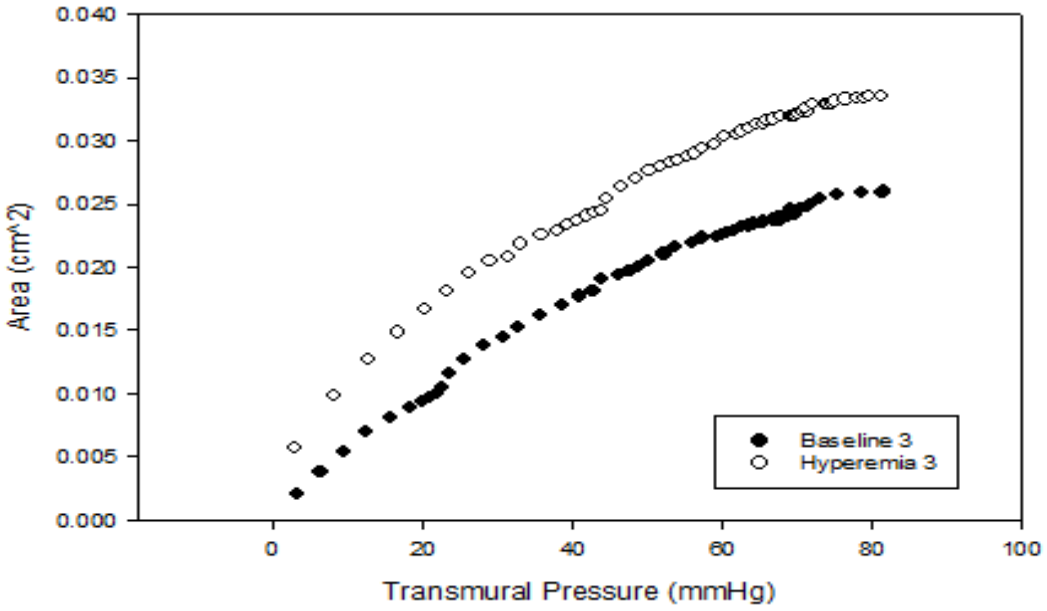

Figure 44. Arterial Lumen Area vs. Arterial Transmural Pressure of Female Participant (F1) 30 Minutes After Cold-Water Immersion. Black data points represent baseline measurements while white data points represent measurements collected during 5-minute reactive hyperemia. Integrated from 0 mmHg to 80 mmHg transmural pressure.

Participant: F2

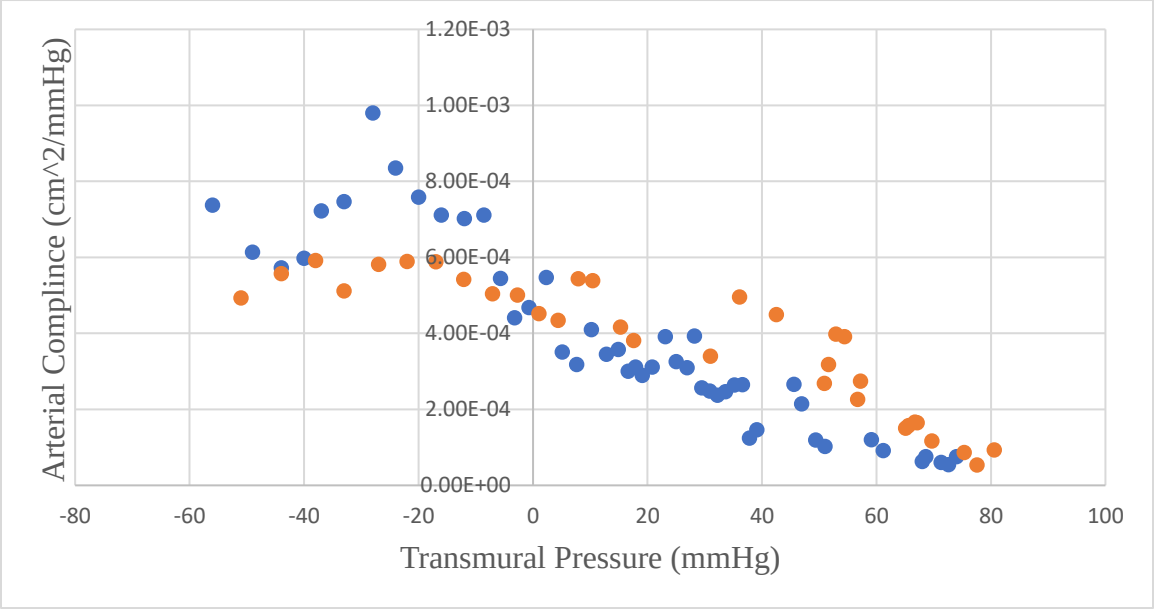

Figure 45. Arterial Area Compliance vs. Transmural Arterial Pressure of Female Participant (F2) 30 Minutes Before Cold-Water Immersion. Blue data points represent baseline measurements while orange data points represent measurements collected during 5-minute reactive hyperemia.

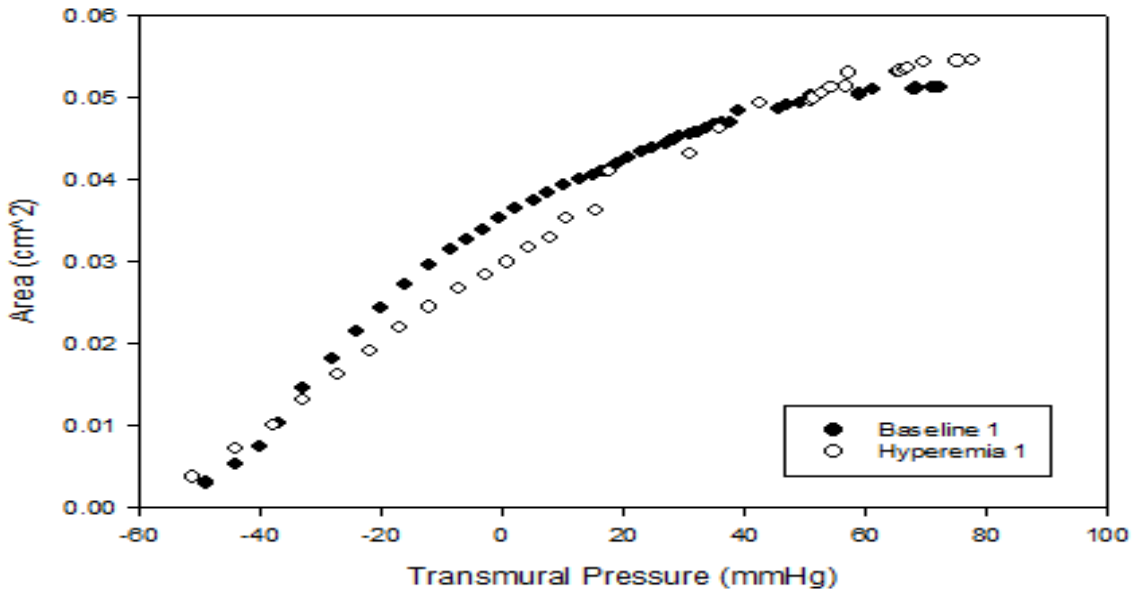

Figure 46. Arterial Lumen Area vs. Arterial Transmural Pressure of Female Participant (F2) 30 Minutes Before Cold-Water Immersion. Black data points represent baseline measurements while white data points represent measurements collected during 5-minute reactive hyperemia.

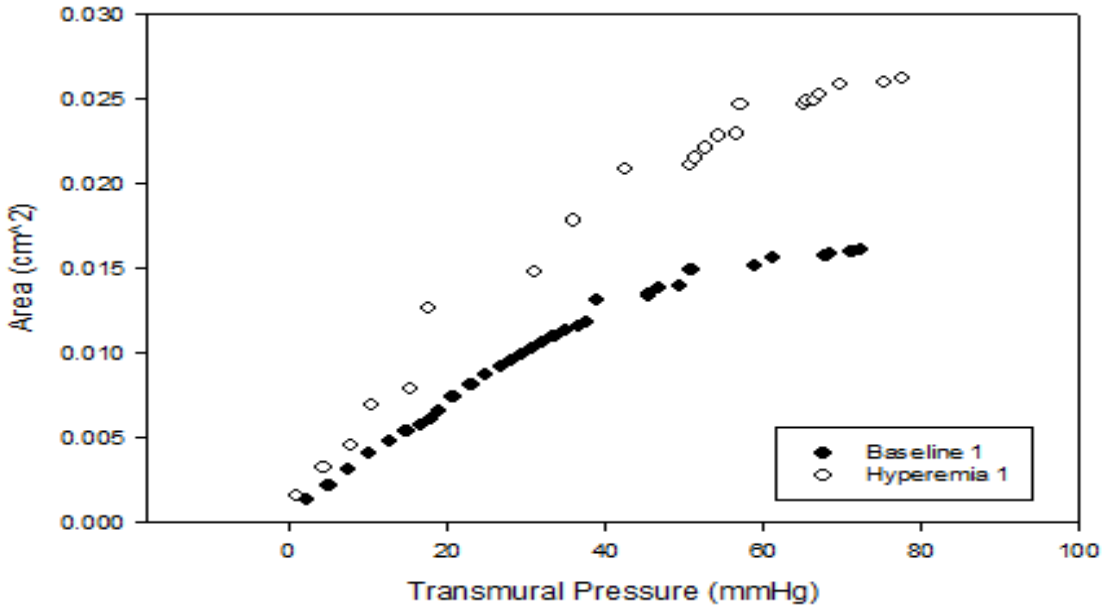

Figure 47. Arterial Lumen Area vs. Arterial Transmural Pressure of Female Participant (F2) 30 Minutes Before Cold-Water Immersion. Black data points represent baseline measurements while white data points represent measurements collected during 5-minute reactive hyperemia. Integrated from 0 mmHg to 80 mmHg transmural pressure.

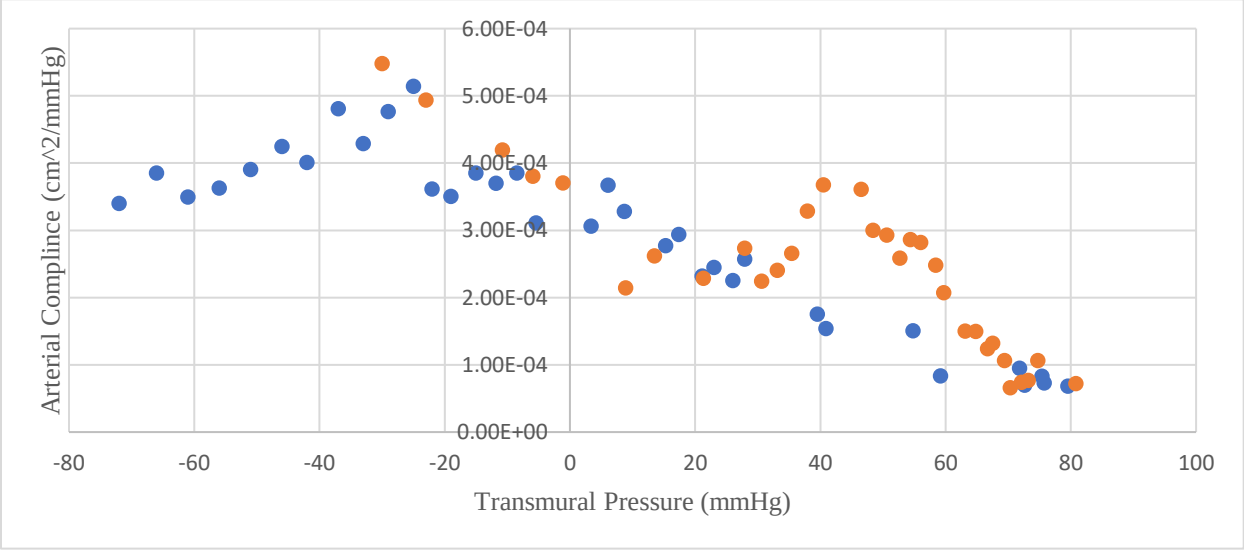

Figure 48. Arterial Area Compliance vs. Transmural Arterial Pressure of Female Participant (F2) Immediately After Cold-Water Immersion. Blue data points represent baseline measurements while orange data points represent measurements collected during 5-minute reactive hyperemia.

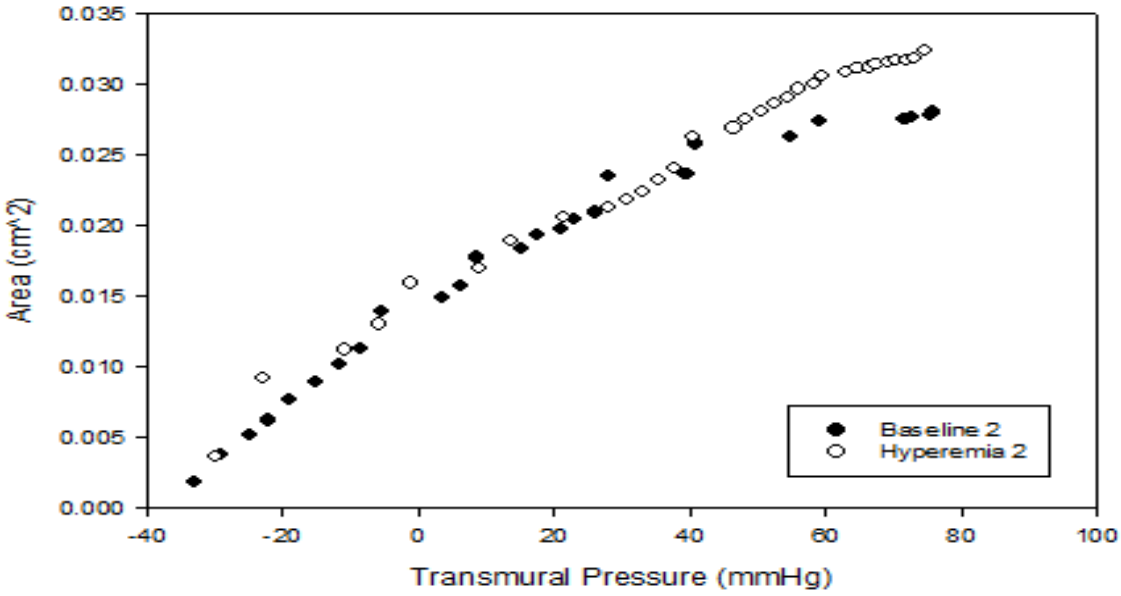

Figure 49. Arterial Lumen Area vs. Arterial Transmural Pressure of Female Participant (F2) Immediately After Cold-Water Immersion. Black data points represent baseline measurements while white data points represent measurements collected during 5-minute reactive hyperemia.

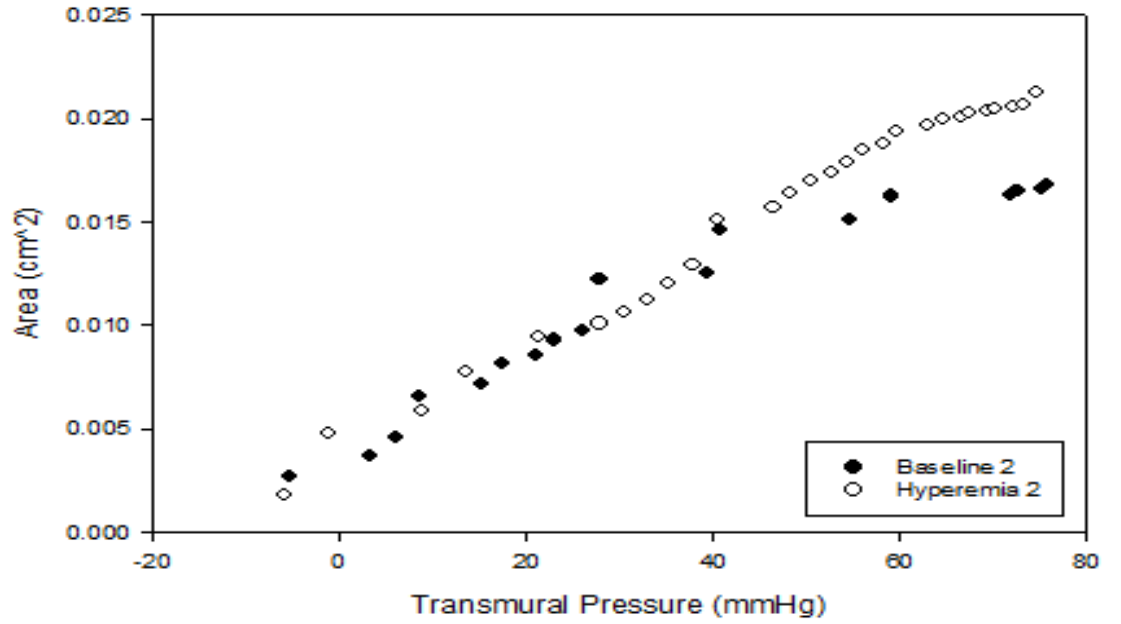

Figure 50. Arterial Lumen Area vs. Arterial Transmural Pressure of Female Participant (F2) Immediately After Before Cold-Water Immersion. Black data points represent baseline measurements while white data points represent measurements collected during 5-minute reactive hyperemia. Integrated from 0 mmHg to 80 mmHg transmural pressure.

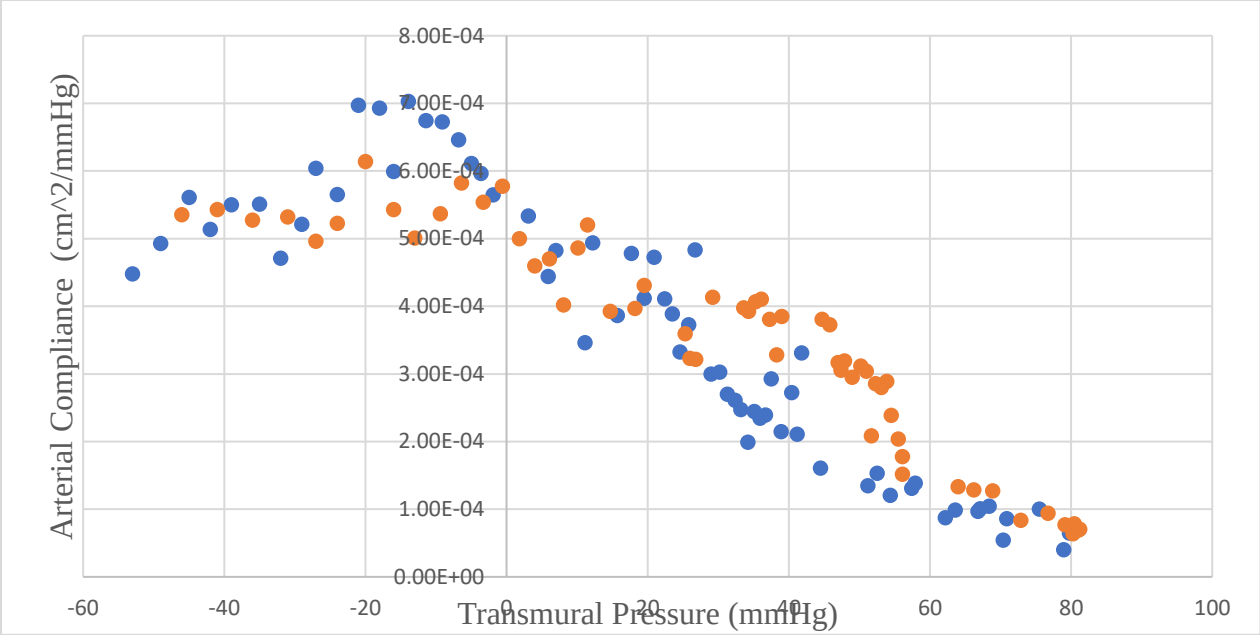

Figure 51. Arterial Area Compliance vs. Transmural Arterial Pressure of Female Participant (F2) 30 Minutes After Cold-Water Immersion. Blue data points represent baseline measurements while orange data points represent measurements collected during 5-minute reactive hyperemia.

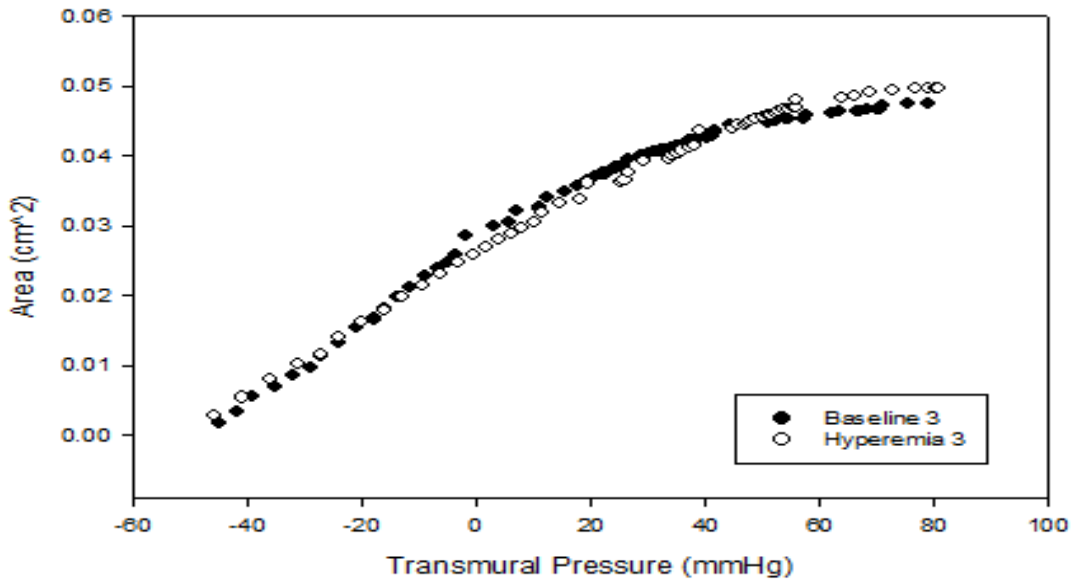

Figure 52. Arterial Lumen Area vs. Arterial Transmural Pressure of Female Participant (F2) 30 Minutes After Cold-Water Immersion. Black data points represent baseline measurements while white data points represent measurements collected during 5-minute reactive hyperemia.

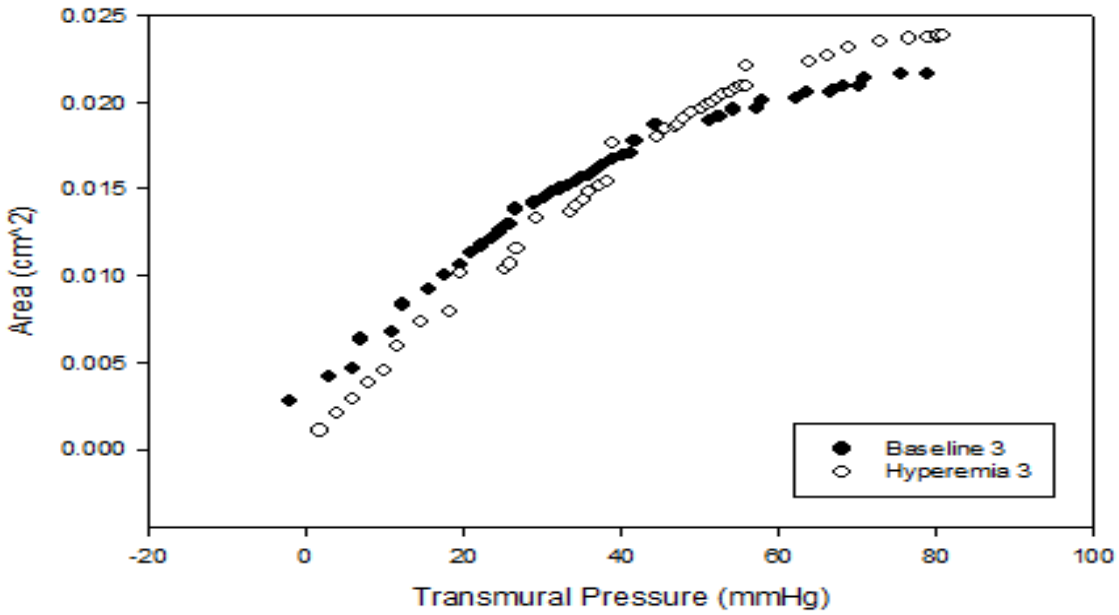

Figure 53. Arterial Lumen Area vs. Arterial Transmural Pressure of Female Participant (F2) 30 Minutes After Cold-Water Immersion. Black data points represent baseline measurements while white data points represent measurements collected during 5-minute reactive hyperemia. Integrated from 0 mmHg to 80 mmHg transmural pressure

Participant: F3

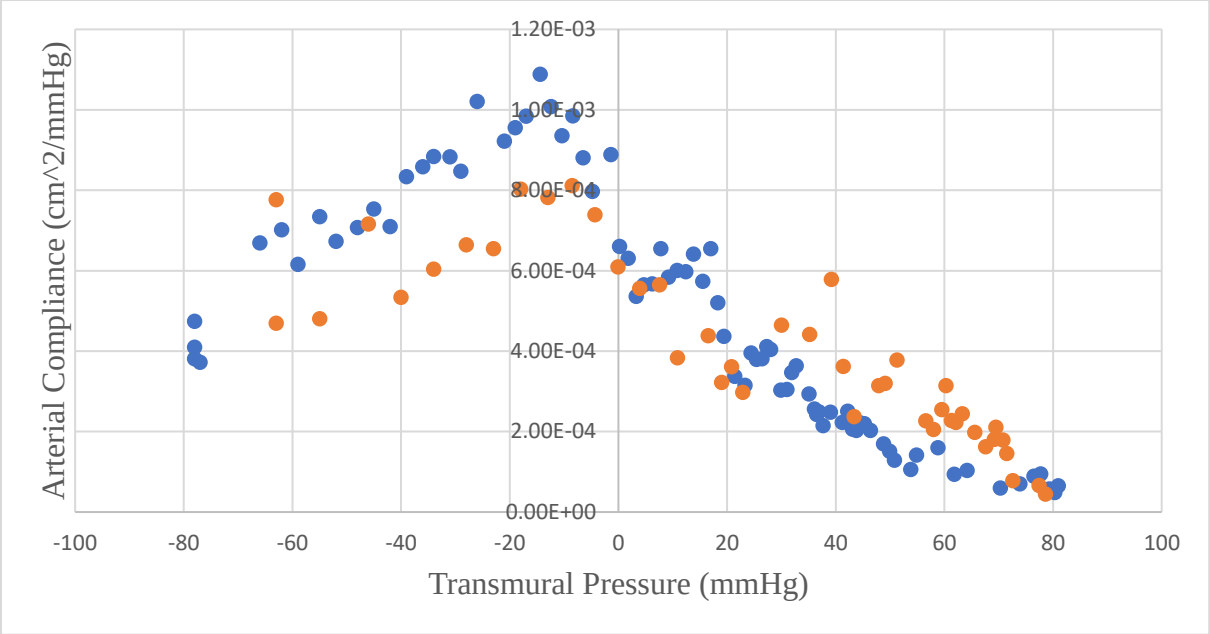

Figure 54. Arterial Area Compliance vs. Transmural Arterial Pressure of Female Participant (F3) 30 Minutes Before Cold-Water Immersion. Blue data points represent baseline measurements while orange data points represent measurements collected during 5-minute reactive hyperemia.

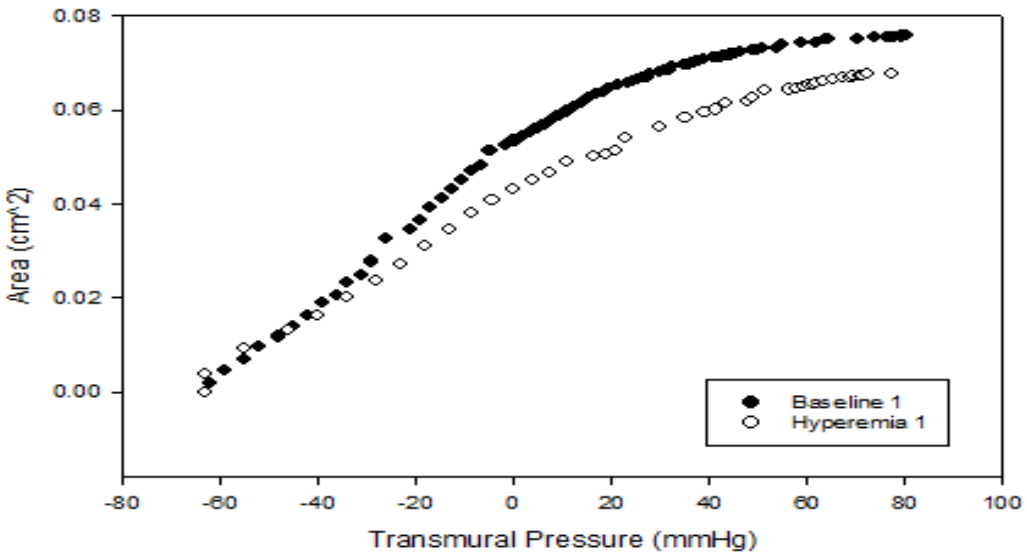

Figure 55. Arterial Lumen Area vs. Arterial Transmural Pressure of Female Participant (F3) 30 Minutes Before Cold-Water Immersion. Black data points represent baseline measurements while white data points represent measurements collected during 5-minute reactive hyperemia.

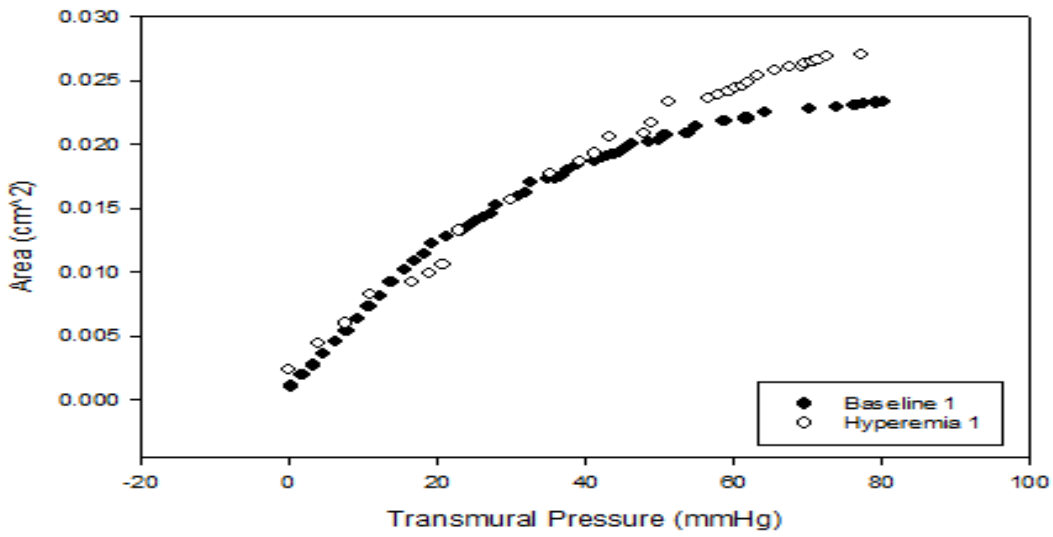

Figure 56. Arterial Lumen Area vs. Arterial Transmural Pressure of Female Participant (F3) 30 Minutes Before Cold-Water Immersion. Black data points represent baseline measurements while white data points represent measurements collected during 5-minute reactive hyperemia. Integrated from 0 mmHg to 80 mmHg transmural pressure.

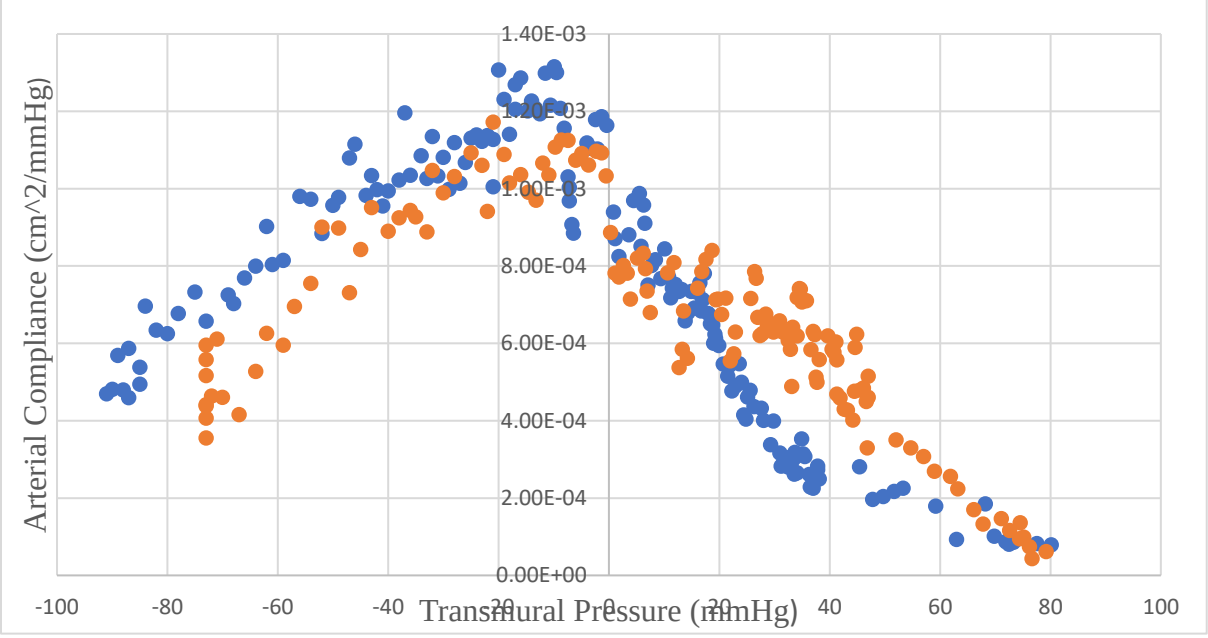

Figure 57. Arterial Area Compliance vs. Transmural Arterial Pressure of Female Participant (F3) Immediately After Cold-Water Immersion. Blue data points represent baseline measurements while orange data points represent measurements collected during 5-minute reactive hyperemia.

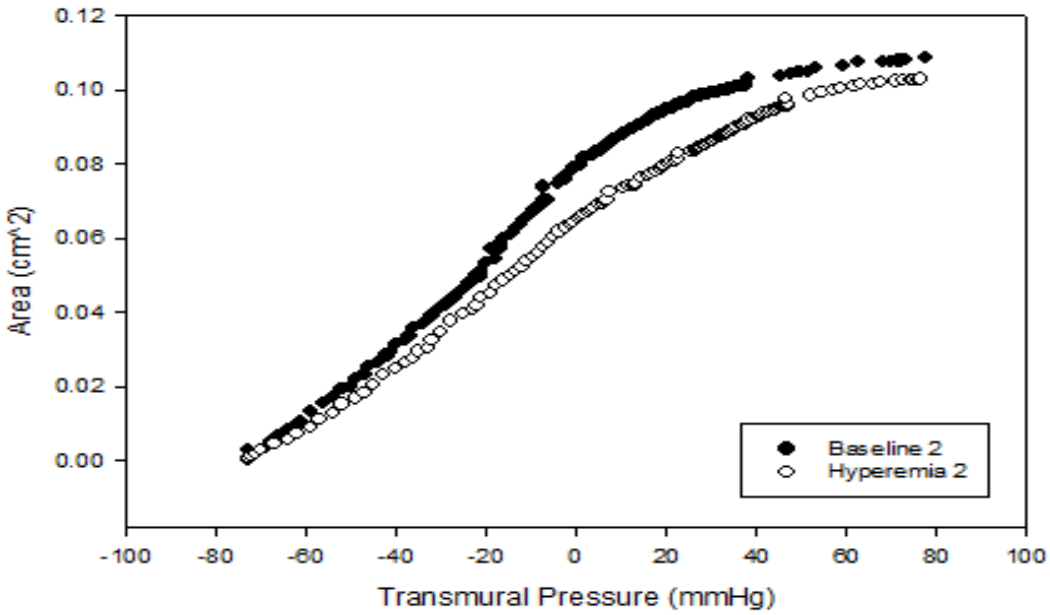

Figure 58. Arterial Lumen Area vs. Arterial Transmural Pressure of Female Participant (F3) Immediately After Cold-Water Immersion. Black data points represent baseline measurements while white data points represent measurements collected during 5-minute reactive hyperemia.

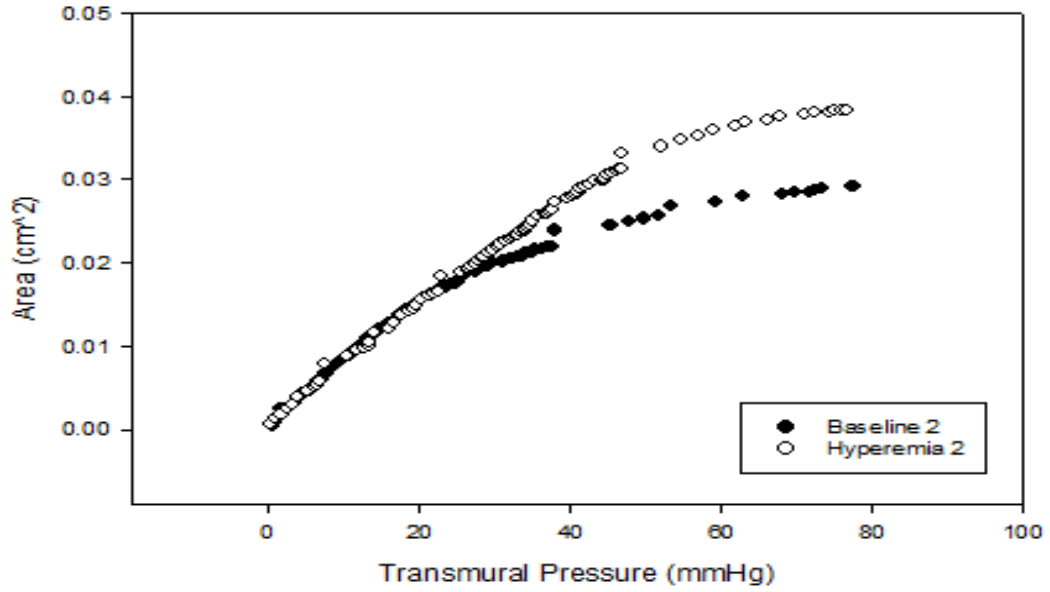

Figure 59. Arterial Lumen Area vs. Arterial Transmural Pressure of Female Participant (F3) Immediately After Cold-Water Immersion. Black data points represent baseline measurements while white data points represent measurements collected during 5-minute reactive hyperemia. Integrated from 0 mmHg to 80 mmHg transmural pressure.

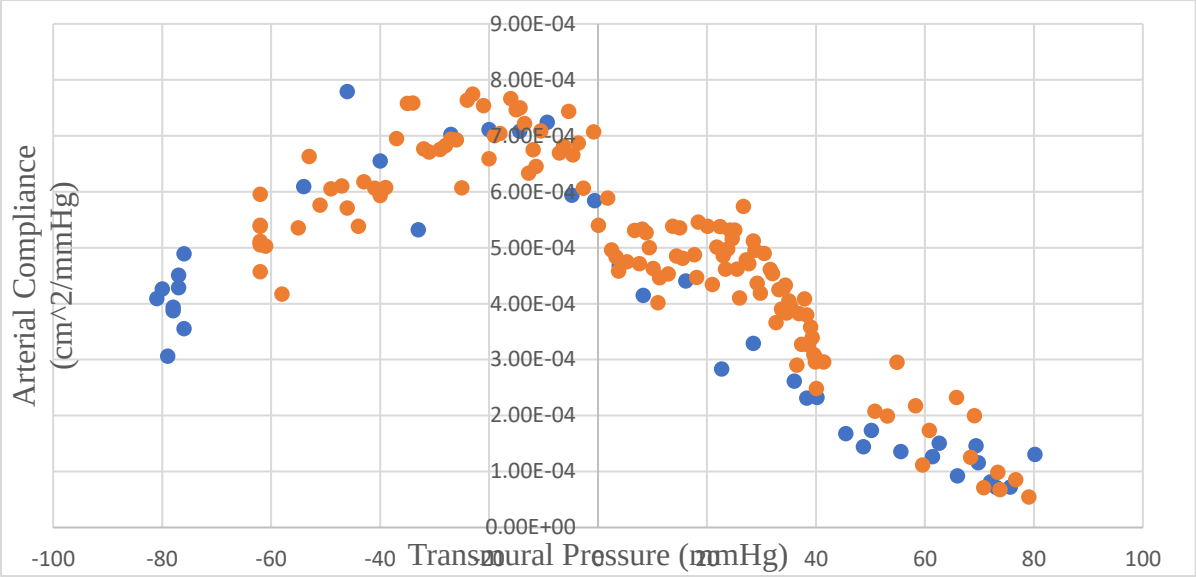

Figure 60. Arterial Area Compliance vs. Transmural Arterial Pressure of Female Participant (F3) 30 Minutes After Cold-Water Immersion. Blue data points represent baseline measurements while orange data points represent measurements collected during 5-minute reactive hyperemia.

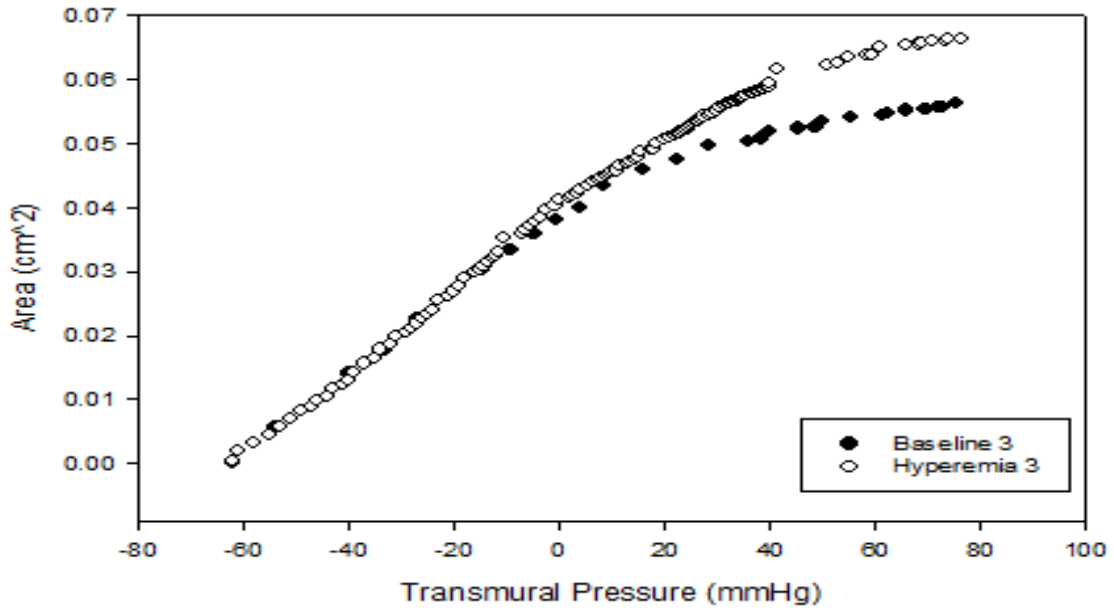

Figure 61. Arterial Lumen Area vs. Arterial Transmural Pressure of Female Participant (F3) 30 Minutes After Cold-Water Immersion. Black data points represent baseline measurements while white data points represent measurements collected during 5-minute reactive hyperemia.

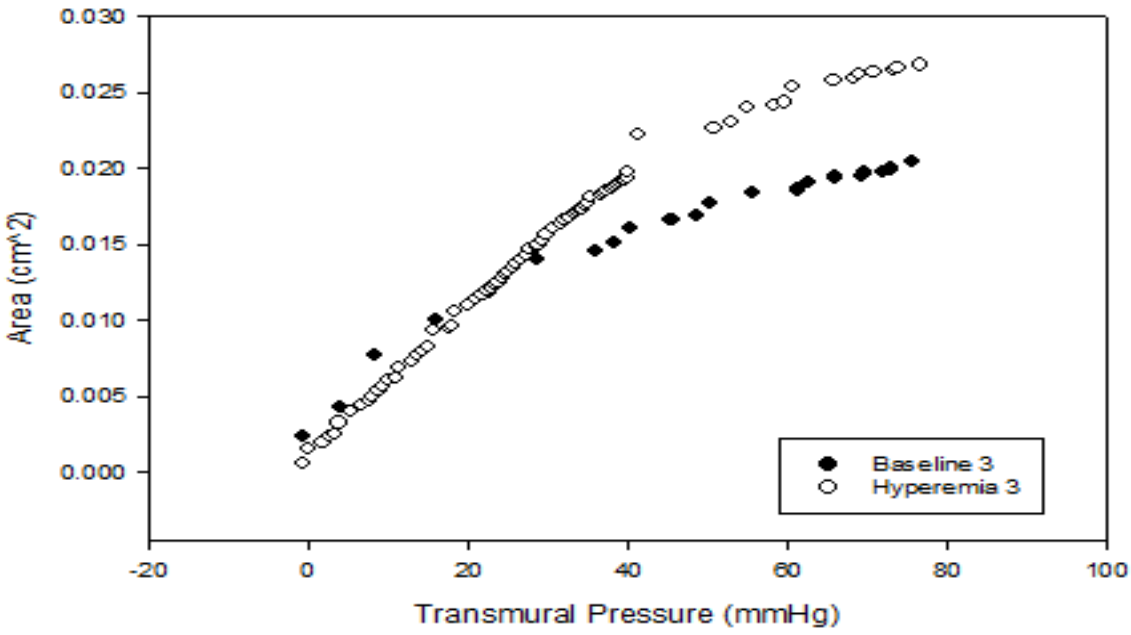

Figure 62. Arterial Lumen Area vs. Arterial Transmural Pressure of Female Participant (F3) 30 Minutes After Cold-Water Immersion. Black data points represent baseline measurements while white data points represent measurements collected during 5-minute reactive hyperemia. Integrated from 0 mmHg to 80 mmHg transmural pressure.

Participant: F4

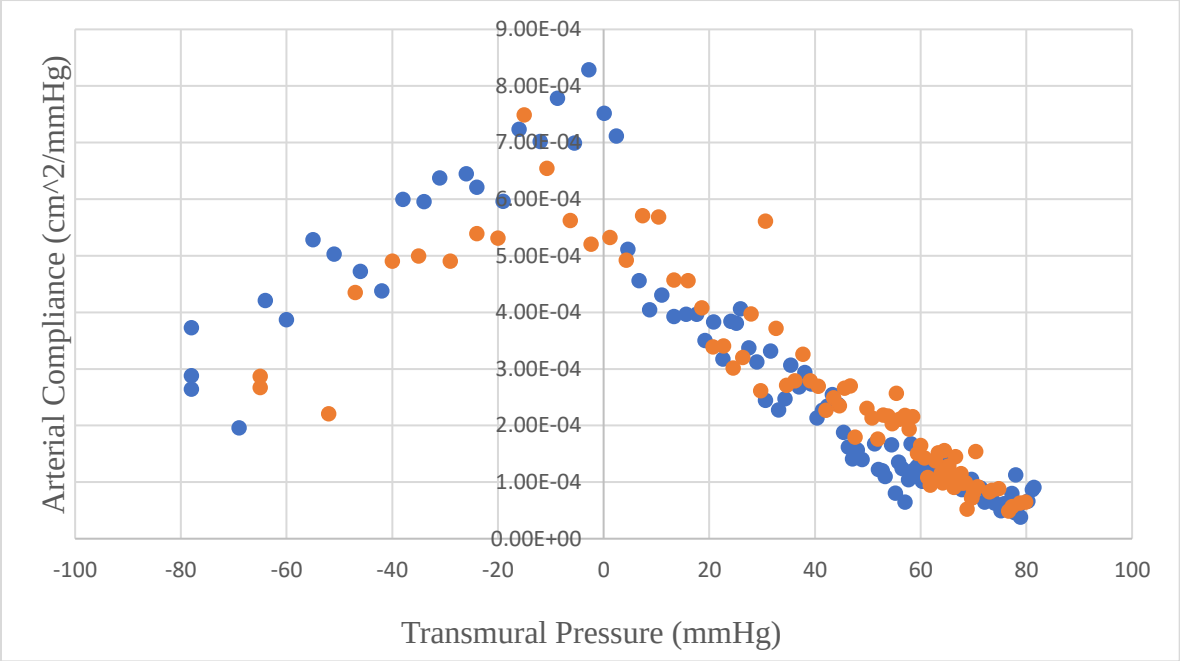

Figure 63. Arterial Area Compliance vs. Transmural Arterial Pressure of Female Participant (F4) 30 Minutes Before Cold-Water Immersion. Blue data points represent baseline measurements while orange data points represent measurements collected during 5-minute reactive hyperemia.

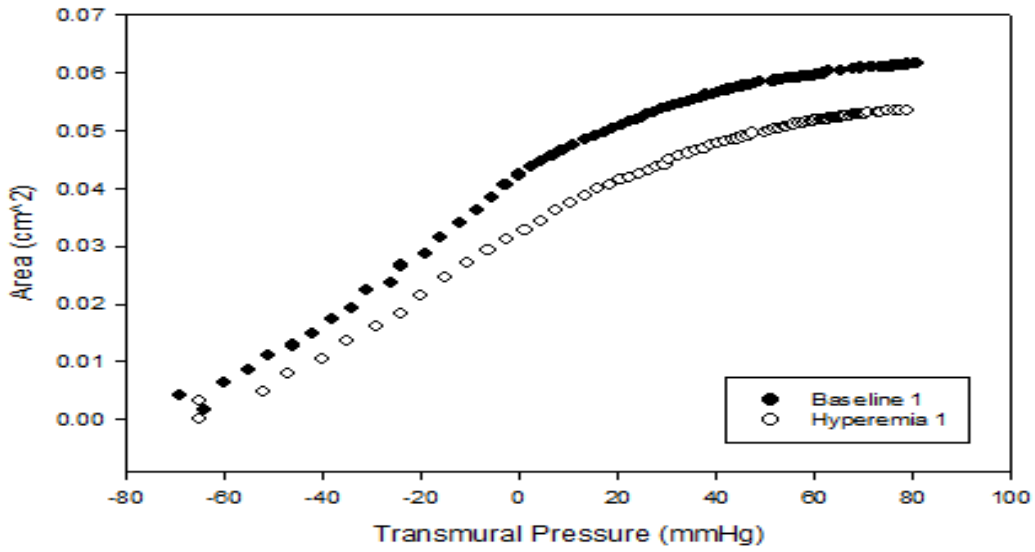

Figure 64. Arterial Lumen Area vs. Arterial Transmural Pressure of Female Participant (F4) 30 Minutes Before Cold-Water Immersion. Black data points represent baseline measurements while white data points represent measurements collected during 5-minute reactive hyperemia.

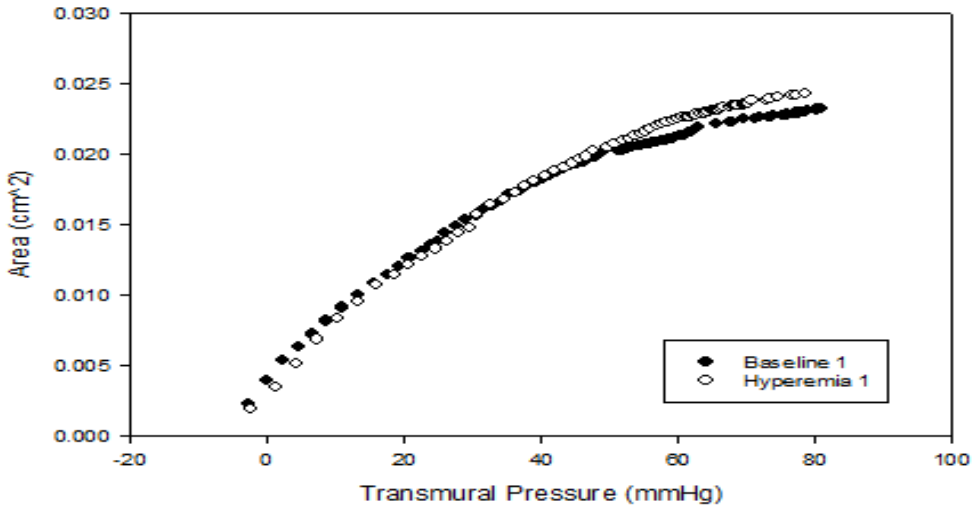

Figure 65. Arterial Lumen Area vs. Arterial Transmural Pressure of Female Participant (F4) 30 Minutes Before Cold-Water Immersion. Black data points represent baseline measurements while white data points represent measurements collected during 5-minute reactive hyperemia. Integrated from 0 mmHg to 80 mmHg transmural pressure.

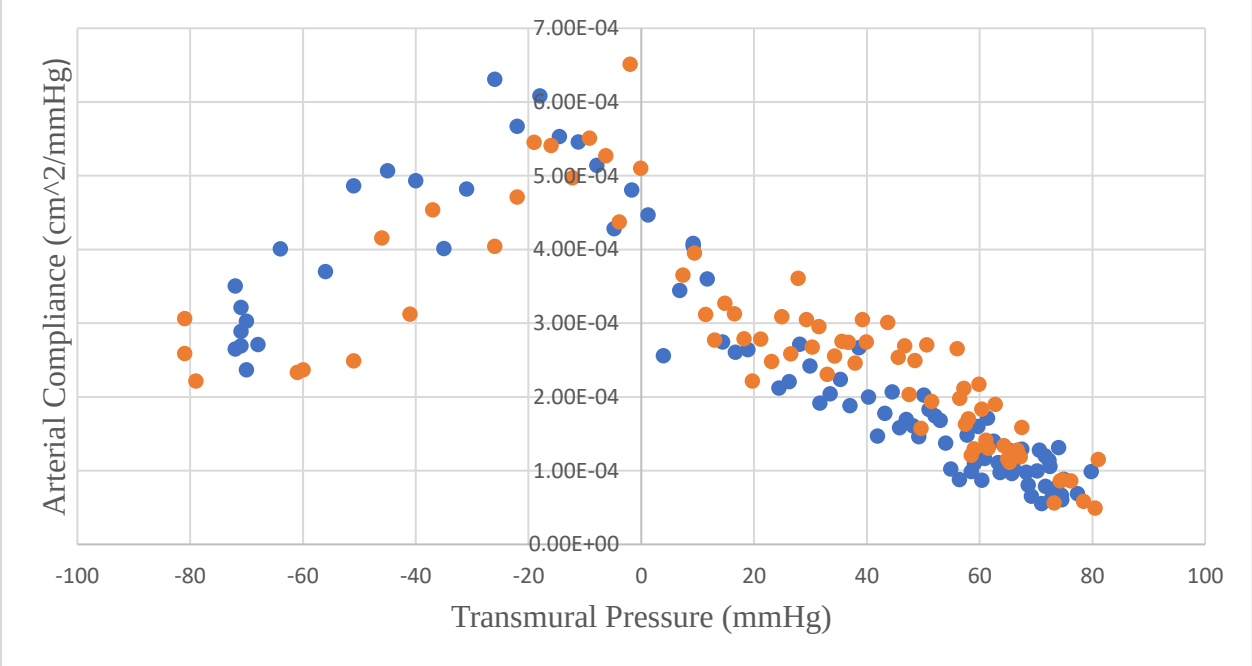

Figure 66. Arterial Area Compliance vs. Transmural Arterial Pressure of Female Participant (F4) Immediately After Cold-Water Immersion. Blue data points represent baseline measurements while orange data points represent measurements collected during 5-minute reactive hyperemia.

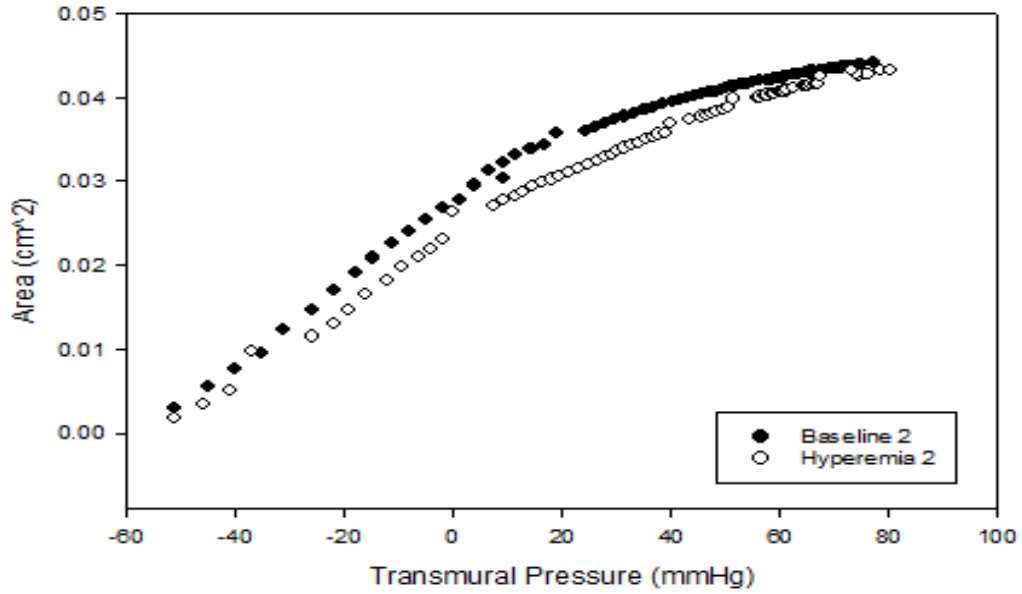

Figure 67. Arterial Lumen Area vs. Arterial Transmural Pressure of Female Participant (F4) Immediately After Cold-Water Immersion. Black data points represent baseline measurements while white data points represent measurements collected during 5-minute reactive hyperemia.

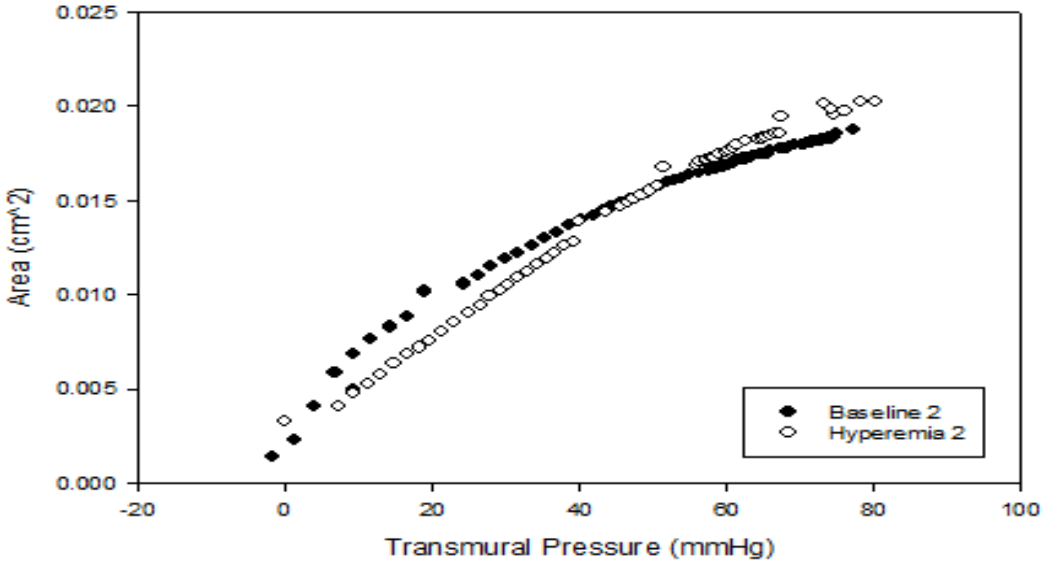

Figure 68. Arterial Lumen Area vs. Arterial Transmural Pressure of Female Participant (F4) Immediately After Cold-Water Immersion. Black data points represent baseline measurements while white data points represent measurements collected during 5-minute reactive hyperemia. Integrated from 0 mmHg to 80 mmHg transmural pressure.

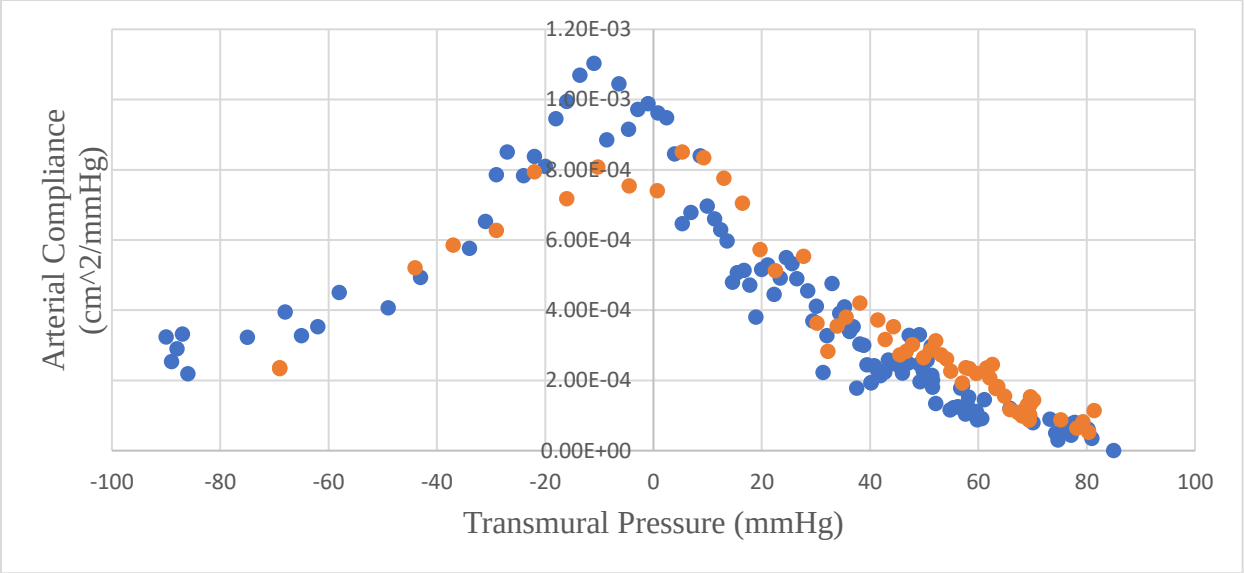

Figure 69. Arterial Area Compliance vs. Transmural Arterial Pressure of Female Participant (F4) 30 Minutes After Cold-Water Immersion. Blue data points represent baseline measurements while orange data points represent measurements collected during 5-minute reactive hyperemia.

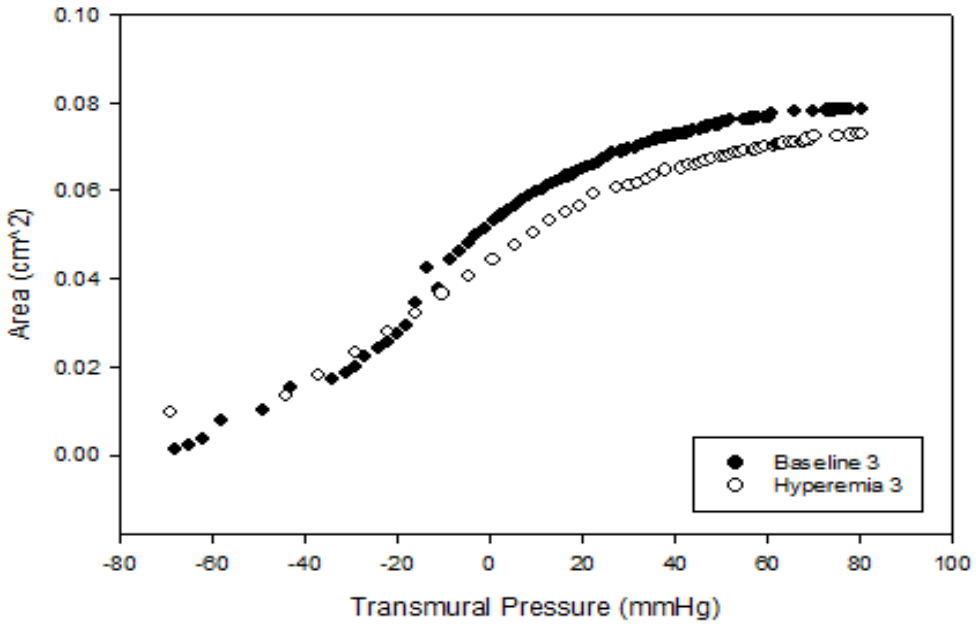

Figure 70. Arterial Lumen Area vs. Arterial Transmural Pressure of Female Participant (F4) 30 Minutes After Cold-Water Immersion. Black data points represent baseline measurements while white data points represent measurements collected during 5-minute reactive hyperemia.

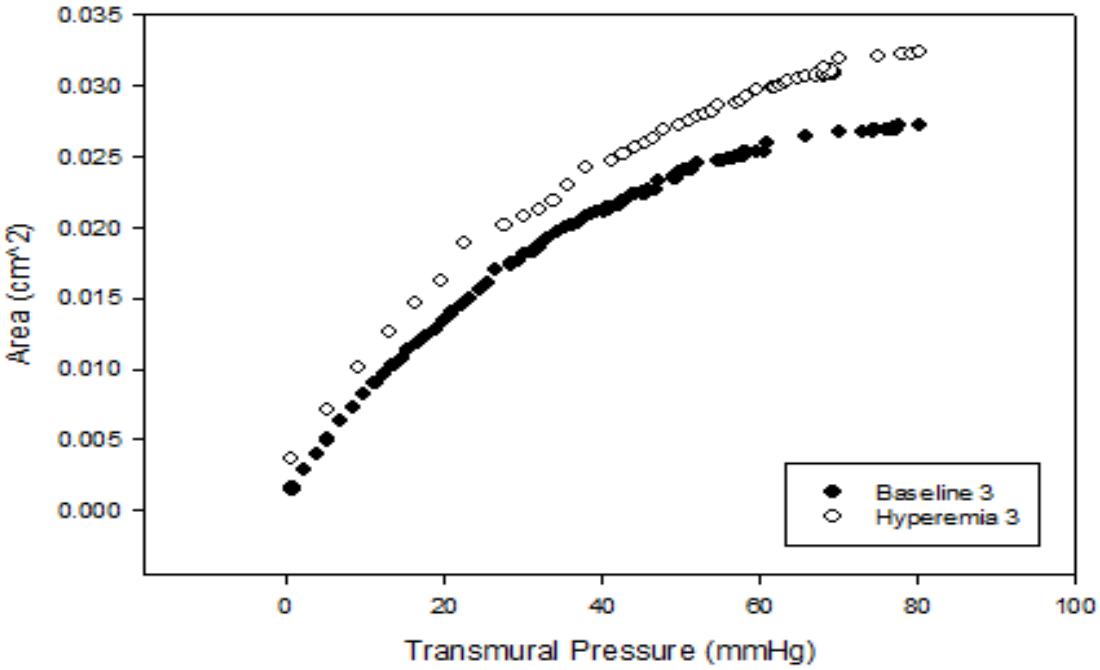

Figure 71. Arterial Lumen Area vs. Arterial Transmural Pressure of Female Participant (F4) 30 Minutes After Cold-Water Immersion. Black data points represent baseline measurements while white data points represent measurements collected during 5-minute reactive hyperemia. Integrated from 0 mmHg to 80 mmHg transmural pressure.

Participant: F5

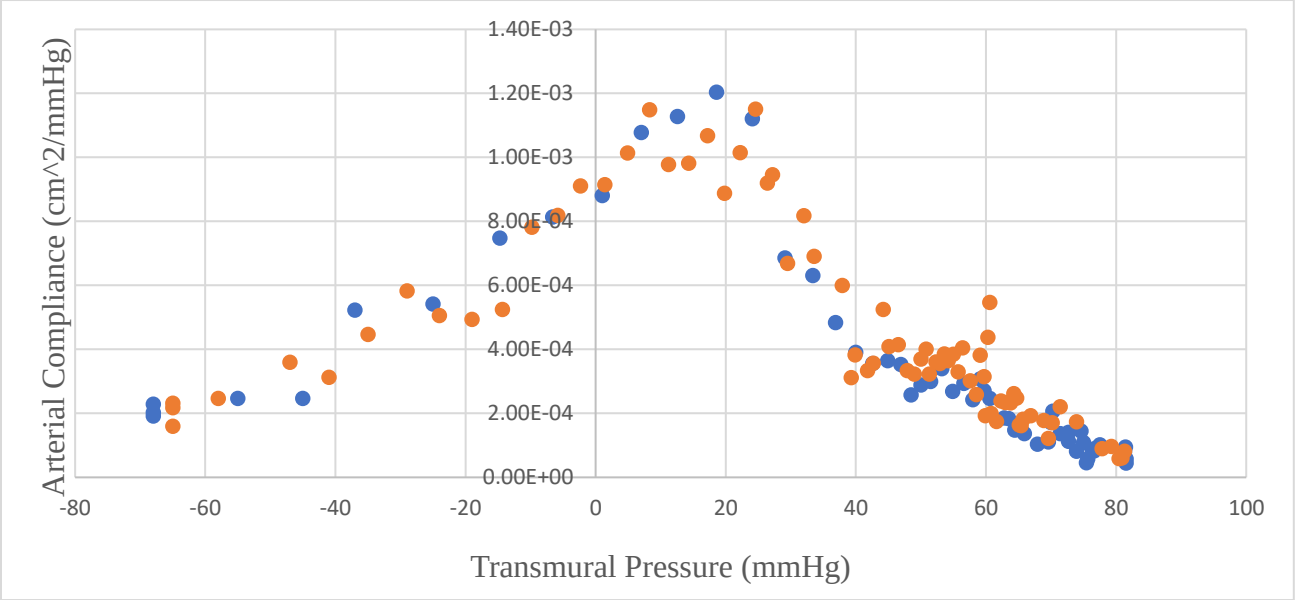

Figure 72. Arterial Area Compliance vs. Transmural Arterial Pressure of Female Participant (F5) 30 Minutes Before Cold-Water Immersion. Blue data points represent baseline measurements while orange data points represent measurements collected during 5-minute reactive hyperemia.

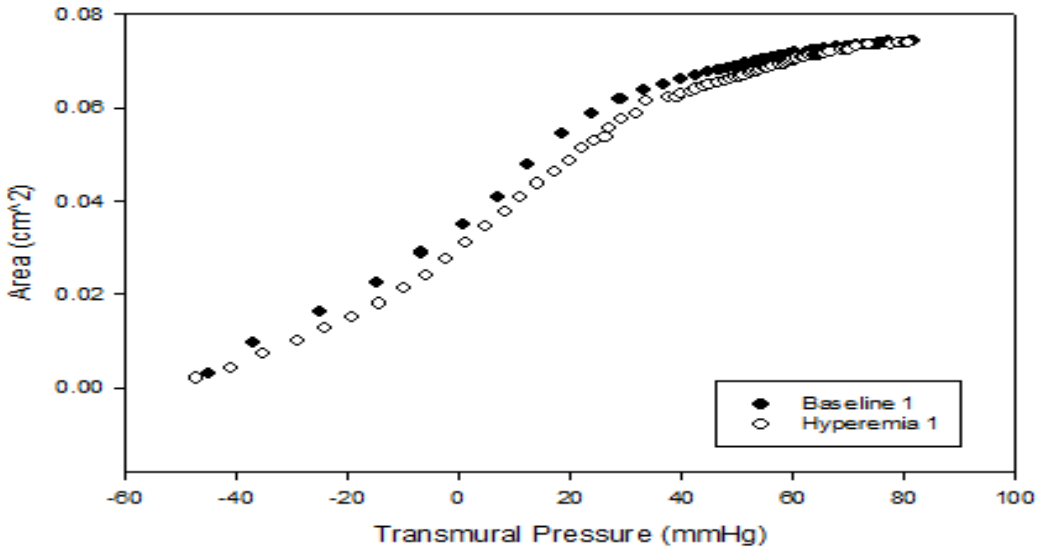

Figure 73. Arterial Lumen Area vs. Arterial Transmural Pressure of Female Participant (F5) 30 Minutes Before Cold-Water Immersion. Black data points represent baseline measurements while white data points represent measurements collected during 5-minute reactive hyperemia.

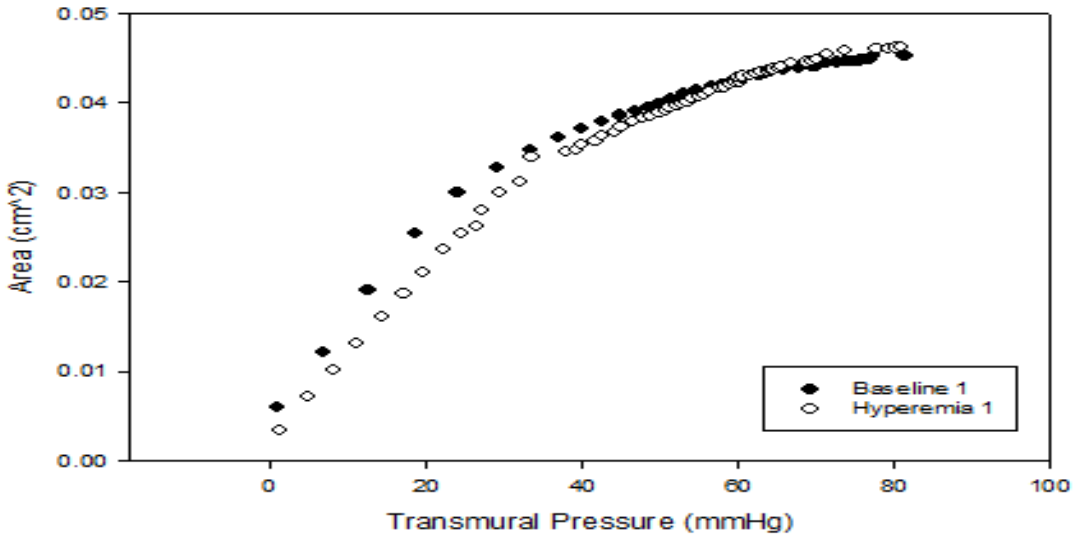

Figure 74. Arterial Lumen Area vs. Arterial Transmural Pressure of Female Participant (F5) 30 Minutes Before Cold-Water Immersion. Black data points represent baseline measurements while white data points represent measurements collected during 5-minute reactive hyperemia. Integrated from 0 mmHg to 80 mmHg transmural pressure.

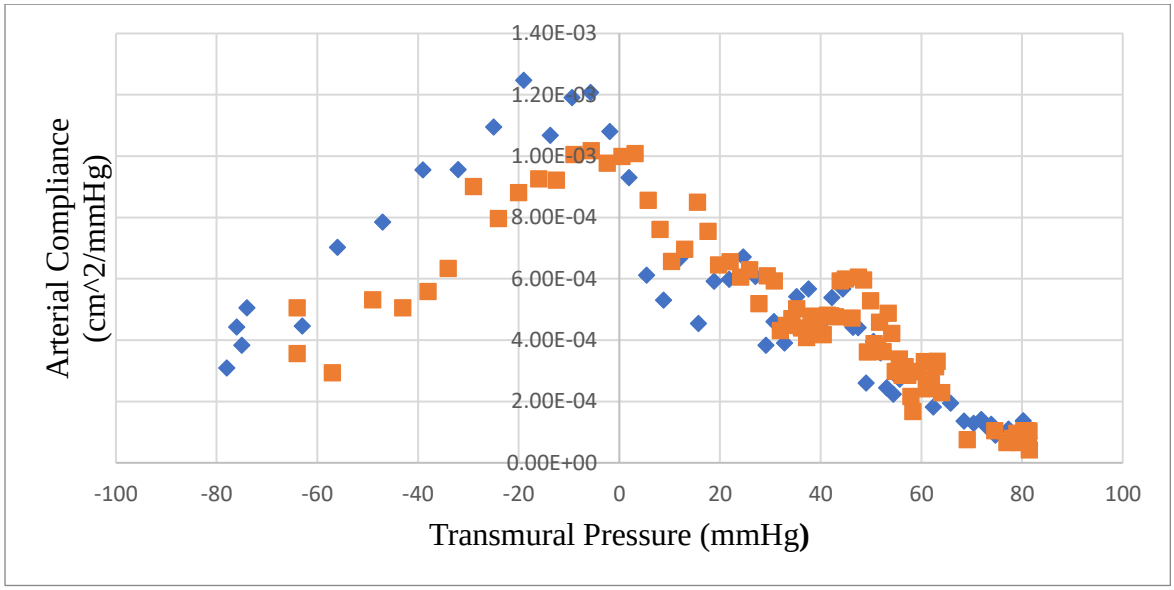

Figure 75. Arterial Area Compliance vs. Transmural Arterial Pressure of Female Participant (F5) Immediately After Cold-Water Immersion. Blue data points represent baseline measurements while orange data points represent measurements collected during 5-minute reactive hyperemia.

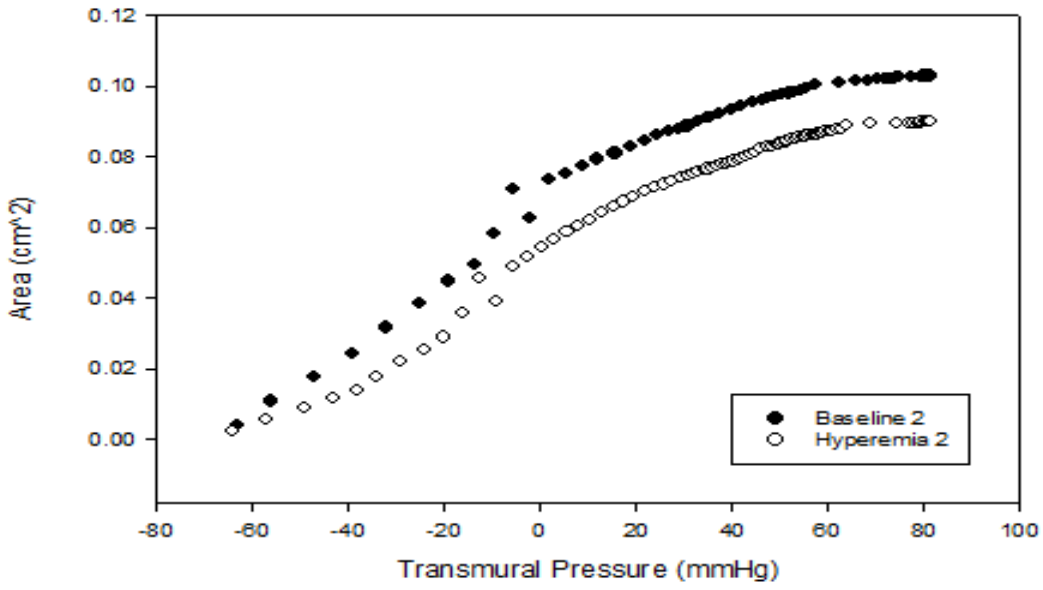

Figure 76. Arterial Lumen Area vs. Arterial Transmural Pressure of Female Participant (F5) Immediately After Cold-Water Immersion. Black data points represent baseline measurements while white data points represent measurements collected during 5-minute reactive hyperemia.

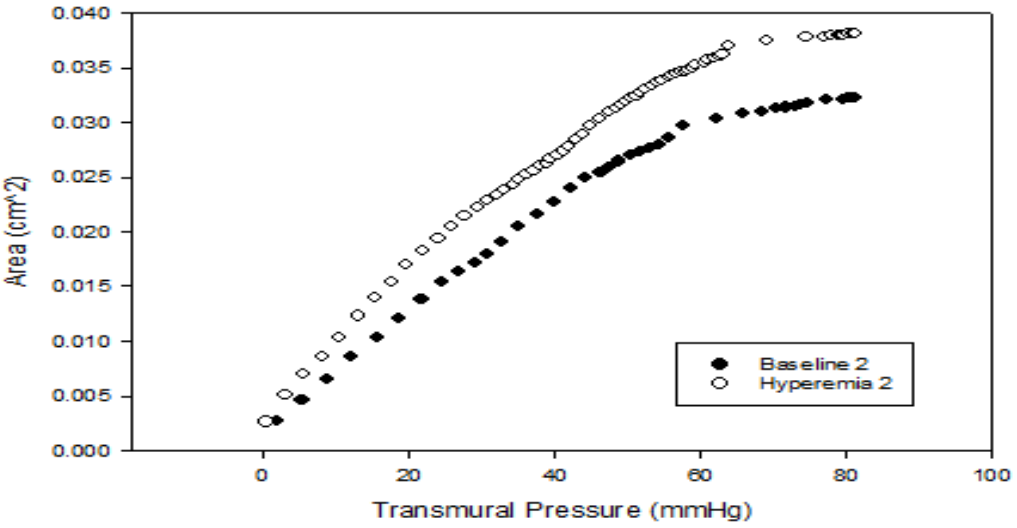

Figure 77. Arterial Lumen Area vs. Arterial Transmural Pressure of Female Participant (F5) Immediately After Cold-Water Immersion. Black data points represent baseline measurements while white data points represent measurements collected during 5-minute reactive hyperemia. Integrated from 0 mmHg to 80 mmHg transmural pressure.

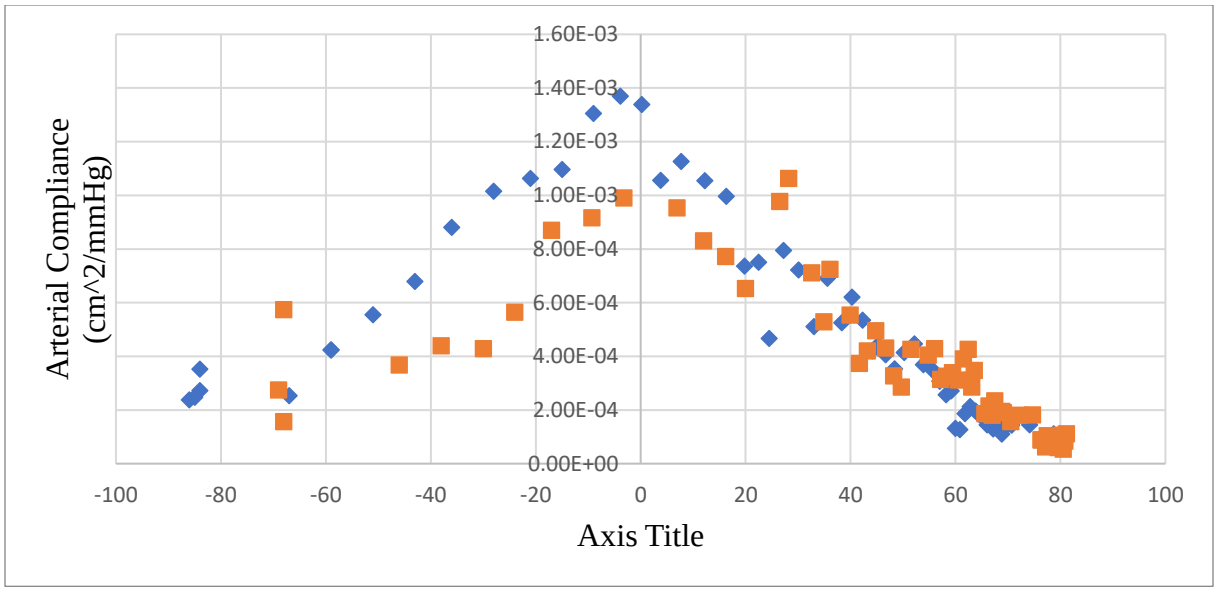

Figure 78. Arterial Area Compliance vs. Transmural Arterial Pressure of Female Participant (F5) 30 Minutes After Cold-Water Immersion. Blue data points represent baseline measurements while orange data points represent measurements collected during 5-minute reactive hyperemia.

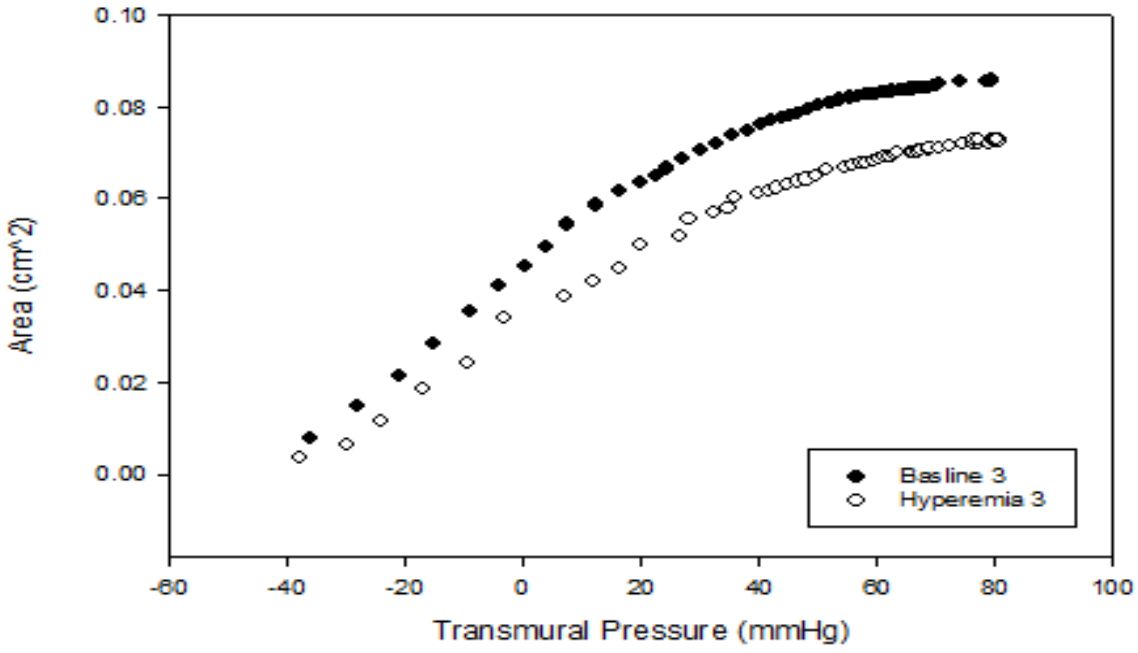

Figure 79. Arterial Lumen Area vs. Arterial Transmural Pressure of Female Participant (F5) 30 Minutes After Cold-Water Immersion. Black data points represent baseline measurements while white data points represent measurements collected during 5-minute reactive hyperemia.

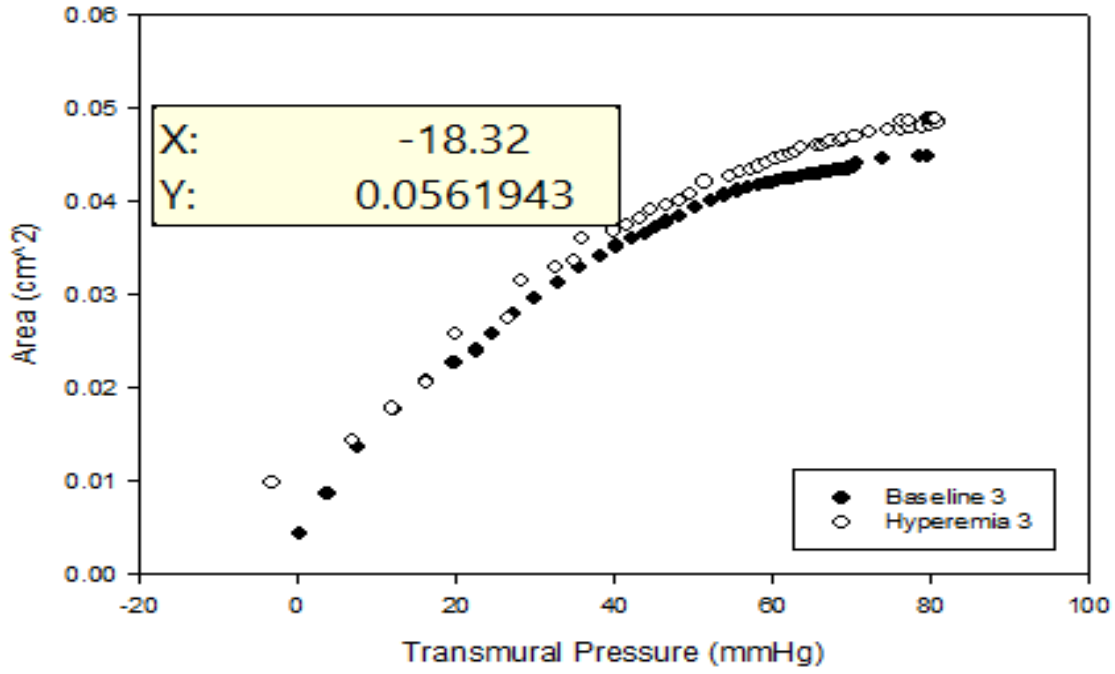

Figure 80. Arterial Lumen Area vs. Arterial Transmural Pressure of Female Participant (F5) 30 Minutes After Cold-Water Immersion. Black data points represent baseline measurements while white data points represent measurements collected during 5-minute reactive hyperemia. Integrated from 0 mmHg to 80 mmHg transmural pressure.

Participant: F6

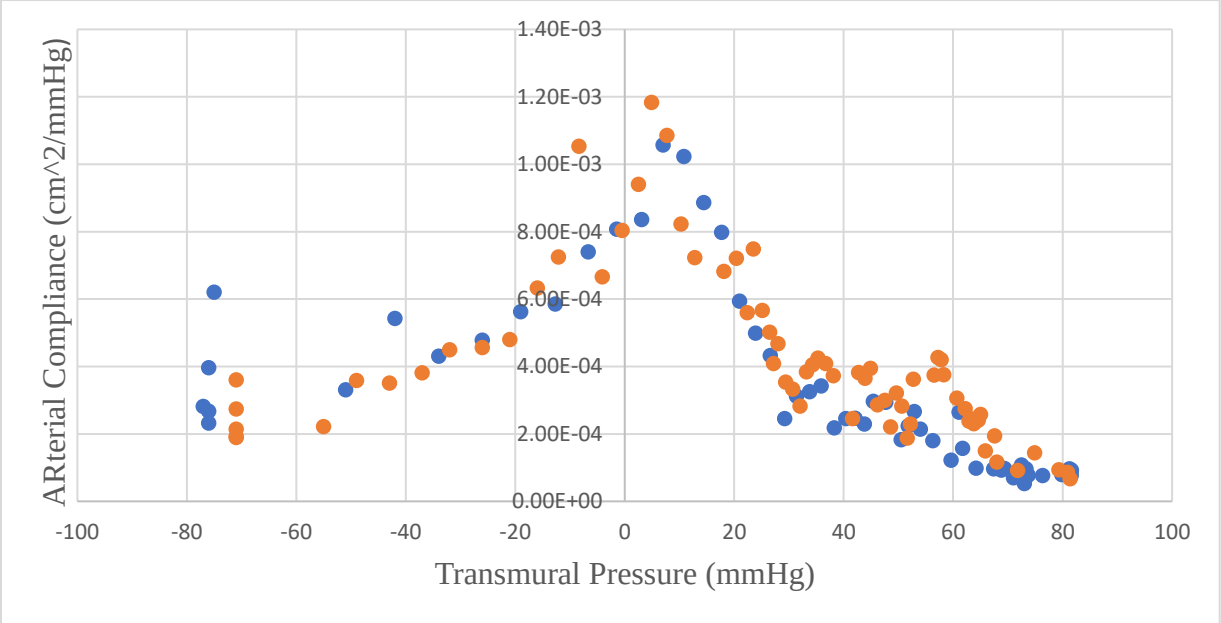

Figure 81. Arterial Area Compliance vs. Transmural Arterial Pressure of Female Participant (F6) 30 Minutes Before Cold-Water Immersion. Blue data points represent baseline measurements while orange data points represent measurements collected during 5-minute reactive hyperemia.

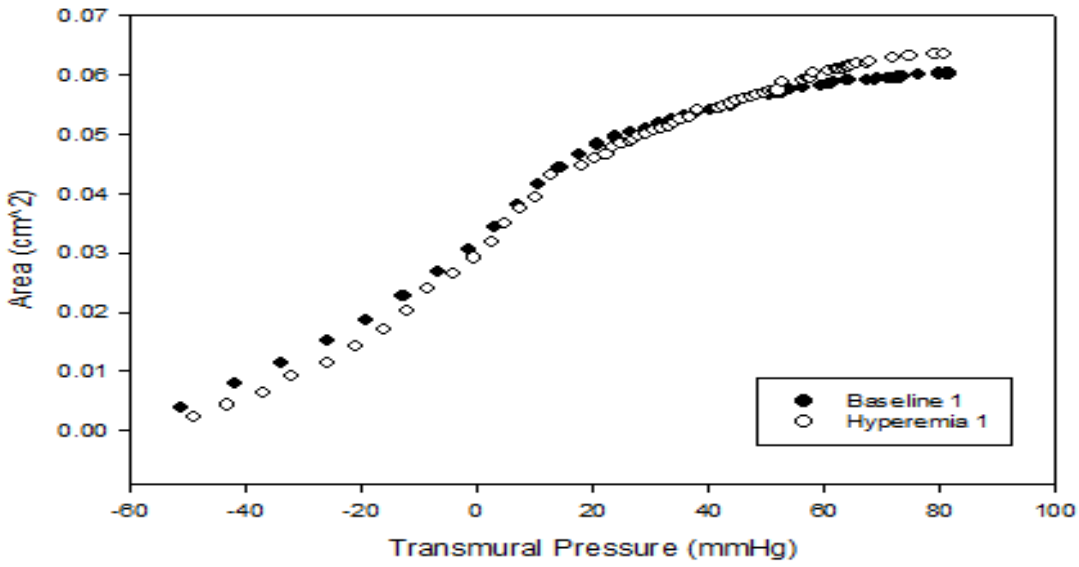

Figure 82. Arterial Lumen Area vs. Arterial Transmural Pressure of Female Participant (F6) 30 Minutes Before Cold-Water Immersion. Black data points represent baseline measurements while white data points represent measurements collected during 5-minute reactive hyperemia.

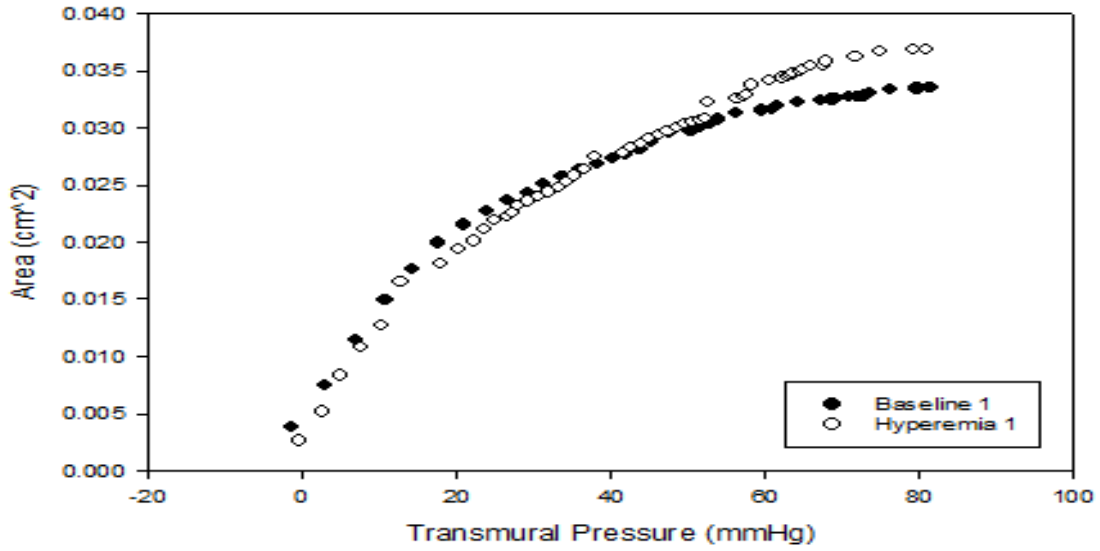

Figure 83. Arterial Lumen Area vs. Arterial Transmural Pressure of Female Participant (F6) 30 Minutes Before Cold-Water Immersion. Black data points represent baseline measurements while white data points represent measurements collected during 5-minute reactive hyperemia. Integrated from 0 mmHg to 80 mmHg transmural pressure.

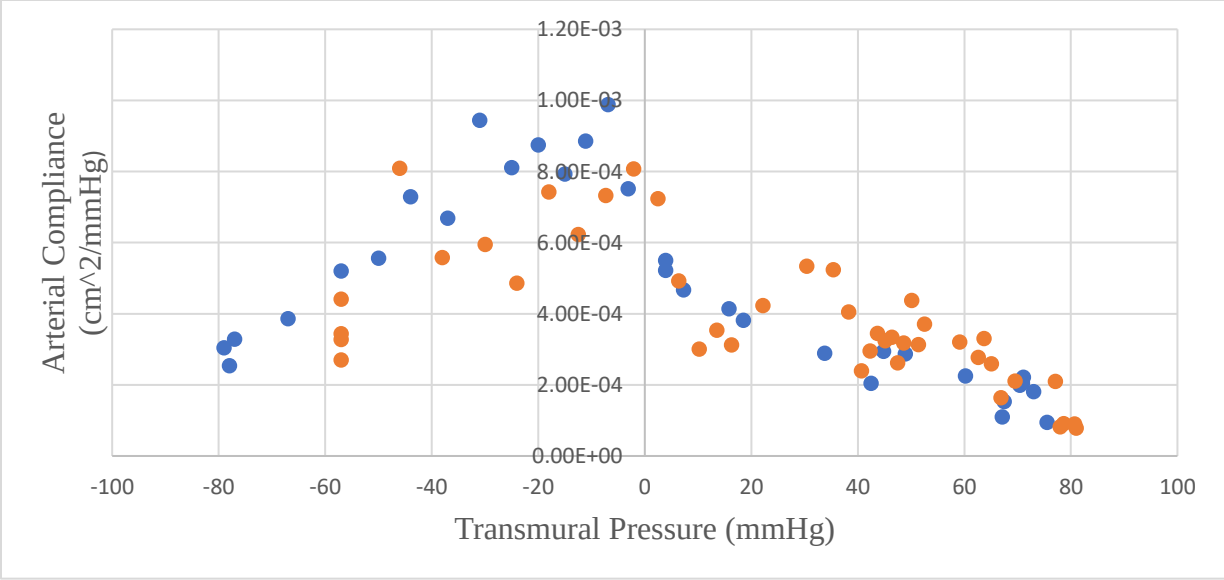

Figure 84. Arterial Area Compliance vs. Transmural Arterial Pressure of Female Participant (F6) Immediately After Cold-Water Immersion. Blue data points represent baseline measurements while orange data points represent measurements collected during 5-minute reactive hyperemia.

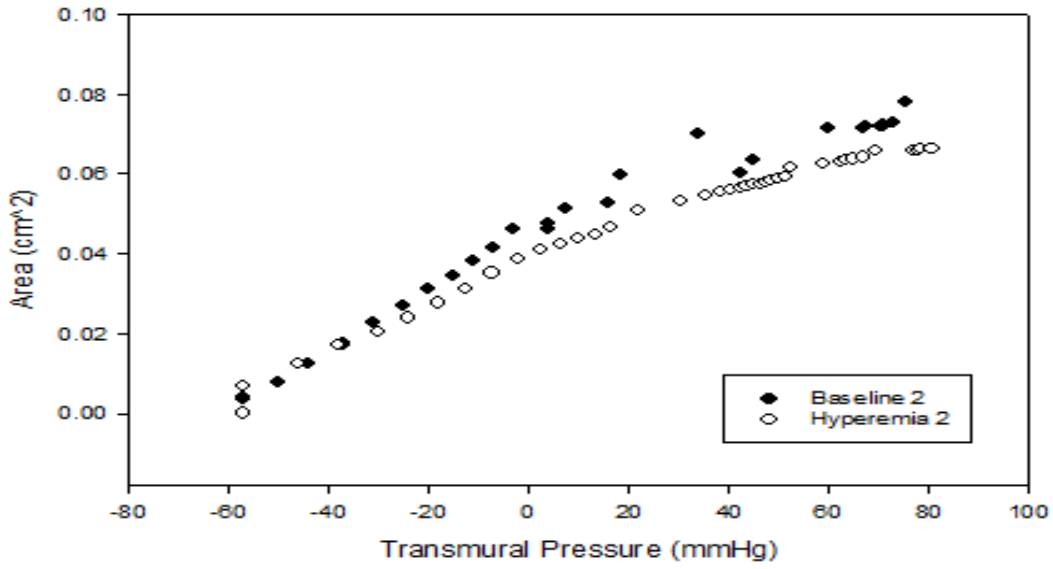

Figure 85. Arterial Lumen Area vs. Arterial Transmural Pressure of Female Participant (F6) Immediately After Cold-Water Immersion. Black data points represent baseline measurements while white data points represent measurements collected during 5-minute reactive hyperemia.

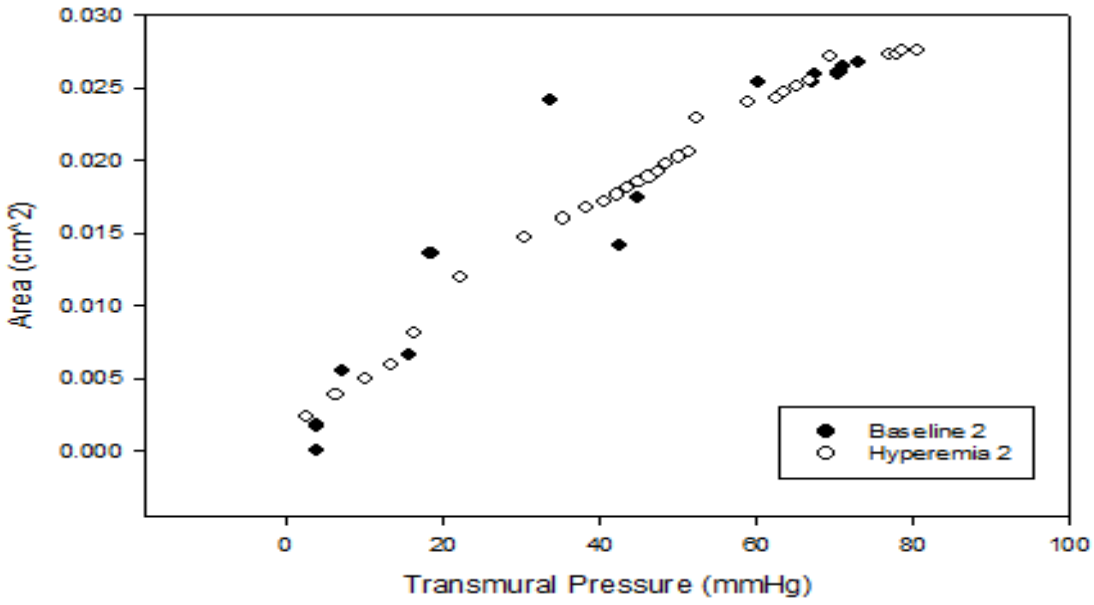

Figure 86. Arterial Lumen Area vs. Arterial Transmural Pressure of Female Participant (F6) Immediately After Cold-Water Immersion. Black data points represent baseline measurements while white data points represent measurements collected during 5-minute reactive hyperemia. Integrated from 0 mmHg to 80 mmHg transmural pressure.

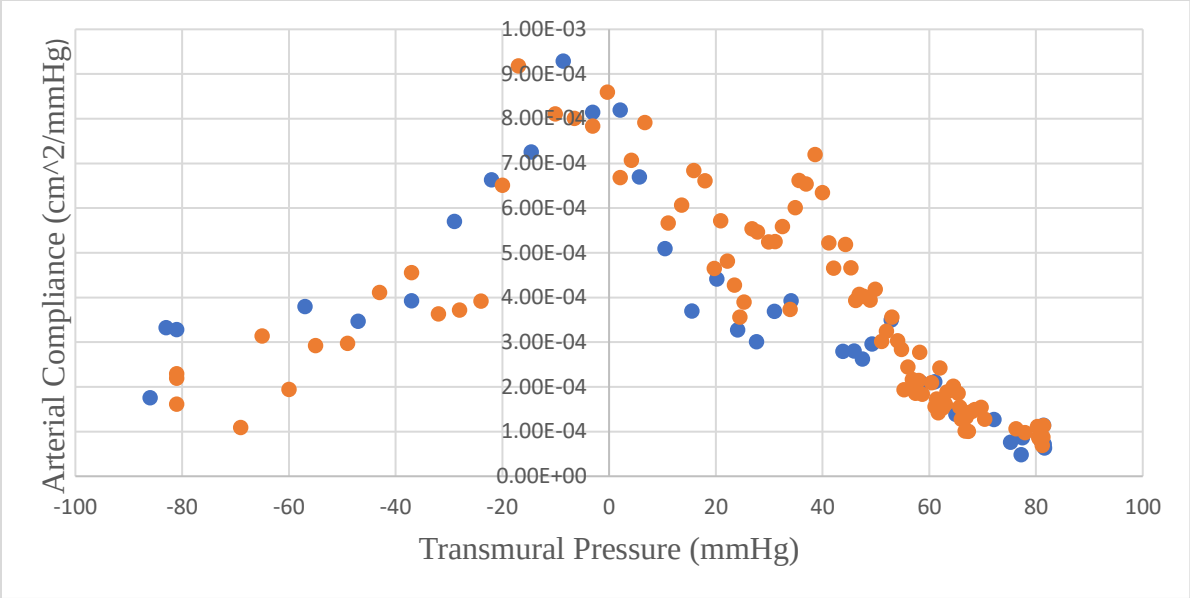

Figure 87. Arterial Area Compliance vs. Transmural Arterial Pressure of Female Participant (F6) 30 Minutes After Cold-Water Immersion. Blue data points represent baseline measurements while orange data points represent measurements collected during 5-minute reactive hyperemia.

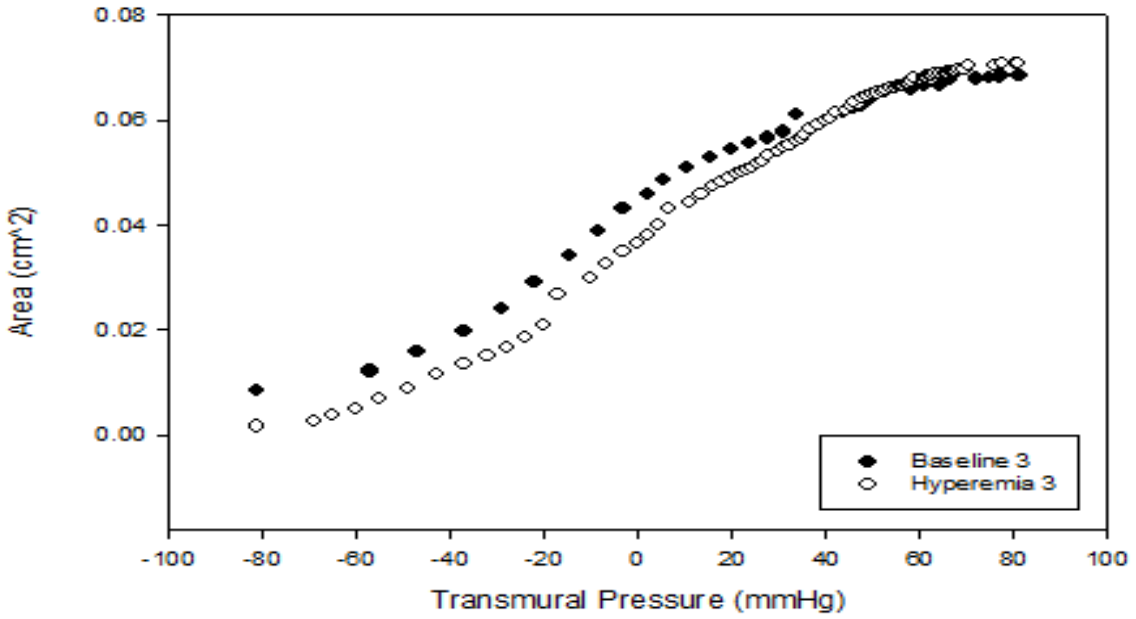

Figure 88. Arterial Lumen Area vs. Arterial Transmural Pressure of Female Participant (F6) 30 Minutes After Cold-Water Immersion. Black data points represent baseline measurements while white data points represent measurements collected during 5-minute reactive hyperemia.

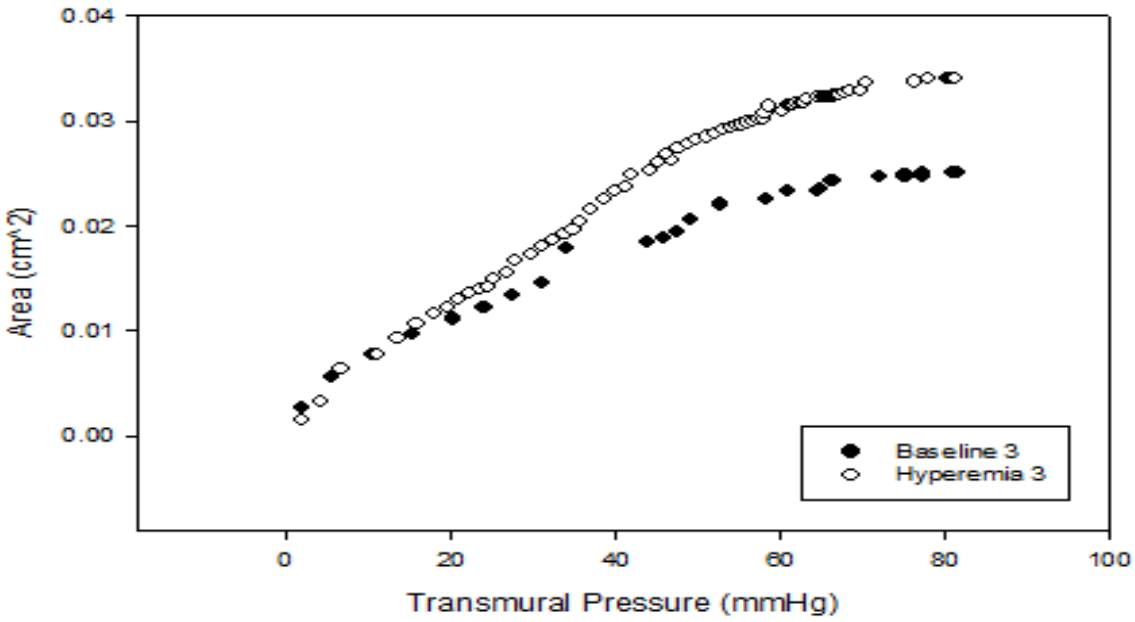

Figure 89. Arterial Lumen Area vs. Arterial Transmural Pressure of Female Participant (F6) 30 Minutes After Cold-Water Immersion. Black data points represent baseline measurements while white data points represent measurements collected during 5-minute reactive hyperemia. Integrated from 0 mmHg to 80 mmHg transmural pressure.

Participant: F7

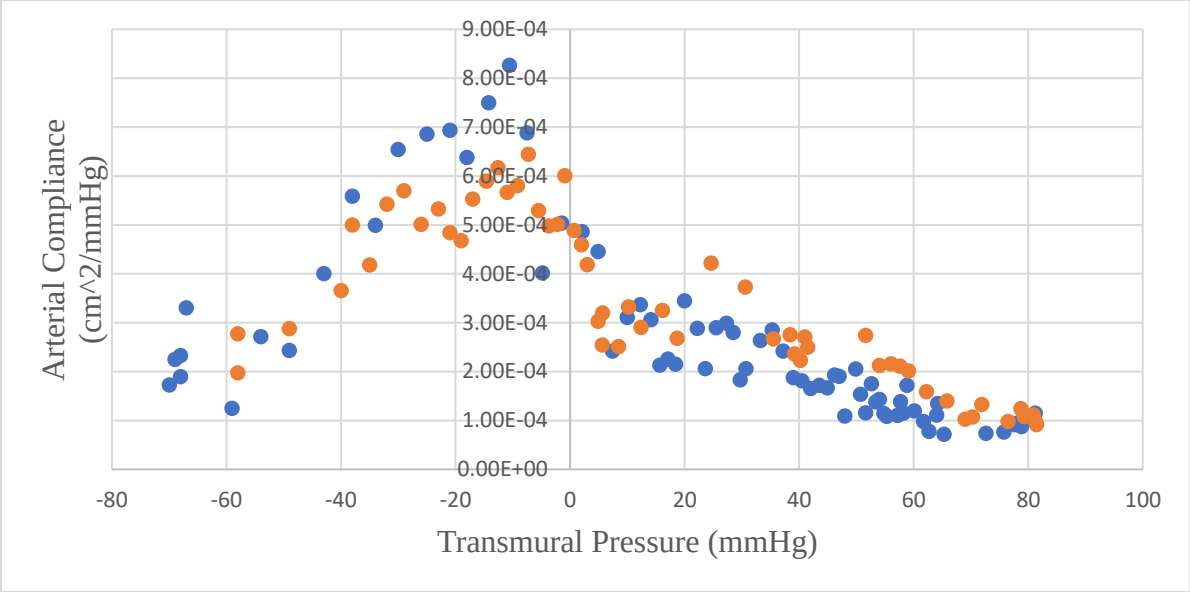

Figure 90. Arterial Area Compliance vs. Transmural Arterial Pressure of Female Participant (F7) 30 Minutes Before Cold-Water Immersion. Blue data points represent baseline measurements while orange data points represent measurements collected during 5-minute reactive hyperemia.

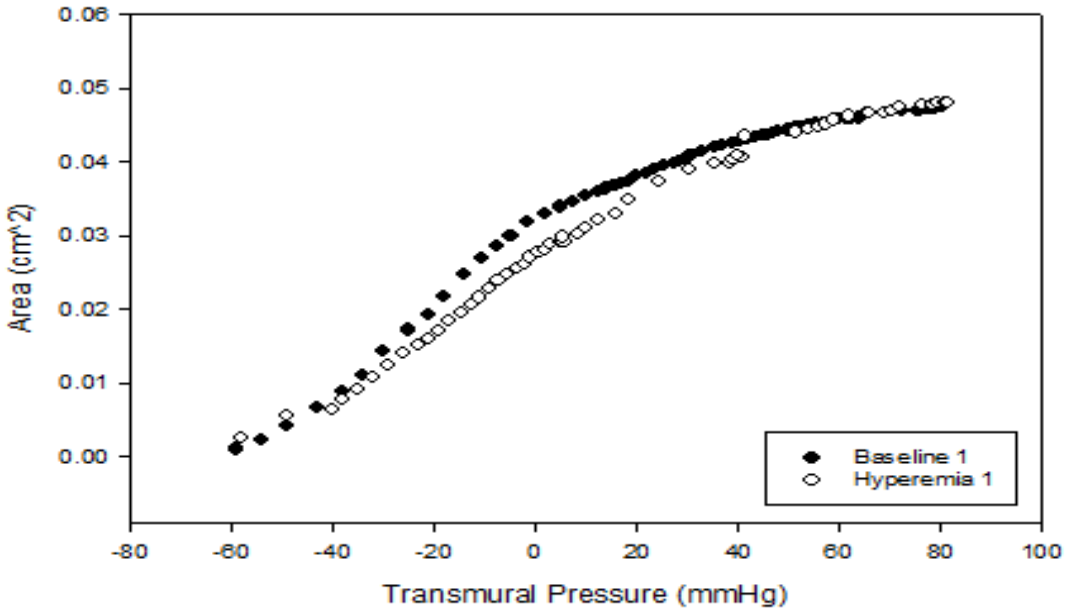

Figure 91. Arterial Lumen Area vs. Arterial Transmural Pressure of Female Participant (F7) 30 Minutes Before Cold-Water Immersion. Black data points represent baseline measurements while white data points represent measurements collected during 5-minute reactive hyperemia.

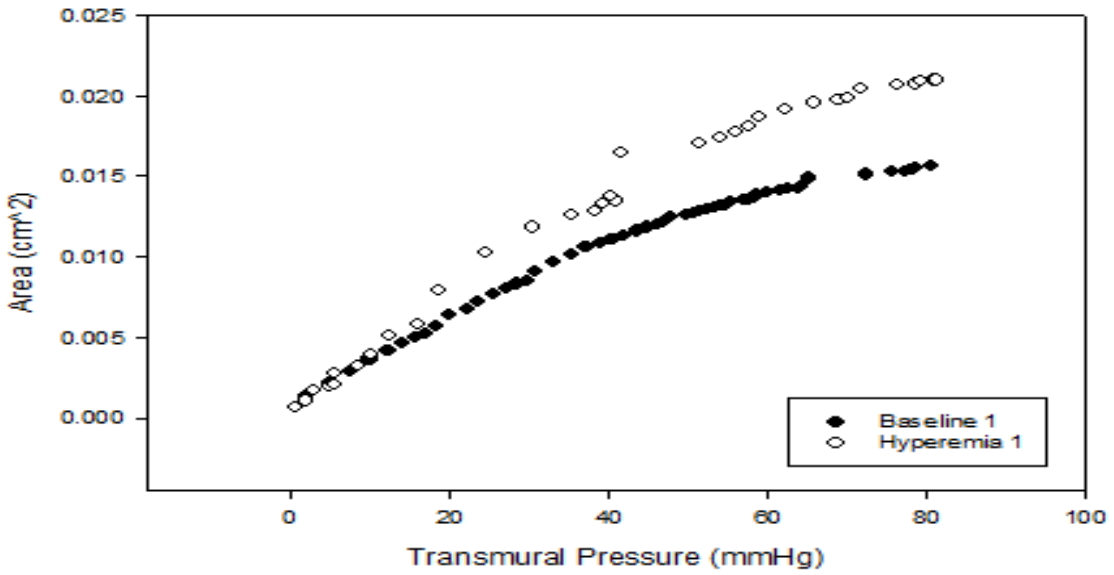

Figure 92. Arterial Lumen Area vs. Arterial Transmural Pressure of Female Participant (F7) 30 Minutes Before Cold-Water Immersion. Black data points represent baseline measurements while white data points represent measurements collected during 5-minute reactive hyperemia. Integrated from 0 mmHg to 80 mmHg transmural pressure.

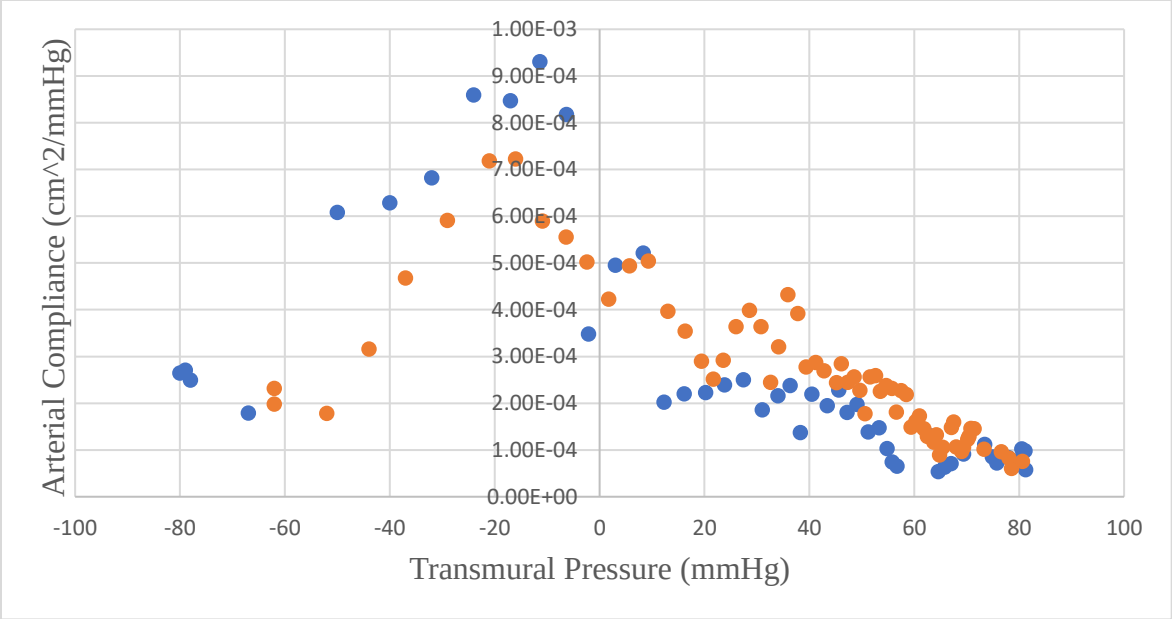

Figure 93. Arterial Area Compliance vs. Transmural Arterial Pressure of Female Participant (F7) Immediately After Cold-Water Immersion. Blue data points represent baseline measurements while orange data points represent measurements collected during 5-minute reactive hyperemia.

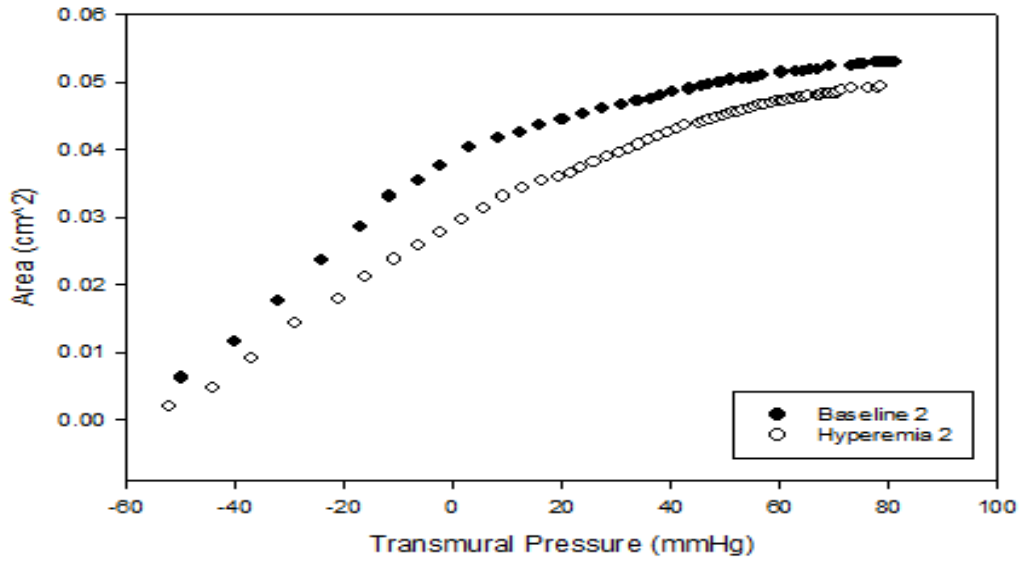

Figure 94. Arterial Lumen Area vs. Arterial Transmural Pressure of Female Participant (F7) Immediately After Cold-Water Immersion. Black data points represent baseline measurements while white data points represent measurements collected during 5-minute reactive hyperemia.

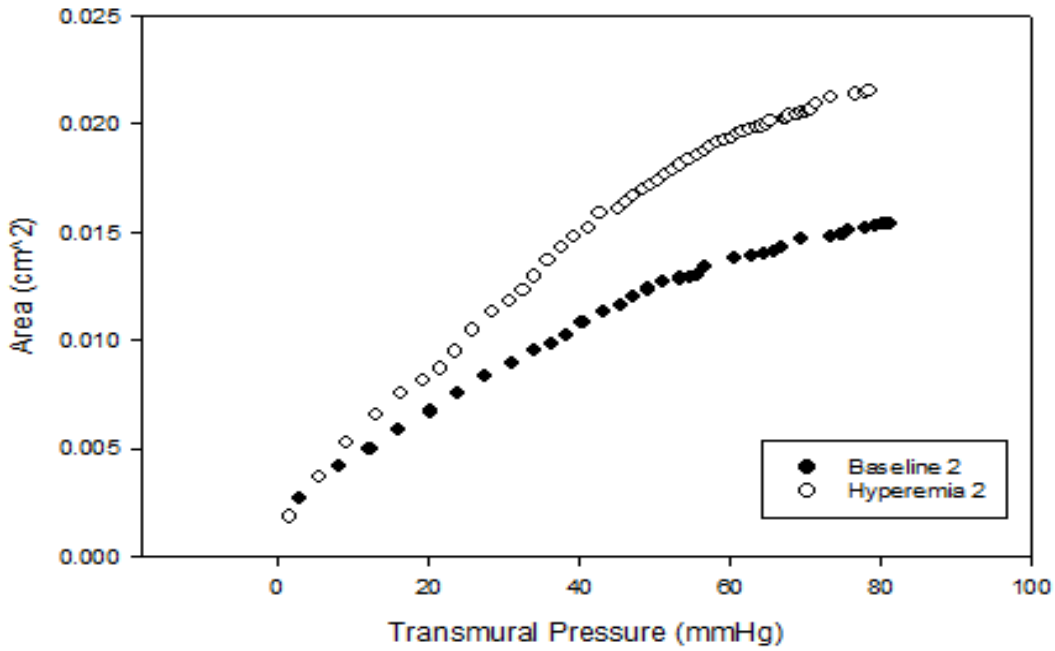

Figure 95. Arterial Lumen Area vs. Arterial Transmural Pressure of Female Participant (F7) Immediately After Cold-Water Immersion. Black data points represent baseline measurements while white data points represent measurements collected during 5-minute reactive hyperemia. Integrated from 0 mmHg to 80 mmHg transmural pressure.

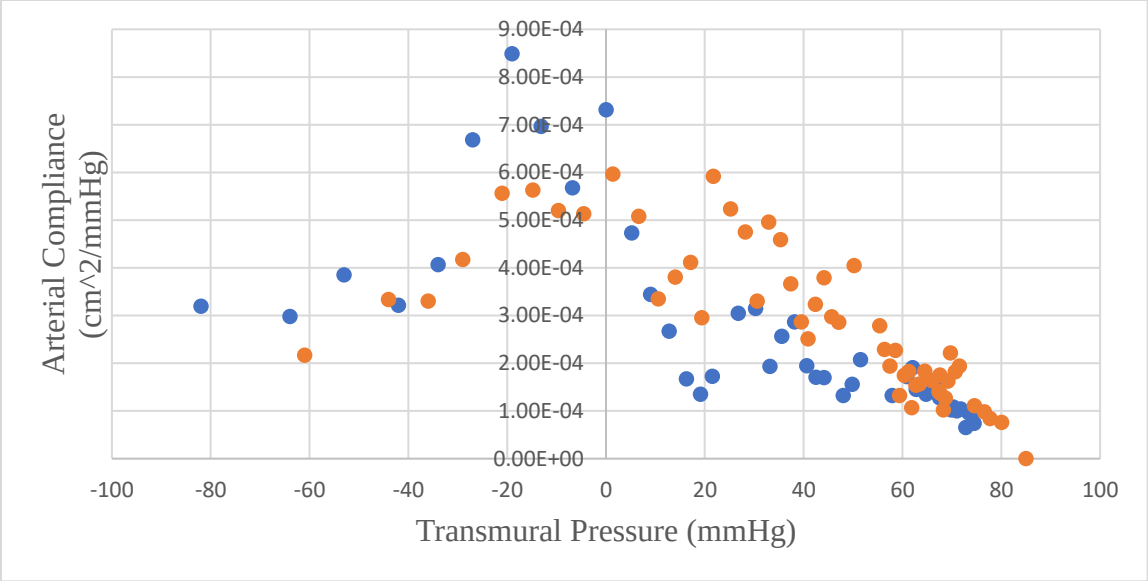

Figure 96. Arterial Area Compliance vs. Transmural Arterial Pressure of Female Participant (F7) 30 Minutes After Cold-Water Immersion. Blue data points represent baseline measurements while orange data points represent measurements collected during 5-minute reactive hyperemia.

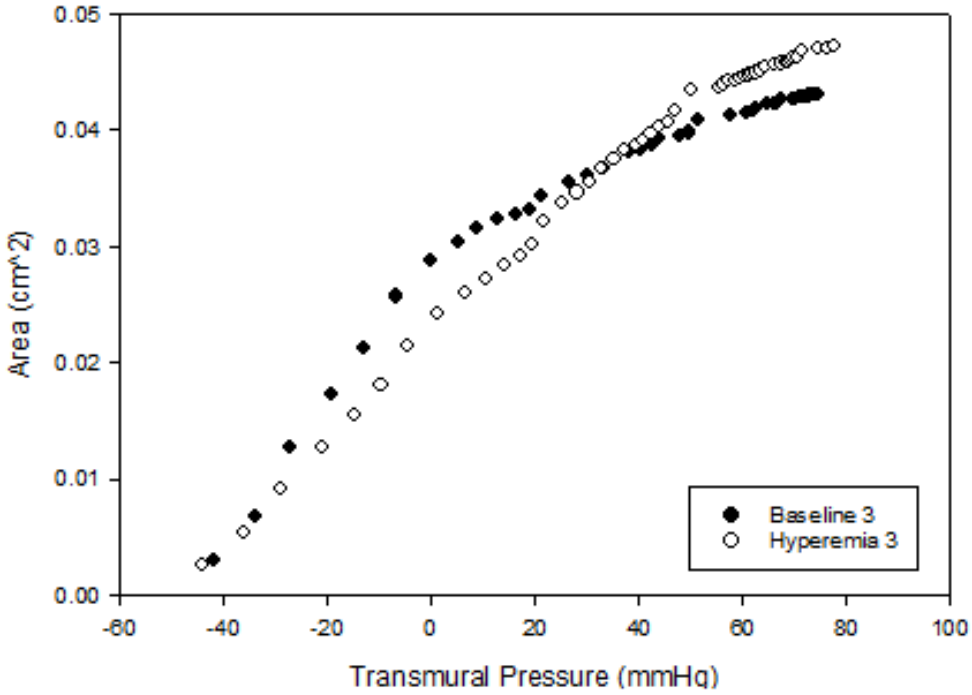

Figure 97. Arterial Lumen Area vs. Arterial Transmural Pressure of Female Participant (F7) 30 Minutes After Cold-Water Immersion. Black data points represent baseline measurements while white data points represent measurements collected during 5-minute reactive hyperemia.

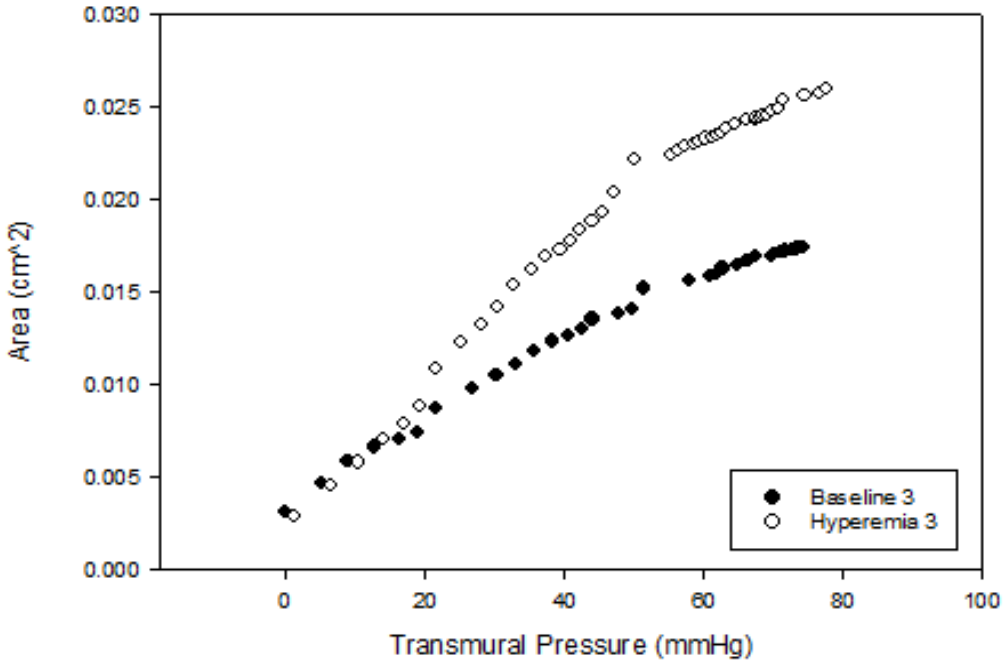

Figure 98. Arterial Lumen Area vs. Arterial Transmural Pressure of Female Participant (F7) 30 Minutes After Cold-Water Immersion. Black data points represent baseline measurements while white data points represent measurements collected during 5-minute reactive hyperemia. Integrated from 0 mmHg to 80 mmHg transmural pressure.

Participant: F8

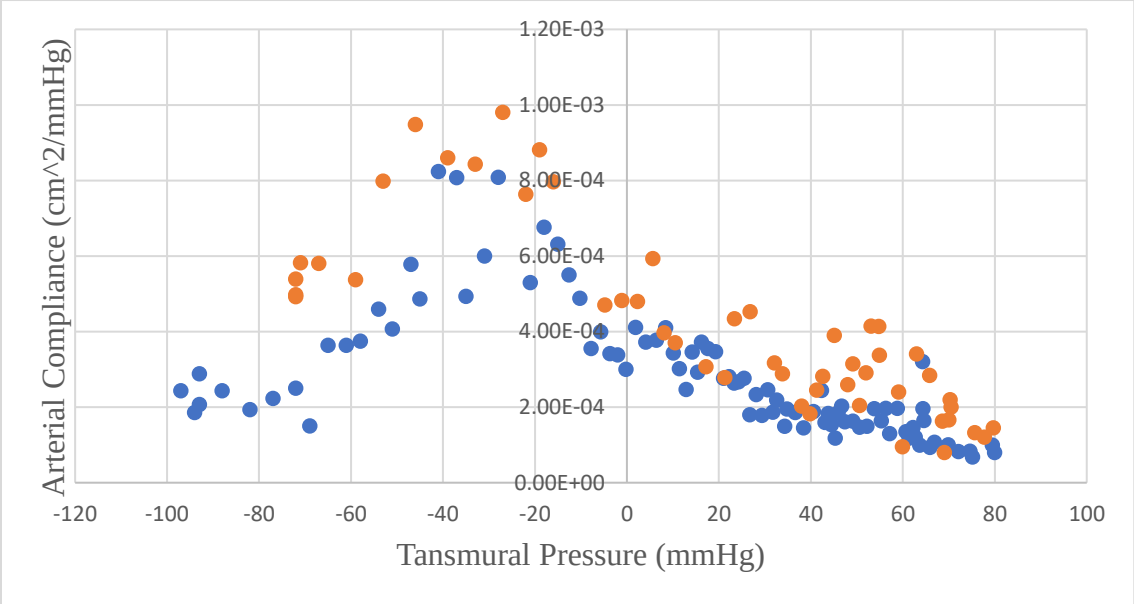

Figure 99. Arterial Area Compliance vs. Transmural Arterial Pressure of Female Participant (F8) 30 Minutes Before Cold-Water Immersion. Blue data points represent baseline measurements while orange data points represent measurements collected during 5-minute reactive hyperemia.

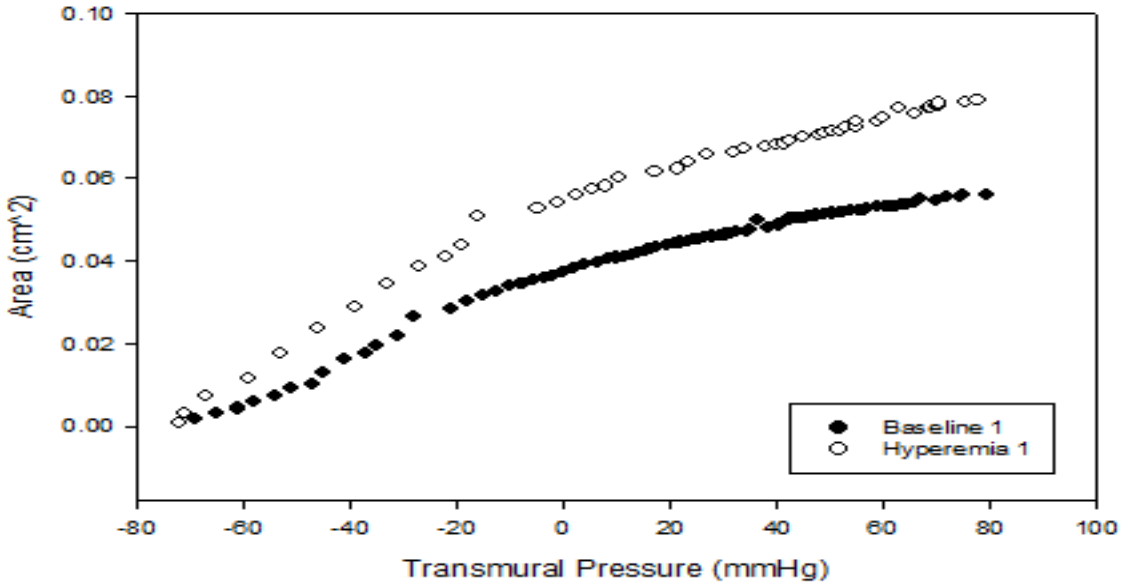

Figure 100. Arterial Lumen Area vs. Arterial Transmural Pressure of Female Participant (F8) 30 Minutes Before Cold-Water Immersion. Black data points represent baseline measurements while white data points represent measurements collected during 5-minute reactive hyperemia.

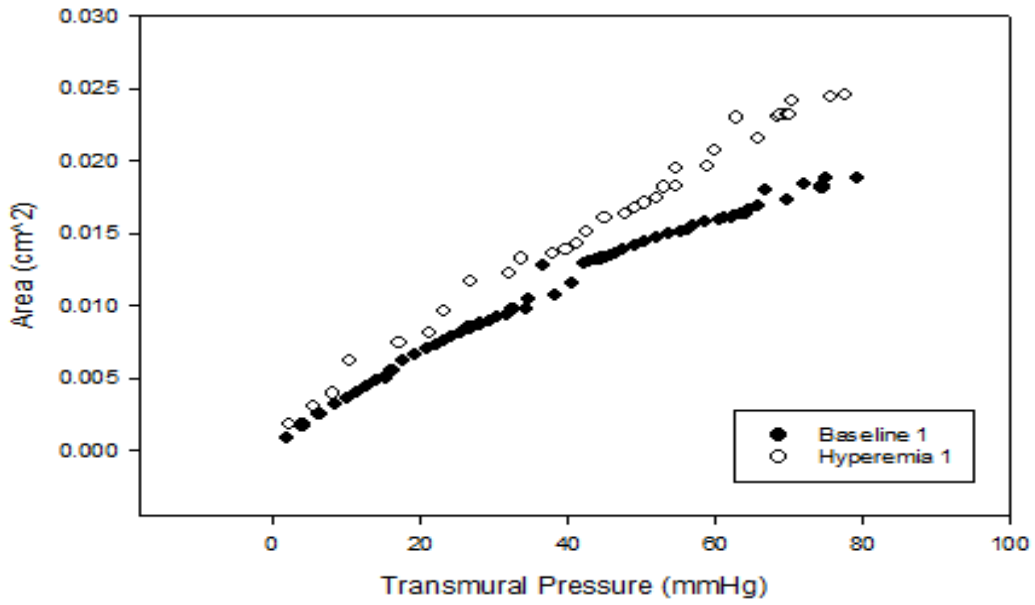

Figure 101. Arterial Lumen Area vs. Arterial Transmural Pressure of Female Participant (F8) 30 Minutes Before Cold-Water Immersion. Black data points represent baseline measurements while white data points represent measurements collected during 5-minute reactive hyperemia. Integrated from 0 mmHg to 80 mmHg transmural pressure.

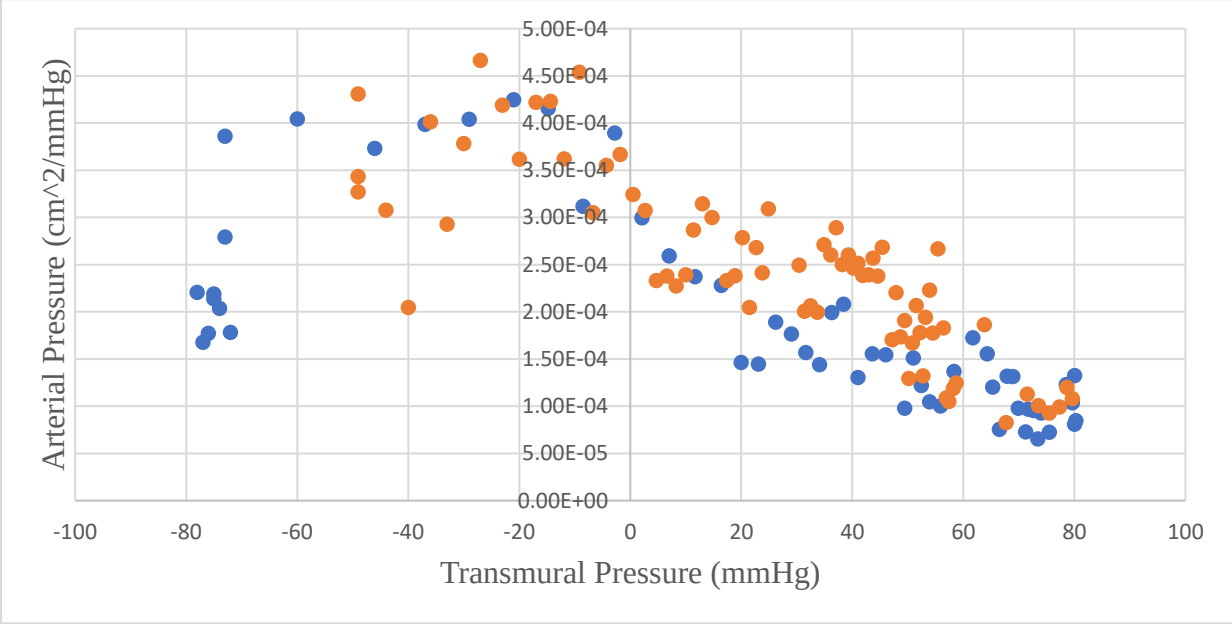

Figure 102. Arterial Area Compliance vs. Transmural Arterial Pressure of Female Participant (F8) Immediately After Cold-Water Immersion. Blue data points represent baseline measurements while orange data points represent measurements collected during 5-minute reactive hyperemia.

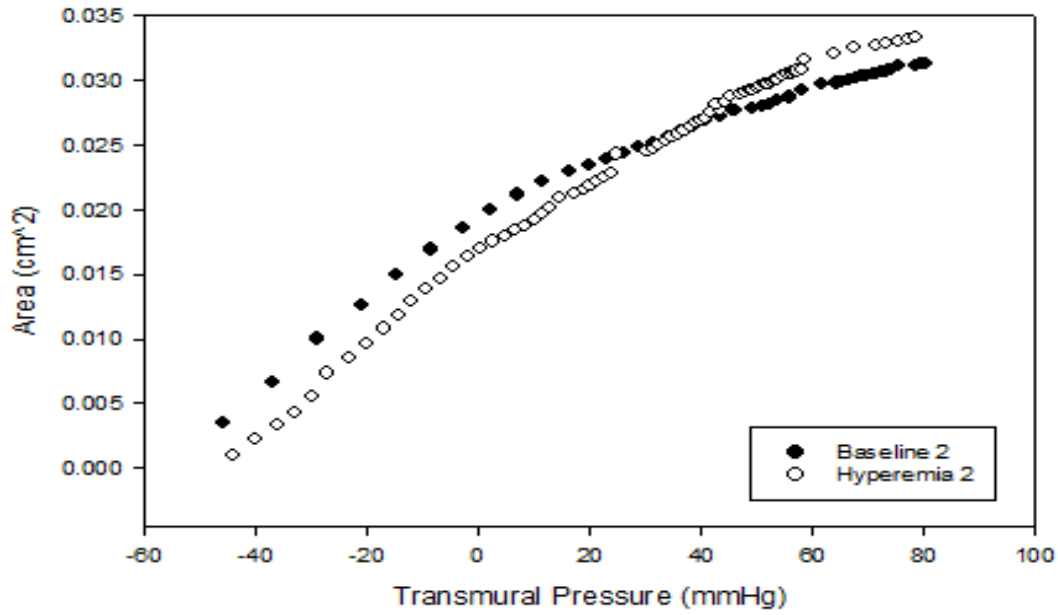

Figure 103. Arterial Lumen Area vs. Arterial Transmural Pressure of Female Participant (F8) Immediately After Cold-Water Immersion. Black data points represent baseline measurements while white data points represent measurements collected during 5-minute reactive hyperemia.

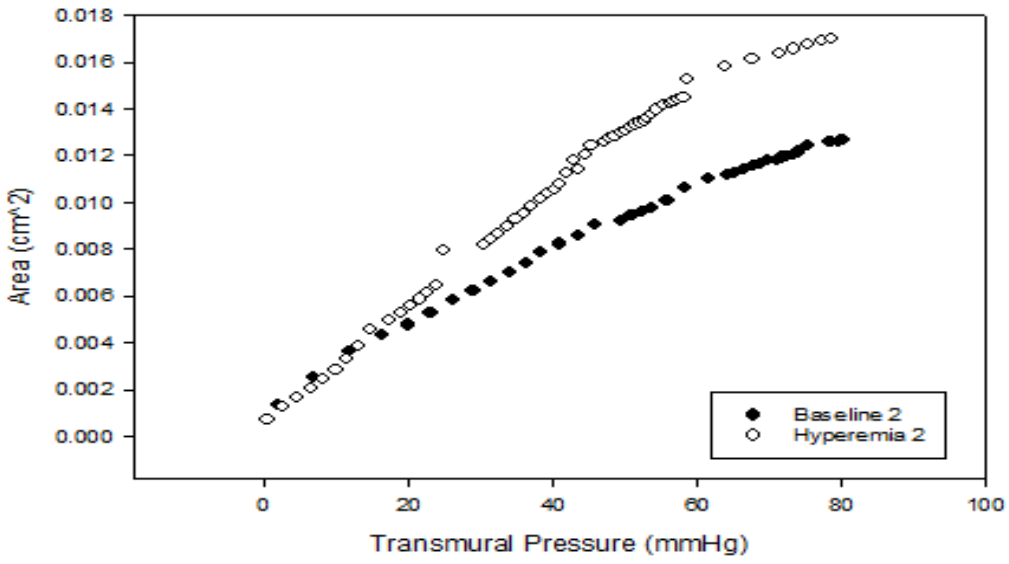

Figure 104. Arterial Lumen Area vs. Arterial Transmural Pressure of Female Participant (F8) Immediately After Cold-Water Immersion. Black data points represent baseline measurements while white data points represent measurements collected during 5-minute reactive hyperemia. Integrated from 0 mmHg to 80 mmHg transmural pressure.

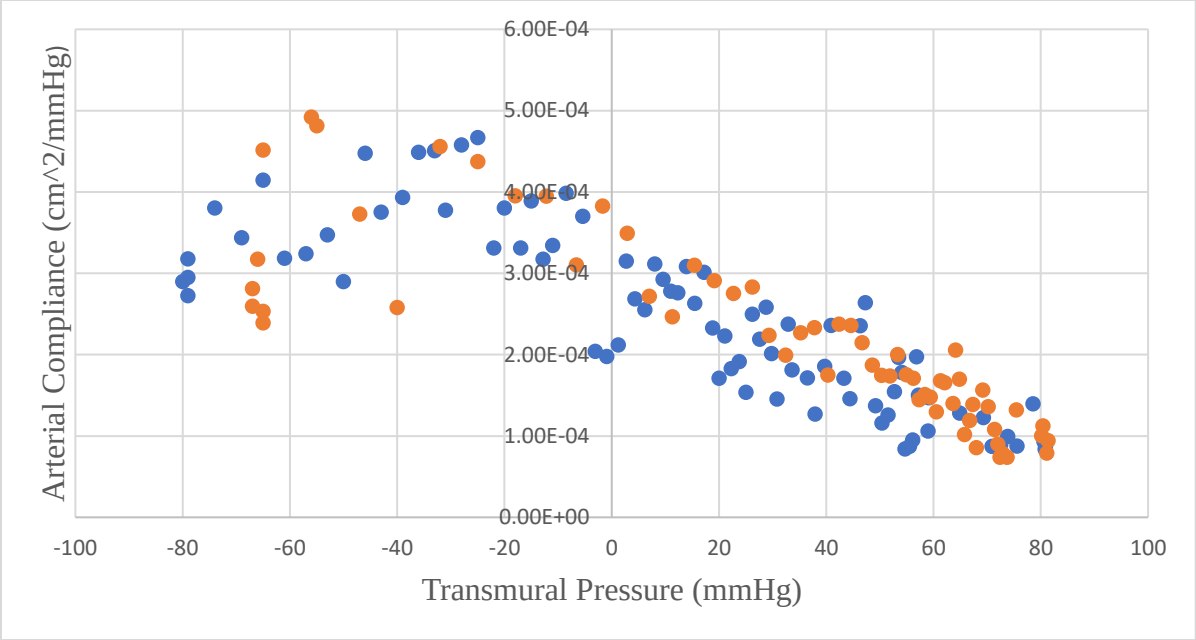

Figure 105. Arterial Area Compliance vs. Transmural Arterial Pressure of Female Participant (F8) 30 Minutes After Cold-Water Immersion. Blue data points represent baseline measurements while orange data points represent measurements collected during 5-minute reactive hyperemia.

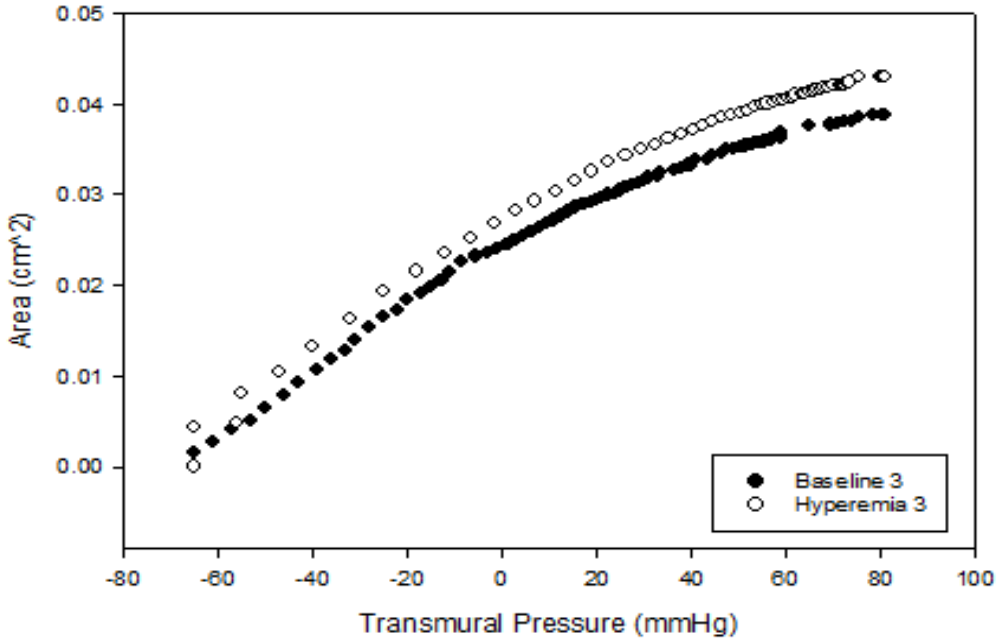

Figure 106. Arterial Lumen Area vs. Arterial Transmural Pressure of Female Participant (F8) 30 Minutes After Cold-Water Immersion. Black data points represent baseline measurements while white data points represent measurements collected during 5-minute reactive hyperemia.

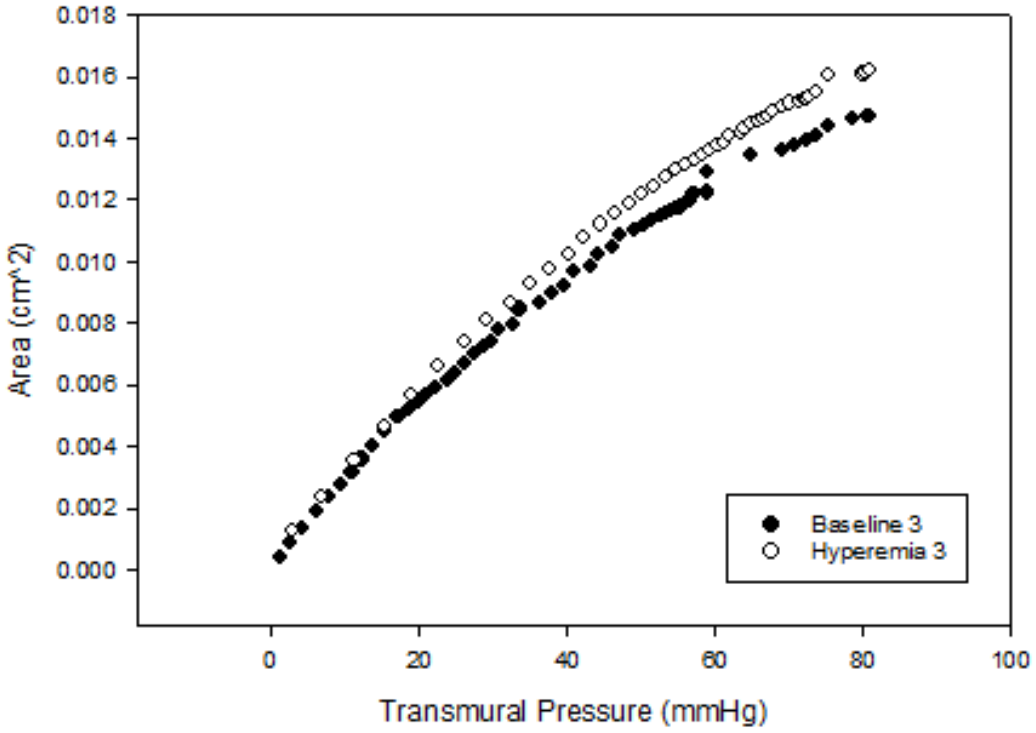

Figure 107. Arterial Lumen Area vs. Arterial Transmural Pressure of Female Participant (F8) 30 Minutes After Cold-Water Immersion. Black data points represent baseline measurements while white data points represent measurements collected during 5-minute reactive hyperemia. Integrated from 0 mmHg to 80 mmHg transmural pressure.

Participant: F9

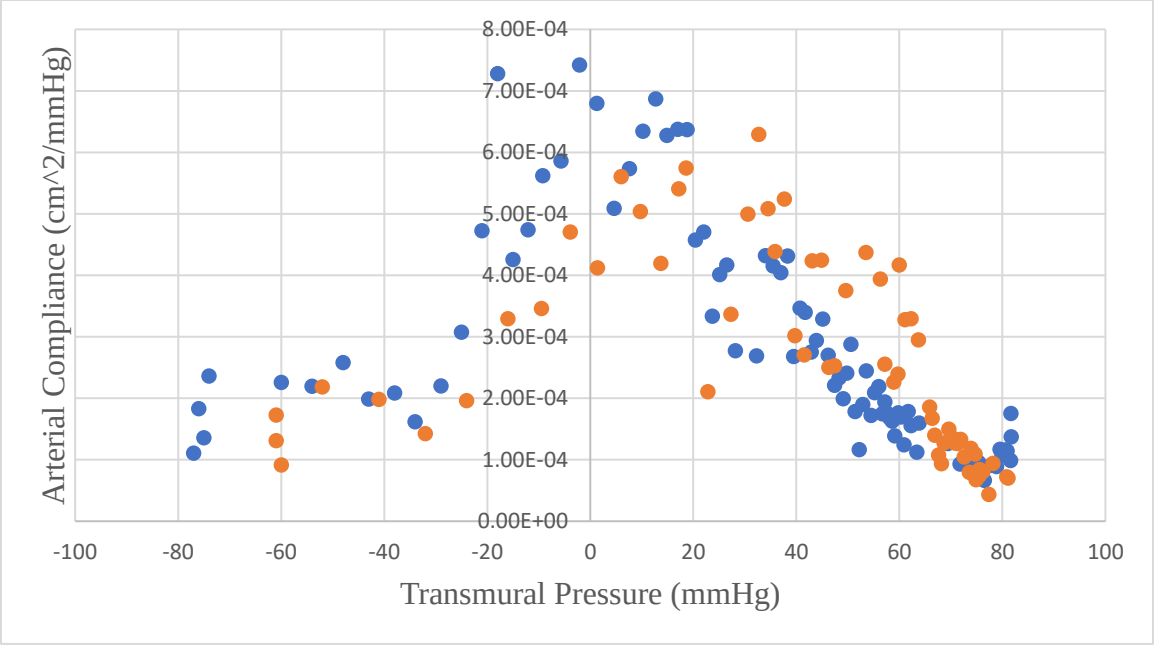

Figure 108. Arterial Area Compliance vs. Transmural Arterial Pressure of Female Participant (F9) 30 Minutes Before Cold-Water Immersion. Blue data points represent baseline measurements while orange data points represent measurements collected during 5-minute reactive hyperemia.

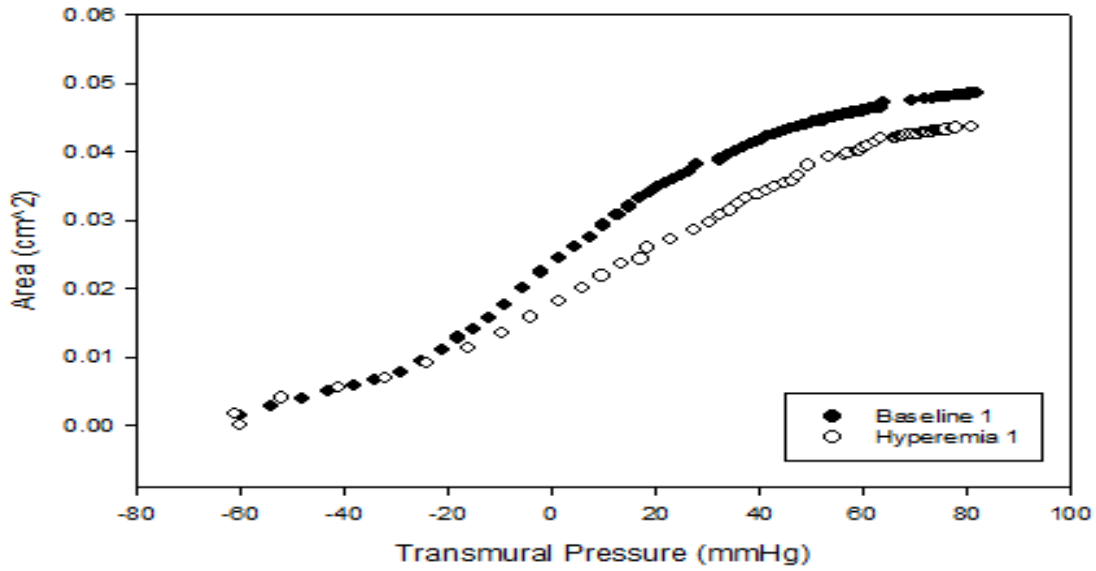

Figure 109. Arterial Lumen Area vs. Arterial Transmural Pressure of Female Participant (F9) 30 Minutes Before Cold-Water Immersion. Black data points represent baseline measurements while white data points represent measurements collected during 5-minute reactive hyperemia.

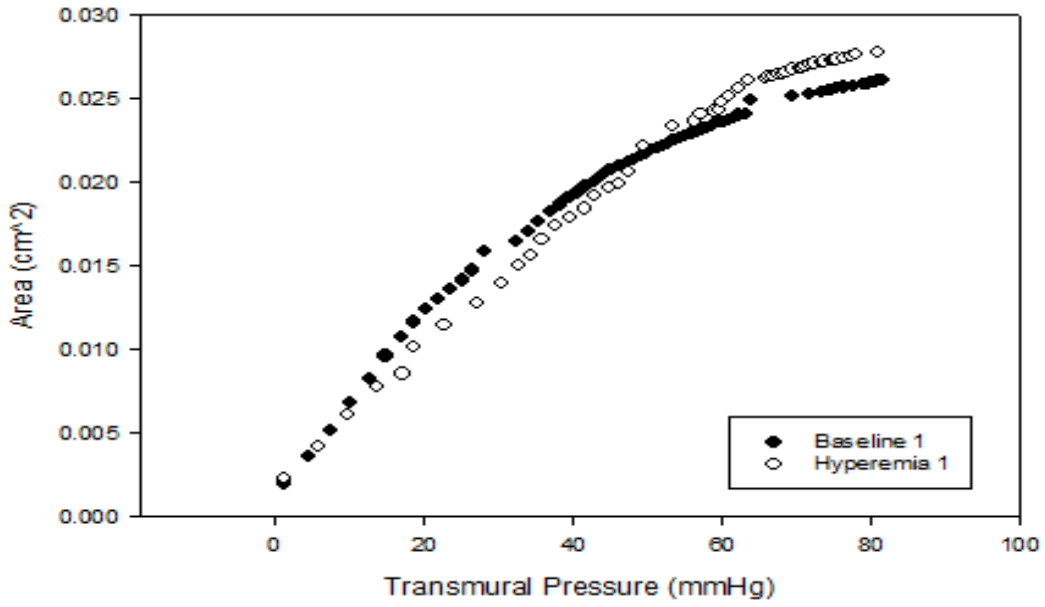

Figure 110. Arterial Lumen Area vs. Arterial Transmural Pressure of Female Participant (F9) 30 Minutes Before Cold-Water Immersion. Black data points represent baseline measurements while white data points represent measurements collected during 5-minute reactive hyperemia. Integrated from 0 mmHg to 80 mmHg transmural pressure.

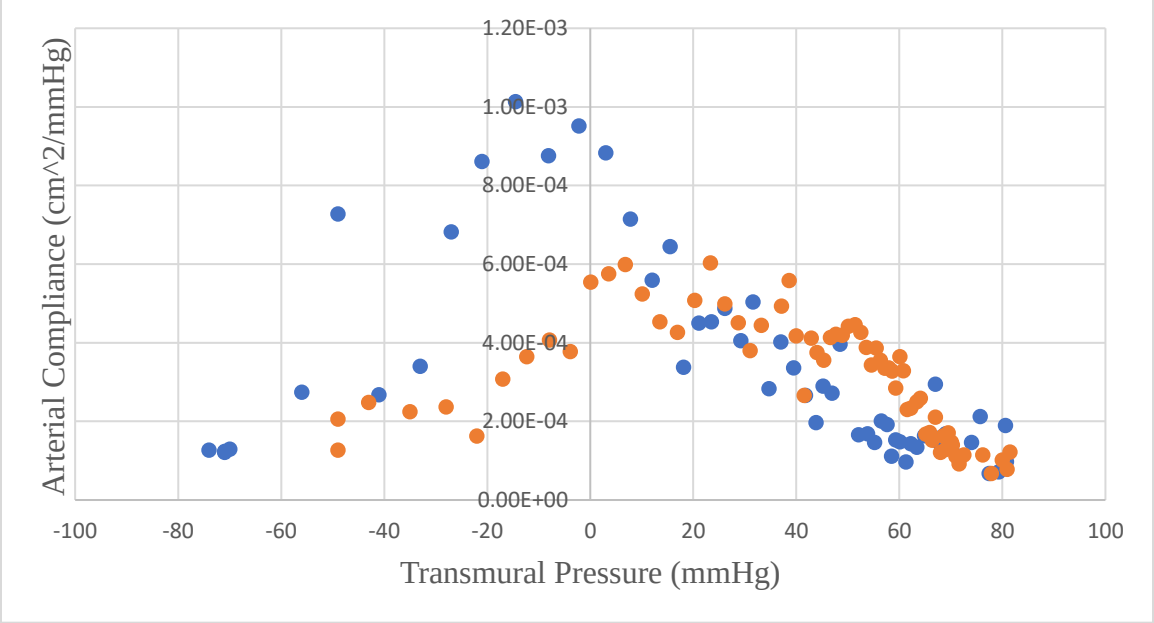

Figure 111. Arterial Area Compliance vs. Transmural Arterial Pressure of Female Participant (F9) Immediately After Cold-Water Immersion. Blue data points represent baseline measurements while orange data points represent measurements collected during 5-minute reactive hyperemia.

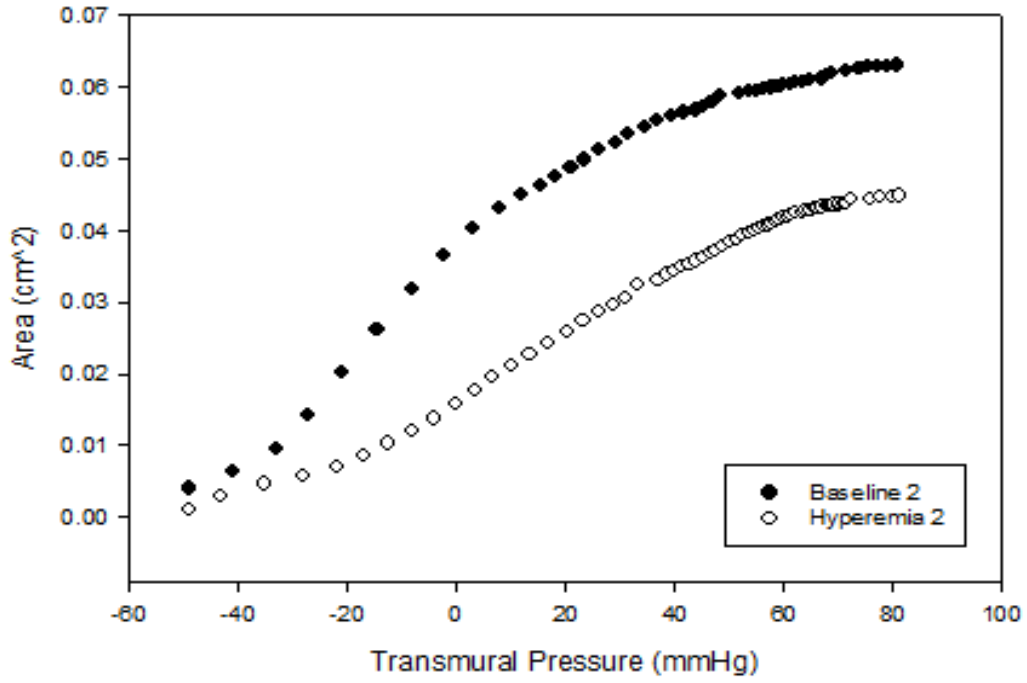

Figure 112. Arterial Lumen Area vs. Arterial Transmural Pressure of Female Participant (F9) Immediately After Cold-Water Immersion. Black data points represent baseline measurements while white data points represent measurements collected during 5-minute reactive hyperemia.

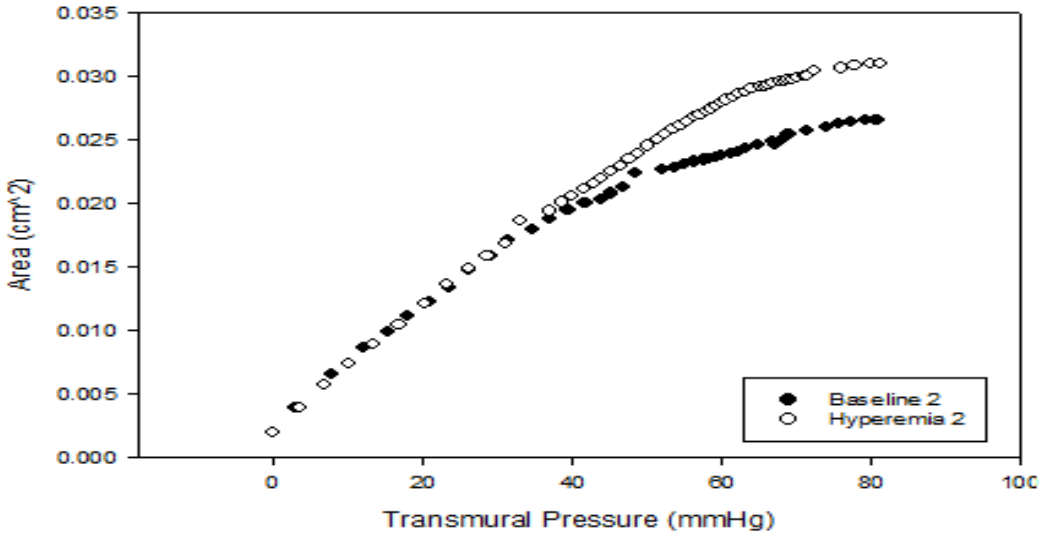

Figure 113. Arterial Lumen Area vs. Arterial Transmural Pressure of Female Participant (F9) Immediately After Cold-Water Immersion. Black data points represent baseline measurements while white data points represent measurements collected during 5-minute reactive hyperemia. Integrated from 0 mmHg to 80 mmHg transmural pressure.

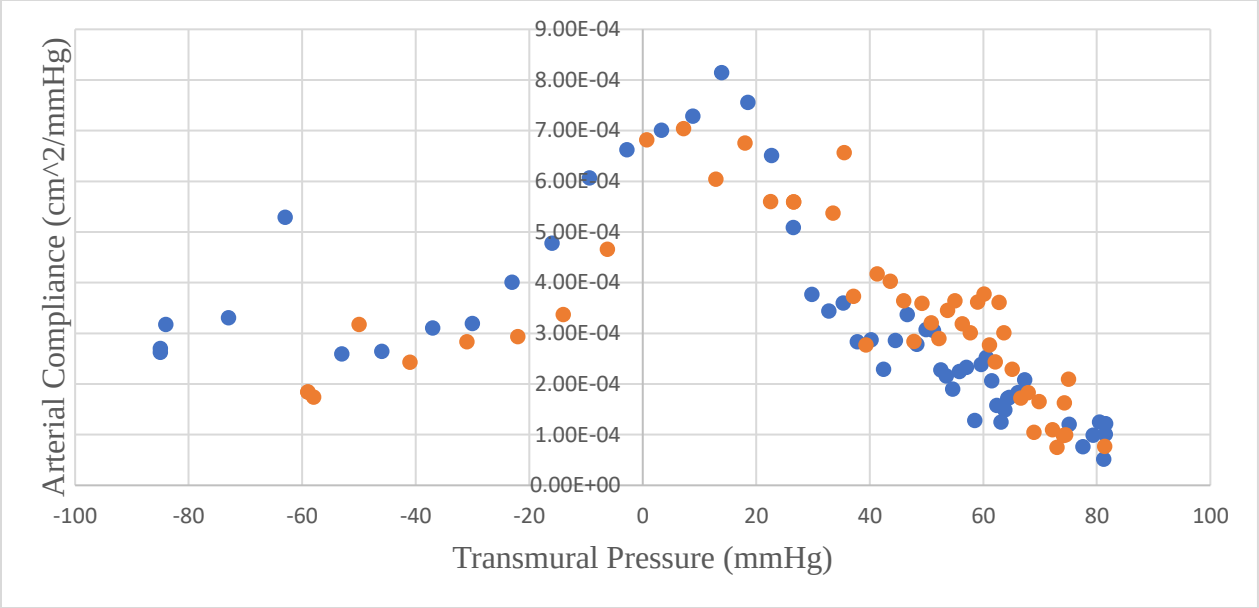

Figure 114. Arterial Area Compliance vs. Transmural Arterial Pressure of Female Participant (F9) 30 Minutes After Cold-Water Immersion. Blue data points represent baseline measurements while orange data points represent measurements collected during 5-minute reactive hyperemia.

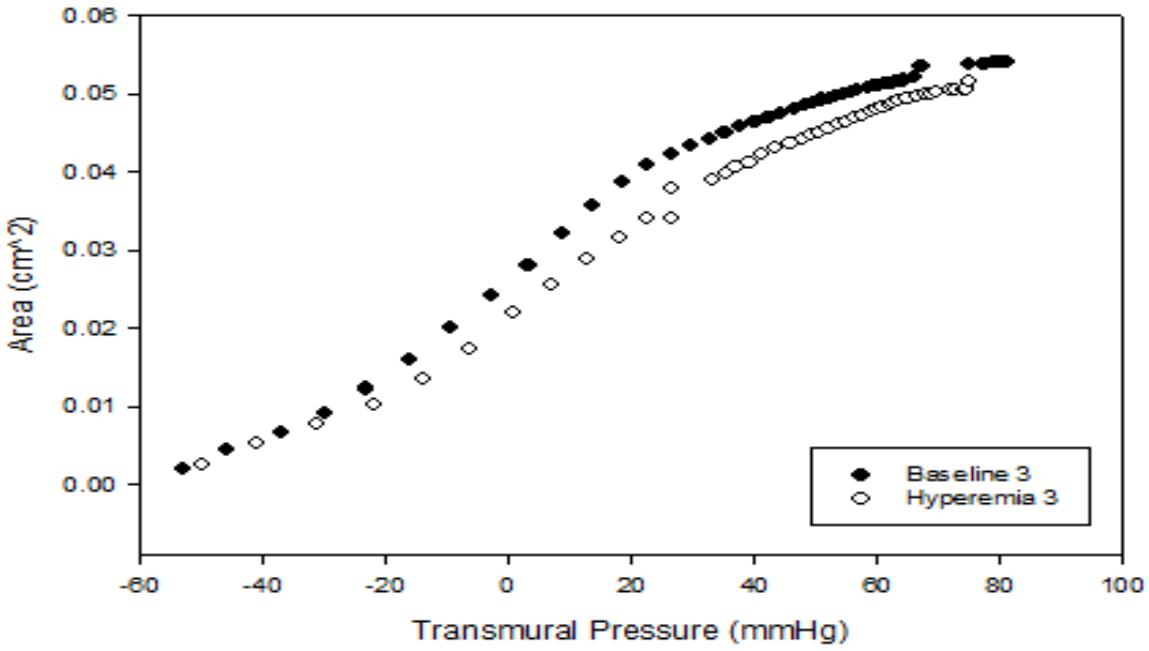

Figure 115. Arterial Lumen Area vs. Arterial Transmural Pressure of Female Participant (F9) 30 Minutes After Cold-Water Immersion. Black data points represent baseline measurements while white data points represent measurements collected during 5-minute reactive hyperemia.

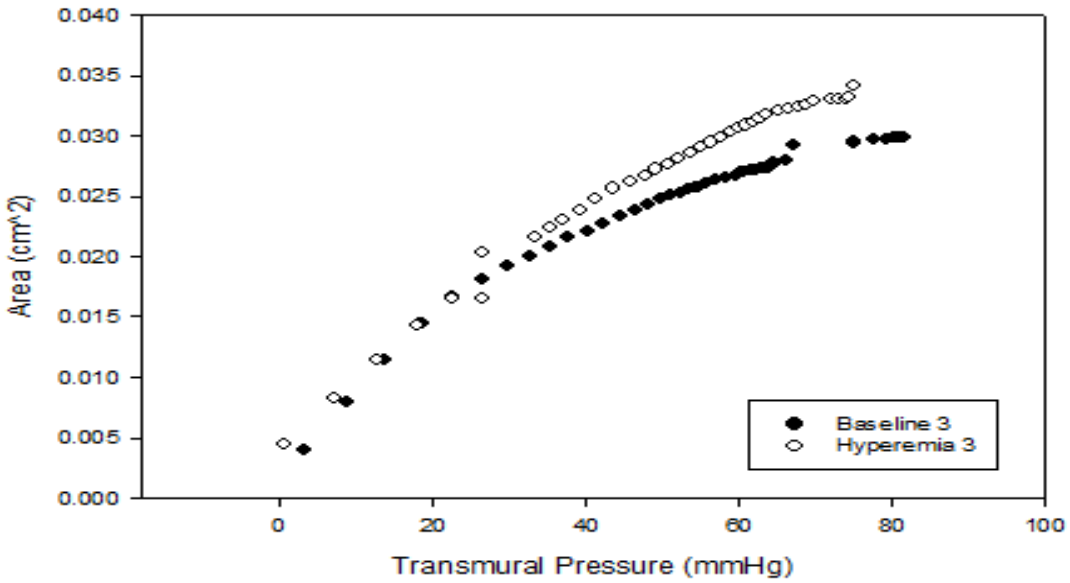

Figure 116. Arterial Lumen Area vs. Arterial Transmural Pressure of Female Participant (F9) 30 Minutes After Cold-Water Immersion. Black data points represent baseline measurements while white data points represent measurements collected during 5-minute reactive hyperemia. Integrated from 0 mmHg to 80 mmHg transmural pressure.

Participant: M1

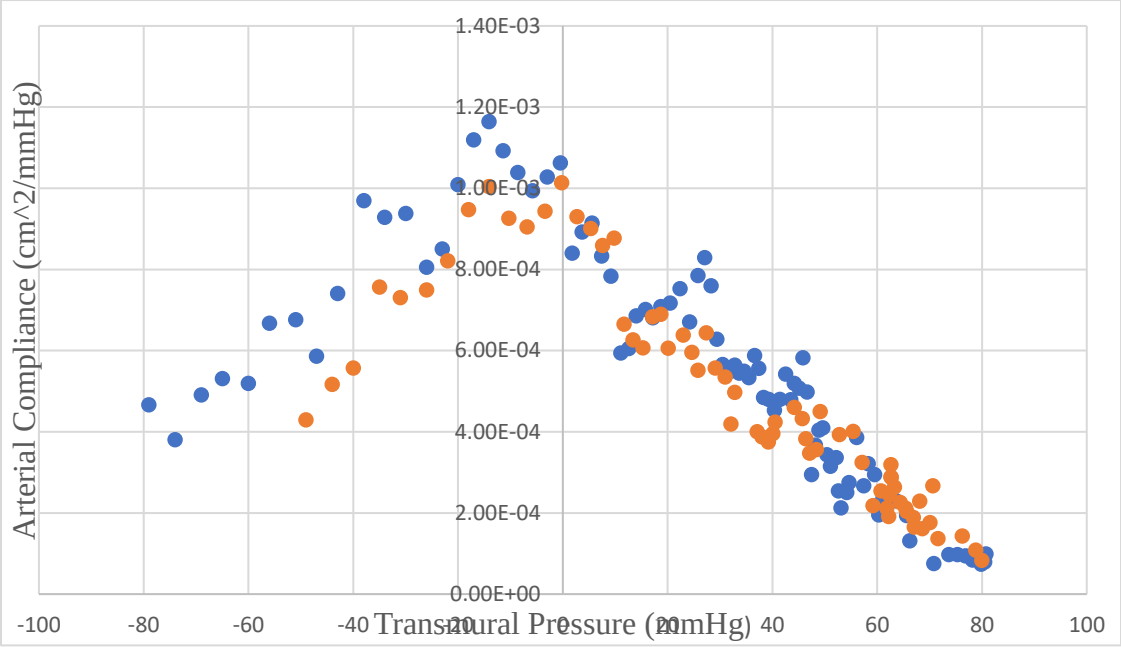

Figure 117. Arterial Area Compliance vs. Transmural Arterial Pressure of Male Participant (M1) 30 Minutes Before Cold-Water Immersion. Blue data points represent baseline measurements while orange data points represent measurements collected during 5-minute reactive hyperemia.

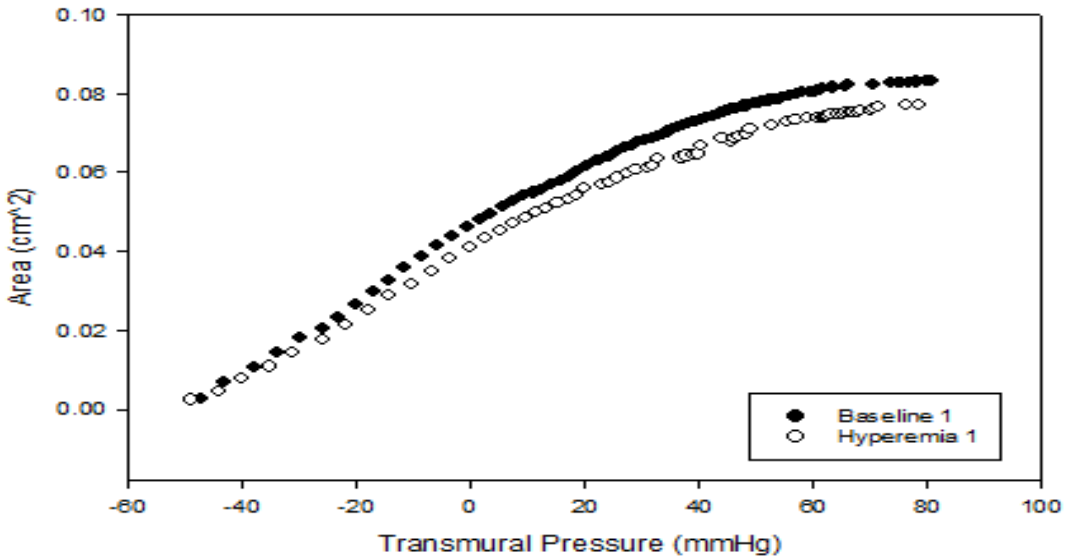

Figure 118. Arterial Lumen Area vs. Arterial Transmural Pressure of Female Participant (M1) 30 Minutes Before Cold-Water Immersion. Black data points represent baseline measurements while white data points represent measurements collected during 5-minute reactive hyperemia.

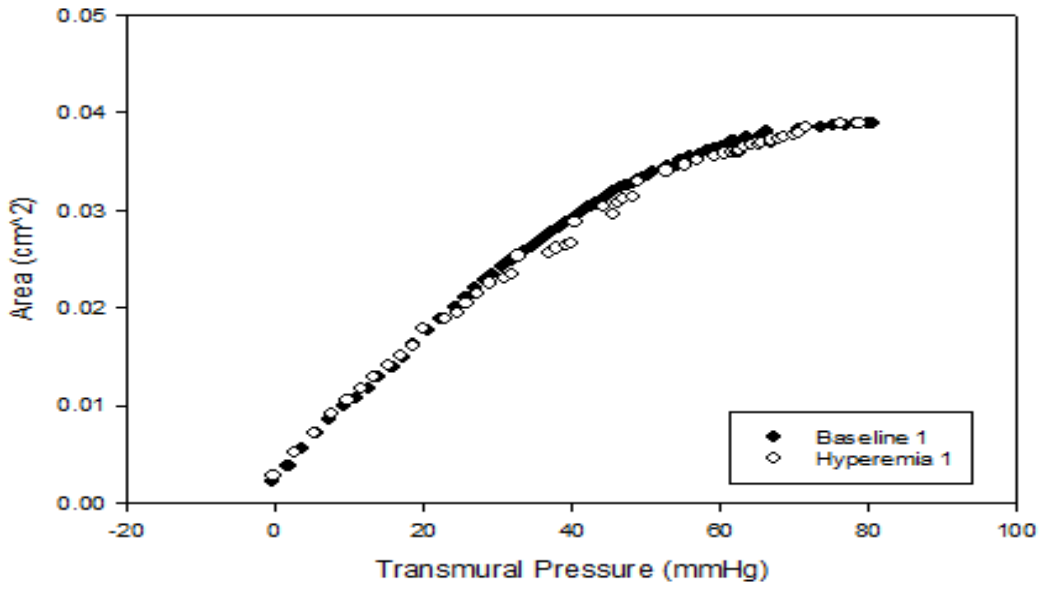

Figure 119. Arterial Lumen Area vs. Arterial Transmural Pressure of Male Participant (M1) 30 Minutes Before Cold-Water Immersion. Black data points represent baseline measurements while white data points represent measurements collected during 5-minute reactive hyperemia. Integrated from 0 mmHg to 80 mmHg transmural pressure.

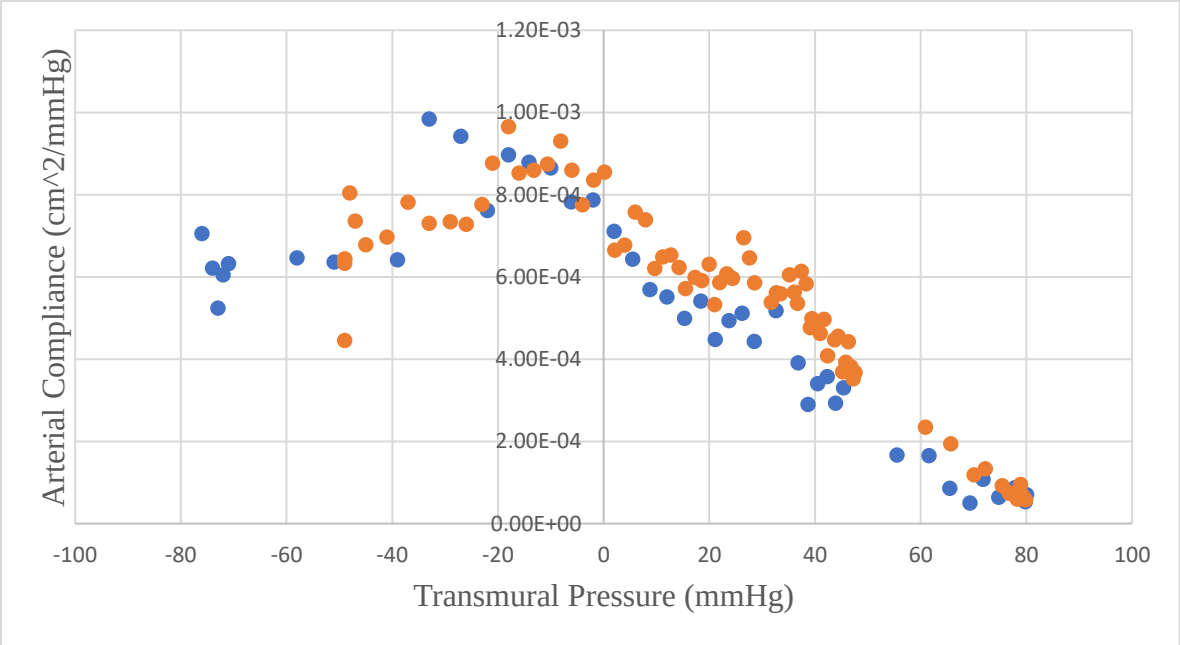

Figure 120. Arterial Area Compliance vs. Transmural Arterial Pressure of Male Participant (M1) Immediately After Cold-Water Immersion. Blue data points represent baseline measurements while orange data points represent measurements collected during 5-minute reactive hyperemia.

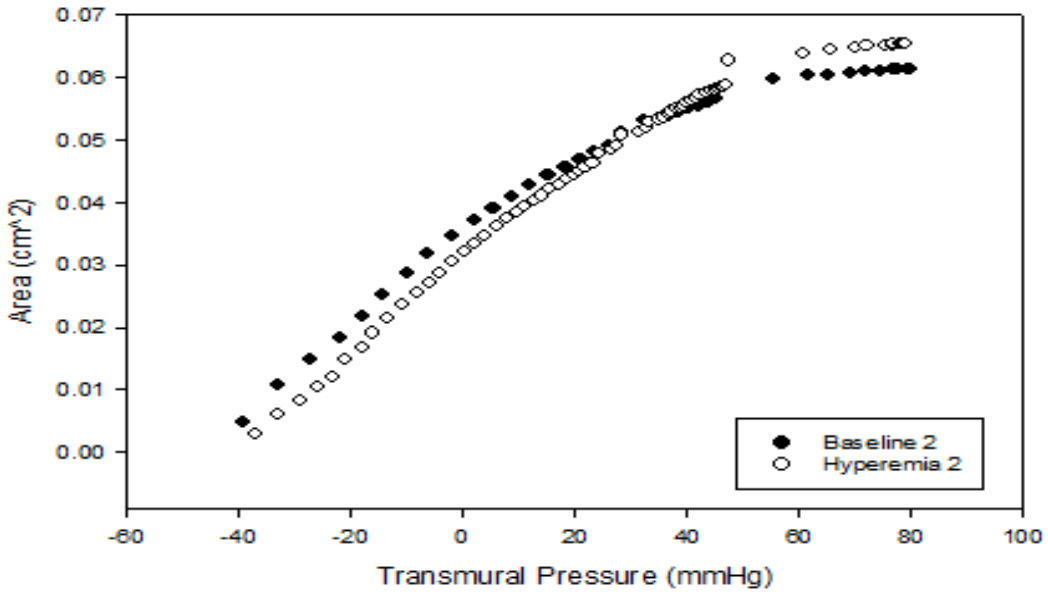

Figure 121. Arterial Lumen Area vs. Arterial Transmural Pressure of Female Participant (M1) Immediately After Cold-Water Immersion. Black data points represent baseline measurements while white data points represent measurements collected during 5-minute reactive hyperemia.

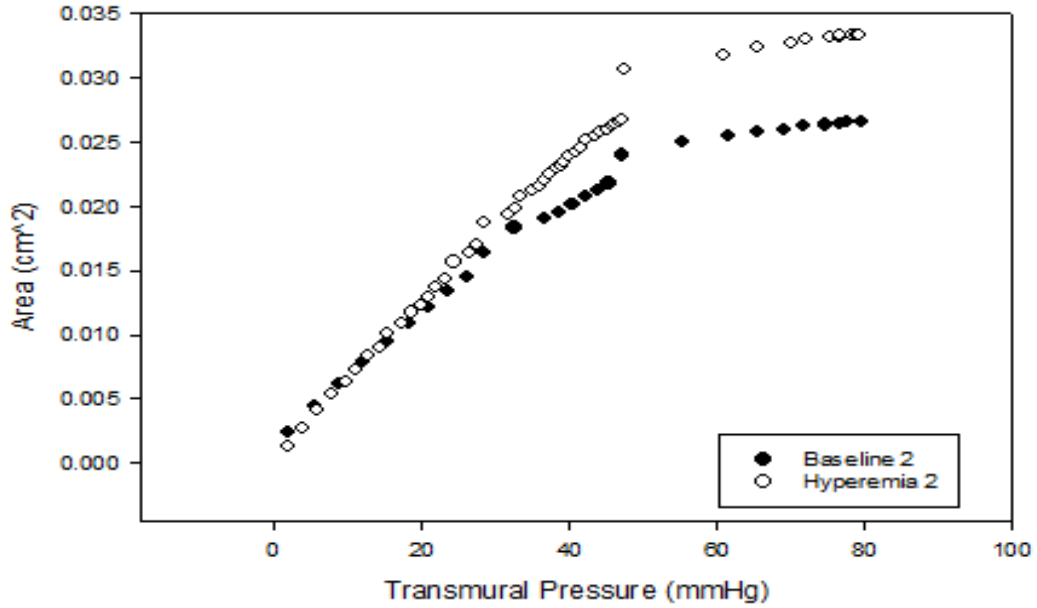

Figure 122. Arterial Lumen Area vs. Arterial Transmural Pressure of Male Participant (M1) Immediately After Cold-Water Immersion. Black data points represent baseline measurements while white data points represent measurements collected during 5-minute reactive hyperemia. Integrated from 0 mmHg to 80 mmHg transmural pressure.

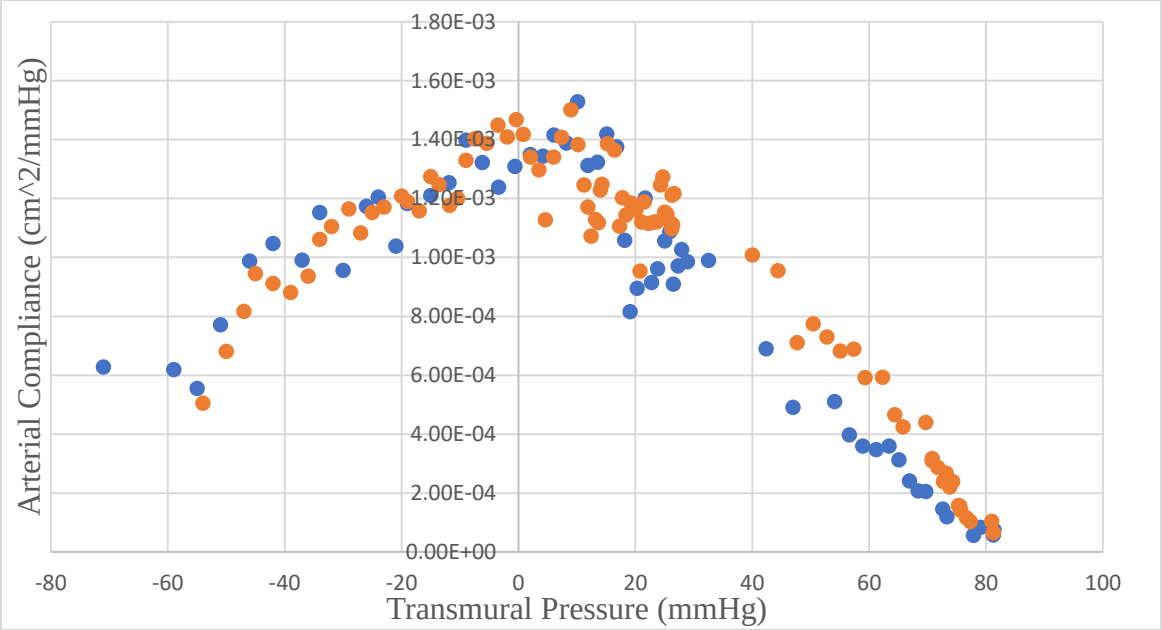

Figure 123. Arterial Area Compliance vs. Transmural Arterial Pressure of Male Participant (M1) 30 Minutes After Cold-Water Immersion. Blue data points represent baseline measurements while orange data points represent measurements collected during 5-minute reactive hyperemia.

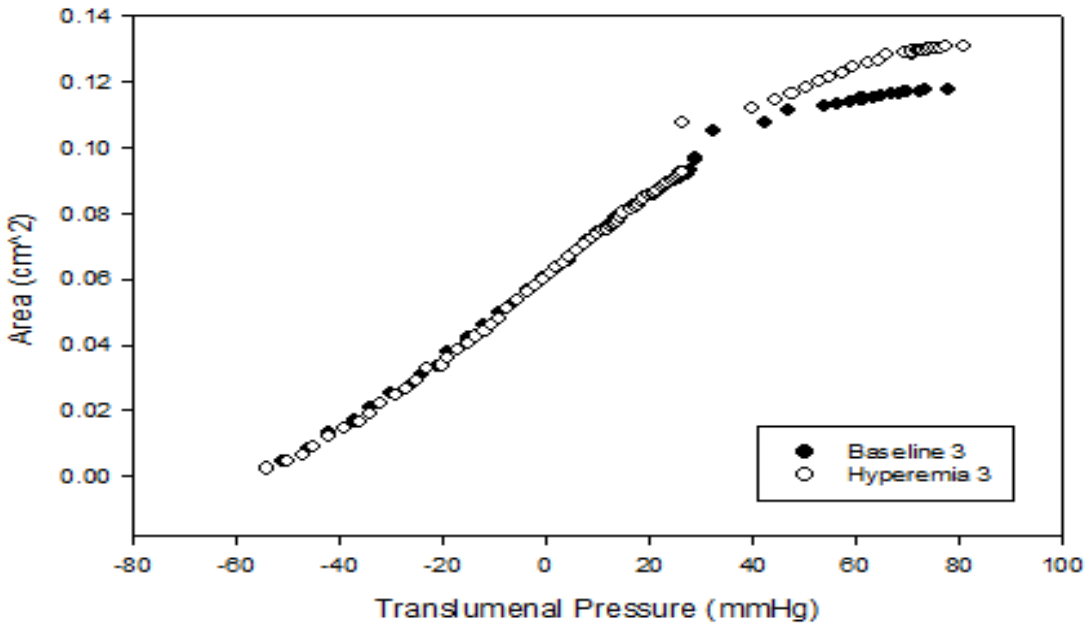

Figure 124. Arterial Lumen Area vs. Arterial Transmural Pressure of Female Participant (M1) 30 Minutes After Cold-Water Immersion. Black data points represent baseline measurements while white data points represent measurements collected during 5-minute reactive hyperemia.

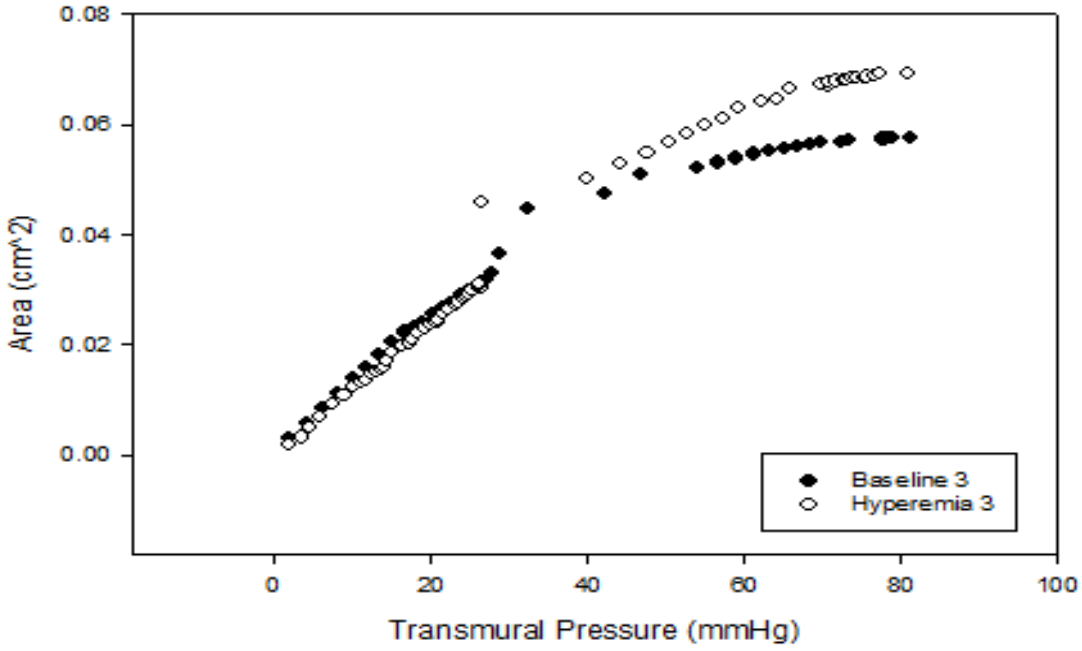

Figure 125. Arterial Lumen Area vs. Arterial Transmural Pressure of Male Participant (M1) 30 Minutes After Cold-Water Immersion. Black data points represent baseline measurements while white data points represent measurements collected during 5-minute reactive hyperemia. Integrated from 0 mmHg to 80 mmHg transmural pressure.

Participant: M2

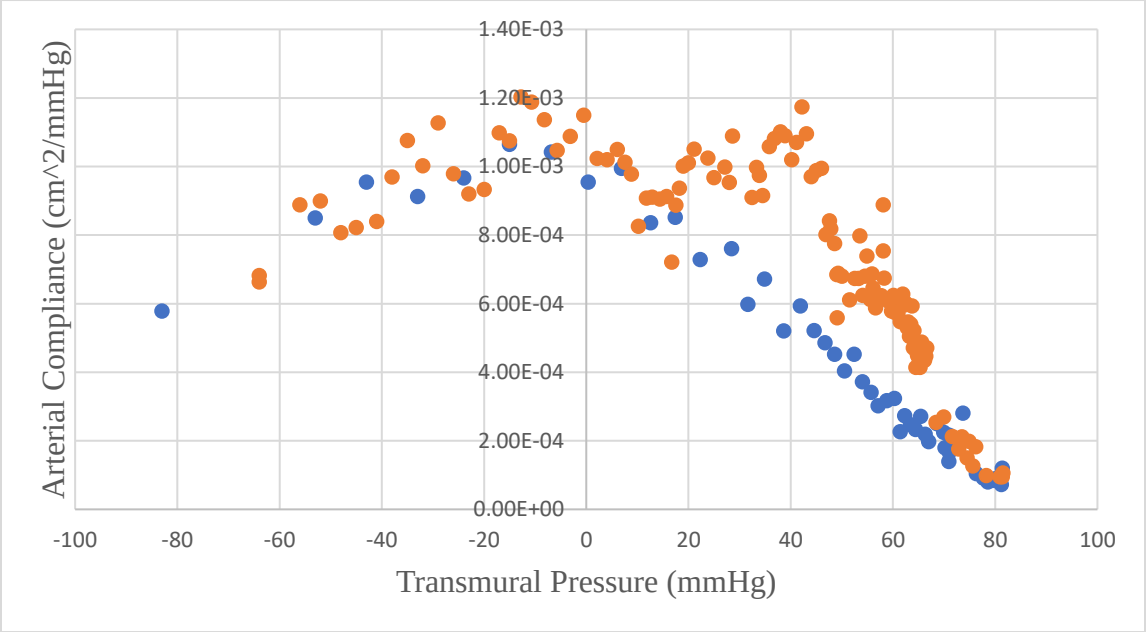

Figure 126. Arterial Area Compliance vs. Transmural Arterial Pressure of Male Participant (M2) 30 Minutes Before Cold-Water Immersion. Blue data points represent baseline measurements while orange data points represent measurements collected during 5-minute reactive hyperemia.

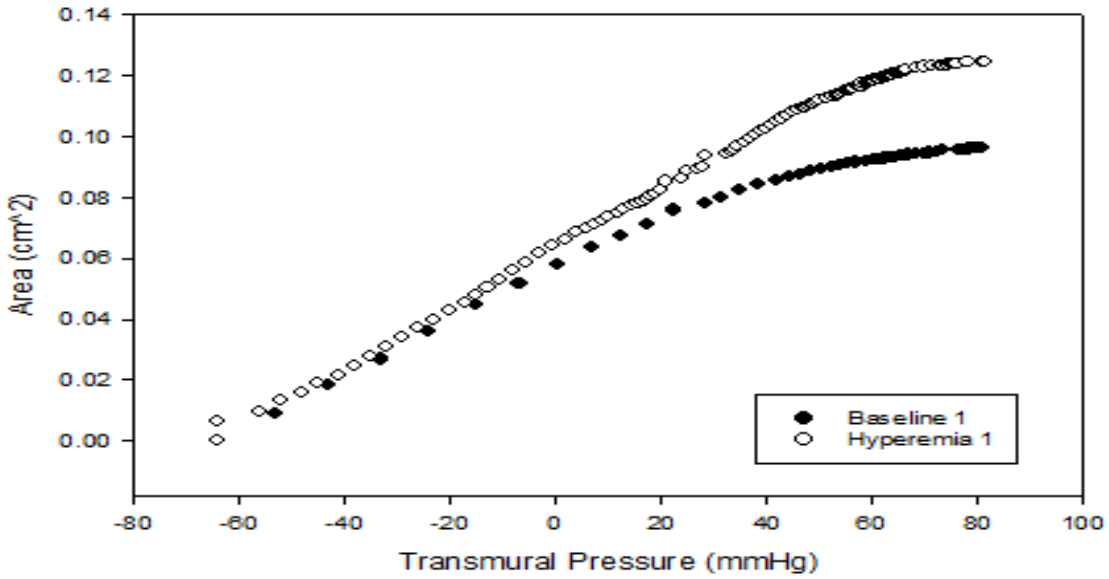

Figure 127. Arterial Lumen Area vs. Arterial Transmural Pressure of Female Participant (M2) 30 Minutes Before Cold-Water Immersion. Black data points represent baseline measurements while white data points represent measurements collected during 5-minute reactive hyperemia.

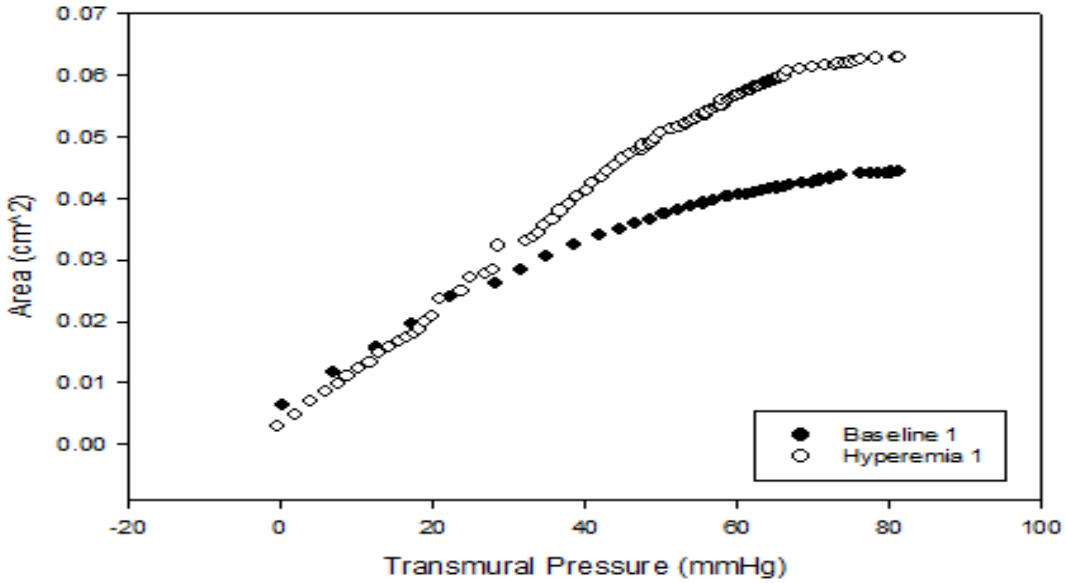

Figure 128. Arterial Lumen Area vs. Arterial Transmural Pressure of Male Participant (M2) 30 Minutes Before Cold-Water Immersion. Black data points represent baseline measurements while white data points represent measurements collected during 5-minute reactive hyperemia. Integrated from 0 mmHg to 80 mmHg transmural pressure.

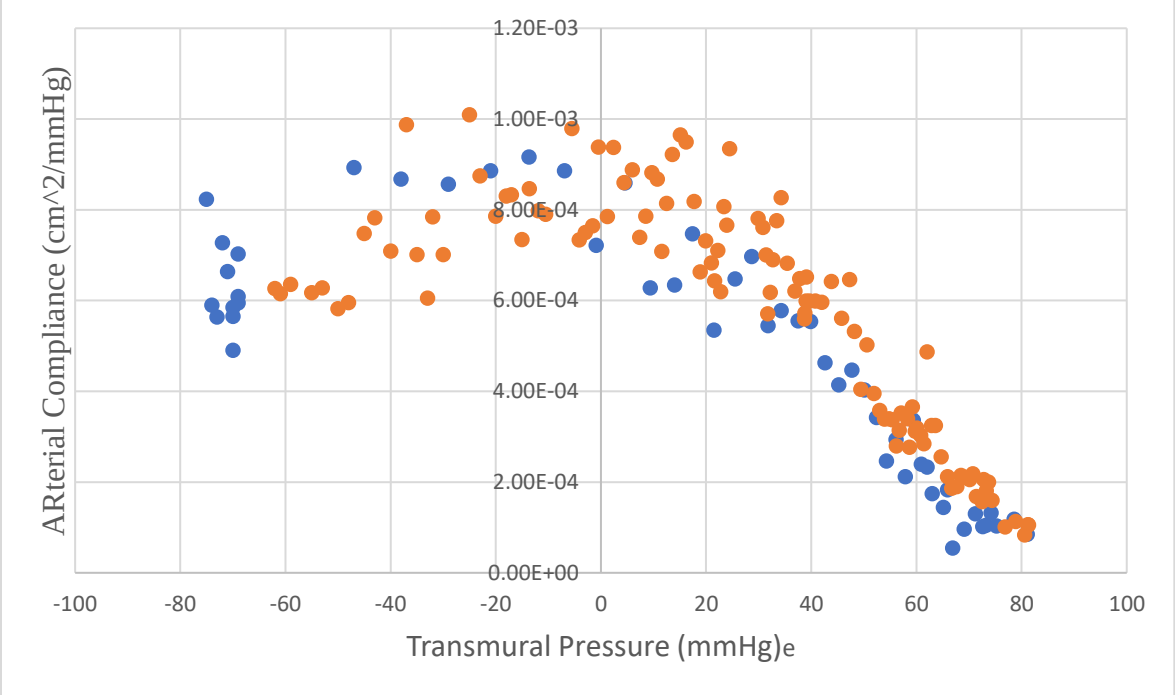

Figure 129. Arterial Area Compliance vs. Transmural Arterial Pressure of Male Participant (M2) Immediately After Cold-Water Immersion. Blue data points represent baseline measurements while orange data points represent measurements collected during 5-minute reactive hyperemia.

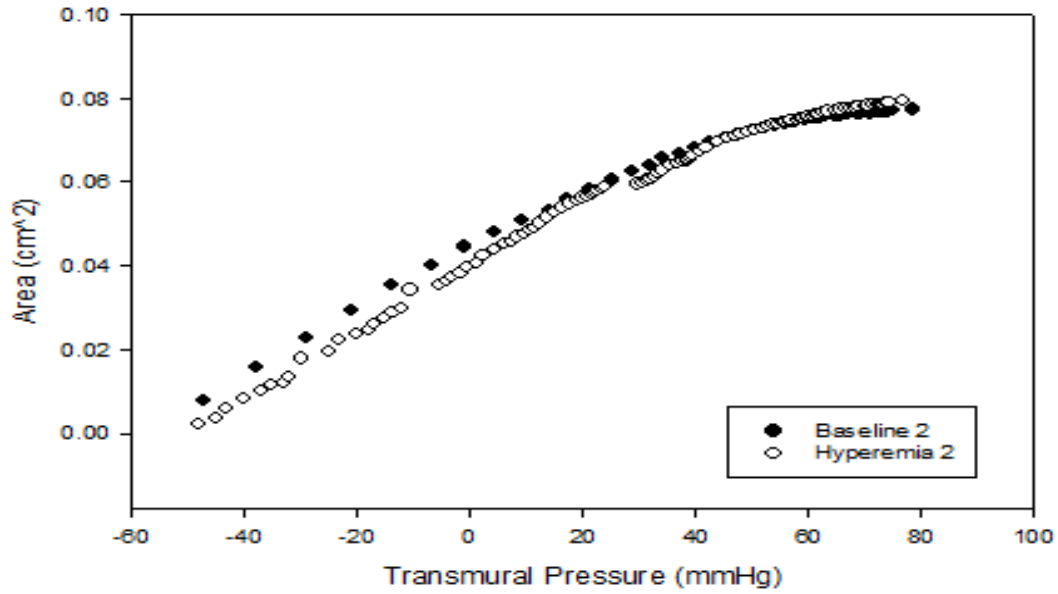

Figure 130. Arterial Lumen Area vs. Arterial Transmural Pressure of Female Participant (M2) Immediately After Cold-Water Immersion. Black data points represent baseline measurements while white data points represent measurements collected during 5-minute reactive hyperemia.

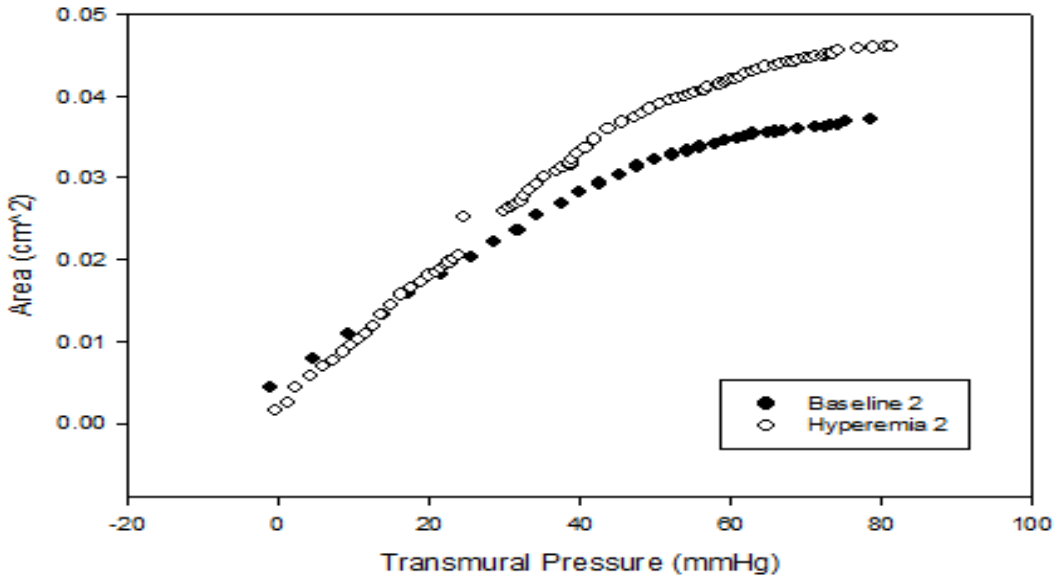

Figure 131. Arterial Lumen Area vs. Arterial Transmural Pressure of Male Participant (M2) Immediately After Cold-Water Immersion. Black data points represent baseline measurements while white data points represent measurements collected during 5-minute reactive hyperemia. Integrated from 0 mmHg to 80 mmHg transmural pressure.

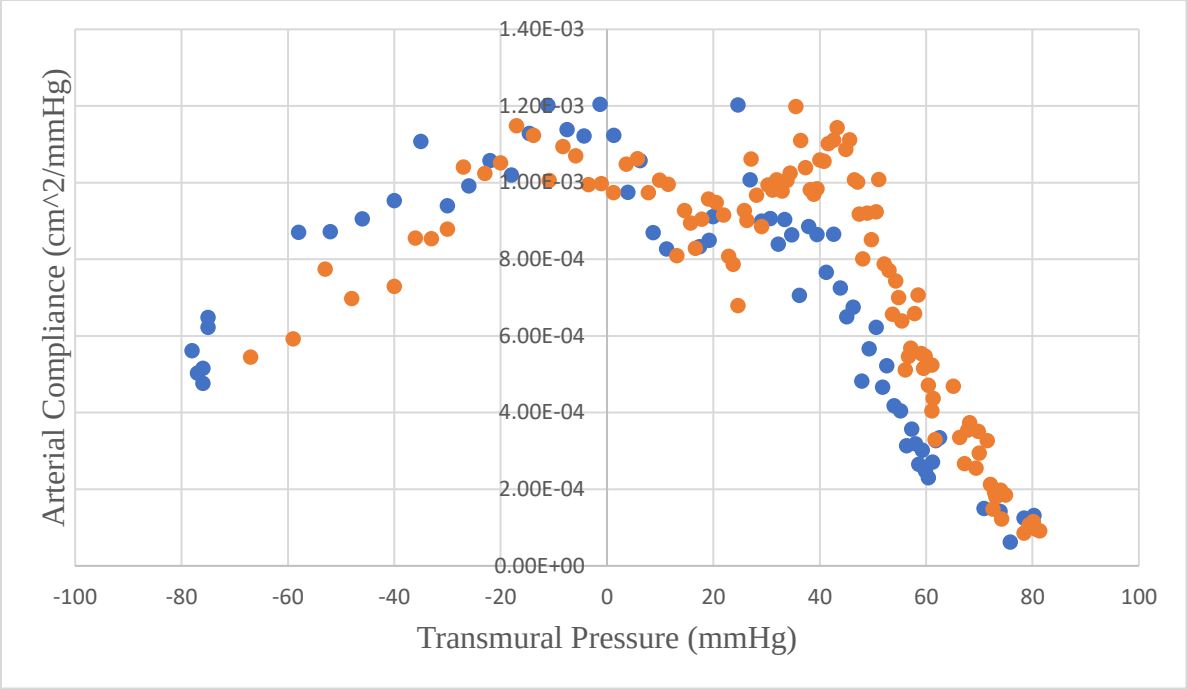

Figure 132. Arterial Area Compliance vs. Transmural Arterial Pressure of Male Participant (M2) 30 Minutes After Cold-Water Immersion. Blue data points represent baseline measurements while orange data points represent measurements collected during 5-minute reactive hyperemia.

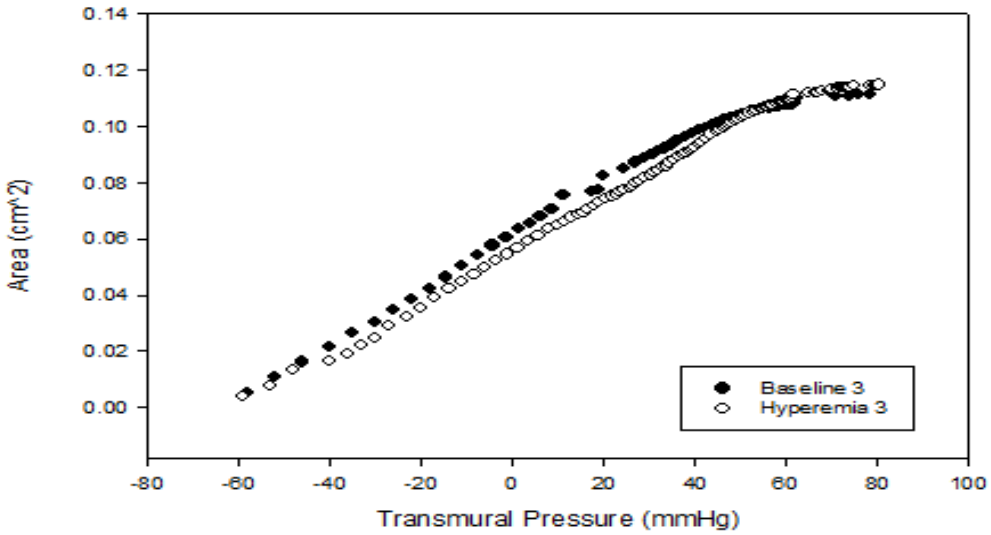

Figure 133. Arterial Lumen Area vs. Arterial Transmural Pressure of Female Participant (M2) 30 Minutes After Cold-Water Immersion. Black data points represent baseline measurements while white data points represent measurements collected during 5-minute reactive hyperemia.

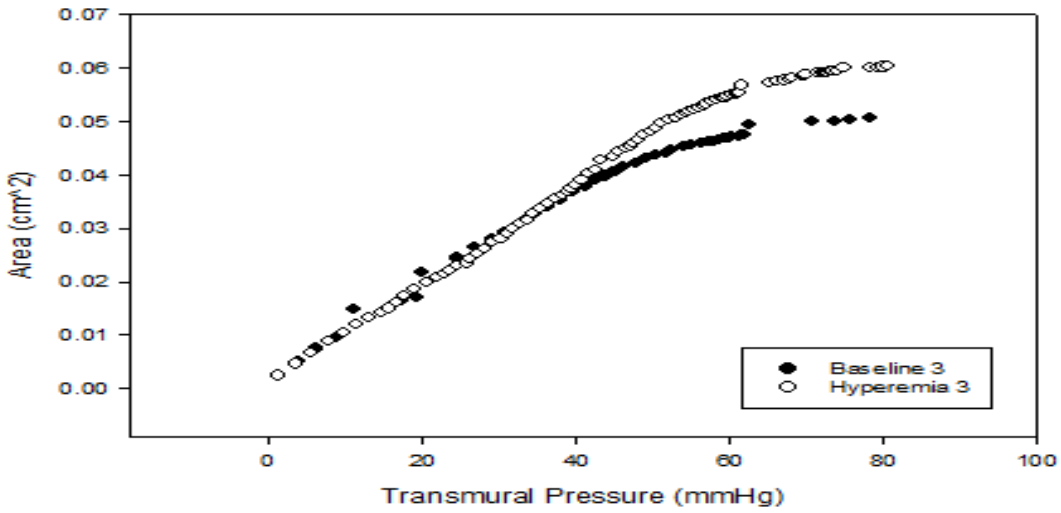

Figure 134. Arterial Lumen Area vs. Arterial Transmural Pressure of Male Participant (M2) 30 Minutes After Cold-Water Immersion. Black data points represent baseline measurements while white data points represent measurements collected during 5-minute reactive hyperemia. Integrated from 0 mmHg to 80 mmHg transmural pressure.

Participant: M3

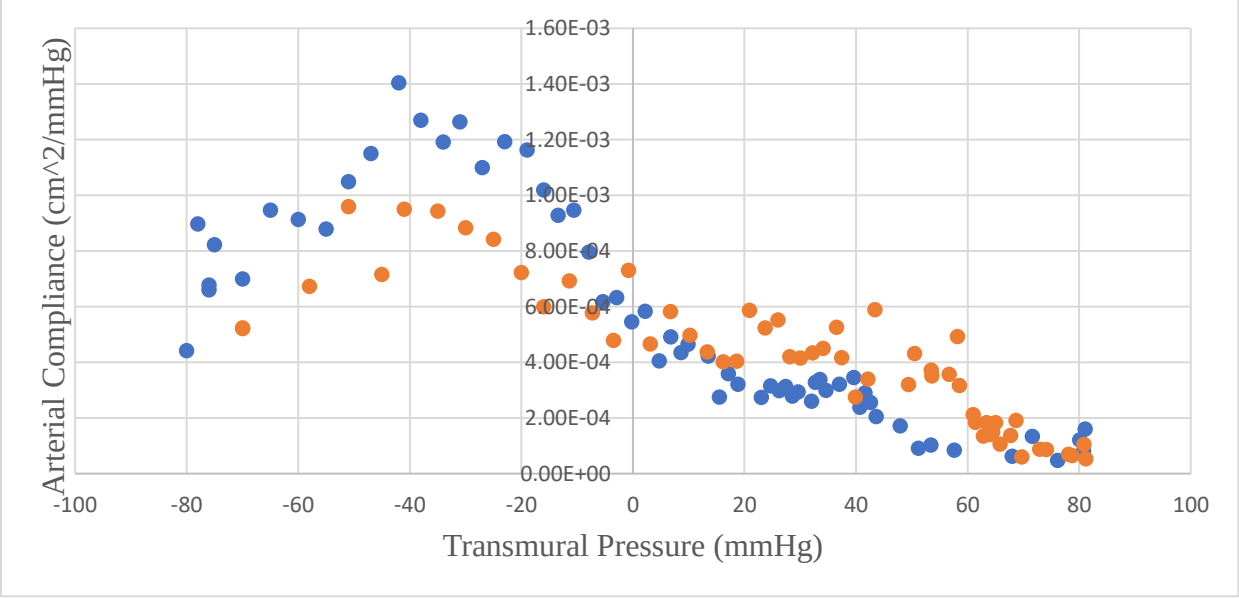

Figure 135. Arterial Area Compliance vs. Transmural Arterial Pressure of Male Participant (M3) 30 Minutes Before Cold-Water Immersion. Blue data points represent baseline measurements while orange data points represent measurements collected during 5-minute reactive hyperemia.

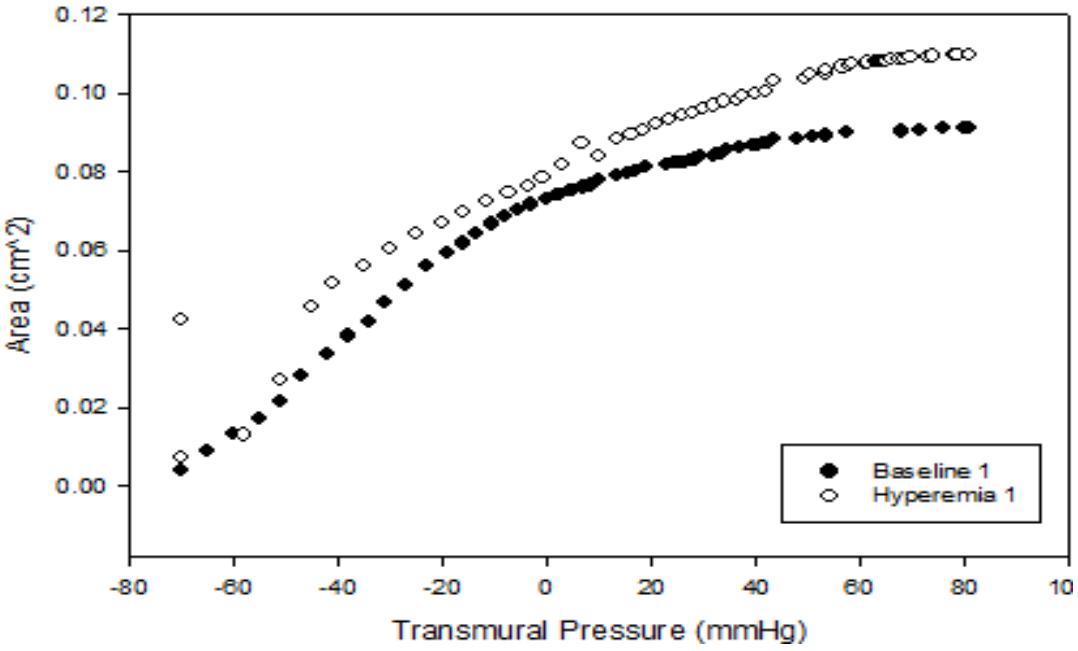

Figure 136. Arterial Lumen Area vs. Arterial Transmural Pressure of Female Participant (M3) 30 Minutes Before Cold-Water Immersion. Black data points represent baseline measurements while white data points represent measurements collected during 5-minute reactive hyperemia.

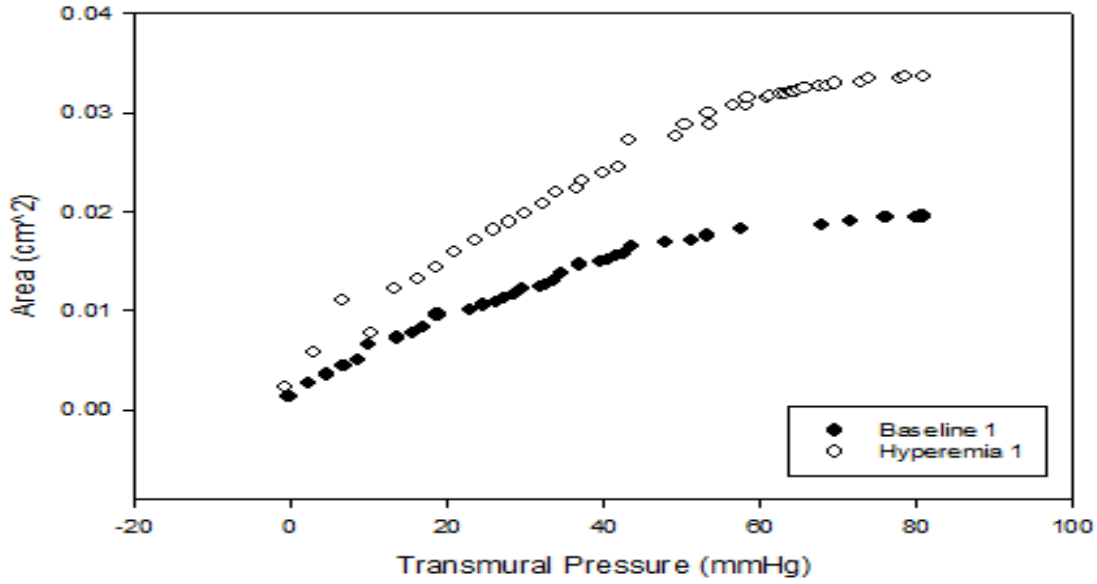

Figure 137. Arterial Lumen Area vs. Arterial Transmural Pressure of Male Participant (M3) 30 Minutes Before Cold-Water Immersion. Black data points represent baseline measurements while white data points represent measurements collected during 5-minute reactive hyperemia. Integrated from 0 mmHg to 80 mmHg transmural pressure.

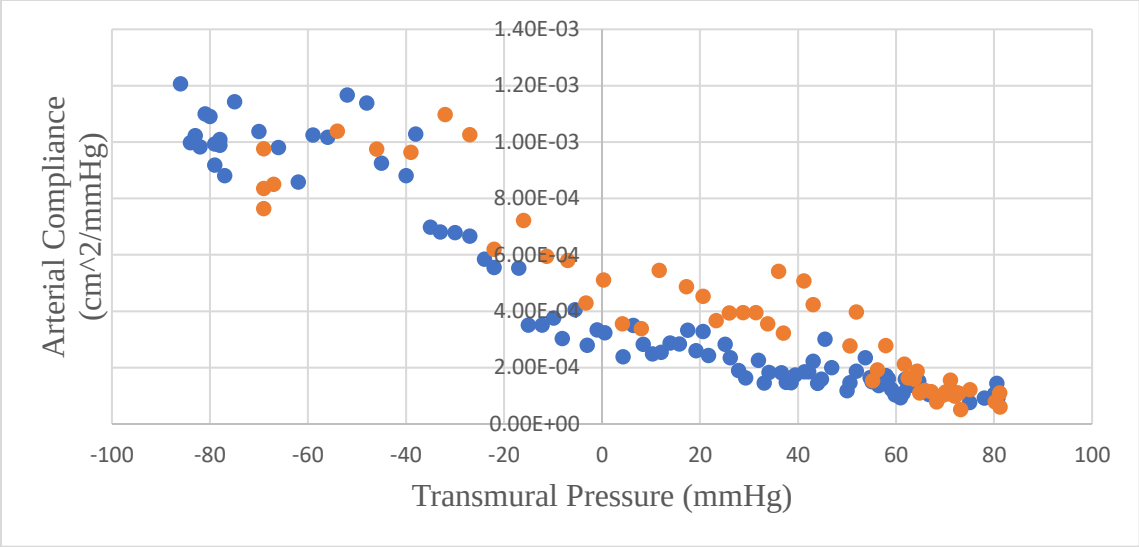

Figure 138. Arterial Area Compliance vs. Transmural Arterial Pressure of Male Participant (M3) Immediately After Cold-Water Immersion. Blue data points represent baseline measurements while orange data points represent measurements collected during 5-minute reactive hyperemia.

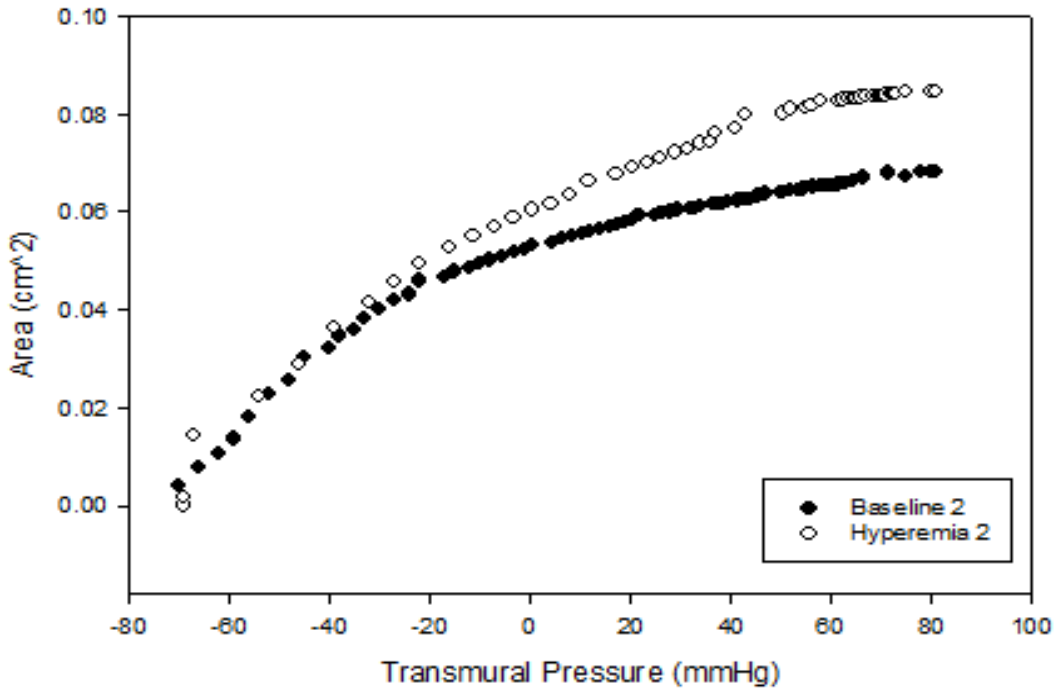

Figure 139. Arterial Lumen Area vs. Arterial Transmural Pressure of Female Participant (M3) Immediately After Cold-Water Immersion. Black data points represent baseline measurements while white data points represent measurements collected during 5-minute reactive hyperemia.

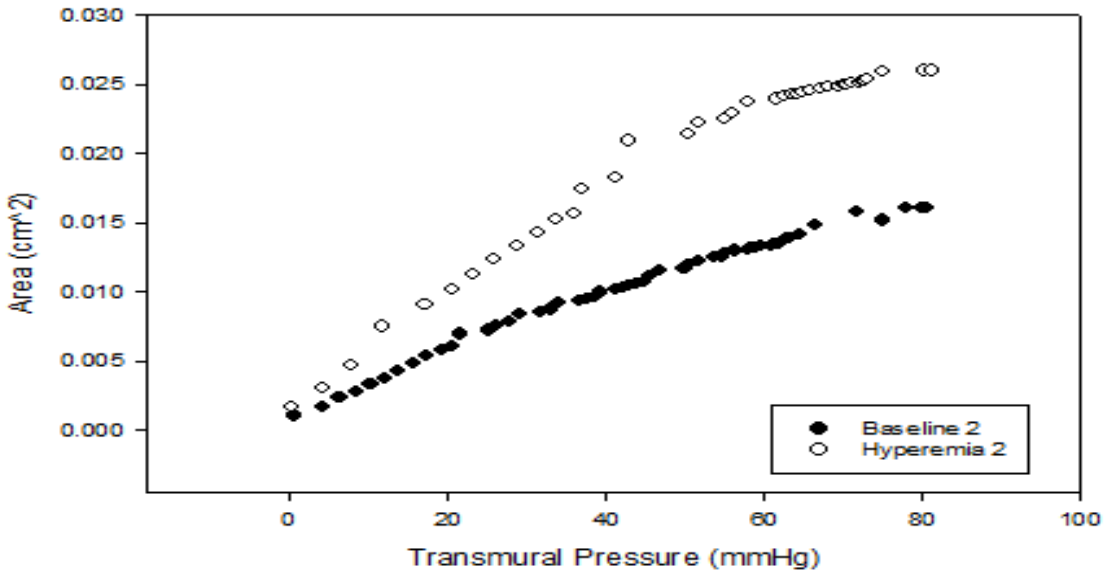

Figure 140. Arterial Lumen Area vs. Arterial Transmural Pressure of Male Participant (M3) Immediately After Cold-Water Immersion. Black data points represent baseline measurements while white data points represent measurements collected during 5-minute reactive hyperemia. Integrated from 0 mmHg to 80 mmHg transmural pressure.

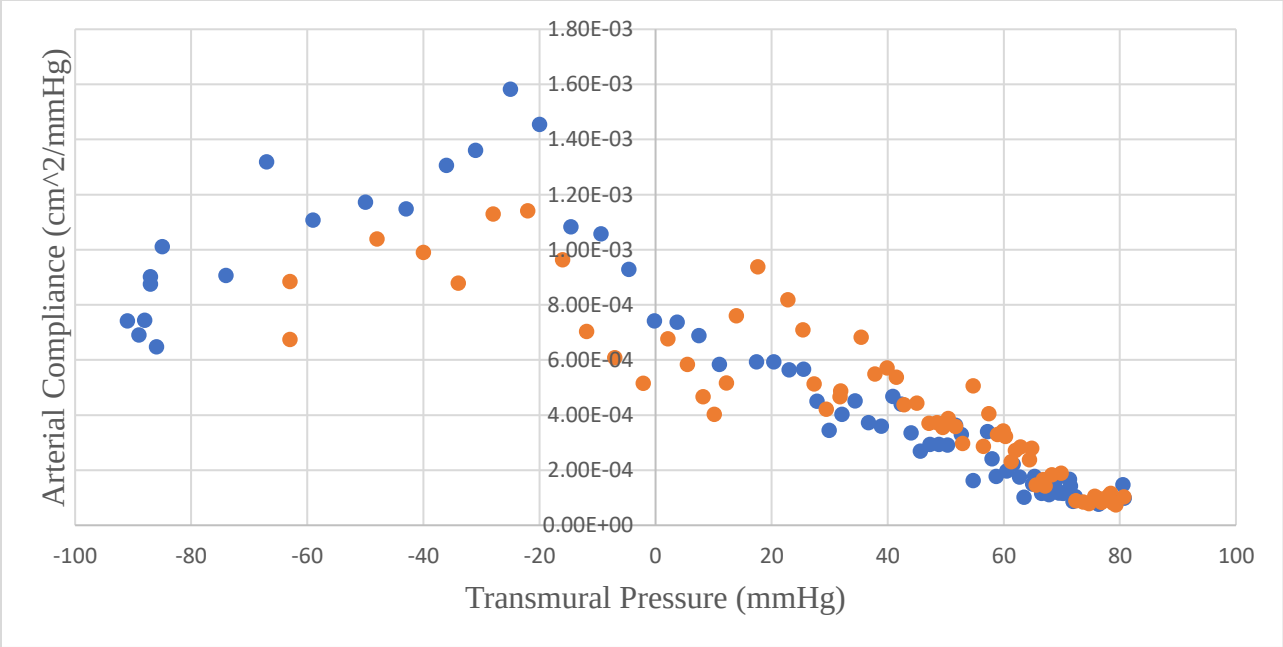

Figure 141. Arterial Area Compliance vs. Transmural Arterial Pressure of Male Participant (M3) 30 Minutes After Cold-Water Immersion. Blue data points represent baseline measurements while orange data points represent measurements collected during 5-minute reactive hyperemia.

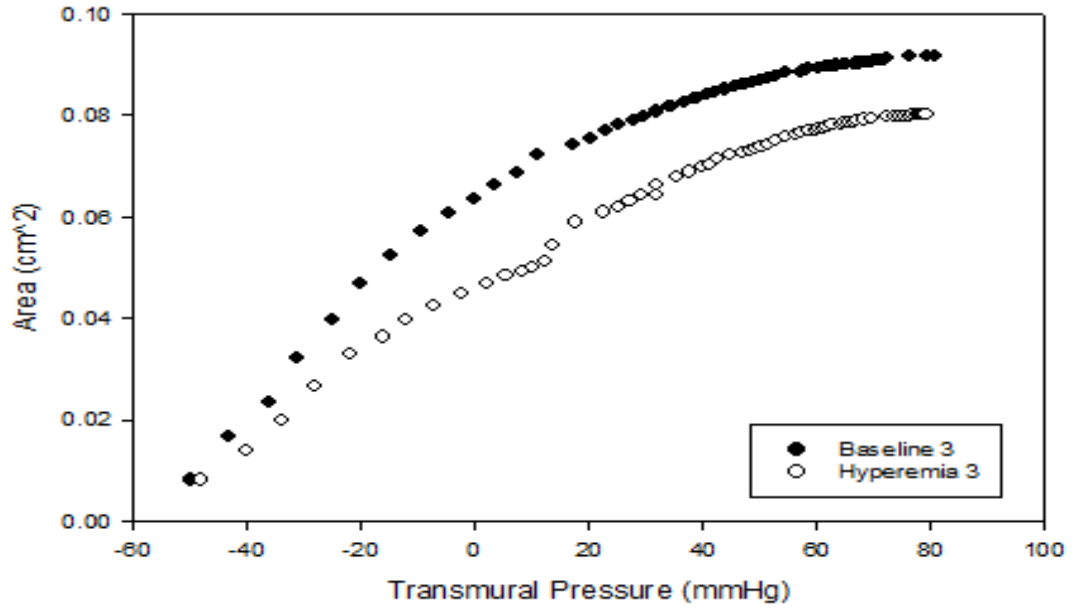

Figure 142. Arterial Lumen Area vs. Arterial Transmural Pressure of Female Participant (M3) 30 Minutes After Cold-Water Immersion. Black data points represent baseline measurements while white data points represent measurements collected during 5-minute reactive hyperemia.

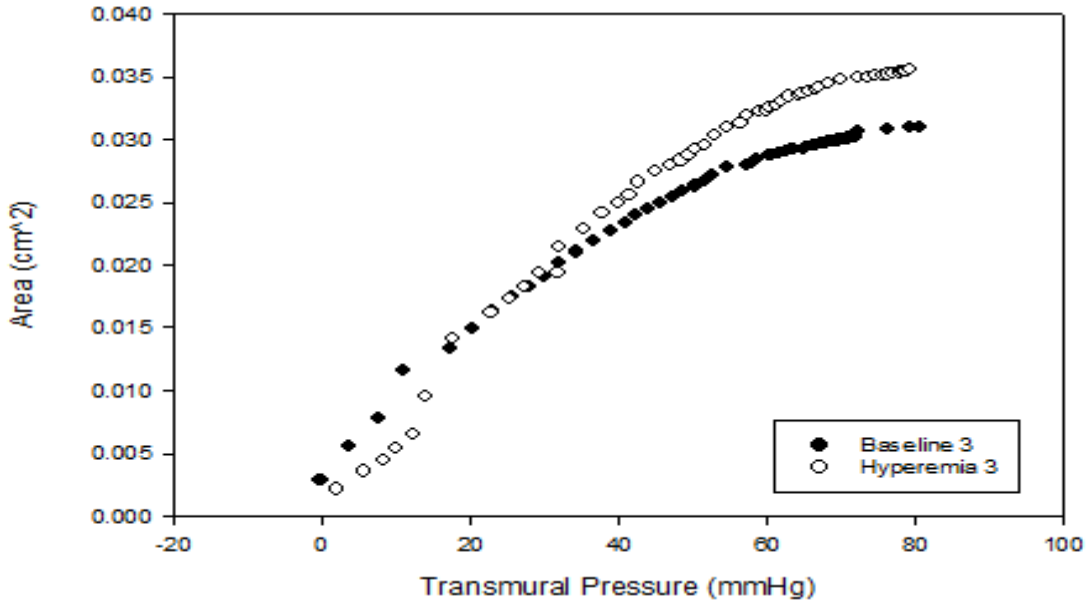

Figure 143. Arterial Lumen Area vs. Arterial Transmural Pressure of Male Participant (M3) 30 Minutes After Cold-Water Immersion. Black data points represent baseline measurements while white data points represent measurements collected during 5-minute reactive hyperemia. Integrated from 0 mmHg to 80 mmHg transmural pressure.

Participant: M4

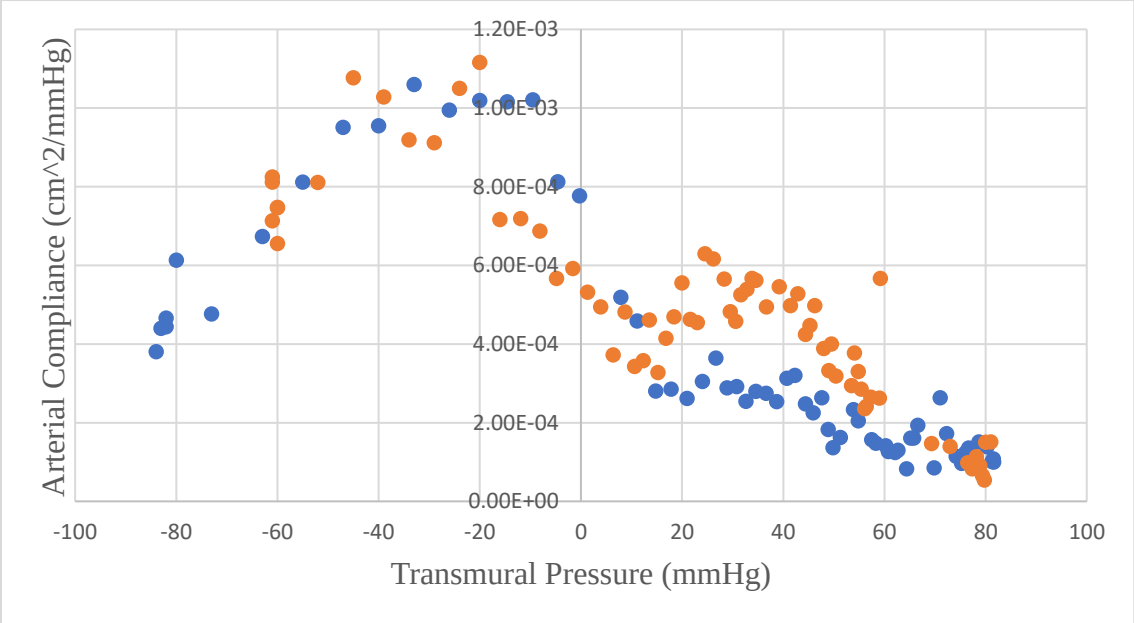

Figure 144. Arterial Area Compliance vs. Transmural Arterial Pressure of Male Participant (M4) 30 Minutes Before Cold-Water Immersion. Blue data points represent baseline measurements while orange data points represent measurements collected during 5-minute reactive hyperemia.

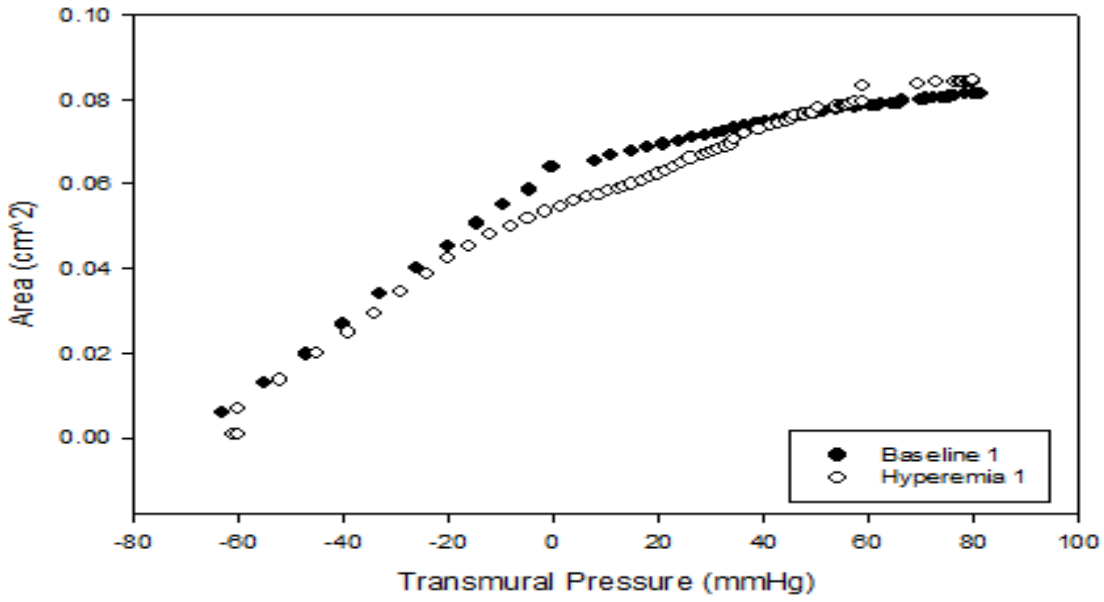

Figure 145. Arterial Lumen Area vs. Arterial Transmural Pressure of Female Participant (M4) 30 Minutes Before Cold-Water Immersion. Black data points represent baseline measurements while white data points represent measurements collected during 5-minute reactive hyperemia.

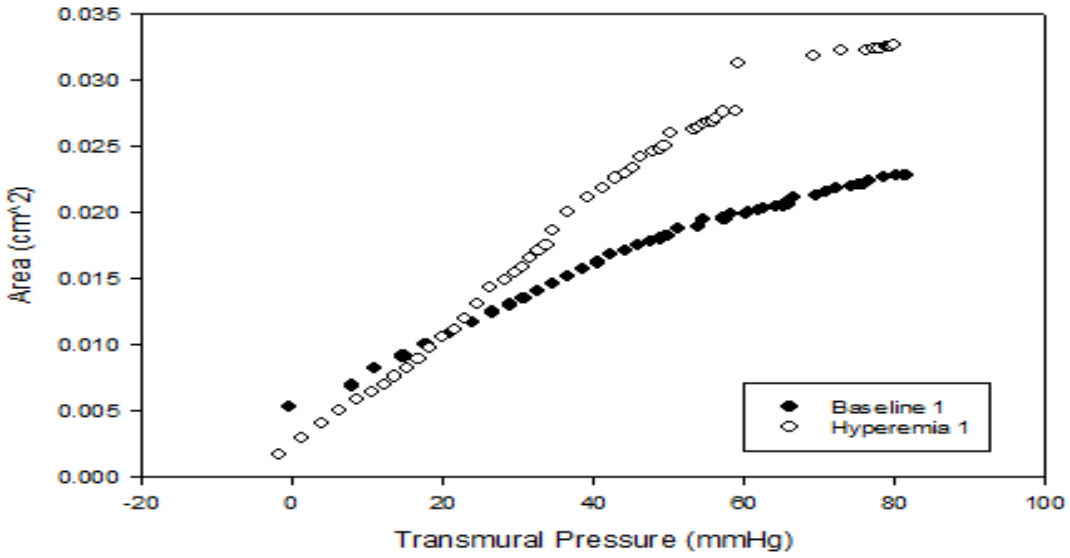

Figure 146. Arterial Lumen Area vs. Arterial Transmural Pressure of Male Participant (M4) 30 Minutes Before Cold-Water Immersion. Black data points represent baseline measurements while white data points represent measurements collected during 5-minute reactive hyperemia. Integrated from 0 mmHg to 80 mmHg transmural pressure.

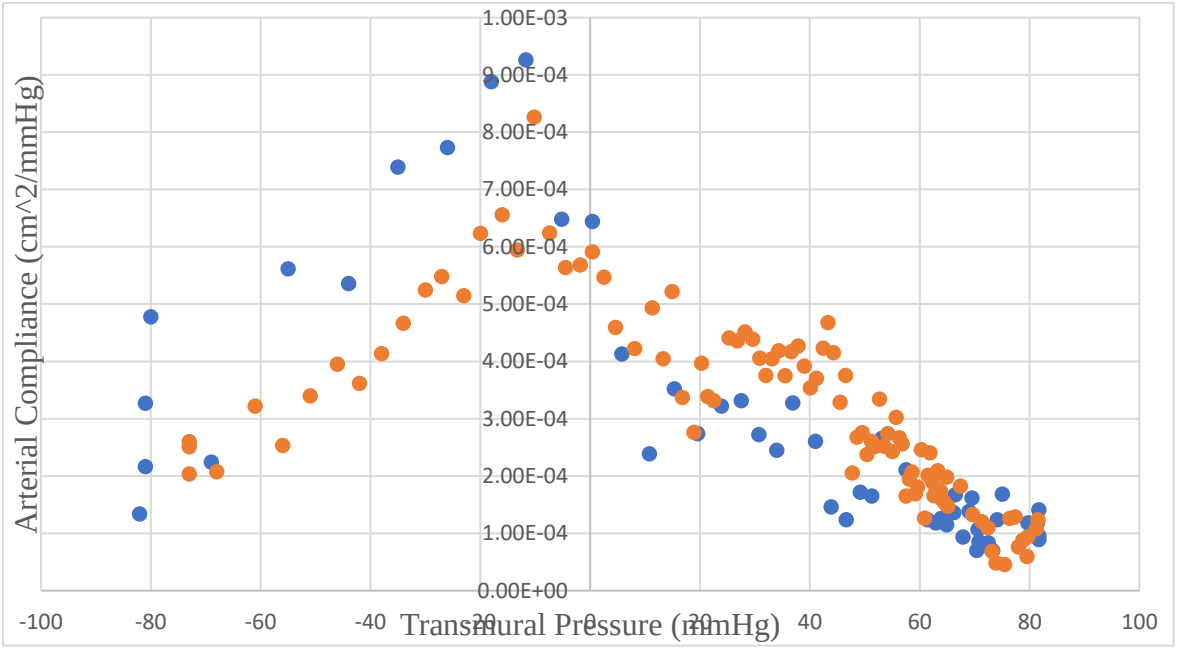

Figure 147. Arterial Area Compliance vs. Transmural Arterial Pressure of Male Participant (M4) Immediately After Cold-Water Immersion. Blue data points represent baseline measurements while orange data points represent measurements collected during 5-minute reactive hyperemia

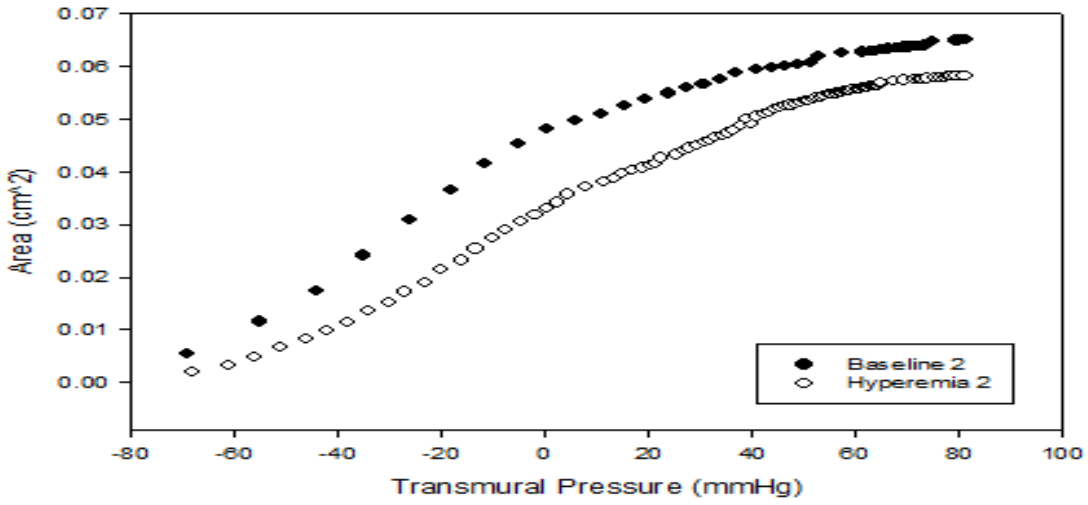

Figure 148. Arterial Lumen Area vs. Arterial Transmural Pressure of Female Participant (M4) Immediately After Cold-Water Immersion. Black data points represent baseline measurements while white data points represent measurements collected during 5-minute reactive hyperemia.

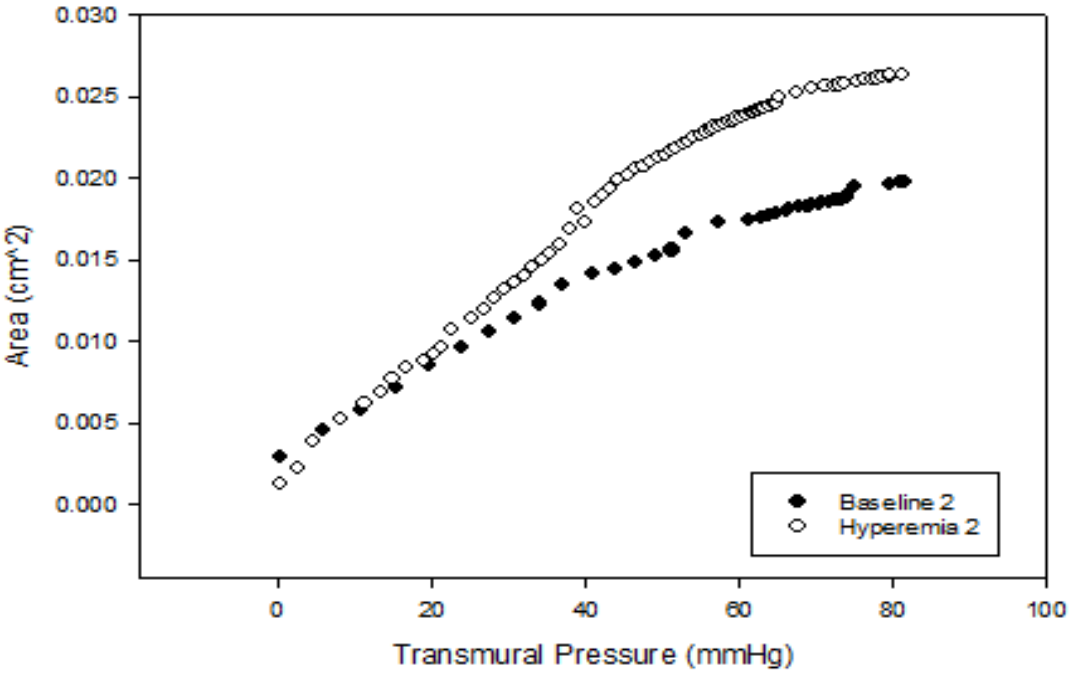

Figure 149. Arterial Lumen Area vs. Arterial Transmural Pressure of Male Participant (M4) Immediately After Cold-Water Immersion. Black data points represent baseline measurements while white data points represent measurements collected during 5-minute reactive hyperemia. Integrated from 0 mmHg to 80 mmHg transmural pressure.

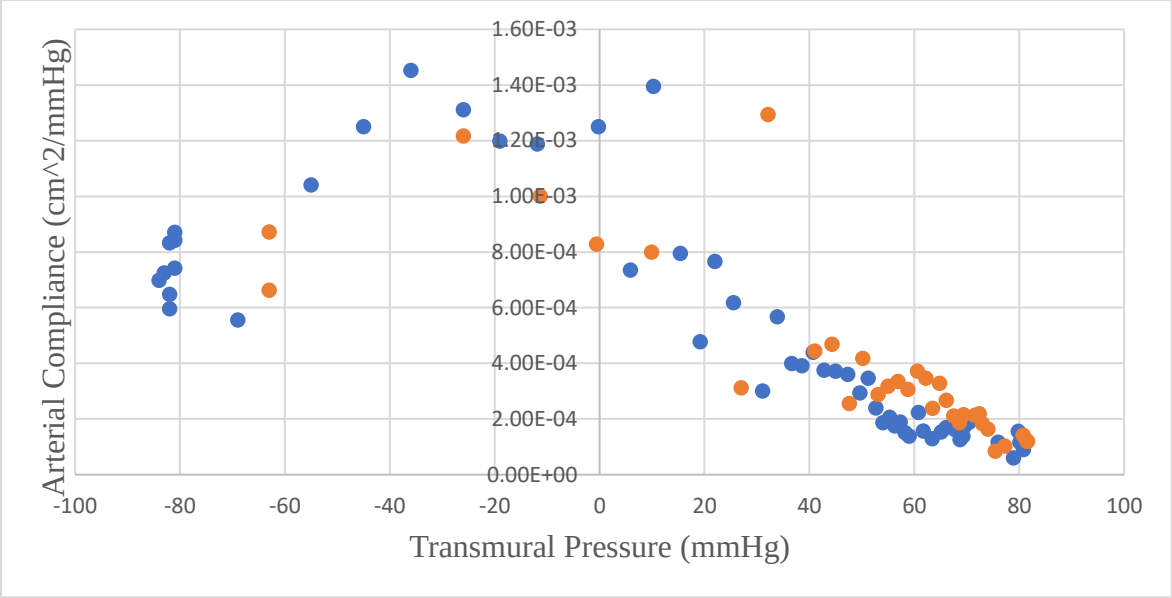

Figure 150. Arterial Area Compliance vs. Transmural Arterial Pressure of Male Participant (M4) 30 Minutes After Cold-Water Immersion. Blue data points represent baseline measurements while orange data points represent measurements collected during 5-minute reactive hyperemia.

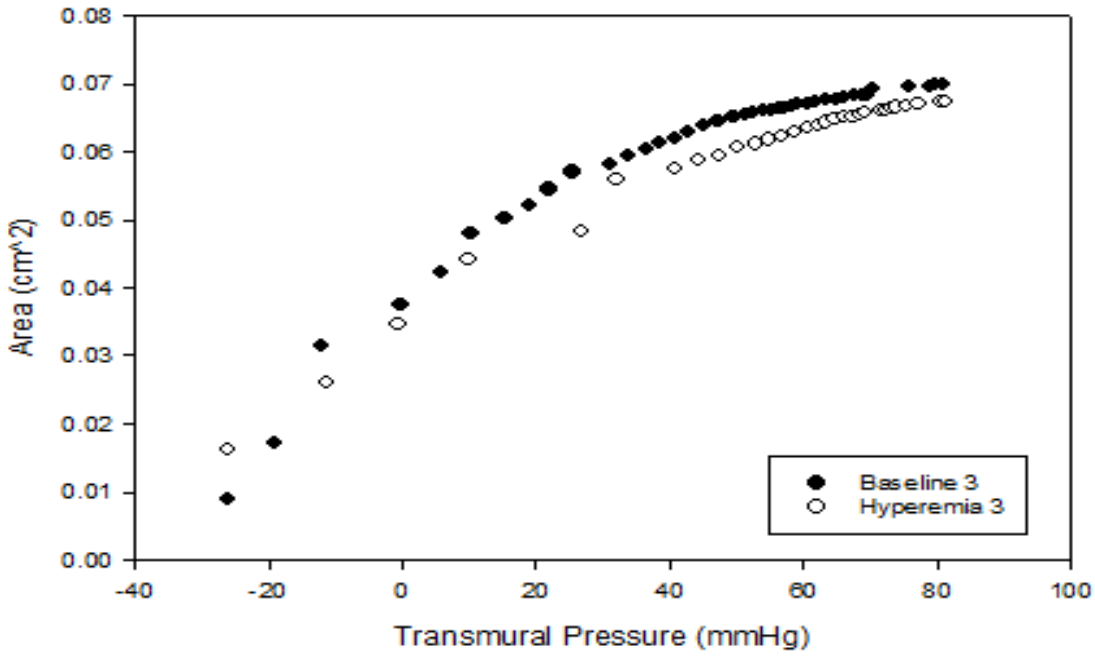

Figure 151. Arterial Lumen Area vs. Arterial Transmural Pressure of Female Participant (M4) 30 Minutes After Cold-Water Immersion. Black data points represent baseline measurements while white data points represent measurements collected during 5-minute reactive hyperemia.

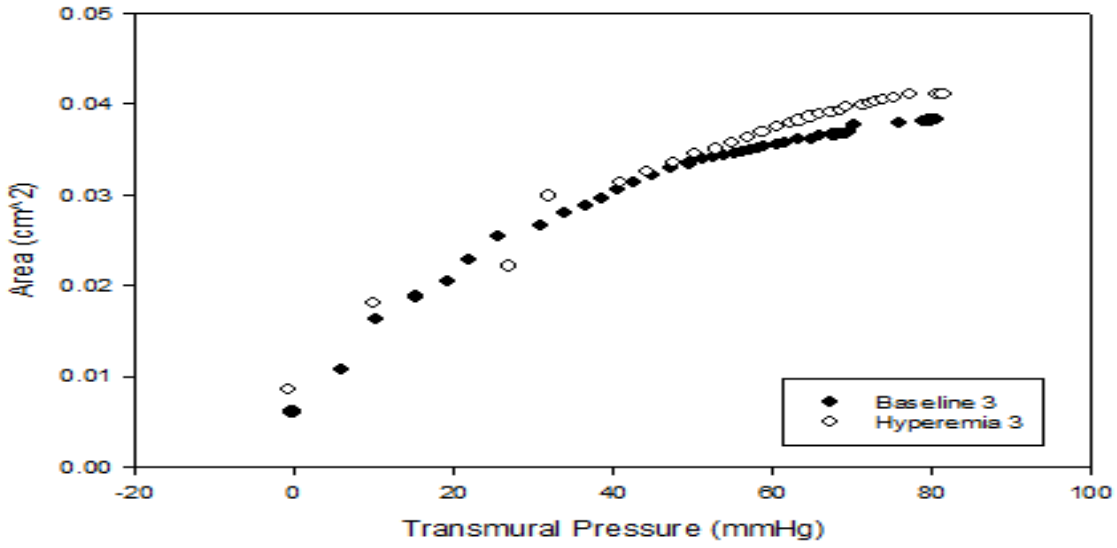

Figure 152. Arterial Lumen Area vs. Arterial Transmural Pressure of Male Participant (M4) 30 Minutes After Cold-Water Immersion. Black data points represent baseline measurements while white data points represent measurements collected during 5-minute reactive hyperemia. Integrated from 0 mmHg to 80 mmHg transmural pressure.

Participant: M5

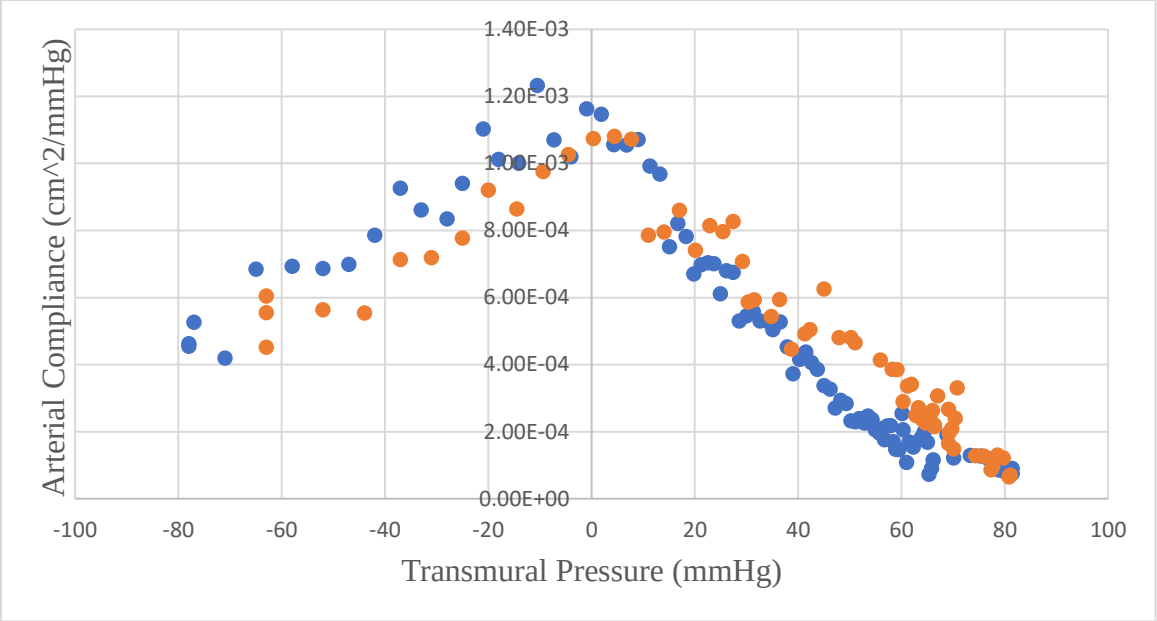

Figure 153. Arterial Area Compliance vs. Transmural Arterial Pressure of Male Participant (M5) 30 Minutes Before Cold-Water Immersion. Blue data points represent baseline measurements while orange data points represent measurements collected during 5-minute reactive hyperemia.

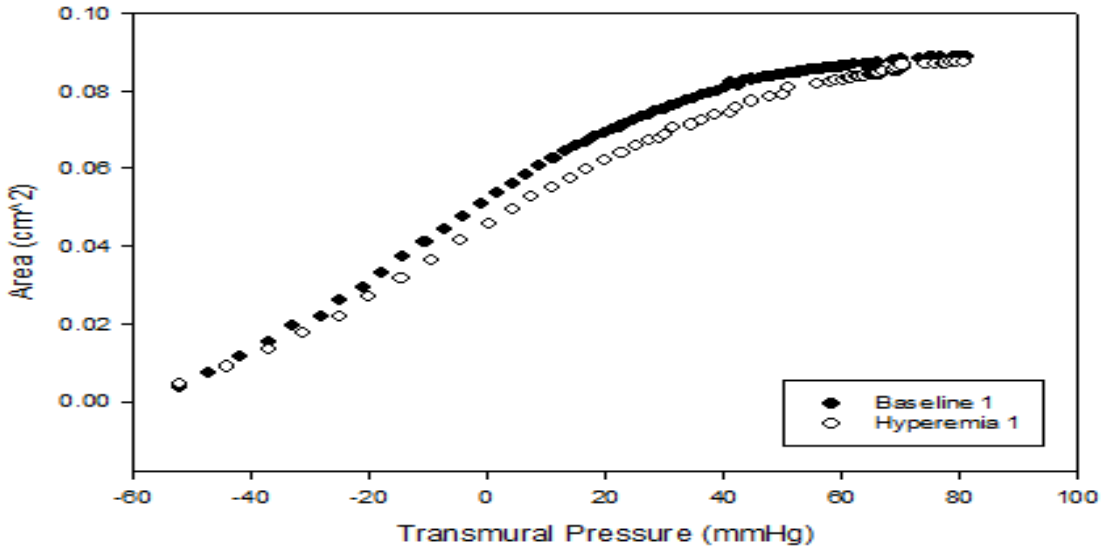

Figure 154. Arterial Lumen Area vs. Arterial Transmural Pressure of Female Participant (M5) 30 Minutes Before Cold-Water Immersion. Black data points represent baseline measurements while white data points represent measurements collected during 5-minute reactive hyperemia.

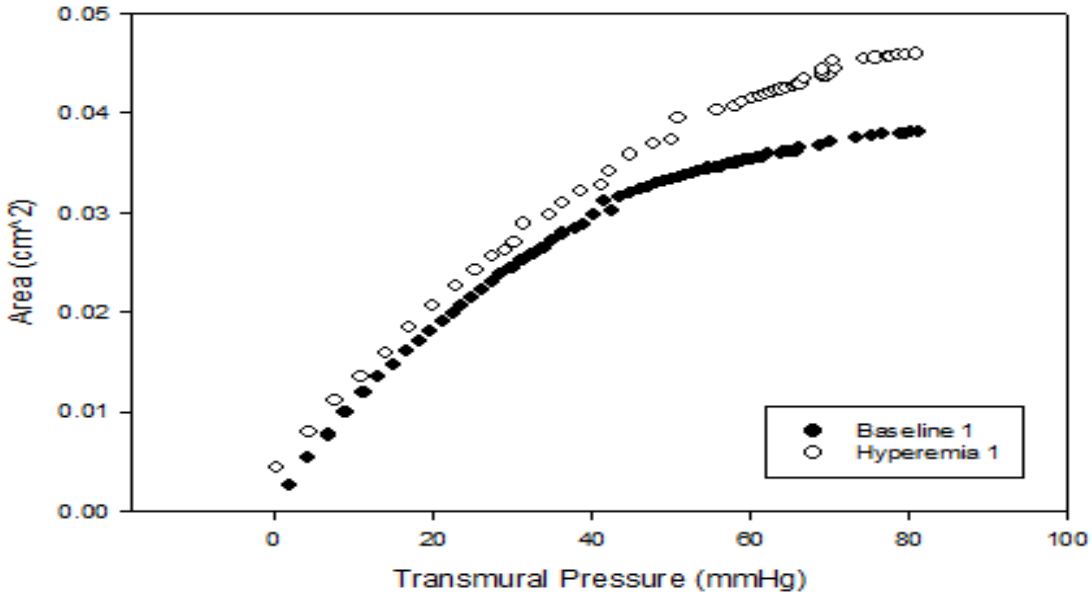

Figure 155. Arterial Lumen Area vs. Arterial Transmural Pressure of Male Participant (M5) 30 Minutes Before Cold-Water Immersion. Black data points represent baseline measurements while white data points represent measurements collected during 5-minute reactive hyperemia. Integrated from 0 mmHg to 80 mmHg transmural pressure.

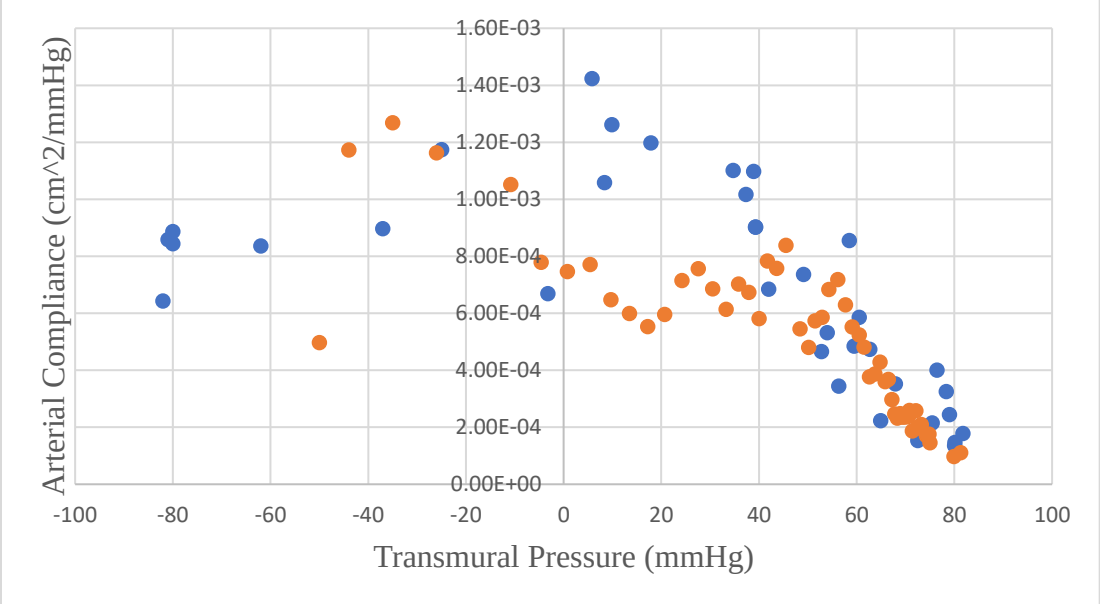

Figure 156. Arterial Area Compliance vs. Transmural Arterial Pressure of Male Participant (M5) Immediately After Cold-Water Immersion. Blue data points represent baseline measurements while orange data points represent measurements collected during 5-minute reactive hyperemia.

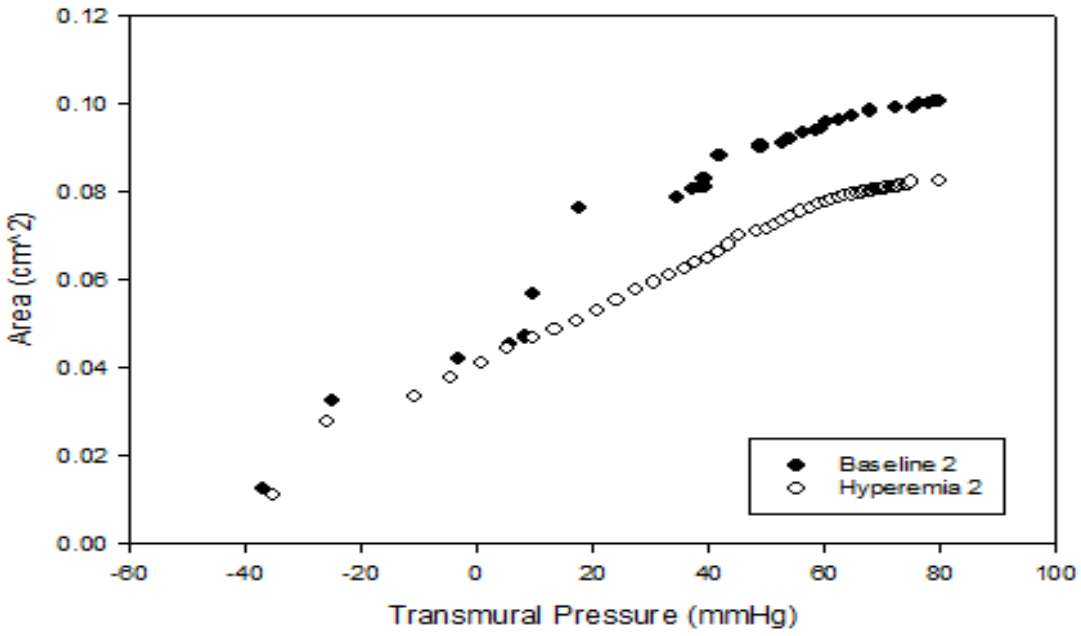

Figure 157. Arterial Lumen Area vs. Arterial Transmural Pressure of Female Participant (M5) Immediately After Cold-Water Immersion. Black data points represent baseline measurements while white data points represent measurements collected during 5-minute reactive hyperemia.

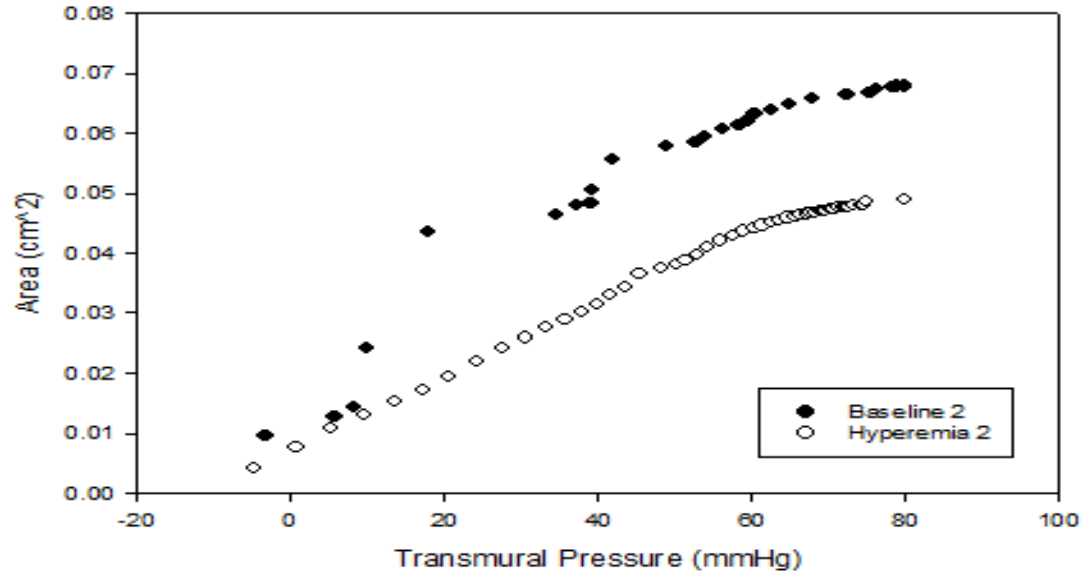

Figure 158.Arterial Lumen Area vs. Arterial Transmural Pressure of Male Participant (M5) Immediately After Cold-Water Immersion. Black data points represent baseline measurements while white data points represent measurements collected during 5-minute reactive hyperemia. Integrated from 0 mmHg to 80 mmHg transmural pressure.

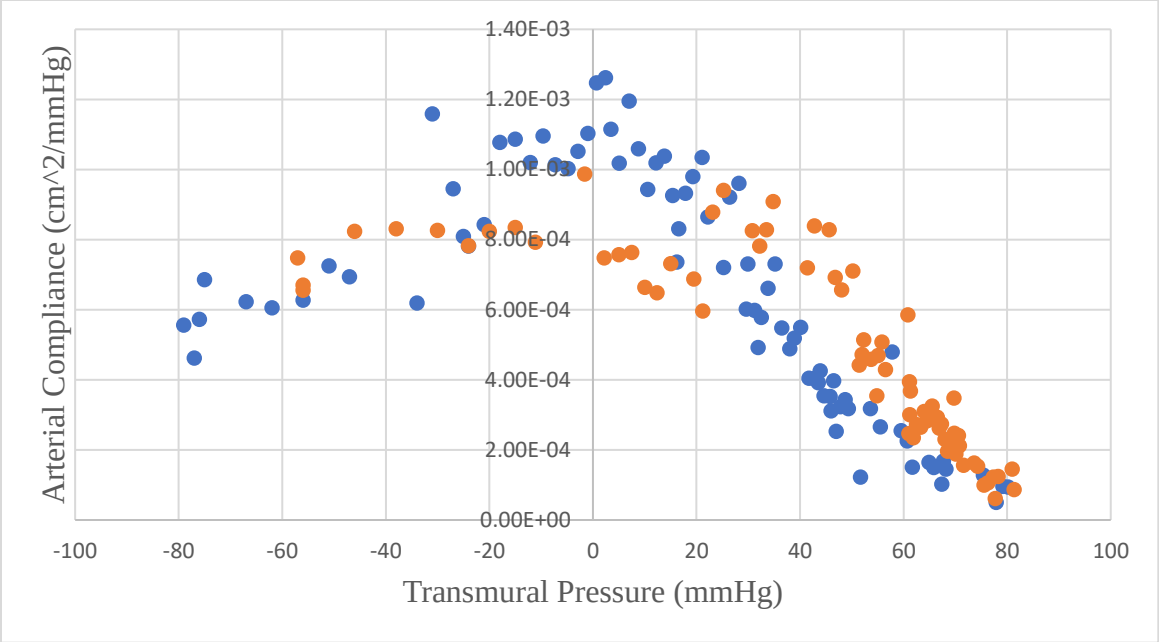

Figure 159.Arterial Area Compliance vs. Transmural Arterial Pressure of Male Participant (M5) 30 Minutes After Cold-Water Immersion. Blue data points represent baseline measurements while orange data points represent measurements collected during 5-minute reactive hyperemia.

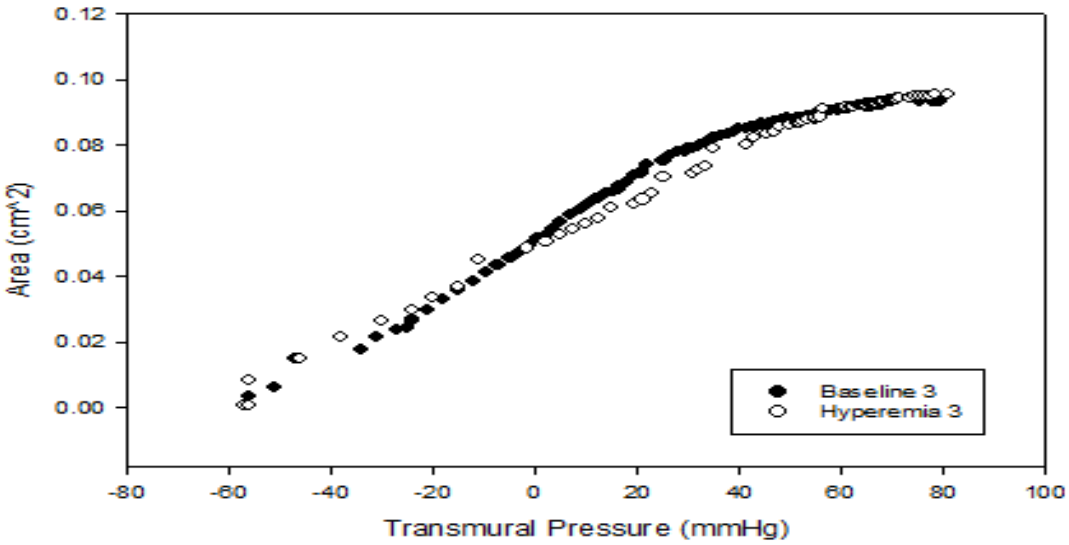

Figure 160. Arterial Lumen Area vs. Arterial Transmural Pressure of Female Participant (M5) 30 Minutes After Cold-Water Immersion. Black data points represent baseline measurements while white data points represent measurements collected during 5-minute reactive hyperemia.

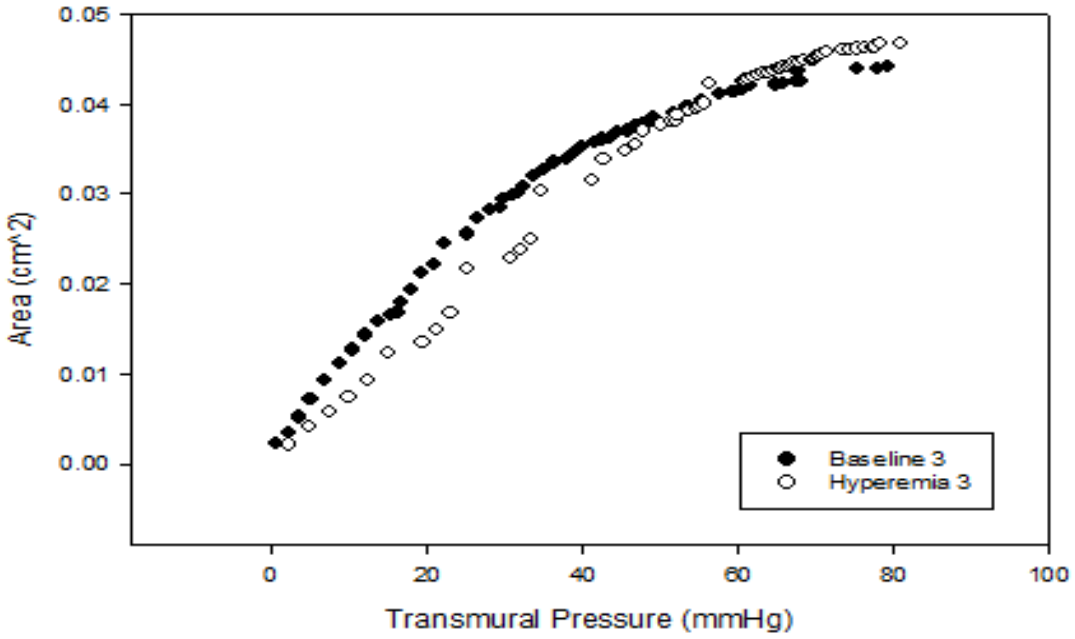

Figure 161. Arterial Lumen Area vs. Arterial Transmural Pressure of Male Participant (M5) 30 Minutes After Cold-Water Immersion. Black data points represent baseline measurements while white data points represent measurements collected during 5-minute reactive hyperemia. Integrated from 0 mmHg to 80 mmHg transmural pressure.